

A11101 909396

NBS  
PUBLICATIONS

NAT'L INST OF STANDARDS & TECH R.I.C.  
  
A11101909396  
/NBS monograph  
QC100 .U556 V172,1983 C.2 NBS-PUB-C 1959



# NBS MONOGRAPH 172

U.S. DEPARTMENT OF COMMERCE / National Bureau of Standards

## Liquefied Natural Gas Densities: Summary of Research Program at the National Bureau of Standards

QC  
100  
.U556  
No.172  
1983  
C. 2

## NATIONAL BUREAU OF STANDARDS

The National Bureau of Standards<sup>1</sup> was established by an act of Congress on March 3, 1901. The Bureau's overall goal is to strengthen and advance the Nation's science and technology and facilitate their effective application for public benefit. To this end, the Bureau conducts research and provides: (1) a basis for the Nation's physical measurement system, (2) scientific and technological services for industry and government, (3) a technical basis for equity in trade, and (4) technical services to promote public safety. The Bureau's technical work is performed by the National Measurement Laboratory, the National Engineering Laboratory, and the Institute for Computer Sciences and Technology.

**THE NATIONAL MEASUREMENT LABORATORY** provides the national system of physical and chemical and materials measurement; coordinates the system with measurement systems of other nations and furnishes essential services leading to accurate and uniform physical and chemical measurement throughout the Nation's scientific community, industry, and commerce; conducts materials research leading to improved methods of measurement, standards, and data on the properties of materials needed by industry, commerce, educational institutions, and Government; provides advisory and research services to other Government agencies; develops, produces, and distributes Standard Reference Materials; and provides calibration services. The Laboratory consists of the following centers:

Absolute Physical Quantities<sup>2</sup> — Radiation Research — Chemical Physics —  
Analytical Chemistry — Materials Science

**THE NATIONAL ENGINEERING LABORATORY** provides technology and technical services to the public and private sectors to address national needs and to solve national problems; conducts research in engineering and applied science in support of these efforts; builds and maintains competence in the necessary disciplines required to carry out this research and technical service; develops engineering data and measurement capabilities; provides engineering measurement traceability services; develops test methods and proposes engineering standards and code changes; develops and proposes new engineering practices; and develops and improves mechanisms to transfer results of its research to the ultimate user. The Laboratory consists of the following centers:

Applied Mathematics — Electronics and Electrical Engineering<sup>2</sup> — Manufacturing  
Engineering — Building Technology — Fire Research — Chemical Engineering<sup>2</sup>

**THE INSTITUTE FOR COMPUTER SCIENCES AND TECHNOLOGY** conducts research and provides scientific and technical services to aid Federal agencies in the selection, acquisition, application, and use of computer technology to improve effectiveness and economy in Government operations in accordance with Public Law 89-306 (40 U.S.C. 759), relevant Executive Orders, and other directives; carries out this mission by managing the Federal Information Processing Standards Program, developing Federal ADP standards guidelines, and managing Federal participation in ADP voluntary standardization activities; provides scientific and technological advisory services and assistance to Federal agencies; and provides the technical foundation for computer-related policies of the Federal Government. The Institute consists of the following centers:

Programming Science and Technology — Computer Systems Engineering.

<sup>1</sup>Headquarters and Laboratories at Gaithersburg, MD, unless otherwise noted;  
mailing address Washington, DC 20234.

<sup>2</sup>Some divisions within the center are located at Boulder, CO 80303.

NATIONAL BUREAU  
OF STANDARDS  
LIBRARY

C.C.  
SC  
100  
U556  
NO 17  
1983  
C.7

# Liquefied Natural Gas Densities: Summary of Research Program at the National Bureau of Standards

W. M. Haynes  
R. D. McCarty  
M. J. Hiza

Chemical Engineering Science Division  
National Engineering Laboratory  
National Bureau of Standards  
Boulder, CO 80303



---

U.S. DEPARTMENT OF COMMERCE, Malcolm Baldrige, Secretary

NATIONAL BUREAU OF STANDARDS, Ernest Ambler, Director

Issued October 1983

Library of Congress Catalog Card Number: 83-600608

**National Bureau of Standards Monograph 172**

Natl. Bur. Stand. (U.S.), Monogr. 172, 241 pages (Oct. 1983)

CODEN: NBSMA6

U.S. GOVERNMENT PRINTING OFFICE  
WASHINGTON: 1983

---

For sale by the Superintendent of Documents, U.S. Government Printing Office, Washington, DC 20402

Price \$

(Add 25 percent for other than U.S. mailing.)

## Contents

	Page
1. Introduction . . . . .	2
2. Major Accomplishments . . . . .	4
2.1 Experimental Apparatus . . . . .	4
2.2 Experimental Measurements . . . . .	6
2.2.1 Pure Fluid Data . . . . .	6
2.2.2 Binary Mixture Data . . . . .	6
2.2.3 Multicomponent Mixture Data . . . . .	7
2.3 Mathematical Models . . . . .	8
3. LNG Density Research at Other Laboratories . . . . .	9
4. Acknowledgments . . . . .	11
5. References . . . . .	13
6. Major Publications of LNG Density Project . . . . .	19
6.1 Reference [5] - Magnetic Suspension Densimeter for Measurements on Fluids of Cryogenic Interest . . . . .	19
6.2 Reference [9] - Simplified Magnetic Suspension Densimeter for Absolute Density Measurements . . . . .	33
6.3 Reference [6] - Apparatus for Density and Dielectric Constant Measurements to 35 MPa on Fluids of Cryogenic Interest . . . . .	37
6.4 Reference [13] - Measurements of the Orthobaric Liquid Densities of Methane, Ethane, Propane, Isobutane, and Normal Butane . . . . .	49
6.5 Reference [14] - Orthobaric Liquid Densities of Normal Butane from 135 to 300 K as Determined with a Magnetic Suspension Densimeter . . . . .	59
6.6 Reference [16] - Orthobaric Liquid Densities and Excess Volumes for Binary Mixtures of Low Molar-Mass Alkanes and Nitrogen Between 105 and 140 K . . . . .	65
6.7 Reference [17] - Orthobaric Liquid Densities and Dielectric Constants of (Methane + 2-Methylpropane) and (Methane + N-Butane) at Low Temperatures . . . . .	89

6.8	Reference [18] - Liquid Mixture Excess Volumes and Total Vapor Pressures Using a Magnetic Suspension Densimeter with Compositions Determined by Chromatographic Analysis: Methane Plus Ethane . . . . .	99
6.9	Reference [20] - Orthobaric Liquid Densities and Excess Volumes for Multicomponent Mixtures of Low Molar-Mass Alkanes and Nitrogen Between 105 and 125 K . . . . .	107
6.10	Reference [21] - Measurements of Orthobaric-Liquid Densities of Multicomponent Mixtures of LNG Components ( $N_2$ , $CH_4$ , $C_2H_6$ , $C_3H_8$ , $CH_3CH(CH_3)CH_3$ , $C_4H_{10}$ , $CH_3CH(CH_3)C_2H_5$ , and $C_5H_{12}$ ) Between 110 and 130 K . . . . .	117
6.11	Reference [34] - Four Mathematical Models for the Prediction of LNG Densities . . . . .	127
6.12	Reference [35] - Mathematical Models for the Prediction of Liquefied-Natural-Gas Densities . . . . .	205
6.13	Reference [25] - An Empirical Excess Volume Model for Estimating Liquefied Natural Gas Densities . . . . .	223
6.14	Reference [22] - Prediction of Liquefied-Natural-Gas (LNG) Densities from New Experimental Dielectric Constant Data .	235

# LIQUEFIED NATURAL GAS DENSITIES: SUMMARY OF RESEARCH

## PROGRAM AT THE NATIONAL BUREAU OF STANDARDS

W. M. Haynes, R. D. McCarty and M. J. Hiza

Chemical Engineering Science Division  
National Engineering Laboratory  
National Bureau of Standards  
Boulder, Colorado 80303

This report summarizes the results of a project concerning the densities of liquefied natural gas (LNG) and its components. This project, initiated in the Properties of Fluids Section of the Cryogenics Division of the National Bureau of Standards in July 1972, was carried out under the sponsorship of a consortium of eighteen energy companies\*.

The experimental part of this project has included the following accomplishments: (a) development of a magnetic suspension densimeter for absolute density measurements on liquids, including liquid mixtures in equilibrium with their vapor, at temperatures from 90 to 300 K; (b) orthobaric liquid density measurements on the major components of LNG, which include nitrogen (95-120 K), methane (105-160 K), ethane (100-270 K), propane (100-288.7 K), isobutane (115-300 K), and normal butane (135-300 K); (c) orthobaric liquid density measurements on approximately thirty-five binary mixtures of the above components for all combinations except nitrogen + butane systems, primarily in the temperature range of 105 to 130 K; and (d) orthobaric liquid density measurements on twenty-seven multicomponent mixtures (105-120 K), including several LNG-like mixtures with up to eight components. The total uncertainty of a single density measurement is approximately 0.1 percent at low temperatures and decreases to approximately 0.06 percent at room temperature. The estimated standard deviation of a single density measurement is less than 0.02 percent.

The density data have been used to optimize, test, and compare several mathematical models as to their suitability for the calculation of LNG densities for custody transfer. Models selected for optimization and testing included an extended corresponding states method, a hard sphere model, a cell model, and an empirical model due to Klosek and McKinley. The ultimate goal of this project was to produce one or more mathematical models that could be used to predict the density of any LNG mixture to within an uncertainty of 0.1 percent from an input of pressure, temperature, and composition. After revisions based on the new experimental data from this project, each of the models

---

\* British Gas Corp., Chicago Bridge and Iron Co., Columbia Gas Service Corp., Distrigas Corp., Easco Gas LNG, Inc., El Paso Natural Gas, Gaz de France, Marathon Oil Co., Mobil Oil Corp., Natural Gas Pipeline Co., Phillips Petroleum Co., Shell International Gas, Ltd., Sonatrach, Southern California Gas Co., Tennessee Gas Pipeline Co., Texas Eastern Transmission Co., Tokyo Gas Co., Ltd., and Transcontinental Gas Pipe Line Corp.

investigated here satisfy this goal for typical LNG compositions. The limitations and ranges of validity of the various models are discussed. Also presented are techniques for predicting LNG densities from dielectric constant measurements and from excess volume calculations.

The last section of this report consists of publications that provide a complete and detailed account of the results of this project.

Key words: binary mixtures; density; experimental data; liquefied natural gas; magnetic suspension densimeter; multicomponent mixtures; prediction methods; pure fluids.

## 1. Introduction

During the past decade liquefied natural gas has become an increasingly important commodity on the world energy market. This trend is expected to continue into the foreseeable future. In the buying and selling of LNG, the basis of custody transfer is its heating value. The determination of the heating value of LNG requires a knowledge of its density, which in turn is dependent upon its composition, temperature, and pressure. Since, for example, an error of one percent in density can result in an inequity of between \$100,000 and \$200,000 (at 1983 prices) per 125,000 m<sup>3</sup> shipload of LNG, the accuracy to which the density of the liquid can be determined is extremely important in transactions involving LNG. A one percent error in density was not uncommon at the time this project was initiated.

There are, at least, two means for determining the density of a large volume of LNG. One method is by direct field measurements using commercially available densimeters. A second method consists of the use of a mathematical model or correlation to calculate a density based on direct measurements of the liquid composition and temperature.

This report describes a project that has been concerned with the determination of the density by the second method. In actual transfer situations it is likely that both methods will be used to complement each other. By either method, the accuracy to which the density can be determined is limited by both practical and state-of-the-art considerations. This has resulted in setting a goal of 0.1 percent for the total uncertainty in the determination of the density of LNG.

In July 1972, a project was initiated at this laboratory with an ultimate goal of providing one or more mathematical models that could be used to calculate the density of any LNG mixture with a total uncertainty of less than 0.1 percent based on a knowledge of the pressure, temperature, and composition of the liquid mixture. The mathematical models would be developed and/or optimized using density data for the major components of LNG and for binary mixtures of these components. Density data for multicomponent mixtures of LNG components would be used to evaluate and compare the performance of the mathematical models. Some of the test mixtures would be selected to simulate commercial LNG compositions. LNG consists primarily of methane (concentration level typically greater than 75 percent) with lesser amounts of ethane (up to 15 percent), propane (up to 5 percent), butanes (up to 2 percent), nitrogen (up to 2 percent), and pentanes plus heavier hydrocarbons (up to 0.5 percent).

The accuracy of a calculational technique based on experimental data can be no better than the input data from which the technique is developed. At the time this project was initiated, comparisons of saturated (orthobaric) liquid density data for the pure components of LNG exhibited differences as large as 0.5 percent, while each investigator was generally claiming inaccuracies of 0.1 percent or less. Furthermore, there were only a few sets of published data for liquid mixtures containing LNG components, especially at low temperatures. These data were generally limited in scope or had claimed inaccuracies larger than the desired 0.1 percent. (The pure fluid and mixture data for LNG components from other investigations are summarized in Section 3 of this report.) Thus, a major task of the LNG density project at this laboratory has been to provide an accurate and internally consistent set of density data for the major components of LNG and for mixtures of these components. (These data could also serve as a basis for calibration or development of gauging and metering methods for LNG and for process design and operation of LNG facilities.)

This project was sponsored by a consortium of eighteen international energy companies, five of which were from countries outside the United States. The sponsors represented both buyers and sellers of LNG. In carrying out this research project, the National Bureau of Standards is serving in its traditional role as an independent third party. All results of this project would be published in the open literature and hopefully gain wide acceptance throughout the LNG industry, since qualified sponsor representatives from all parts of the

international LNG market would have closely scrutinized the progress of this project throughout its entirety.

The major purpose of this report is to incorporate under a single cover a complete account of the LNG density project. The major accomplishments of the project are summarized in Section 2, while the detailed results are presented in the papers that comprise Section 6. Most of these papers are reprints of publications, while a few are presented in their existing, prepublished form. During the course of this research, several papers [1-4] have been published that presented a summary or status report of the project. These papers are not included in Section 6. The present report serves as the final report to the sponsors of this project.

## 2. Major Accomplishments

### 2.1 Experimental Apparatus

The experimental technique selected for performing the density measurements for this project had to satisfy relatively stringent criteria. It must be capable of absolute density measurements of high accuracy and precision on a liquid, including mixtures, in equilibrium with vapor at cryogenic temperatures and at pressures to approximately 4 MPa using an optical cell. A magnetic suspension densimeter, based on an application of Archimedes' principle, was developed for this purpose.

Two apparatus [5,6], each incorporating a magnetic suspension technique in the density determination, were constructed for the measurements on liquids, including liquid mixtures, associated with this project. For both apparatus, the total uncertainty of a single density measurement, which is taken as three times the standard deviation plus the systematic error, is approximately 0.1 percent at low temperatures and decreases to approximately 0.06 percent at room temperature. The estimated standard deviation of a single density measurement is less than 0.02 percent.

A brief description of the method for determining densities with either apparatus is as follows. A small magnetic buoy is freely suspended in the fluid whose density is to be determined. The density of the buoy is significantly greater (by approximately an order of magnitude) than the density of the fluids investigated here. The force necessary to lift the buoy is supplied by one or more air-core solenoids. The buoy is maintained at a stable (vertical) position

through the automatic regulation of an electronic servocircuit containing the lift coil and either a differential transformer [5] or a differential capacitor [7] that detects the motion of the buoy. The horizontal position of the buoy is maintained by the axially symmetrical, diverging field of the lift coil.

When the buoy is supported at the same position in vacuum and in the fluid of interest, the upward magnetic force on the buoy supplied by the air-core solenoids gives a means for measuring the density of the fluid since this is the force that must be added to the buoyant force to balance the downward gravitational force. Thus, the density is deduced from measurements of the currents in the support coils necessary to support the buoy in vacuum and in the fluid of interest at the same temperature and at the same vertical position (determined with a 125X microscope).

The mass and volume of the buoy must be determined from independent measurements. The mass was determined using an analytical microbalance. The volume of the buoy at room temperature was determined by using distilled water as a reference fluid of known density. Thermal expansion data [8] for barium ferrite, the material from which the buoy was fabricated, were obtained so that the volume of the buoy at low temperatures could be calculated.

The first apparatus [5] could be used at temperatures between 90 and 300 K and at pressures to 5 MPa. After initial tests with a three-coil arrangement to support the buoy, the densimeter was simplified considerably by reducing to a system employing only one coil [9]. The second apparatus [6], which employed exactly the same technique for determining density, was significantly different from, and more versatile than, the first apparatus. The second apparatus contained a concentric cylinder capacitor that was used to make dielectric constant measurements on the same liquid samples for which density data were obtained. The major reason for the construction of the second apparatus was a need in other research projects (e.g., PVT and dielectric constant measurements on liquid propane [10], isobutane [11], and normal butane [12]) for a higher pressure capability (35 MPa) for the magnetic suspension densimeter. The extension to higher pressures was not needed in the LNG density project.

It should be noted that the second apparatus gave no improvement over the first in the accuracy to which the density could be determined. The consistency of the density data from both apparatus should be equivalent to that for either

apparatus alone. To ensure that this was the case, measurements on liquid methane were used as a control throughout the project with both apparatus.

## 2.2 Experimental Measurements

### 2.2.1 Pure Fluid Data

The first experimental measurements for the LNG density project consisted of the acquisition of orthobaric liquid density data for the major components of LNG. Comprehensive results were obtained for nitrogen (95-120 K) [5], methane (105-160 K) [5,13], ethane (100-270 K) [13], propane (100-288.7 K) [13], isobutane (115-300 K) [13], and normal butane (135-300 K) [13,14]. Detailed comparisons between the data from this project and independent results demonstrated the need for an accurate and internally consistent set of data for the major components of LNG. Differences as large as 0.5 percent between the density data of independent investigators were common. At the time this project was initiated, there were no published data for normal butane at low temperatures. (In the course of evaluating the performance of the magnetic suspension densimeter, density data were also obtained for saturated liquid argon (100-120 K) and ethylene (105-200 K) [15].)

### 2.2.2 Binary Mixture Data

Next, orthobaric liquid density measurements were carried out on thirty-five binary mixtures [16-18] containing the major components of LNG. Most of the binary mixture data was taken in the temperature range of 105 to 140 K. All binary combinations of the six major components of LNG were investigated in this project, with the exception of the nitrogen + isobutane and nitrogen + normal butane systems.

Prior to the LNG density project, no low temperature, liquid density data could be found in the literature for the following systems: nitrogen + ethane, nitrogen + propane, ethane + isobutane, propane + isobutane, propane + normal butane, and isobutane + normal butane, all of which have been investigated here. All of the binary mixture measurements were carried out on liquid samples condensed into the cell from gravimetrically prepared gas mixtures. This was considered to be the most accurate method to fix the compositions of the liquid mixtures. For all mixtures containing nitrogen and/or methane, total vapor pressures have also been measured. For the methane-rich binary mixtures containing either isobutane or normal butane, dielectric constant data [17] were obtained simultaneously with the density results.

Extensive comparisons of the binary mixture data from the present study have been made with available literature data. In general, differences were less than 0.1 percent, except that the density data here for the ethane + propane system exhibited approximately an 0.8 percent discrepancy when compared with the data of Shana'a and Canfield [19]. This was inconsistent with comparisons with the same authors for the methane + ethane and methane + propane systems as well as for pure fluid results, where the agreement was typically better than 0.1 percent.

### 2.2.3 Multicomponent Mixture Data

In order to evaluate and test the mathematical models that have been developed and optimized using the binary mixture and pure component data, orthobaric liquid density measurements have been performed on twenty-seven multicomponent mixtures [20,21] of LNG components, primarily in the temperature range of 110 to 120 K. The multicomponent mixtures investigated in this project ranged from ternary mixtures (methane and binary combinations of nitrogen, ethane, propane, and normal butane) to four- to eight-component methane-rich (75-90 mole percent) mixtures containing up to 5 mole percent nitrogen, 15 mole percent ethane, 7 mole percent propane, 5 mole percent butanes, and 0.44 mole percent pentanes.

The compositions of some of the six- to eight-component mixtures were selected to simulate commercial LNG mixtures. The compositions of other multicomponent mixtures were chosen to provide severe tests of the mathematical models and to complement the use of binary mixture data in the optimization of the models. Except for three of the multicomponent mixtures, the compositions were determined from the preparation of the gas mixtures by gravimetric means. For the other three mixtures, the compositions were determined by gas chromatographic analysis using a thermal conductivity detector. The chromatograph was calibrated with a gravimetrically prepared mixture. Vapor pressure data have also been obtained for the multicomponent mixtures. For those multicomponent mixtures investigated with the second apparatus, dielectric constant measurements [22] were performed simultaneously with the density measurements.

Although the pure fluid and binary mixture measurements from this project have not included data for pentanes, five multicomponent mixtures containing pentanes [21] have been investigated. It was thought that densities of these systems could be predicted with the mathematical models using existing pure fluid data for the pentanes from other sources [23,24] and predicting the interaction

parameters for binary mixtures containing pentanes from the behavior of the binary mixtures studied in the LNG density project. (Expressions for representing the pentane data of Orrit and Laupretre [24] are reported by Hiza [25].) High accuracy in these predictions is not required since LNG mixtures contain relatively small fractions of pentanes.

### 2.3 Mathematical Models

As mentioned earlier, one method of determining the density of LNG is to predict that density with a mathematical model of the equation of state, given the pressure, temperature, and composition of the LNG. The ultimate goal of this study was to produce such a model (or models) that would be accurate to within 0.1 percent of the true density. The scope of this study was limited to saturated liquids over a temperature range of 105 to 140 K with pressures to 2 MPa. The components of LNG were assumed to be  $N_2$ ,  $CH_4$ ,  $C_2H_6$ ,  $C_3H_8$ ,  $iC_4H_{10}$ ,  $nC_4H_{10}$ ,  $iC_5H_{12}$ , and  $nC_5H_{12}$ .

Four models were chosen to fit to the experimental data. Each of the selected models represents a different approach to modeling the equation of state of a fluid. These are an extended corresponding states model [26-27], a hard sphere model [28], a cell model [29-31], and a graphical model due to Klosek and McKinley [32]. During the course of optimizing the four models using the experimental data, it became necessary to revise the functional form of the model proposed by Klosek and McKinley. No revisions of the functional form of the other three models were necessary, and only the adjustable parameters were changed to achieve the desired fit of the experimental data. The final result was that all four of the models originally chosen can be used to predict the density of LNG to within 0.1 percent of the true density, given the temperature, pressure, and composition of the LNG. Details of the fitting procedures, comparisons to experimental data, and computer program listings are given in references [33-35].

Also during the course of this study, an excess volume model was developed by Hiza [25]. This model also achieves the 0.1 percent criteria outlined above under the same restrictions as the other models. Lastly, a model has been developed by Haynes and McCarty [22] that does not require either the temperature or pressure as input information (all of the other models require a minimum of temperature as input and most require both temperature and pressure). This model

requires an input of dielectric constant and composition of the LNG and predicts the density to within 0.15 percent of the experimental value.

All of the models have restrictions on pressure, temperature, and composition ranges, which must be defined for each model. The models are of widely ranging computational complexity. The selection of a particular model is dependent on the needs and objectives of the individual user. However, on the basis of the accuracy of the calculated density of a commercial LNG mixture, each of the models appears to be equally acceptable.

One final comment about accuracy should be emphasized. No mathematical model of the equation of state can be more accurate than the experimental data to which it has been fit. Therefore, all of the accuracy claims are dependent upon the accuracy of the experimental data from this study, which were used almost exclusively to optimize and test the models.

### 3. LNG Density Research at Other Laboratories

Due to the widespread interest in reliable data and the prediction of properties of multicomponent liquefied natural gas mixtures, in particular saturated liquid (bubble point) densities, a number of independent research programs were conducted from which a significant amount of density results have been published in the open literature. These include the studies at Gaz de France\* (Morlet [36]), Air Products and Chemicals, Inc.\* (Klosek and McKinley [32]), Institute of Gas Technology (Gonzalez, et al. [37,38], Huebler, et al. [39]), University of Kansas (Huang, et al. [40], Jensen and Kurata [41]), University of Oklahoma (Shana'a and Canfield [19]), Shell Research, Ltd.\* (Boyle and Reece [42], McClune [23]), University of Wyoming (Miller, et al. [28,43-46]), and Societe Nationale Elf Aquitaine\* (Roche, et al. [47,48], Orrit and Laupretre [24,49], and Orrit [50]). There is considerable variation in the precision and accuracy of measurement and in the completeness of the data published from these studies. Therefore, the contributions of these programs to the precise knowledge of the density behavior of LNG mixtures are also quite variable.

From comparisons with these independent results, it appears that the data from the University of Wyoming are the most precise and are uniformly consistent

---

\* Certain companies are identified in this paper for the purpose of clarity only. Such identification does not imply any type of endorsement by the National Bureau of Standards.

with the results of the NBS program. Direct comparisons of measurement precision were also made between the NBS densimeter and the Wyoming apparatus. Measurements were made at the University of Wyoming on one binary mixture and four multicomponent mixtures, prepared at NBS, with the apparatus calibrated with pure methane densities determined with the NBS densimeter [46]. Densities for the binary mixture and three of the multicomponent mixtures were also measured with the NBS densimeter. Comparisons were made through the extended corresponding states model when measured temperatures were not exactly the same. The maximum difference found was 0.10 percent for one multicomponent mixture point; the remaining differences were less than 0.03 percent and random. Though the Wyoming program was carefully planned, measurements for some of the important binary mixtures (e.g., nitrogen + ethane, nitrogen + propane, ethane + propane, etc.) were not included, and the accuracy of the molar volume results (though not that of derived excess volumes) depends directly on the accuracy of the density data of the low temperature liquid used to calibrate the apparatus.

The most extensive experimental measurements are those from the Elf Aquitaine program. Their precision of measurement does not appear to be quite as good as the measurements of the University of Wyoming, and there is a systematic bias of about -0.1 percent in a sample of multicomponent mixtures data [49] compared to the extended corresponding states model optimized to the NBS results. Though not all of the important binary mixtures were included in their study, it is notable that measurements were made on a nearly equimolar mixture of ethane + propane [50]. Excess volumes derived from these data and their pure fluid data between 105 and 140 K are in excellent agreement with those of the NBS program. Most of their  $V^E$  values are between -0.01 and -0.04 cm<sup>3</sup>/mol compared to -0.03 to -0.05 cm<sup>3</sup>/mol for a comparable mixture from the present study and about -0.49 cm<sup>3</sup>/mol from the University of Oklahoma data at 108.15 K for a mixture containing 58.52 mole percent ethane.

With the exception of this large discrepancy in the University of Oklahoma data for the ethane + propane mixture, the remainder of the data from the University of Oklahoma, as well as those from Shell Research, Ltd., are of comparable precision as those from the University of Wyoming and from Elf Aquitaine. From the Shell Research, Ltd. program, only the pure component density data have been published. None of the remaining programs have provided data approaching the precision and accuracy goals desired for custody transfer.

The programs of Elf Aquitaine and Shell Research, Ltd. provide the only low temperature experimental densities for pure isopentane and normal pentane, and these data sets are in good agreement, i.e., within about 0.1 percent. With the small concentrations of pentanes normally encountered in LNG mixtures, and the fact that the densities from these investigations are generally within about 0.1 percent of the NBS values for the lower molar mass alkanes, it was felt that additional measurements on the pure pentanes were unnecessary. In the NBS program, the pentanes were included only in multicomponent mixtures, with compositions much like LNG mixtures that would be encountered in practice. These measurements were made to provide proof that the mathematical models developed could properly account for the presence of pentanes.

Compared to the LNG research programs noted above, the NBS program is unique in that a single set of data is provided of uniformly high precision and accuracy for all of the pure components (i.e., nitrogen and the lower mass alkanes through the butanes), all the possible binary combinations where liquid phase separation does not occur, the important ternary combinations, and multicomponent mixtures that contain the highest probable amounts of nitrogen, butanes, and pentanes. The measurement method employed is a sophisticated state-of-the-art method for which a detailed analysis of the measurement uncertainties have been made and published, and statistical control of the experiments was assured throughout the program by repeating measurements of the density of liquid methane with each experimental run. The mathematical models optimized to the data are representative of existing theoretical and empirical models in wide use, from the most simple to the most complex. The concurrent experimental and mathematical modeling efforts also served to guarantee that sufficient data were obtained to optimize and to identify the inherent limitations of each.

#### 4. Acknowledgments

The contributions of the members of the LNG Density Project Steering Committee are gratefully acknowledged. The Steering Committee, comprised of representatives from each of the sponsoring companies, met quarterly from May 11, 1972 to February 15, 1979. The critique of research progress and numerous suggestions offered by the members were extremely valuable. Special thanks are due Martin R. Cines of the Phillips Petroleum Company who served as Chairman of the LNG Density Project Steering Committee during that time, and who played a major role in obtaining sponsors for this project. Thanks are also due Louis A.

Sarkes of the American Gas Association for his general support of LNG properties research and for his contributions to this project. The AGA coordinated the funding from the sponsoring companies for this project. L. James Kemp of Southern California Gas Company assumed Chairmanship of the Steering Committee following the retirement of Martin R. Cines from Phillips Petroleum Company. The authors would like to express their appreciation to Karen A. Bowie and Lawrence G. Liberman for their assistance in the preparation of the manuscript.

## 5. References

- [1] Haynes, W. M.; Hiza, M. J.; McCarty, R. D. Densities of LNG for custody transfer. Proceedings of Fifth International Conference on LNG, Vol. 2; 1977 August 29-September 1; Dusseldorf, Germany. Chicago, Ill.: Institute of Gas Technology; Section III, Paper 11. 36 p.
- [2] Haynes, W. M.; McCarty, R. D. The density of liquefied natural gas. Proceeding of the Fifty-Eighth Annual (GPA) Convention of the Gas Processors Association; 1979 March 19-21; Denver, Colo.: Gas Processors Association, Tulsa, Okla. 10-16.
- [3] Diller, D. E. LNG density determination. Hydrocarbon Processing 56(4): 142-144; 1977 April.
- [4] McCarty, R. D. LNG densities for custody transfer. Proceedings of the Fifty-Sixth International School of Hydrocarbon Measurements; 1981 April 14-16; Norman, Okla. 515-517.
- [5] Haynes, W. M.; Hiza, M. J.; Frederick, N. V. Magnetic suspension densimeter for measurements on fluids of cryogenic interest. Rev. Sci. Instrum. 47(10): 1237-1250; 1976 October.
- [6] Haynes, W. M. Apparatus for density and dielectric constant measurements to 35 MPa on fluids of cryogenic interest. J. Res. Nat. Bur. Stand. (U.S.) 88(4): 241-252; 1983 July-August.
- [7] Frederick, N. V.; Haynes, W. M. Differential capacitance sensor as position detector for a magnetic suspension densimeter, Rev. Sci. Instrum. 50(9): 1154-1155; 1979 September.
- [8] Clark, A. F.; Haynes, W. M.; Deason, V. A.; Trapani, R. J.; Low temperature thermal expansion of barium ferrite. Cryogenics 16(5): 267-270; 1976 May.
- [9] Haynes, W. M. Simplified magnetic suspension densimeter for absolute density measurements. Rev. Sci. Instrum. 48(1): 39-41; 1977 January.
- [10] Haynes, W. M. Measurements of densities and dielectric constants of liquid propane from 90 to 300 K at pressures to 35 MPa. J. Chem. Thermodynamics 15(5): 419-424; 1983 May.
- [11] Haynes, W. M. Measurements of densities and dielectric constants of liquid isobutane from 120 to 300 K at pressures to 35 MPa. J. Chem. Eng. Data. to be published.
- [12] Haynes, W. M. Measurements of densities and dielectric constants of liquid normal butane from 140 to 300 K at pressures to 35 MPa. J. Chem. Thermodynamics 15(9): 801-805; 1983 September.

- [13] Haynes, W. M.; Hiza, M. J. Measurements of the orthobaric liquid densities of methane, ethane, propane, isobutane, and normal butane. *J. Chem. Thermodynamics* 9(2): 179-187; 1977 February.
- [14] Haynes, W. M.; Hiza, M. J. Orthobaric liquid densities of normal butane from 135 to 300 K as determined with a magnetic suspension densimeter. *Advances in Cryogenic Engineering*, Vol 21. K. D. Timmerhaus and D. H. Weitzel, ed. New York, NY: Plenum Press; 1976. 516-521.
- [15] Haynes, W. M. Measurements of the orthobaric liquid densities of argon (100-120 K) and ethylene (105-200 K). *Cryogenics* 18(10): 621-623; 1978 October.
- [16] Hiza, M. J.; Haynes, W. M.; Parrish, W. R. Orthobaric liquid densities and excess volumes for binary mixtures of low molar-mass alkanes and nitrogen between 105 and 140 K. *J. Chem. Thermodynamics* 9(9): 873-896; 1977 September.
- [17] Haynes, W. M. Orthobaric liquid densities and dielectric constants of (methane + 2-methylpropane) and (methane + n-butane) at low temperatures. *J. Chem. Thermodynamics* 15(10): 903-911; 1983 October.
- [18] Hiza, M. J.; Haynes, W. M. Liquid mixture excess volumes and total vapor pressures using a magnetic suspension densimeter with compositions determined by chromatographic analysis: methane plus ethane. *Advances in Cryogenic Engineering*, Vol 23. K. D. Timmerhaus, ed. New York, NY: Plenum Press; 1976. 594-601.
- [19] Shana'a, M. Y.; Canfield, F. B. Liquid density and excess volume of light hydrocarbon mixtures at -165°C. *Trans. Faraday Soc.* 64(549): 2281-2286; 1968 September.
- [20] Hiza, M. J.; Haynes, W. M. Orthobaric liquid densities and excess volumes for multicomponent mixtures of low molar-mass alkanes and nitrogen between 105 and 125 K. *J. Chem. Thermodynamics* 12(1): 1-10; 1980 January.
- [21] Haynes, W. M. Measurements of orthobaric-liquid densities of multicomponent mixtures of LNG components ( $N_2$ ,  $CH_4$ ,  $C_2H_6$ ,  $C_3H_8$ ,  $CH_3CH(CH_3)CH_3$ ,  $C_4H_{10}$ ,  $CH_3Cn(CH_3)C_2H_5$ , and  $C_5H_{12}$ ) between 110 and 130 K. *J. Chem. Thermodynamics* 14(7): 603-612; 1982 July.
- [22] Haynes, W. M.; McCarty, R. D. Prediction of liquefied-natural-gas (LNG) densities from new experimental dielectric constant data. *Cryogenics* 23(8): 421-426; 1983 August.

- [23] McClune, C. R. Measurement of the densities of liquefied hydrocarbons from -100 to -180°C (173 to 93 K). *Cryogenics* 16(5): 289-295; 1976 May.
- [24] Orrit, J.; Laupretre, J. M. Density of liquefied natural gas constituents. *Advances in Cryogenic Engineering*, Vol. 23. K. D. Timmerhaus, ed. New York, NY: Plenum Press; 1978. 573-579.
- [25] Hiza, M. J. An empirical excess volume model for estimating liquefied natural gas densities. *Fluid Phase Equilibria* 2(2): 27-38; 1978 August.
- [26] Rowlinson, J. S.; Watson, I. D. The prediction of the thermodynamic properties of fluids and fluid mixtures - I. The principle of corresponding states and its extensions. *Chem. Eng. Sci.* 24(10): 1565-1574; 1969 October.
- [27] Mollerup, J.; Rowlinson, J. S. The prediction of the densities of liquefied natural gas and of lower molecular weight hydrocarbons. *Chem. Eng. Sci.* 29(6): 1373-1382; 1974 June.
- [28] Rodosevich, J. B.; Miller, R. C. Calculation of LNG excess volumes by a modified hard-sphere model. *Advances in Cryogenic Engineering*, Vol. 19. K. D. Timmerhaus, ed. New York, NY: Plenum Press; 1974. 339-345.
- [29] Renon, H.; Eckert, C. A.; Prausnitz, J. M. Molecular thermodynamics of simple liquids. *Ind. Eng. Chem. Fundam.* 6(1): 52-58; 1967 February.
- [30] Eckert, C. A.; Renon, H.; Prausnitz, J. M. Molecular thermodynamics of simple liquids. *Ind. Eng. Chem. Fundam.* 6(1): 58-67; 1967 February.
- [31] Albright, M. A. A model for the precise calculation of liquefied natural gas densities. NGPA Tech. Pub. TP-3. 1973.
- [32] Klosek, J.; McKinley, C. Densities of liquefied natural gas and of low molecular weight hydrocarbons. White, J. W.; Neumann, A. E. S., ed. *Proceeding of the First International Conference on LNG*; 1968 April 7-12; Chicago, Ill. Chicago, Ill.: Institute of Gas Technology; Session 5, Paper 22. 15 p.
- [33] McCarty, R. D. A comparison of mathematical models for the prediction of LNG densities. *Nat. Bur. Stand. (U.S.) NBSIR* 77-867; 1977 October. 60 p.
- [34] McCarty, R. D. Four mathematical models for the prediction of LNG densities. *Nat. Bur. Stand. (U.S.) Tech. note* 1030; 1980 December. 76 p.
- [35] McCarty, R. D. Mathematical models for the prediction of liquefied-natural-gas densities. *J. Chem. Thermodynamics* 14(9): 837-854; 1982 September.

- [36] Morlet, J. The density and miscibility of liquefied hydrocarbon gases at low temperatures. *Rev. Inst. Francais Petrole* 18: 127-143; 1963 January.
- [37] Gonzalez, M. H.; Subramanian, T. K.; Kao, R. L.; Lee, A. L. Physical properties of natural gases at cryogenic conditions. White, J.W.; Neumann, A. E. S., ed. *Proceedings of the First International Conference on LNG*; 1968 April 7-12; Chicago, Ill. Chicago, Ill.: Institute of Gas Technology; Session 5, Paper 21. 38 p.
- [38] Gonzalez, M. H.; Lee, A. L. Dew and bubble points of simulated natural gases. *J. Chem. Eng. Data* 13(2): 172-176; 1968 April.
- [39] Huebler, J.; Eakin, B. E.; Lee, A. L. Physical properties of natural gas at cryogenic conditions. *Proceedings of the Second International Conference on LNG, Vol. I*; 1970 October 19-23; Paris, France. Chicago, Ill.: Institute of Gas Technology; Session 2, Paper 9. 10 p.
- [40] Huang, E. T. S.; Swift, G. W.; Kurata, F. Viscosities and densities of methane-propane mixtures at low temperatures and high pressures. *AIChE J.* 13(5): 846-850; 1967 September.
- [41] Jensen, R. H.; Kurata, F. Density of liquefied natural gas. *J. Petrol. Tech.* 21: 683-691; 1969 June.
- [42] Boyle, G. J.; Reece, D. Bulk measurement of LNG. *Proceedings of the Second International Conference on LNG, Vol. I*; 1970 October 19-23; Paris, France. Chicago, Ill.: Institute of Gas Technology; Session 2, Paper 5. 14 p.
- [43] Rodosevich, J. B.; Miller, R. C. Experimental liquid mixture densities for testing and improving correlations for liquefied natural gas. *AIChE J.* 19(4): 729-735; 1973 July.
- [44] Miller, R. C. Estimating the densities of natural gas mixtures. *Chem. Eng.* 81(23): 134-135; 1974 October.
- [45] Pan, W. P.; Mady, M. H.; Miller, R. C. Dielectric constants and Clausius-Mossotti functions for simple liquid mixtures: systems containing nitrogen, argon and light hydrocarbons. *AIChE J.* 21(2): 283-289; 1975 March.
- [46] Miller, R. C.; Hiza, M. J. Experimental molar volumes for some LNG-related saturated liquid mixtures. *Fluid Phase Equilibria* 2(1): 49-57; 1978 August.

- [47] Rocne, Y.; Perret, J.; Bochirol, L. Density of LNG and of its constituents. Proceedings of the Second International Conference on LNG, Vol. I; 1970 October 19-23; Paris, France. Chicago, Ill.: Institute of Gas Technology; Session 2, Paper 8. 8 p.
- [48] Roche, Y.; Perret, J.; Bochirol, L.; Brauns, P. Density of LNG and of its constituents. White, J. W., ed. Proceedings of the Third International Conference on LNG; 1972 September 24-28; Washington, D.C. Chicago, Ill.: Institute of Gas Technology; Session II, Paper 13. 11 p.
- [49] Orrit, J.; Laupretre, J. M. A calculational method for obtaining the density of a liquefied natural gas. Advances in Cryogenic Engineering, Vol. 23. K. D. Timmerhaus, ed. New York, NY: Plenum Press; 1978. 566-579.
- [50] Orrit, J. E. Densities of liquefied natural gas components mixtures. (submitted to Fluid Phase Equilibria) 1983 January.



## 6.1 Reference [5]

**Magnetic suspension densimeter for measurements on fluids of cryogenic interest\***

W. M. Haynes, M. J. Hiza, and N. V. Frederick

*National Bureau of Standards, Institute for Basic Standards, Cryogenics Division, Boulder, Colorado 80302*

(Received 24 June 1976)

An apparatus incorporating a magnetic suspension technique has been developed for density measurements on liquids and liquid mixtures, particularly at saturation, at temperatures between 90 and 300 K and at pressures to 5 MPa (approximately 50 atm). The feasibility of adapting this method, previously used at room temperature, for low temperature use had been demonstrated in an earlier study with a density measurement on saturated liquid nitrogen near its normal boiling point. The present apparatus, which is significantly improved, and in most respects different from the earlier model, is described in detail. It includes a cryostat for continuous wide-range temperature control, a windowed equilibrium cell particularly suited for studies of liquid mixtures, and a new electronic servocircuit with a linear differential transformer for position control of the magnetic buoy. Extensive tests and density measurements have been carried out to evaluate the performance of this apparatus. Densities of saturated liquid nitrogen between 95 and 120 K and saturated liquid methane between 105 and 160 K are reported. The estimated standard deviation of a single density measurement is less than 0.02%. The total systematic error in the measurement process from known sources is approximately 0.05%. The total uncertainty of a single density measurement, which is taken as three times the standard deviation plus the systematic error, is approximately 0.1%. Comprehensive comparisons of the present results with previous experimental data are presented.

**1. INTRODUCTION**

With the advent of large-scale liquefaction and global transport of natural gas, accurate equilibrium liquid-phase densities have become important for custody transfer. The density data for liquefied natural gas mixtures and their components have been generally characterized by the existence of large discrepancies (approximately 0.5%) between different sets of data for the pure components and by a limited amount of mixture data. Hence, an apparatus has been developed to provide accurate, consistent, and comprehensive density data for liquefied natural gas mixtures and their predominant pure components at saturation conditions. These measurements will serve as a data base for testing and optimizing selected mathematical models (correlations) useful in predicting the densities of liquefied natural gas. In the present paper the apparatus and experimental procedures are described in detail and representative measurements for two components of liquefied natural gas are presented.

A magnetic suspension densimeter, which is based on an application of Archimedes' principle, has been selected for the present measurements primarily because this instrument is suitable for an independent, direct determination of the density of a saturated liquid over wide ranges of temperature and pressure within the precision and accuracy required for anticipated technical applications. In an earlier study,<sup>1</sup> the

feasibility of adapting the magnetic suspension technique for density measurements at low temperature was demonstrated with a measurement on saturated liquid nitrogen near its normal boiling point. The present apparatus (see Fig. 1 for a scaled assembly drawing), which is a much improved version of the earlier model, incorporates a three-coil support system,<sup>2</sup> a cryostat for temperature control at any temperature between 90 and 300 K, a windowed equilibrium cell suitable for projected studies on liquid mixtures at pressures to 5 MPa, and a new electronic servocircuit with a linear differential transformer that serves as a position sensor for a barium ferrite magnetic buoy.

The present work has included an extensive evaluation of the use of a magnetic suspension densimeter for absolute density measurements. (Here the term "absolute density" is used to indicate that cryogenic fluids were not used to calibrate the instrument.) Results of performance tests along with densities for saturated liquid nitrogen between 95 and 120 K and saturated liquid methane between 105 and 160 K are presented in this paper to demonstrate the low temperature performance of this new apparatus. The estimated standard deviation of a single density measurement is less than 0.02%. The total uncertainty of a single measurement, which is taken as the sum of the systematic error and three times the standard deviation, is approximately 0.1%.

In Sec. II the general principles of a magnetic

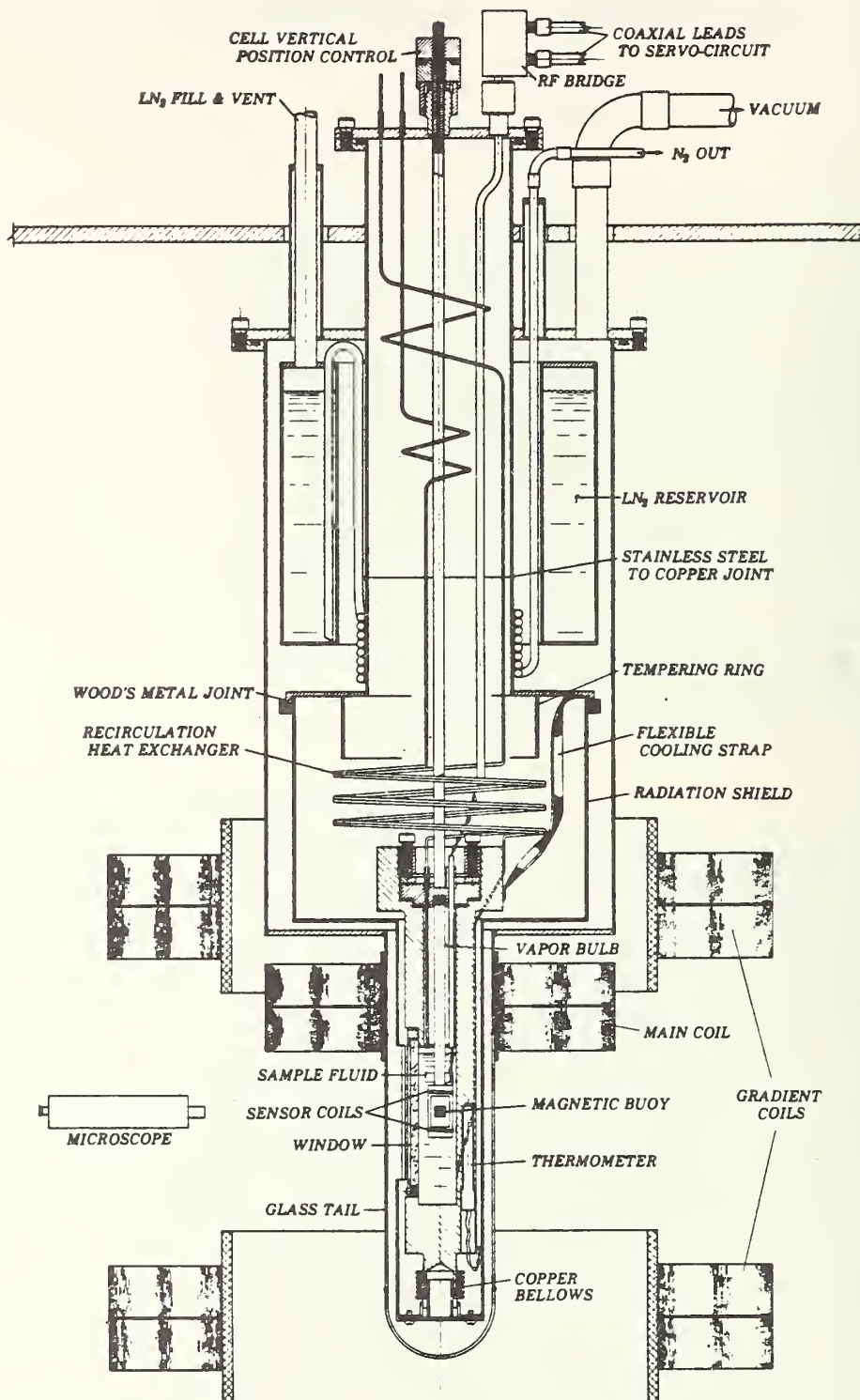


FIG. 1. Assembly drawing (approximately to scale) of a magnetic suspension densimeter for cryogenic fluids.

suspension densimeter are outlined. Section III is devoted to a detailed description of the experimental apparatus. A comprehensive discussion of the experi-

mental procedures and measurements is given in Sec. IV. In Sec. V a summary of performance tests carried out in evaluating the instrument is presented. This sec-

tion also deals with the uncertainties in the density measurements. Finally, the experimental data for saturated liquid nitrogen and methane, along with comparisons with independent measurements, are reported in Sec. VI.

## II. PRINCIPLES OF OPERATION

A piece of magnetic material is magnetically suspended in a fluid at a stable equilibrium position through the use of a closed-loop servosystem. When the float (or buoy) is in free support, there are three forces acting on it. In the present system the magnetic float is more dense than the fluid in which it is suspended; thus, an upward magnetic force is added to the buoyancy force to balance the downward gravitational force.

In the present work a three-coil (air-core) system<sup>2</sup> is used to supply the magnetic force. The three coils are aligned coaxially. Each coil is symmetric about an axis in common with the cylindrical axis of the magnetic buoy. The three coils consist of a main coil, which supplies the major part of the field necessary to lift the float, and a pair of gradient coils. The horizontal position of the float, which is in the shape of a right circular cylinder (length/diameter > 1) magnetized along its cylindrical axis, is maintained by the axially symmetrical, diverging field of the main coil. The magnetic force on the ferromagnetic buoy is given by

$$F_{\text{mag}} = M \frac{dH}{dZ}, \quad (1)$$

where  $M$  is the total magnetic moment of the buoy and  $dH/dZ$  is the variation of the external field intensity along the common cylindrical axis of the coils. For the present system the float is a permanent magnet for which the total magnetic moment (excluding temperature dependence) can be represented by

$$M = M_0 + M_I(H), \quad (2)$$

where  $M_0$  is the permanent moment, and  $M_I(H)$  is the induced moment resulting from an applied field.

At a fixed position along the cylindrical axis of an air-core solenoid,

$$H = kI \quad (3)$$

and

$$\frac{dH}{dZ} = k'I, \quad (4)$$

where  $I$  is the solenoid current and  $k$  and  $k'$  are constants dependent upon the number of turns and dimensions of the coil.

As mentioned earlier, the float is supported at a position relative to the main coil such that its horizontal position is fixed. This results in the float being supported at a distance below the main coil slightly larger than the inside radius of this coil. The float is sup-

ported approximately midway between the gradient coils. These coils are connected in series such that their magnetic field intensity contributions cancel at the float position. (For a Helmholtz coil arrangement the magnetic fields would add at the midpoint.) Thus, the magnetic field intensity at the float position is due solely to the main coil contribution. Similarly, the magnetic field gradients of the gradient coils add at the float position.

For this three-coil arrangement and with a constant main coil current ( $I_M$ ) (and subsequently the magnetic moment of the float does not change), the density of the fluid ( $\rho$ ) is related to the gradient coil current ( $I_G$ ) by the following relation:

$$\rho = A + BI_G, \quad (5)$$

where  $A$  and  $B$  are constants to be determined by calibration with fluids of known density. This relationship is valid whether the float is magnetically hard or soft. Knowledge of the mass and volume of the float is not required to obtain relative density results using Eq. (5). However, since the magnetic moment of the float is temperature dependent, the constants  $A$  and  $B$  would have to be determined at each temperature of interest.

At low temperatures at least two fluids of known density, one of which may be "vacuum," are needed for calibrating the instrument for use in performing relative density measurements. However, the densities of low temperature fluids are not known to sufficient accuracy to permit them to be used as calibration fluids and, in fact, this had been one of the major motivations for developing an independent technique for density measurements on cryogenic fluids.

In the previous work by Haynes and Stewart,<sup>1</sup> a new method was demonstrated for determining absolute densities using the same three-coil arrangement, but which is dependent upon the magnetic properties of the buoy material. If one uses a permanent magnetic material for the float and its induced moment is zero or, at least, very small compared to the permanent moment, then the magnetic force on the float is given by the relation.

$$F_{\text{mag}} = C'I_M + D'I_G, \quad (6)$$

where  $C'$  and  $D'$  are constants depending on the relative position of the coils and float, the magnetic moment of the float, and the dimensions and number of turns of the support coils. One should note that for Eq. (6) the main coil current ( $I_M$ ) is not held constant. Now the density of the fluid is given by the expression.

$$\rho = (m - CI_M - DI_G)/V, \quad (7)$$

where  $m$  and  $V$  are the mass and volume of the float. The acceleration of gravity has been included in the constants  $C$  and  $D$ . (The mass and volume of the float must be determined by independent measurements.) The validity of this equation can be tested experimentally. For measurements in a vacuum, Eq. (7) reduces to the following relation:

$$m = CI_M + DI_G \quad (8)$$

It should be emphasized that the critical assumption in deriving Eq. (7) is that there is no induced moment in the buoy resulting from changes in the magnetic field intensity over the range of magnetic fields needed for the density measurements. (For the present measurements this includes fields between 0.006 and 0.016 T.)

The current in the gradient coils has been measured as a function of the current in the main coil while the float was suspended at a constant height in a given fluid, usually vacuum, at constant temperature. The currents were fitted by the method of least squares to either Eq. (6) or Eq. (8). The quality of this fit indicated the validity of the assumption concerning the dependence of the magnetic moment upon the magnetic field. (Results will be presented in a later section.) For the present measurements the main coil current, and thus the magnetic field, could be varied over a range amounting to 25% of its maximum value. The minimum ratio of  $I_M/I_G$  was determined by the loss of horizontal stability of the float.

From the above discussion it should be apparent that relative density measurements using Eq. (5) ( $I_M$  constant) can be carried out to complement the results of absolute measurements using Eq. (7) with the same three-coil arrangement. In performing measurements using Eq. (7) for which the main coil current is varied over a considerable range, it is experimentally difficult to fix or determine the position of the main coil from vacuum to liquid measurements within the desired precision. This problem does not arise when making relative density measurements for which the main coil current is held constant. In principle, both procedures should give identical density ratios for the same fluids at constant temperature. In practice, the relative density measurements can be carried out to deduce the systematic error in the absolute density measurements that depends on the magnitude of the main coil current. These tests have been performed in the present work and will be discussed in a later section.

### III. APPARATUS

#### A. General considerations and cryostat

An assembly drawing (approximately to scale) of the major components of the apparatus is shown in Fig. 1. The general dimensions and configuration of the cryostat and equilibrium cell were determined by the dimensions and configuration of the main coil and the two gradient coils. (See Table I for coil dimensions.)

Criteria considered essential, and which have been satisfied, in the design of the apparatus are as follows: (a) all materials of construction in close proximity to the magnetic suspension assembly are nonmagnetic; (b) the entire assembly is rigidly supported so that the relative position of the buoy, microscope, and support coils

TABLE I. Parameters of support coils.

	Main coil	Gradient coils
Length	6.0 cm	6.2 cm
Inside diameter	7.4 cm	25.4 cm
Outside diameter	20.24 cm	38.6 cm
Number of turns	5000	5000

can be maintained; (c) the magnetic buoy and the liquid level are visible within a windowed cell capable of withstanding working pressures up to 5 MPa; (d) the volume occupied by the liquid sample within the cell is sufficiently large to render the unavoidable vapor volume of the access tubing, etc., insignificant within the accuracy goals of experiments involving liquid mixtures; (e) temperature gradients along the length of the working space of the cell are monitored and reduced to a practical minimum, i.e., less than a total of 10 mK; (f) the rate of refrigeration of the equilibrium cell is adjustable and continuous; and (g) the temperature of the cell can be controlled at any temperature between 90 and 300 K.

A concrete block structure provides a stable support for the cryostat, the coils, and the microscope. The cryostat assembly is suspended from an aluminum plate that spans the top of the concrete structure. The stainless steel central support tube of the cryostat is attached to this aluminum plate with a brass collar (not shown in Fig. 1). The lower end of the stainless steel tube is soldered to a copper tube to which a heat exchanger is soldered.

Refrigeration is provided by continuous transfer of liquid nitrogen from the cryostat reservoir through the heat exchanger. Regulation of the refrigeration rate is accomplished by controlling the nitrogen vent rate to the atmosphere.

Refrigeration is supplied to the bottom of the equilibrium cell through the copper radiation shield and to the top of the cell through two copper braided straps. The radiation shield, which contains a slit aperture in a position corresponding to the cell window, is attached to a copper plate at the top of the shield with Wood's metal to facilitate removal of the shield and alignment of the shield within the glass tail section. The glass tail is connected to the stainless steel vacuum jacket through a stainless steel-to-glass transition joint.

#### B. Equilibrium cell

The equilibrium cell, made of electrolytic tough pitch copper, has an overall length of approximately 30 cm, including the copper-plated bellows at the bottom. The cell closure is a compression fitting with a silver-plated, solid copper O-ring. The closure plug, threaded backing ring, and compression screws are stainless steel. The top of the cell is held in alignment by a stainless steel tube, which is brazed to the closure plug and extends through the uppermost cryostat plate. The upper end of the cell support tube

is threaded through a nut and bearing assembly to allow small adjustments in the vertical position of the cell and thus the vertical position of the magnetic buoy. The bottom of the cell is thermally anchored to the radiation shield by mechanical attachment of a flanged bellows section. A thin coat of commercially available conducting grease is used to enhance thermal contact between the bellows flange and the shield. Two thermal links of copper braid are also mechanically attached to the top of the cell from the top plate of the radiation shield using thin coats of conducting grease between the contact surfaces.

The outside diameter of the main part of the cell is 4.13 cm and that of the closure section is 7.60 cm. The internal working space is 1.99 cm in diameter and approximately 20 cm long. More than half of the internal volume, however, is occupied by the magnetic buoy-sensor coils assembly ( $\sim 10 \text{ cm}^3$ ) and the vapor bulb ( $\sim 35 \text{ cm}^3$ ). The vapor bulb is a slip fit in the top section of the cell and is attached directly to the closure plug. The internal free volume of the cell is approximately  $20.5 \text{ cm}^3$ . Anticipating measurements on mixtures, the volume ( $\sim 0.3 \text{ cm}^3$ ) in the annulus between the vapor bulb and the cell wall has been made as small as possible, since this is normally part of the vapor volume.

The electrical lead-throughs for the sensor coils consist of three No. 32 coated copper wires encapsulated with an epoxy adhesive in a copper capillary tube. This tube extends through the closure plug to the bottom of the vapor bulb. The epoxy adhesive, an alumina-filled resin with elevated temperature curing agent, was selected based on an earlier study<sup>3</sup> of low temperature properties of epoxy adhesives. By pressurizing with helium gas while the adhesive was hot, the entire length of the capillary tube was filled with adhesive to minimize the available vapor volume in the equilibrium cell.

The cell window was designed to allow viewing the liquid sample from the base of the vapor bulb down to 2 cm from the bottom of the liquid space. The viewing slit is 0.6 cm wide  $\times$  7.5 cm long. The window consists of a piece of tempered Pyrex<sup>4</sup> glass of 0.32-cm thickness with semicircular ends and chamfered edges. The seal between the glass and the cell is made with indium wire compressed in a racetrack groove machined in a flat surface on the cell. The glass is compressed against the indium seal with a hardened beryllium copper plate secured by stainless steel screws. A rubber asbestos pad is placed between the beryllium copper plate and the glass to relieve thermal and mechanical strains. The maximum working pressure of the equilibrium cell is limited by the maximum working pressure of the window.

### C. Magnetic buoy

The buoy is a barium ferrite ( $\text{BaFe}_{12}\text{O}_{19}$ ) magnet in the shape of a right circular cylinder magnetized

along its cylindrical axis. Its length and diameter are approximately 0.64 and 0.51 cm, respectively.

Barium ferrite is a magnetically hard, ceramic material with a density of approximately  $5 \times 10^3 \text{ kg/m}^3$ . It is somewhat porous and has a high electrical resistivity. The buoy used in the present work has been permanently magnetized in a saturation field of 1 T. After initial cycling over maximum ranges of temperature (90–300 K) and magnetic field intensity ( $0\text{--}1.3 \times 10^4 \text{ A/m}$ ) the barium ferrite magnet exhibited no hysteresis over the ranges of currents and temperatures needed in the density measurements. The magnet is operating in a very small segment ( $5\text{--}13 \times 10^3 \text{ A/m}$ ) of a broad hysteresis loop. The slope of the  $B$ -vs- $H$  curve is small and constant. The change in the magnetic moment of the float with temperature varies from 0.2%/K at 300 K to 0.1%/K at 100 K, as determined from the present measurements in vacuum. This variation in the magnetic moment with temperature results in a random error in the density of approximately 0.002% at 100 K, increasing to 0.004% at 300 K. This estimate is based on a reproducibility in the temperature of 2 mK from vacuum to liquid measurements.

Since the barium ferrite magnet is porous, it must be coated with a material which does not allow fluid to penetrate into the buoy. Copper was found suitable for this purpose. After a piece of barium ferrite was ground into the shape of a right circular cylinder with chamfered edges (0.25 mm deep), a conducting layer of copper was uniformly plated onto the ceramic magnet by chemical reduction. On top of this conducting layer, copper was electroplated to a thickness of approximately 0.25–0.50 mm: a much thicker coating resulted at the edges. Then most of the copper was removed with a diamond tool until the copper-plated barium ferrite magnet was in the shape of a right circular cylinder without chamfered edges. The final buoy had a minimum of 0.06 mm of copper over the cylindrical surface and the end faces and at least 0.25 mm on the edges where the magnet had been chamfered. The edges were built up to a thicker coating since the plating strength would be weakest at these locations. (For density measurements it is not necessary that the plating be symmetric about the center of mass of the buoy.) Gold was flashed ( $10^{-3} \text{ mm}$ ) over the entire copper surface as a protective coating.

### D. Electromagnetic support coils

Each of the coils is composed of two separate coils of 2500 turns of epoxy-coated aluminum foil of approximately 0.025-mm thickness. The foil for the main coil has a width of 2.5 cm while that for the gradient coils is 3.0 cm. Selected coil parameters are given in Table I.

Each of the gradient coils is rigidly supported by three aluminum rods resting on the concrete structure. The gradient coils have a separation distance of approximately 23 cm. No effort has been made to control the

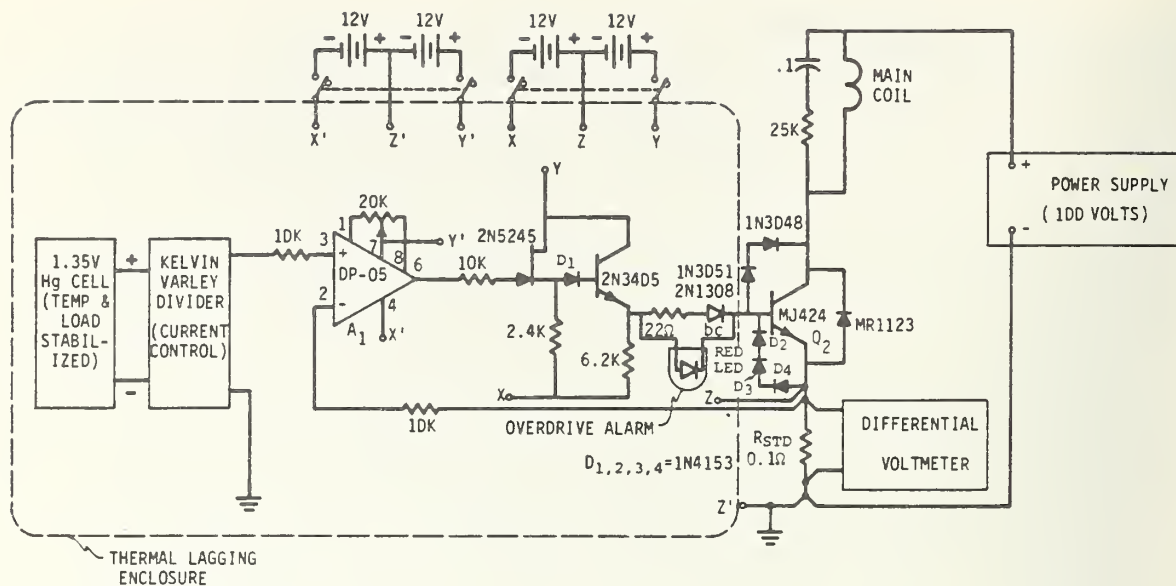


FIG. 2. Current control circuit for main coil.

position of the gradient coils except through the control of the laboratory temperature. The  $dH/dZ$  of the gradient coils changes very slowly ( $2.5 \times 10^{-4}/\text{cm}$ ) from a maximum at the float position. Since the change in  $dH/dZ$  with position for the main coil is two orders of magnitude larger than that for the gradient coils, special care has been taken to minimize changes in the position of the main coil.

First, the main coil is supported at its midplane so that thermal expansion effects inside the coil are minimized. A circular copper plate has been soldered to the brass tube on which the main coil is wound. A coil of aluminum foil (2500 turns) is clamped tightly to each side of the copper plate with a thin layer of vacuum grease between the aluminum foil and copper for maximum thermal contact. The copper plate (and thus the coil) is supported by quartz rods extending to the concrete structure. Thus, any changes in the position of the midplane of the coil due to room temperature changes would be negligible. Copper plates with cooling water have been placed on the outside faces of each section of the main coil such that the average temperature of the main coil is below room temperature for maximum current (1 A). However, for absolute density measurements, the temperature of the main coil changes from vacuum to liquid measurements (1.2 K for nitrogen at 100 K) since a larger current is required to support the float in vacuum than in the liquid for a given gradient coil current.

### E. Support system electronics

The current in the main coil, which contributes the major portion of the magnetic force necessary to lift the buoy, is provided by the circuit of Fig. 2. The circuit

functions as follows: The main coil current flows through a stable resistor  $R_{STD}$  ( $0.1 \Omega$ ) in the emitter of  $Q_2$  (the current-controlling transistor). The voltage developed across  $R_{STD}$  is compared with a reference voltage from a Kelvin-Varley voltage divider by amplifier  $A_1$ . The output of  $A_1$  drives the base of  $Q_2$  and controls the current through  $R_{STD}$  and the main coil. Since the loop gain of this circuit is exceedingly high ( $>10^6$ ) and the thermal drifts are very low, the long-term stability of the main coil current is of the order of 0.001%. This current controller has a temperature coefficient of the order of 5 ppm/K and a sensitivity to power supply variations of less than  $2 \times 10^{-6}$  A/V. A slow drift of the coil current of  $2.5 \times 10^{-6}$  A/h has negligible effect on the density measurements since the main coil current is measured each time that the gradient coil current is determined. (It should be noted that the precision and accuracy of the density results depend on the short-term stability and not the absolute accuracy of the standard resistor.)

The gradient coils are included in a control circuit (Figs. 3 and 4) that senses and maintains the vertical position of the buoy. The requirements for stability of a magnetic support or levitation system are discussed in detail in Refs. 5 and 6 and will not be repeated here. Suffice it to say that the characteristic equation for a magnetic levitation system has a root with a positive real part, and for system stability the plot of the frequency response of the characteristic equation (the Nyquist plot) must encircle the origin once in the counterclockwise sense. This is accomplished by the dual-lead network composed of  $R_1$ ,  $R_2$ ,  $C_1$ , and  $C_2$  in Fig. 4. A dual-lead network is required for this system since minimization of the steady state offset or buoy position change requires at least a first-order integrator



current control amplifier for the main-coil constant-current source is the same as that for the gradient coils.

Perhaps the most interesting part of the support system is the position sensor. In the past, position sensing has been accomplished by either optical<sup>7,8</sup> (light beam-photomultiplier tube arrangement) or electronic<sup>9-12</sup> (inductance pickup coil or differential transformer) means. The requirements of small size, low power dissipation, high sensitivity, the ability to withstand high pressure and low temperatures, and exceptional dimensional integrity resulted in the use of a linear differential transformer (LDT) wound on a machinable glass ceramic form. The LDT consists of a pair of coils equally spaced about a transverse rectangular opening in the ceramic form inside which the buoy is suspended. Each coil is wound with 34 turns of double silk-wrapped 50/44 Litz wire in circumferential grooves of 2.8-mm width and 6.1-mm depth. The outside diameter of the coils and the ceramic holder is 17.3 mm. The complete transformer assembly has been potted with a low-viscosity epoxy resin to prevent intrusion of the pressurized fluid into the windings.

The sensitivity of the LDT as measured at the phase-sensitive detector (synchronous detector) is of the order of 1 V/mm. The noise voltage at the sensor amplifier input is less than  $10^{-6}$  V/Hz<sup>1/2</sup>. The operational amplifiers in the compensation circuit have very low offset drifts and are thermally lagged to a large copper block in the amplifier chassis. Consequently, the vertical movement of the buoy due to operational amplifier drifts and rf amplifier noise is less than  $10^{-5}$  mm.

The LDT is the major component of a ratio-transformer-type bridge. Part of the bridge is located at the top of the cryostat and is connected to the LDT through long coaxial lines. The bridge is constructed so as to remove proximity effects of the outer conductors of the coaxial lines. The neutral position of the buoy is controlled by a small variable capacitor between the center lead and one side of the LDT. Conductance balance is achieved with a resistor connected across the capacitor. Unbalance in the LDT due to the inductance of the long leads is minimized by tuning the two halves of the LDT to resonance with matched capacitors (as large as possible for the 0.5-MHz exciting signal). These capacitors are connected near the LDT outside the sample cell but inside the vacuum space.

#### IV. EXPERIMENTAL MEASUREMENTS AND PROCEDURES

##### A. Temperature and pressure

The techniques and instrumentation for the measurement and control of the temperature and pressure are standard. The primary temperature sensor, calibrated on the IPTS 1968, is a platinum resistance thermometer secured in a well at the base of the equilibrium cell with Wood's metal. The calibration of the thermometer

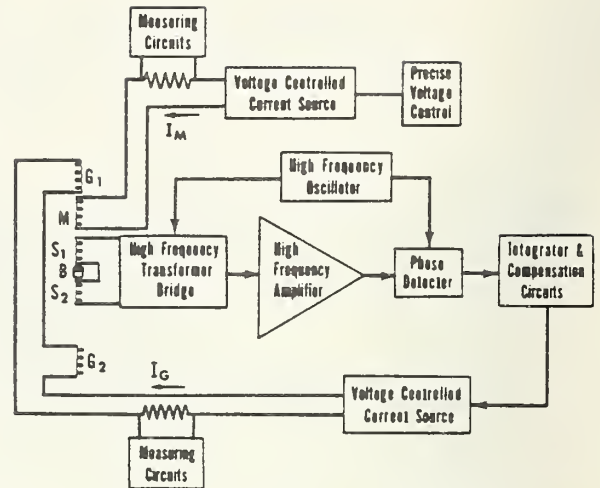


FIG. 5. Block diagram of a magnetic suspension densimeter:  $G_1$ ,  $G_2$ —gradient coils; M—main coil;  $S_1$ ,  $S_2$ —sensing coils; B—magnetic buoy.

has been checked against vapor pressure measurements on liquid methane and nitrogen.

The uncertainty of the calibration is approximately 0.002 K. Due to the specifications of the potentiometric measuring system, uncertainties in the temperature amount to a maximum of 0.010 K at 110 K, increasing to 0.030 K at 300 K. The temperature of the sample holder is controlled to better than 0.005 K, approximately the same as the reproducibility of the temperature measurements.

A current of 1 mA for the thermometer is supplied by an electronic constant current source. The voltage drop across a 100  $\Omega$  calibrated standard resistor in series with the thermometer is monitored continuously with a six-digit differential voltmeter. With this setup the uncertainty and repeatability of the current is approximately 0.002%. The voltmeter is checked periodically against a microvolt potentiometer using a calibrated standard cell.

The total uncertainty in the reported temperatures in Sec. VI is believed to be less than 0.03 K. (At room temperature it would be less than 0.04 K.) The 0.03-K total uncertainty consists of approximately 0.025-K systematic error and 0.005-K random error. The systematic error was determined from the uncertainties in the calibration of the thermometer and in the potentiometric measuring system.

The temperature of the cell is regulated by balancing coarsely variable cooling with precisely controlled electric heating. A control heater near the bottom of the cell is connected to a dc power regulator, which is part of a measuring/regulation system that also includes a six-dial microvolt potentiometer and a microvolt amplifier. A second heater at the top of the cell is connected to a manual power supply. Independent heaters at the top and bottom of the cell are used to minimize temperature gradients along the length of the cell.

Temperature gradients are detected by monitoring the vapor pressure of the liquid in the vapor bulb.

Pressures below 7 bars are measured with a 0- to 7-bar spiral quartz Bourdon gauge. This gauge has a resolution of less than  $3.5 \times 10^{-4}$  bar. It has been calibrated against an air dead-weight gauge giving an uncertainty of approximately 0.1% over the full range. For pressures above 7 bars, a double-revolution 0- to 20-bar Bourdon gauge is used. It has also been calibrated against the air dead-weight gauge and can be read to the nearest 0.005 bar.

Vapor pressure measurements have been used in the present work primarily as a means of monitoring temperature gradients. They have also been used as a check against the calibration of the platinum resistance thermometer. In general, the vapor pressures for methane have been consistently lower than those of Prydz and Goodwin.<sup>13</sup> This pressure difference corresponds to a temperature difference of 0.01–0.02 K. The discrepancies between the nitrogen vapor pressures of the present work and those of Wagner<sup>14</sup> correspond to an average temperature difference of less than 0.015 K, with no particular trend observed.

## B. Position of buoy

The accuracy and precision of the density measurements depend on being able to suspend the float at the same position relative to the support coils in vacuum and in the test liquid at the same temperature. A 125 $\times$  filar micrometer microscope is used to determine the position of the float. It has a resolution of approximately  $5 \times 10^{-4}$  mm. The maximum error in the position determination is  $2 \times 10^{-3}$  mm, which corresponds to an error in density of less than 0.03%.

This error includes approximately equal contributions from the alignment of the microscope, so that the "apparent" position of the float is independent of the index of refraction of the fluid inside the sample cell, and from the repositioning of the float for vacuum and liquid measurements. The first contribution would be a systematic error while the second is random. The precision of the density measurements depends primarily on the reproducibility of the position of the buoy from vacuum to liquid measurements.

As mentioned above, the microscope must be aligned so that the "apparent" position of the float does not depend on the index of refraction of the fluid inside the sample cell. In viewing the float inside the cell one must look through the glass tail of the cryostat and the sample holder window. The "apparent" position of the float would be dependent on the refractive index of the fluid inside the cell unless the light rays are perpendicular to the interface between the test liquid and the inside surface of the sample holder window.

The procedure for adjusting or aligning the microscope is as follows. First, the float is positioned at rest on the ceramic holder at the same horizontal position as when in support. Then a fiducial mark on the

float is observed under two experimental conditions, i.e., with the float first immersed in gas and then immersed in liquid. Both methane and nitrogen were used to carry out this procedure. During this procedure the microscope tilt is adjusted so that the "apparent" position of the float does not depend on the refractive index of the fluid inside the cell within the resolution of the microscope. The temperature of the cell is controlled to better than 0.01 K during these observations. Care is taken to ascertain that the float is observed through the same parts of the windows as during the density measurements. Necessarily a different part of the float is observed. This presents no special problem since there are diamond tool marks the entire length of the float that can be used as reference lines. This procedure has been repeated frequently during the course of the reported measurements. It has been found that a readjustment of the microscope tilt is necessary only if the apparatus is perturbed by disassembly.

## C. Volume of buoy

Absolute density measurements [Eq. (7)] with a magnetic suspension densimeter require a determination of the volume of the magnetic buoy. In the past this has been accomplished either by using distilled water as a reference fluid of known density<sup>15</sup> or by making direct length and diameter measurements on a uniformly constructed float.<sup>1</sup> Here the volume has been determined by the first method.

The volume ( $0.13485 \text{ cm}^3$  at 300 K) of the magnetic buoy was determined within 0.02%. The distilled water was vacuum distilled to remove air. Any problems with bubbles inside the cell were rectified by pressurizing the water with helium gas. The volume of the buoy has been measured three times at 300 K and once at 290 K. These four measurements gave a standard deviation of 0.005% using thermal expansion data for barium ferrite to calculate the volume change from 290 to 300 K. This resulted in a 99% confidence interval of  $\pm 0.015\%$ . The systematic error in the volume determination depends on the uncertainty in the density of water. This should be less than 0.005%.<sup>16</sup>

The present paper reports density data for cryogenic fluids. Thermal expansion data for barium ferrite were used to calculate the volume of the float at low temperatures. Recently the linear thermal expansion of polycrystalline barium ferrite was measured at this laboratory at temperatures from 76 to 293 K with a quartz tube dilatometer.<sup>17</sup> The volume of the float at 100 K is approximately 0.4% less than the room temperature value.

Barium ferrite is somewhat anisotropic and its thermal expansion was measured both parallel and perpendicular to the magnetization direction. An anisotropy of 15–20% was observed. The estimated overall uncertainty of the thermal expansion measurements would correspond to an error of 6% in the adjustment to the volume. This would produce an uncertainty of approximately

0.02% in the volume at 120 K. The uncertainty in the adjustment to the volume due to the contraction of the copper plating is negligible.

The effect of pressure on the volume of the float is negligible at the highest pressures encountered in the present work. The bulk modulus for barium ferrite should be less than that for copper, which is  $1.35 \times 10^{11}$  Pa.<sup>18</sup> This value would correspond to a volume correction of approximately 0.001% at 2.5 MPa, the vapor pressure of nitrogen at 120 K.

#### D. Mass of buoy

The mass of the magnetic buoy was determined with a 10-g capacity equal-arm microbalance. A calibrated class M weight set was used in the weighings. Precautions were taken to assure that the copper plating and gold protective coating provided an impervious barrier to liquids under pressure. The buoy was rapidly cycled between room temperature and 76 K. It was then immersed in liquid ethanol at 5-atm pressure and room temperature for 4 h. The buoy was weighed twice after removal from the ethanol bath. The average of these weighings was 9  $\mu\text{g}$  higher than the mean of the initial four weighings. A significantly larger increase in the mass was expected if the plating on the float contained a pinhole that allowed ethanol to penetrate into the porous ceramic. Thus, at room temperature, the metallic coating appeared to be impervious after thermal cycling. The reproducibility of liquid methane density measurements (see experimental results) after many cycles between room temperature and 100–140 K is further evidence of the resistance of the metallic coatings to damage from thermal cycling.

The final mass of the magnetic buoy (0.73706 g) was taken as the mean of all weighings, including the weighings after immersion in ethanol, corrected for air buoyancy. A 99% confidence interval for the six weighings, based on a standard deviation of 6  $\mu\text{g}$ , was  $\pm 10$   $\mu\text{g}$ . The systematic error in the mass determination, resulting primarily from the weight set calibration, is believed to be less than 5  $\mu\text{g}$ .

### V. EVALUATION OF PERFORMANCE OF MAGNETIC SUSPENSION DENSIMETER

#### A. Performance tests

The use of Eq. (7) for obtaining absolute densities has again been verified experimentally<sup>1</sup>. The gradient coil current has been measured as a function of the main coil current over a range of approximately 20% of the maximum main coil current. These measurements were carried out while supporting the float in a given fluid (including vacuum) at constant height at a fixed temperature. The various pairs of  $I_M$  and  $I_G$  were fitted by the method of least squares to Eq. (7). The residual standard deviation, with the gradient coil current as the dependent variable, was less than  $10^{-5}$  A. Examination of the residuals showed that they were

random and well approximated by a normal probability distribution. These results demonstrated that within the precision of the current measurements the magnetic moment of the barium ferrite float is independent of the magnetic field intensity over the range of fields (0.006–0.016 T) considered in the present work.

Other coil configurations have been tried that gave results that substantiated the observations given above. First the bottom gradient coil was disconnected resulting in a two-coil system. The values of the constant ( $C$ ) in Eq. (7) for the two- and three-coil arrangements under otherwise identical experimental conditions were in agreement within the experimental uncertainty. In other words, the magnetic moment of the float (contained in  $C$ ) remains constant for significantly different magnetic field intensities.

Next the pair of approximately identical (gradient) coils were connected to the constant current source in a Helmholtz arrangement. The main coil was connected into the servosystem. The float was first supported at a constant height at fixed temperature by the force supplied by only the main coil. The float was located at the midpoint of the Helmholtz coils while the current in the Helmholtz coils was increased to 0.6 A. There was an insignificant change in the main coil current ( $10^{-4}$  A) for this relatively enormous change in the magnetic field intensity (about an order of magnitude more than for the typical data point). The results of these tests demonstrated that this technique could be used for absolute density measurements.

In carrying out density measurements with this technique, the position of the main coil must remain fixed over a wide range of currents for the vacuum and liquid measurements. This means that the "constant"  $k'$  in Eq. (4) and the constants  $C$  and  $D$ , in Eq. (7) must be independent of the current in the coil. It was hoped that the measures exercised in controlling the temperature and position of the main coil (see Sec. III D) would result in such behavior. It was experimentally impracticable to determine if  $k'$  was a constant by monitoring the position of the coil. However, the effect of a change in the current in the main coil on the density measurements could be obtained in another manner. As shown in Sec. II the fluid density is linearly proportional to the current in the gradient coils if the main coil current is held constant. Not only is the position of the main coil fixed, but also the magnetic field intensity at the midpoint of the gradient coils (float position) is constant. Relative measurements [Eq. (5)] carried out with vacuum, nitrogen, methane, and propane at 110 K were not consistent with the density ratios computed from absolute measurements [Eq. (7)] for the same fluids. These results showed that the "constants" ( $k'$ ,  $C$ , and  $D$ ) vary slightly with the main coil current. This variation produces a density error relative to the difference between main coil currents for vacuum and liquid measurements (constant  $I_G$ ) of approximately 1.4%/A. This corresponds to a density adjustment of 0.1–0.2%/(g/cm<sup>3</sup>) to the results from Eq.

TABLE II. Estimated uncertainties in density measurements.

Systematic errors	Percent error in density					
	Methane		Nitrogen		Normal butane	
	105 K	160 K	95 K	120 K	135 K	300 K
Mass of float (Sec. IV D)	±0.002	±0.002	±0.002	±0.002	±0.002	±0.002
Volume of float at 300 K (Sec. IV C)	±0.02	±0.02	±0.02	±0.02	±0.02	±0.02
Thermal expansion coefficient of barium ferrite (Sec. IV C)	±0.022	±0.017	±0.023	±0.021	±0.020	±0.001
Position of float (Sec. IV B)	±0.015	±0.018	±0.010	±0.012	±0.009	±0.009
Position of main coil, determined from relative measurements, Eq. (5) (Sec. V A)	±0.02	±0.02	±0.02	±0.02	±0.02	±0.02
Temperature of sample fluid (Sec. IV A)	±0.010	±0.021	±0.023	±0.076	±0.004	±0.008
Three times standard deviation	±0.045	±0.054	±0.030	±0.036	±0.027	±0.027
Total uncertainty <sup>a</sup>	±0.09	±0.10	±0.07	±0.12	±0.06	±0.06

<sup>a</sup> The total uncertainty was determined from the square root of the sum of the squares of the systematic errors added to three times the standard deviation.

(7). Since all measurements are based on the volume determination using distilled water as a reference fluid of known density, the adjustment must be applied relative to this point.

A further check on this density-dependent adjustment was accomplished by measuring the densities of two other fluids of known density at room temperature. The densities of liquid samples of normal pentane and ethanol were determined by the Mass and Volume Section of the Mechanics Division of the National Bureau of Standards in Washington, DC, to an estimated inaccuracy of less than 0.01%. Measurements on these fluids at 300 K with the present apparatus using Eq. (7), combined with the adjustment based on the relative density measurements at low temperature, gave densities that agreed with the reference values to better than 0.02%. Thus, the densities presented in this paper based on absolute measurements [Eq. (7)] have been adjusted slightly to be consistent with the results of

relative measurements [Eq. (5)]. The density difference between the relative and absolute measurements, expressed in terms of the difference in main coil currents between the vacuum and liquid points ( $I_v - I_l$ ) for a constant gradient coil current, is independent of temperature. The temperature dependence of the magnetic moment of the float must be included if the difference is expressed in terms of density.

The relative measurements were carried out using the same experimental setup and parameters (mass, volume, and position) as the absolute measurements. Thus the total uncertainty in the adjustment determination should only include the random error in the measurement process. Thus an estimated uncertainty of ±0.02% in the adjustment is based on the comparisons with the reference fluids since this density difference was larger than a 99% confidence interval from a fit of the differences between relative and absolute measurements.

## B. Error analysis

Evaluation of the experimental parameters involved in the present work showed that the uncertainty in the density measurements depends primarily on the uncertainties in the determination of the volume of the float, the relative position of the float and the main coil, and the temperature of the sample fluid. The precision of the density measurements is inversely proportional to the difference between the density of the fluid and the density of the float. This variation with density cannot be observed for the measurements reported in this paper because of the density range covered. The precision also varies with temperature, corresponding to the change in the magnetic moment of the float with temperature.

Table II summarizes the uncertainties in the density measurements for the nitrogen and methane results presented in this paper. Normal butane is also included in this table, primarily to show the performance of the instrument at higher temperatures. Normal butane densities, determined with this instrument at tempera-

TABLE III. Experimental results for saturated liquid nitrogen (molecular weight = 28.0134).

T (K)	$\rho_{exp}$ (mol/l)	$\rho_{calc}$ (mol/l)	$100(\rho_{exp} - \rho_{calc}) / \rho_{calc}$
95.000	25.6731	25.6755	-0.009
100.000	24.6400	24.6391	0.004
105.000	23.4998	23.4988	0.005
110.000	22.2079	22.2071	0.004
115.000	20.6719	20.6748	-0.014
120.000	18.6818	18.6856	-0.020
100.000	24.6361	24.6391	-0.012
105.000	23.4963	23.4988	-0.011
110.000	22.2044	22.2071	-0.012
115.000	20.6787	20.6748	0.019
120.010	18.6800	18.6808	-0.004
95.075	25.6624	25.6605	0.007
100.075	24.6207	24.6229	-0.009
105.075	23.4841	23.4807	0.015
110.075	22.1840	22.1862	-0.010
115.075	20.6490	20.6492	-0.001
117.575	19.7356	19.7326	0.015
120.075	18.6525	18.6497	0.015

tures between 135 and 300 K, will be presented in a forthcoming paper.

The standard deviation given in the table for methane at 105 K was based on twelve measurements. The other standard deviations were computed relative to the density and temperature of this point. Standard deviations at the other temperatures and densities could not be estimated from statistical analysis since sufficient repetitive measurements were not taken for these points. Measurements on more dense fluids, such as argon and krypton, have demonstrated the expected variation of the precision with density. Measurements near room temperature, especially those on distilled water, have exhibited the expected improvement in the precision as the temperature is increased.

The total uncertainty of a single density measurement was taken as the square root of the sum of the squares of the systematic errors plus an allowance of three times the standard deviation for random error.

## VI. EXPERIMENTAL RESULTS

### A. Nitrogen

The experimental saturated liquid densities for nitrogen are presented as a function of temperature (IPTS 1968) in Table III. The explanation for some of the nitrogen points not being at integral temperatures involves the presence of a temperature gradient along the length of the cell in some of the initial measurements with this apparatus. Each of the data points was taken from a new charge of nitrogen. For each datum point the vacuum measurements were carried out immediately before or after the liquid measurements. The same procedure was used for methane. The three data sets for nitrogen over the temperature range of 95– or 100–120 K were obtained at approximately six-month intervals. Of the two data sets at integral temperatures, one was taken with methane, and the other with nitrogen, in the vapor bulb. The third set was taken with no liquid in the vapor bulb. (For the 120.010-K point a slight temperature gradient was applied to remove bubbles from the sample liquid inside the cell.)

The nitrogen samples were taken from commercially available, research grade gas. A purity specification of 99.99 mol% was given by the supplier. The gas has been analyzed chromatographically with a thermal conductivity detector and found to be within the specified purity. The nitrogen gas was passed through a room temperature molecular sieve trap, primarily for removal of water.

The saturated liquid densities ( $\rho$ ) of nitrogen have been fitted as a function of temperature ( $T$ ) by the method of least squares to an equation of the following form:

$$\rho - \rho_c = a \left(1 - \frac{T}{T_c}\right)^{0.35} + \sum_{i=1}^3 b_i \left(1 - \frac{T}{T_c}\right)^{1+(i-1)/3}. \quad (9)$$

TABLE IV. Parameters of Eq. (9) for nitrogen.

$a = 19.39217^a$	$(0.11)^b$	$b_3 = 23.32977$	$(4.8)$	$\rho_c = 11.21$	$\text{mol/l}$
$b_1 = 26.01408$	$(2.5)$	$T_c = 126.20$	$\text{K}$	$\sigma = 0.016\%$	
$b_2 = -39.49759$	$(6.5)$				

<sup>a</sup> These coefficients ( $a, b_1, b_2, b_3$ ) and those in Table VI were obtained from a least-squares program in which the experimental densities in  $\text{g/cm}^3$  to five digits were converted to molar densities within the program.

<sup>b</sup> Standard errors of coefficients in parentheses.

$\rho_c$  and  $T_c$  are selected values of the critical density and temperature and  $a, b_i$  are coefficients determined by least squares. Equation (9) consists of a scaling law modification<sup>19</sup> to a generalized Guggenheim equation.<sup>20</sup> The parameters of Eq. (9) for nitrogen, along with the residual standard deviation ( $\sigma$ ) of the fit and the standard errors of the coefficients, are given in Table IV. The standard errors of the calculated densities in Table III are not presented since they are significantly smaller than the standard deviation. The main purpose of the above expression is to facilitate comparisons with independent measurements. The choice of the critical point parameters is arbitrary in the sense that the critical point density can be varied by as much as 5% and the critical point temperature by 0.2% without changing the fit of the data within the estimated precision of the present measurements. For nitrogen the critical point values were obtained from the PVT data compilation of Jacobson<sup>21</sup>.

In Fig. 6 independent experimental data available in the literature are compared with the expression representing the present nitrogen data over the temperature range of the present measurements. The present data are also shown. The experimental temperatures

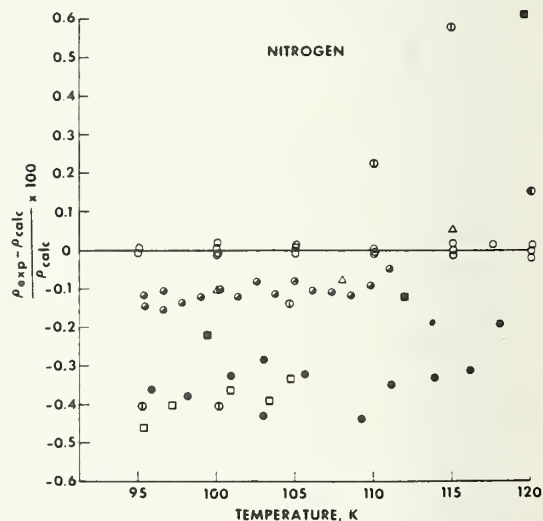


FIG. 6. Deviation plot of experimental densities of saturated liquid nitrogen compared with values calculated from Eq. (9) using parameters from Table IV: ○ present data, ● Brauns,<sup>22</sup> ● Weber,<sup>23</sup> △ Rodosevich and Miller,<sup>24</sup> ● Goldman and Scrase,<sup>25</sup> □ Terry *et al.*,<sup>26</sup> ○ Streett and Staveley,<sup>27</sup> ■ Mathias *et al.*<sup>28</sup>

TABLE V. Results for saturated liquid methane (molecular weight = 16.04303).

Temperature (K)	Mean density (mol/l)	Standard deviation (%)	Number of data points
105.000	26.9458	0.015	12
110.000	26.4985	0.019	11
115.000	26.0443	0.014	12
120.000	25.5721	0.016	17
125.000	25.0845	0.016	18
130.000	24.5775	0.017	16
135.000	24.0540	0.016	23
140.000	23.5067	0.018	5
145.000	22.9312	0.014	5
150.000	22.3218	—	2
160.000	20.9876	—	2

of other measurements have not been adjusted to the temperature scale of the present results.

The data of Brauns,<sup>22</sup> Weber,<sup>23</sup> and Rodosevich and Miller,<sup>24</sup> each obtained with a technique different from that used here, fall within 0.15% of the present results. The densities of Goldman and Scrase<sup>25</sup> and Terry *et al.*<sup>26</sup> are consistently lower than the present results by approximately 0.3–0.4%. This pattern is also followed for methane by Terry *et al.* and preliminary analysis of recent results for argon and krypton obtained with the magnetic suspension densimeter indicate comparisons with Terry *et al.*, for these fluids exhibit the same behavior.

## B. Methane

Methane has been used as a control fluid throughout the entirety of a project that has included density measurements on six pure fluids and, at least, thirty mixtures of these components. As a result, well over one hundred data points have been accumulated for saturated liquid methane, primarily in the temperature range 105–150 K. Although these experimental data are not presented in this paper, the results of an analysis of the methane data are helpful in evaluating the performance of the magnetic suspension densimeter used in the present work. More than ten data points were obtained at each 5-K interval between 105 and 135 K. The mean of the experimental densities, along with the standard deviation and the number of points at each temperature, are given in Table V. (The standard deviations are not given at 150 and 160 K since there are only two data points at each of these temperatures.) Each of the data points represents a new methane sample. The vapor bulb contained liquid methane for all points.

TABLE VI. Parameters of Eq. (9) for methane.

$a = 18.65812$	(0.035) <sup>a</sup>	$T_c = 190.555$ K
$b_1 = 6.712030$	(0.21)	$\rho_c = 10.16$ mol/l
$b_2 = -0.9472020$	(0.20)	$\sigma = 0.016\%$

<sup>a</sup> Standard errors of coefficients in parentheses.

The liquid samples were obtained from either of two cylinders of different batches of commercial, research grade methane. The purity for each cylinder as specified by the supplier is 99.99 mol% minimum. Analyses in this laboratory substantiated these specifications. As with nitrogen the methane gas was passed through a room temperature molecular sieve trap to remove moisture and any heavy contaminants not detected by analysis.

The 123 experimental data points have been fitted by the method of least squares to Eq. (9). Only three coefficients were needed to fit the methane data within the precision of the measurements. The fourth term in the equation was not statistically significant. The coefficients of Eq. (9), the standard errors of the coefficients, the residual standard deviation ( $\sigma$ ) of the fit, and a selected critical density<sup>29</sup> and temperature<sup>30</sup> are given in Table VI for methane. Equation (9), with the coefficients for methane, has been used to compare the present results with experimental data from independent investigators. The methane data from the present work are not shown on the deviation plot because of the large number of points. All of the experimental densities of methane obtained in the present work will be presented in tabular form in a future publication.

For saturated liquid methane there have been considerably more measurements than for saturated liquid nitrogen. All of the other measurements were obtained with techniques different from that of the present work. Some of the older, less precise data have been included in Fig. 7 for the sake of completeness. It is satisfying that the relatively recent data of Orrit and Olives,<sup>31</sup> McClune,<sup>32</sup> Goodwin and Prydz,<sup>33</sup> and Shana'a and

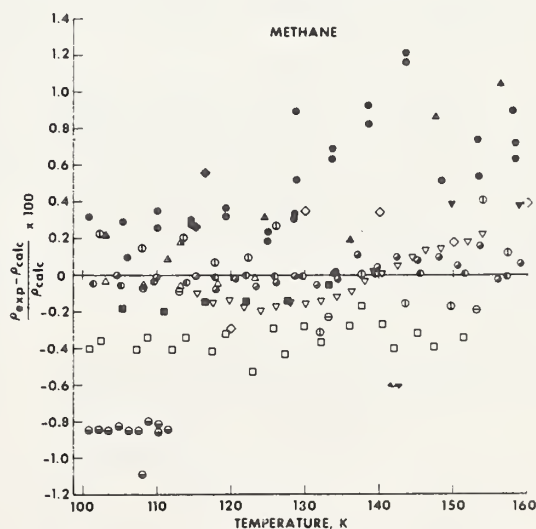


Fig. 7. Deviation plot of experimental densities of saturated liquid methane compared with values calculated from Eq. (9) using parameters from Table VI: □ Terry *et al.*,<sup>26</sup> ● Orrit and Olives,<sup>31</sup> △ McClune,<sup>32</sup> ● Goodwin and Prydz,<sup>33</sup> ⊗ Shana'a and Canfield,<sup>34</sup> ▽ Vennix,<sup>35</sup> ○ Grigor,<sup>36</sup> ▽ Davenport *et al.*,<sup>37</sup> ■ Klosek and McKinley,<sup>38</sup> ⊖ Sinor and Kurata,<sup>39</sup> △ Jensen and Kurata,<sup>40</sup> ▲ Bloomer and Parent,<sup>41</sup> ⊙ Fuks *et al.*,<sup>42</sup> ● Keyes *et al.*,<sup>43</sup> ◆ Moran,<sup>44</sup> ◇ Van Itterbeek *et al.*<sup>45</sup>

Canfield<sup>34</sup> agree with the present results within 0.1%. However, as mentioned earlier, the densities of Terry *et al.*<sup>26</sup> are systematically lower than the present results by 0.3–0.4%. The extrapolated densities of Vennix<sup>35</sup> at approximately 150 and 160 K are 0.4% larger than the present results although the discrepancy at 140 K is approximately 0.01%.

### C. Other fluids

To demonstrate the performance of the magnetic suspension densimeter at low temperature, this paper presents only a representative cross section of the data that have been taken in the present work. Data have recently been obtained for other pure fluids (ethane, propane, isobutane, normal butane, argon, and krypton) over a density range extending to 2.3 g/cm<sup>3</sup> (krypton) and over a temperature range extending to 300 K (isobutane and normal butane). These data will be published in the near future.

### ACKNOWLEDGMENTS

The authors would like to express their appreciation to the following individuals who have made significant contributions to the development of this apparatus. M. R. Cines of Phillips Petroleum Co., Chairman of the LNG Density Project Steering Committee, was instrumental in the development of support for this project. W. G. Layne, D. L. Smith, and A. N. DiSalvo assisted in the design and fabrication of the apparatus. J. E. Cruz designed some of the electronics associated with the refrigeration and temperature control systems. J. R. Whetstone determined the densities of liquid samples of normal pentane and ethanol, which were used as reference fluids. P. V. Tryon assisted with the statistical analysis of the data.

\* This work was carried out at the National Bureau of Standards under the sponsorship of British Gas Corp., Chicago Bridge and Iron Co., Columbia Gas Service Corp., Distrigas Corp., Easco Gas LNG, Inc., El Paso Natural Gas, Gaz de France, Marathon Oil Co., Mobil R and D Corp., Natural Gas Pipeline Co., Phillips Petroleum Co., Shell International Gas, Ltd., Sonatrach, Southern California Gas Co., Tennessee Gas Pipeline, Texas Eastern Transmission Co., Tokyo Gas Co., Ltd., and Transcontinental Gas Pipe Line Corp., through a grant administered by the American Gas Association, Inc.

<sup>1</sup> W. M. Haynes and J. W. Stewart, *Rev. Sci. Instrum.* **42**, 1142 (1971).

<sup>2</sup> J. W. Beams, *Rev. Sci. Instrum.* **40**, 167 (1969).

<sup>3</sup> R. M. McClintock and M. J. Hiza, *Mod. Plast.* **35**, 172 (1958).

<sup>4</sup> The use of a trade name for clarity and completeness does not

signify an endorsement or recommendation by the National Bureau of Standards.

<sup>5</sup> J. B. Breazeale, Ph.D. thesis, University of Virginia (1955).

<sup>6</sup> H. S. Morton, Jr., Ph.D. thesis, University of Virginia (1953).

<sup>7</sup> J. P. Senter, *Rev. Sci. Instrum.* **40**, 334 (1969).

<sup>8</sup> J. W. Beams, C. W. Hulburt, W. E. Lotz, Jr., and R. M. Montague, Jr., *Rev. Sci. Instrum.* **26**, 1181 (1955).

<sup>9</sup> S. P. Almeida and T. H. Crouch, *Rev. Sci. Instrum.* **42**, 1344 (1971).

<sup>10</sup> M. G. Hodgins and J. W. Beams, *Rev. Sci. Instrum.* **42**, 1455 (1971).

<sup>11</sup> J. L. Hales, *J. Phys. E* **3**, 855 (1970).

<sup>12</sup> S. C. Greer, M. R. Moldover, and R. Hocken, *Rev. Sci. Instrum.* **45**, 1462 (1974).

<sup>13</sup> R. Prydz and R. D. Goodwin, *J. Chem. Thermodyn.* **4**, 127 (1972).

<sup>14</sup> W. Wagner, *Cryogenics* **13**, 470 (1973).

<sup>15</sup> J. W. Beams and A. M. Clarke, *Rev. Sci. Instrum.* **33**, 750 (1962).

<sup>16</sup> M. Menaché and G. Girard, *Metrologia* **9**, 62 (1973).

<sup>17</sup> A. F. Clark, W. M. Haynes, V. A. Deason, and R. J. Trapani, *Cryogenics* **16**, 267 (1976).

<sup>18</sup> G. Simmons and H. Wang, *Single Crystal Elastic Constants and Calculated Aggregate Properties: A Handbook* (MIT Press, Cambridge, MA, 1971), p. 181.

<sup>19</sup> R. D. McCarty, *Natl. Bur. Stand. (U.S.) Intern. Rept.* 74-357 (1974).

<sup>20</sup> Y. C. Hou and J. J. Martin, *AIChE J.* **5**, 125 (1959).

<sup>21</sup> R. T. Jacobsen, Ph.D. thesis, Washington State University (1972).

<sup>22</sup> P. Brauns (private communication, 1973).

<sup>23</sup> L. A. Weber, *J. Chem. Thermodyn.* **2**, 839 (1970).

<sup>24</sup> J. B. Rodosevich and R. C. Miller, *AIChE J.* **19**, 729 (1973).

<sup>25</sup> K. Goldman and N. G. Scrase, *Physica* **44**, 555 (1969).

<sup>26</sup> M. J. Terry, J. T. Lynch, M. Bunclark, K. R. Mancell, and L. A. K. Staveley, *J. Chem. Thermodyn.* **1**, 413 (1969).

<sup>27</sup> W. B. Streett and L. A. K. Staveley, *Adv. Cryog. Eng.* **13**, 363 (1968).

<sup>28</sup> E. Mathias, H. K. Onnes, and C. A. Crommelin, *Commun. Leiden* **145C**, 19 (1914).

<sup>29</sup> J. D. Olson, *J. Chem. Phys.* **63**, 474 (1975).

<sup>30</sup> R. D. Goodwin, *Natl. Bur. Stand. (U.S.) Tech. Note No.* 653 (1974).

<sup>31</sup> J. Orrit and J. Olives, distributed at 4th International Conference on Liquefied Natural Gas, Algeria (1974).

<sup>32</sup> C. R. McClune, *Cryogenics* **16**, 289 (1976).

<sup>33</sup> R. D. Goodwin and R. Prydz, *J. Res. Natl. Bur. Std. (U.S.)* **76A**, 81 (1972).

<sup>34</sup> M. Y. Shana'a and F. B. Canfield, *Trans. Faraday Soc.* **64**, 2281 (1968).

<sup>35</sup> A. J. Vennix, Ph.D. thesis, Rice University (1965).

<sup>36</sup> A. F. Grigor, Ph.D. thesis, Pennsylvania State University (1966).

<sup>37</sup> A. J. Davenport, J. S. Rowlinson, and G. Saville, *Trans. Faraday Soc.* **62**, 322 (1966).

<sup>38</sup> J. Klosek and C. McKinley, *Proceedings of the First International Conference on LNG*, Chicago (1968), Paper 22.

<sup>39</sup> J. E. Sinor and F. Kurata, *J. Chem. Eng. Data* **11**, 1 (1966).

<sup>40</sup> R. H. Jensen and F. Kurata, *J. Petrol. Technol.* **21**, 683 (1969).

<sup>41</sup> O. T. Bloomer and J. D. Parent, *Chem. Eng. Progr. Symp. Ser.* **49**, 11 (1952).

<sup>42</sup> S. Fuks, J. C. Legros, and A. Bellemans, *Physica* **31**, 606 (1965).

<sup>43</sup> F. G. Keyes, R. S. Taylor, and L. B. Smith, *J. Math. Phys.* **1**, 211 (1922).

<sup>44</sup> D. W. Moran, Ph.D. thesis, Imperial College, University of London (1959).

<sup>45</sup> A. Van Itterbeek, O. Verbeke, and K. Staes, *Physica* **29**, 742 (1963).

## Simplified magnetic suspension densimeter for absolute density measurements\*

W. M. Haynes

National Bureau of Standards, Institute for Basic Standards, Boulder, Colorado 80302

(Received 24 September 1976)

A magnetic suspension densimeter, incorporating three support coils, has been reduced to a system using only one coil. This simplifies considerably the design of the apparatus and the procedures involved in the measurements. This instrument can be used for absolute density measurements; i.e., it does not have to be calibrated with reference fluids of known density.

During the past two decades the magnetic suspension densimeter<sup>1-17</sup> has evolved into a versatile research instrument that has been used routinely for liquid density measurements to a precision of ten parts per million. (Reference 14 presents a detailed review of the principles, applications, and development of the magnetic densimeter.) In the original design (Fig. 1) of the instrument a piece of soft ferromagnetic material is suspended in a fluid of unknown density by the magnetic force produced by a single solenoid. The magnetic force on the buoy is given by the relation

$$F_{\text{mag}} = M \frac{dH}{dZ}, \quad (1)$$

where  $M$  is the magnetic moment of the buoy,  $H$  is the axial magnetic field intensity of the air core solenoid, and  $Z$  is the distance along the vertical. The density ( $\rho$ ) of the fluid is related to the current ( $I$ ) in the support coil by

$$\rho = A + BI^2, \quad (2)$$

where  $A$  and  $B$  are constants to be determined by calibration of the instrument with reference fluids of known density. The above relation is based on the assumption that the magnetic moment of the buoy is linearly proportional to the magnetic field intensity.

It is not unusual for the magnetic susceptibility of the magnetically soft material of the buoy to vary slowly with  $H$ . Thus a relatively large number of reference fluids are required to calibrate a one-coil instrument to maintain a given precision over its entire operating range. The precision is inversely proportional to the difference between the density of the fluid and the density of the buoy. To cover an extended density range it is necessary to construct and calibrate buoys of different densities. The calibration of the instrument must be checked periodically to test the buoy material for hysteresis.

These procedural tasks were reduced considerably with the development of a three-coil support system<sup>5</sup> (Fig. 2) which allows variations in  $dH/dZ$  while  $H$  is held constant. The three-coil arrangement consists of a main coil, which supplies the major part of the force necessary

to support the buoy, and a pair of gradient coils connected in such a way that at the buoy position their magnetic fields cancel and their magnetic field gradients add. The magnetic moment of the buoy is held constant; it depends only on the stability of the constant current source that supplies the main coil current. In the first applications of the three-coil arrangement (with a magnetically soft buoy) the instrument still had to be calibrated but now the density range for a given buoy was increased significantly over that for a single-coil system. Also the calibration was simplified since the density was linearly proportional to the current in the gradient coils for a constant main coil current. The buoy may be either magnetically soft or hard for the three-coil system.

Recently, in the adaptation of the magnetic suspension densimeter for use at low temperatures,<sup>11,17</sup> the same three-coil arrangement (Fig. 2) was employed to determine the force on a magnetic material in a nonuniform field; i.e., it was used to determine the variation of the magnetic susceptibility of the buoy material with  $H$  over the range of magnetic fields needed for the density measurements. It was found that the magnetic force on a barium ferrite buoy could be represented by the expression

$$F_{\text{mag}} = M \left( \frac{dH_M}{dZ} + \frac{dH_G}{dZ} \right) = CI_M + DI_G, \quad (3)$$

where the subscripts denote the main and gradient coils.

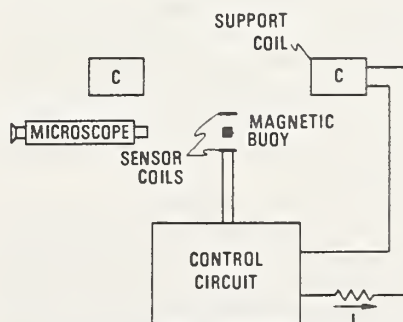


FIG. 1. Schematic diagram of a magnetic suspension densimeter with one support coil.

This result demonstrated that, over the range of magnetic fields considered (0.006–0.016 T), there was no induced moment in the barium ferrite buoy (a magnetically hard material with a permanent moment). Therefore, it was possible to determine fluid densities without the use of calibration fluids. The instrument constants [ $C$ ,  $D$  in Eq. (3)] could be determined from measurements of the gradient coil current as a function of the main coil current while the buoy was supported at a fixed position at constant temperature in vacuum. The mass and volume of the buoy must be determined from independent measurements.

Now that it had been determined with the three-coil arrangement (Fig. 2) that the magnetic moment of the barium ferrite buoy was independent of the magnetic field strength over the range of magnetic fields needed for the desired density measurements, the instrument could be simplified considerably by reducing to a one-coil system (Fig. 1). The magnetic force on the buoy depended only on the magnetic field gradient ( $dH/dZ$ ) and not on the magnetic field intensity ( $H$ ). Thus the single (main) coil was connected into the servosystem and the gradient coils were eliminated.

It should be noted that a one-coil system can be used for absolute density measurements as long as the variation in the magnetic moment of the buoy with magnetic field intensity is known. This information could be obtained by techniques other than that used in the present work, e.g., a vibrating sample magnetometer. This is mentioned to emphasize that, with a knowledge of  $M(H)$  of the magnetic buoy material, the initial apparatus design could be simplified significantly with the use of only one coil.

To carry out density measurements with the one-coil system with a barium ferrite buoy, first the current necessary to support the buoy in vacuum ( $I_v$ ) at a given position and temperature must be determined. Then the current necessary to support the buoy in a liquid ( $I_f$ ) of unknown density at the same position and temperature is measured. The density of the fluid is related to this current ratio by

$$\rho = \frac{m}{V} \left( 1 - \frac{I_f}{I_v} \right), \quad (4)$$

where  $m$  and  $V$  are the mass and volume of the buoy. It should be emphasized that no reference fluids are required for calibration of the one-coil system (or the three-coil system) used in the present work. However, the volume of the float may best be determined near room temperature using distilled water as a reference fluid of known density and, in fact, this procedure was used in the present work.<sup>17</sup>

There are several obvious advantages of the one-coil system over one using three coils; most are involved with the experimental design and procedures. With elimination of the two gradient coils and the alignment problems associated with them, the design and construction of the apparatus are much simpler. The constant current source is no longer needed. The

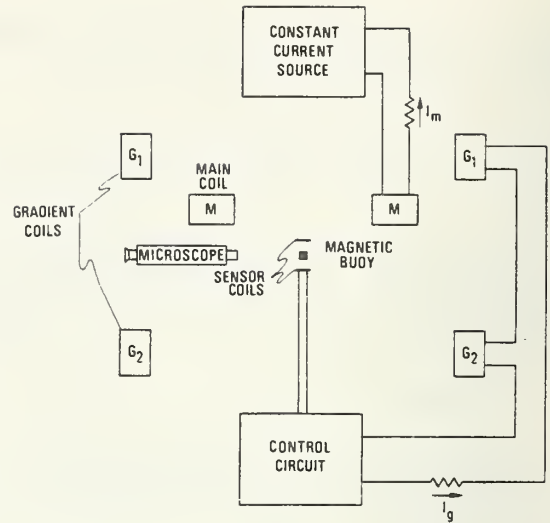


FIG. 2. Schematic diagram of a magnetic suspension densimeter with three support coils.

vacuum points for a single-coil system require only a single current measurement, while those for a three-coil system require a series of measurements of  $I_M$  and  $I_G$  while holding the buoy at a fixed position. Then the currents must be fitted by the method of least squares to Eq. (3) to obtain the instrument constants. Also the error analysis is less complicated with a one-coil system.

There is one inherent disadvantage in the method for obtaining absolute densities with either the one-coil or three-coil systems where the magnetic force depends only on  $dH/dZ$ . The change in  $dH/dZ$  with position is significantly larger than the change in the product of  $H$  and  $dH/dZ$  with position. Thus a very precise determination ( $10^{-3}$  mm) of the separation distance of the main coil and buoy was required in the present work and has been described in Ref. 17.

Experimental densities have been determined for saturated liquid argon and methane at temperatures between 100 and 120 K with both the three-coil and one-coil systems. The results agreed within the imprecision of the measurements, which was approximately 0.015% for methane and 0.005% for argon. Thus the simpler one-coil system is now utilized for all density measurements with the present instrument.

The servosystem that is used with the single coil was originally connected to the gradient coils in the three-coil system. No modifications to the servosystem as described in Ref. 17 were required for its use with the single coil.

The present series of density measurements in this laboratory with the magnetic suspension densimeter represented a nontypical use of the instrument. In the past the instrument has been used for highly precise (usually less than 0.001%) measurements over a short density range at a single temperature. Here a relatively modest precision (less than 0.02%) was the result of

measurements over large density (0.3–2.3 g/cm<sup>3</sup>) and temperature (95–300 K) ranges with a single buoy. The total uncertainty of the present measurements was approximately 0.1%.

In order to obtain the highest precision and accuracy with the present instrument it was necessary to perform vacuum measurements immediately before or after the liquid measurements. The possible use of the instrument without repeating the vacuum measurements for each datum point has been investigated. In other words the precision and accuracy of the instrument has been estimated, based on a single series of vacuum measurements as a function of temperature at the beginning (and/or end) of a set of density measurements without regard to the temperature and magnetic field cycling of the buoy. The separation distance of the coil and the buoy must be maintained throughout the set of measurements.

In the present setup the position of the main coil was fixed as described in Ref. 17. The position of the float was determined with a 125× microscope and the buoy could be returned to a desired position either electronically or mechanically. Over a period of several months during the course of density measurements at low temperatures on several different fluids, the sample cell was cycled between approximately 100 to 130 K and 300 K more than twenty times. The standard deviation of the vacuum measurements at low temperatures was of the order of 0.05% with no systematic trend observed. This was a measure of the thermal hysteresis of the magnetic moment of the barium ferrite buoy over rather large temperature cycles. This result demonstrated that densities with a total uncertainty of approximately 0.2% could be expected without repeating

vacuum measurements for each datum point. Thus, for density data in which the highest precision and accuracy are not required, the use of a one-coil system and a barium ferrite buoy would result in a relatively simple and efficient measurement process that requires few vacuum measurements.

\* This work was carried out at the National Bureau of Standards under the sponsorship of British Gas Corp., Chicago Bridge and Iron Co., Columbia Gas Service Corp., Distrigas Corp., Easco Gas LNG, Inc., El Paso Natural Gas, Gaz de France, Marathon Oil Co., Mobil R and D Corp., Natural Gas Pipeline Co., Phillips Petroleum Co., Shell International Gas, Ltd., Sonatrach, Southern California Gas Co., Tennessee Gas Pipeline, Texas Eastern Transmission Co., Tokyo Gas Co., Ltd., and Transcontinental Gas Pipe Line Corp., through a grant administered by the American Gas Association, Inc.

<sup>1</sup> J. W. Beams, C. W. Hulbert, W. E. Lotz, Jr., and R. M. Montague, Jr., *Rev. Sci. Instrum.* **26**, 1181 (1955).

<sup>2</sup> J. W. Beams and A. M. Clarke, *Rev. Sci. Instrum.* **33**, 750 (1962).

<sup>3</sup> A. M. Clarke, D. W. Kupke, and J. W. Beams, *J. Phys. Chem.* **67**, 929 (1963).

<sup>4</sup> D. V. Ulrich, D. W. Kupke, and J. W. Beams, *Proc. Nat. Acad. Sci. U.S.A.* **52**, 349 (1964).

<sup>5</sup> J. W. Beams, *Rev. Sci. Instrum.* **40**, 167 (1969).

<sup>6</sup> J. P. Senter, *Rev. Sci. Instrum.* **40**, 334 (1969).

<sup>7</sup> P. F. Fahey, D. W. Kupke, and J. W. Beams, *Proc. Nat. Acad. Sci. U.S.A.* **63**, 548 (1969).

<sup>8</sup> A. M. Wims, D. McIntyre, and F. Hynne, *J. Chem. Phys.* **50**, 616 (1969).

<sup>9</sup> R. Goodrich, D. F. Swinehart, M. J. Kelly, and F. J. Reithel, *Anal. Biochem.* **28**, 25 (1969).

<sup>10</sup> J. L. Hales, *J. Phys. E* **3**, 855 (1970).

<sup>11</sup> W. M. Haynes and J. W. Stewart, *Rev. Sci. Instrum.* **42**, 1142 (1971).

<sup>12</sup> S. P. Almeida and T. H. Crouch, *Rev. Sci. Instrum.* **42**, 1344 (1971).

<sup>13</sup> M. G. Hodgins and J. W. Beams, *Rev. Sci. Instrum.* **42**, 1455 (1971).

<sup>14</sup> D. W. Kupke and J. W. Beams, *Methods Enzymol.* **26**, 74 (1973).

<sup>15</sup> S. C. Greer, M. R. Moldover, and R. Hocken, *Rev. Sci. Instrum.* **45**, 1462 (1974).

<sup>16</sup> S. C. Greer, T. E. Block, and C. M. Knobler, *Phys. Rev. Lett.* **34**, 250 (1975).

<sup>17</sup> W. M. Haynes, M. J. Hiza, and N. V. Frederick, *Rev. Sci. Instrum.* **47**, 1237 (1976).



# Apparatus for Density and Dielectric Constant Measurements to 35 MPa on Fluids of Cryogenic Interest

W. M. Haynes and N. V. Frederick  
National Bureau of Standards, Boulder, CO 80303

Accepted: March 11, 1983

An apparatus has been developed for simultaneous measurements of fluid densities and dielectric constants at temperatures from 70 to 320 K and at pressures to 35 MPa. A magnetic suspension technique, based on an application of Archimedes' principle, is employed in the density determination, while a concentric cylinder capacitor is used for obtaining the dielectric constant data. The apparatus can be used not only for determining densities and dielectric constants of compressed gases and liquids (including mixtures), but for saturated liquid and vapor properties as well. Also included is the capability for acquiring liquid-vapor equilibrium data for mixtures. The total uncertainty of a single density measurement is estimated to be approximately 0.1% for densities as low as 50 kg/m<sup>3</sup>; at lower densities, the uncertainty increases. The imprecision of the density data is typically less than 0.02%. The total uncertainty in the dielectric constants is approximately 0.01%. Experimental data for a 0.85 CH<sub>4</sub>+0.15 C<sub>2</sub>H<sub>6</sub> mixture are given here to demonstrate the performance of the apparatus.

Key words: Clausius-Mossotti function; compressed fluid; concentric cylinder capacitor; density; dielectric constant; excess volume; magnetic suspension densimeter; methane-ethane mixture; saturated liquid; vapor pressure.

## 1. Introduction

A magnetic suspension densimeter [1,2]<sup>1</sup> was used in a large-scale program to measure the orthobaric liquid densities of the major components [1,3,4] of liquefied natural gas (LNG) and mixtures [5-9] of these components. This technique, based on an application of Archimedes' principle, was selected for the LNG density project for several reasons:

- 1) It is capable of absolute density measurements of high accuracy and precision over wide ranges of

**About the Authors, Paper:** W. M. Haynes is with NBS' Chemical Engineering Science Division, and N. V. Frederick with its Electromagnetic Technology Division. The work reported on was carried out at NBS under the sponsorship of the American Gas Association, Inc. and the National Aeronautics and Space Administration.

<sup>1</sup> Figures in brackets indicate literature references at the end of this paper.

- density, temperature, and pressure.
- 2) Calibration fluids are not required.
- 3) The technique can be used not only to measure densities of compressed fluids, but also to measure liquid and vapor densities along the coexistence boundary.

The measurements for the LNG density project were concentrated in the temperature range from 100-140 K at pressures typically less than 0.2 MPa. The apparatus was designed for a maximum pressure of 5 MPa. Near the end of the LNG density project, the pressure range of the densimeter was expanded to at least 35 MPa. The expansion was because of a need to map the PVT surfaces of fluids with critical points significantly above ambient temperature. (A gas expansion technique [10-13] used at this laboratory for PVT measurements on cryogenic fluids could not be used for this application.) The expansion of the densimeter's pressure capability resulted in a new instrument, described here, significantly different from and more versatile than the previous one [1] developed specifically for the LNG density project.

Although many of the components of the new densimeter changed, the technique used is the same. To detect the position of the magnetic buoy, a linear differential capacitance sensor [12], compatible with the higher pressure environment, has been developed to replace an inductance sensor. Although the properties of the buoy had been well characterized in the previous work [1], it was necessary to determine the effect of pressure on its volume. A new support coil for lifting the buoy and a new microscope lens combination for determining the position of the buoy were also required in adapting the technique to higher pressures.

Since the dielectric constant of a fluid is closely related to its density through the Clausius-Mossotti function, a concentric cylinder capacitor was added inside the sample cell to enable simultaneous measurements of dielectric constant and density on the same fluid samples. Dielectric constant measurements can serve as simple and reliable substitutes for density measurements. The addition of the capacitor was motivated to some extent by the fact that some commercial densimeters being developed for custody transfer applications in LNG transactions include devices based on capacitance measurements.

The new apparatus incorporates a cryostat design different from that employed with the previous densimeter, but similar to ones used with other instruments [10-13] in this laboratory. The cryostat is suitable for continuous temperature control between 70 and 320 K. A new high-pressure window design developed for the equilibrium cell allows the position of the buoy to be determined by optical means. With the new cell and cryostat, it was not possible to change the position of the buoy by mechanical means; this is now accomplished electronically.

The apparatus can also be used for liquid-vapor equilibrium measurements on mixtures. Means have been provided for mixing (recirculation of vapor through liquid), sampling of vapor and liquid, and subsequent composition analysis. Compared to the previous densimeter [1], improvements have been made in the characterization of the temperature, pressure, and composition of the fluid samples. With the previous apparatus [1], it was possible to observe the liquid-vapor interface through a window that extended most of the length of the sample space. In adapting the magnetic suspension densimeter for pressures to 35 MPa over a wide temperature range, it was not practical to retain this feature. This feature, although convenient, was not essential for any of the measurements performed with the new apparatus.

The new apparatus was first used to complete

measurements for the LNG density project [7,9]. Extensive tests were made to ensure that the density results obtained with the new apparatus were in agreement with those from the previous apparatus. The consistency of the density data was one of the most important considerations in the development of mathematical models [15-18] for predictions of mixture (LNG) densities. The apparatus was then used to measure the densities and dielectric constants of liquid propane [19-20], isobutane [19,21], and normal butane [19,22] over temperature ranges from their triple points to 300 K at pressures to 35 MPa.

## 2. Measurement Methods

### 2.1 Density

In the magnetic suspension densimeter used, a piece of magnetic material (barium ferrite magnetic buoy in the shape of a right circular cylinder magnetized along its cylindrical axis) is suspended freely by the force produced from the axial magnetic field of a single air-core solenoid. The vertical motion of the magnetic buoy is controlled by the automatic regulation of the solenoid current with a closed-loop servocircuit that includes a differential capacitance sensor to detect the position of the buoy. (The horizontal position of the buoy is maintained by the axially symmetrical, diverging field of the solenoid.) In the present system, the magnetic buoy is more dense than the fluids in which it is suspended. Thus, an upward magnetic force is added to the buoyant force to balance the downward gravitational force.

In earlier work [2] with a densimeter that utilized a three-solenoid arrangement to supply the magnetic force, it was found that the magnetic moment of a barium ferrite buoy was independent of magnetic field intensity over the range of fields (0.006-0.016 T) needed to support the buoy. Barium ferrite is a magnetically hard material with a permanent moment. This meant that a one-coil system could be used to determine fluid densities without the need of calibration fluids. To carry out density measurements with a one-coil system and a barium ferrite buoy, first the current ( $I_v$ ) necessary to support the buoy in vacuum at a given position (buoy-coil separation distance) and temperature is measured. Then the current ( $I_f$ ) necessary to support the buoy in a fluid of unknown density at the same position and temperature is determined. The density ( $\rho$ ) of the fluid is related to these currents by the relation,

$$\rho = \frac{m}{V} \left( 1 - \frac{I_f}{I_v} \right), \quad (1)$$

where  $m$  and  $V$  are the mass and volume of the buoy. Measurement procedures for using this equation to determine fluid densities for the instrument developed in the present work are discussed later. Also presented is a detailed description of the magnetic suspension system.

## 2.2 Dielectric Constant

A stable concentric cylinder capacitor was used for dielectric constant measurements. First, the capacitance ( $C$ ) with the fluid (of unknown dielectric constant) between the cylindrical electrodes is measured. Then, at the same temperature, the vacuum capacitance ( $C_0$ ) is determined. The dielectric constant ( $\epsilon$ ) is calculated from the relation,

$$\epsilon = C/C_0. \quad (2)$$

## 3. Apparatus

### 3.1 Cryostat

The major features of the cryostat are shown to scale in figure 1, an assembly drawing of the apparatus. This cryostat is similar to some used previously at this laboratory [10-13]. Those modifications necessary to adapt the cryostat for use with a magnetic suspension densimeter will be emphasized.

The cryostat was supported by a 1.3-cm-thick aluminum plate suspended from concrete block columns at a height 2.3 m above floor level. The aluminum plate was reinforced with 10-cm-wide stainless steel channel beams so that the position of the cryostat was independent of the amount of liquid nitrogen in the reservoir. Apparent changes in the buoy-coil separation distance resulted if the position of the cryostat was not maintained during the course of measurements. The aluminum plate from which the cryostat was suspended could be leveled and clamped in place using four bolts in contact with the concrete block columns.

The cryostat was fabricated from nonmagnetic materials. The inner cylinders or cans (liquid nitrogen reservoir, cold ring, guard ring, shield, cold wall) were copper; the outer vacuum jacket and access tubes were primarily stainless steel; and the flanges, support plates, and fittings were mostly brass. The various cylindrical portions of the cryostat and the central support (reflux) tube had to be aligned (concentric and vertical) so the buoy could be suspended symmetrically about the cylindrical axis of the differential capacitance sensor. Many of the dimensions of the cryostat components were

determined by the dimensions of the high-pressure cell and the support coil. The outside diameter of the stainless steel vacuum jacket is 20.3 cm while the outside diameter of the glass tail of the cryostat is 9.0 cm. There is 0.4-cm clearance on the diameter between the cryostat tail and the support coil. The

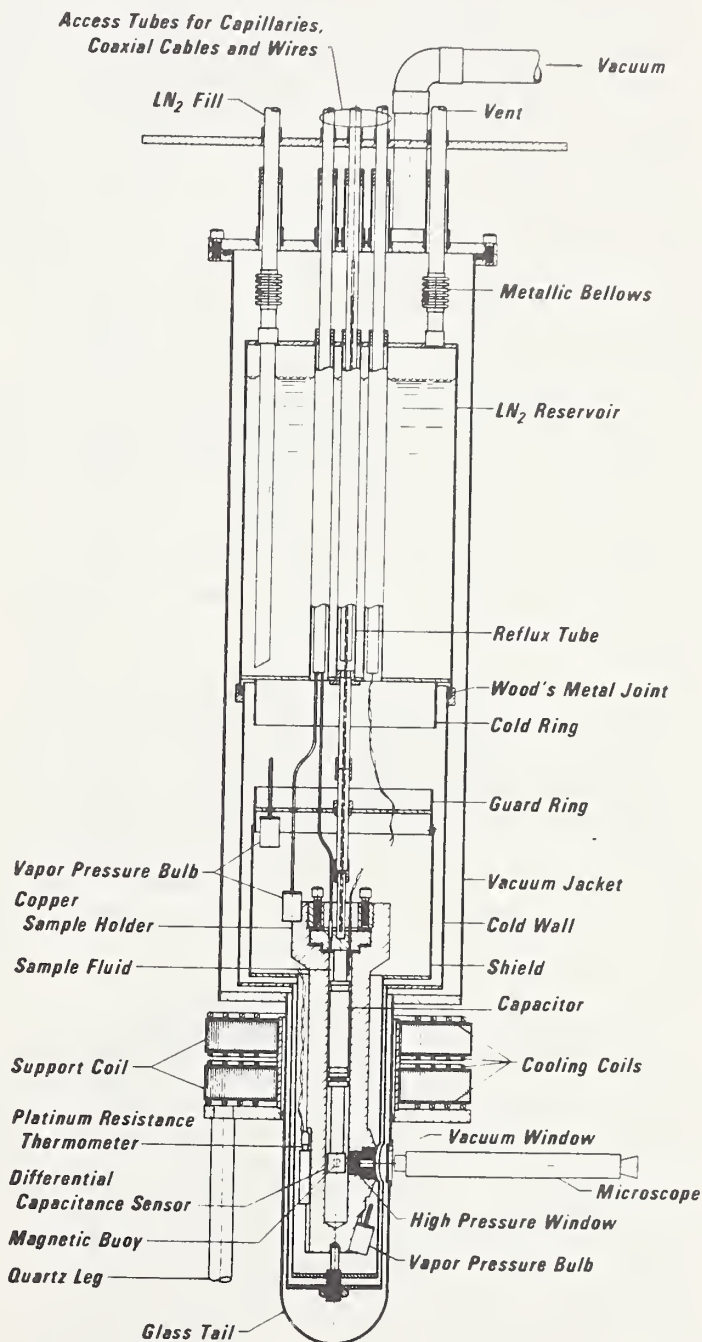


Figure 1—Assembly drawing (approximately to scale) of an apparatus for density and dielectric constant measurements to 35 MPa on cryogenic fluids.

overall length of the cryostat is approximately 94 cm.

The liquid nitrogen reservoir has a capacity of approximately  $7 \times 10^3 \text{ cm}^3$  and needs refilling under normal conditions about every 16 h. Metallic bellows were placed in the fill and vent lines of the reservoir to eliminate relative movement, as a function of temperature, between the cell and the outer stainless steel jacket of the cryostat. This step was necessary to maintain alignment of the capacitance sensor and buoy located inside the cell with the support coil located outside the cryostat, independent of the experimental conditions. Five access tubes, which passed through the liquid nitrogen reservoir, were available for introducing capillaries, coaxial cables, and wires into the vacuum space and cell inside the cryostat.

The cryostat was comprised of one large vacuum space; holes (3 cm diameter) were cut into the electroformed copper cylinders attached to the liquid nitrogen reservoir and the guard ring for visual observation of the buoy. With this arrangement it was not feasible to use exchange gas for fast-cooling the cell. The exchange gas would have been in direct contact with the outer stainless steel can which included a glass tail as its lower section. The glass tail was connected to the outer jacket through a stainless steel-to-glass transition joint; to ensure integrity of this seal, the joint should be kept at a temperature near ambient.

Fast-cooling of the cell was accomplished using the refluxing action of nitrogen in the central support tube. The maximum cooling rate was approximately 50 K/h. The reflux tube is evacuated during measurements when the cell is controlled at a desired temperature. For additional cooling, three flexible copper braided straps (not shown in fig. 1), each with a cross sectional area of  $5 \text{ mm}^2$  per strap, have been connected symmetrically from the top of the cold shield to the cell.

The cryostat was designed to facilitate ease in assembly and disassembly and to minimize alignment problems of critical components. All demountable joints had enough latitude to make alignment reasonably straightforward. The outer vacuum jacket was attached to the top of the cryostat through a rubber o-ring seal using a split-ring assembly not shown in the drawing. The inner cans were attached with either Wood's metal or screws. Once the joints were secured, the entire structure was rigid, and no problems with alignment were encountered after numerous temperature cycles. A nut and bolt (fiberglass) arrangement was installed between the cold shield and the bottom of the cell to eliminate pendulous vibrations of the cell.

### 3.2 Equilibrium Sample Cell

Figure 2 is a detailed cross sectional diagram of the copper equilibrium cell. The overall dimensions of the cell used here are roughly the same as for the cell used with the earlier version [1] of the magnetic suspension densimeter, except for an increase in the wall thickness required for use at higher pressures. The new cell has an overall length of approximately 29.5 cm, primarily determined by the position at which the buoy must be suspended relative to the diverging field of the support coil for horizontal stability of the buoy. The outside diameter of the main part of the cell is 4.44 cm, while

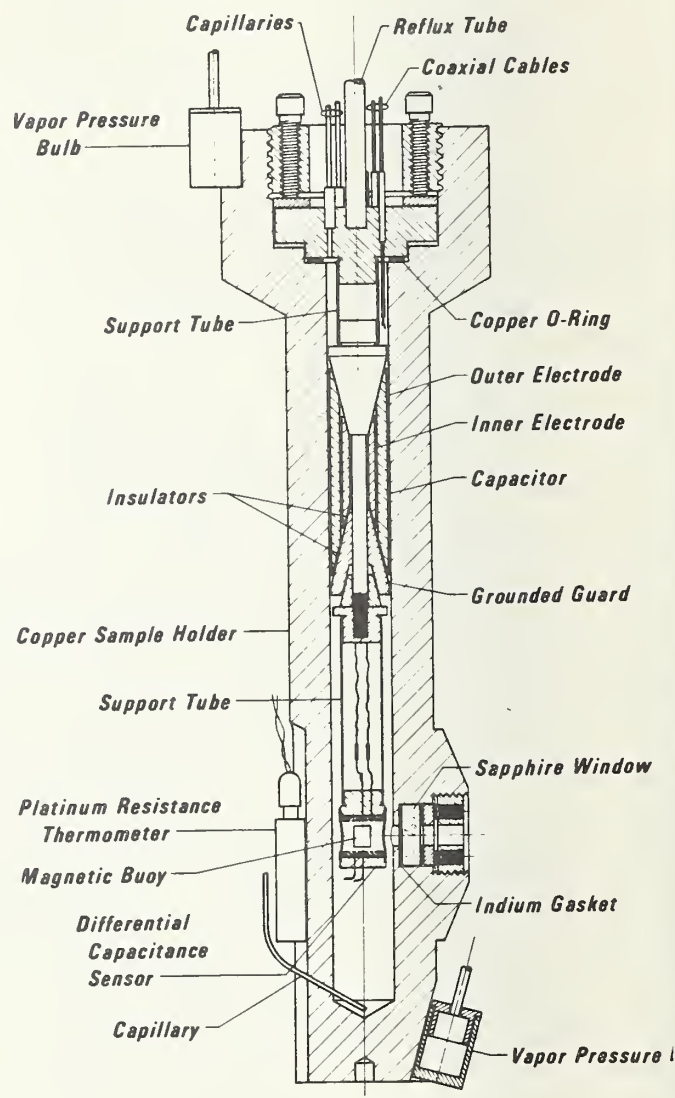


Figure 2—The equilibrium cell.

the top closure section has a diameter of 8.10 cm. The dimensions of the internal sample space are 1.90 cm diameter by approximately 23 cm length. About one third of the internal volume is occupied by the concentric cylinder capacitor and the magnetic buoy-capacitance sensor assembly. This results in an internal free volume of approximately  $43 \text{ cm}^3$ , as determined by filling the cell with water.

To facilitate easy access to the assemblies inside the cell, a flange-gasketed seal was used to close the cell. The seal was effected by compressing a silver-plated, solid copper O-ring between a stainless steel plug and a smooth, flat ledge of the copper cell. This assembly was similar to that used earlier [1]. A thin-walled stainless steel tube, used to support the cell, was soldered into the cell lid (the stainless steel closure plug). This support tube was also used for reflux gas as described earlier.

For visual observation of the magnetic buoy position, a new window assembly for pressures to 35 MPa has been developed. The assembly consists of a sapphire disk (1.90 cm diameter by 0.63 cm thickness) with chamfered edges, indium gasket, asbestos-rubber backing ring to relieve thermal and mechanical strains, and stainless steel plug and ring with four stainless steel set screws to provide a pressure- and vacuum-tight seal. It has a 0.63 cm diameter viewing area. An effort was made to minimize the size of the high pressure window assembly, especially in the horizontal direction. This effort resulted from an attempt to minimize the inner diameter of the support coil so current and power in the coil were not excessively large.

A total of four capillaries has been introduced into the sample space. Two capillaries are soldered into collars in the cell lid; the other two are soldered into the cell wall with their ends terminating at the bottom of the sample space. This makes it possible to fill the cell from either the top or bottom, or from both simultaneously. Filling procedures can be critical when condensing liquid mixtures into the cell. Under normal conditions, a pair of capillaries, one at the top and one at the bottom, is available for recirculating the vapor through the liquid for mixing; the other capillary at the top is for pressure measurements while the free capillary at the bottom can be used for liquid sampling. By having capillaries at both ends of the cell, it is easy to remove low vapor pressure liquids from the cell.

At approximately the same height at which the magnetic buoy is suspended, a platinum resistance thermometer has been soldered with indium into a closed-end copper tube that has been soft-soldered into

a groove cut lengthwise in the cell wall. Vapor pressure bulbs fabricated from copper (each with an internal volume of approximately  $2 \text{ cm}^3$ ) have been installed at the ends of the cell in close thermal contact (soft-solder) with the outside surface. These bulbs, along with differential thermocouples (chromel-constantan) secured at the same positions, are used to monitor temperature differences between the ends of the cell. Four independent heaters of 110 to 160  $\Omega$  each for temperature control have been wound bifilarly at different positions along the length of the cell.

A total of six coaxial cables enter through the lid of the cell into the sample space in pressure-tight assemblies. Three of the cables are for the capacitance sensor, two for the cylindrical capacitor, and one is a spare. Each coaxial cable consists of an outer stainless steel sheath of 0.51 mm diameter insulated from a 0.13 mm diameter inner conductor with polytetrafluoroethylene. These cables have been found to be leak-tight along short lengths at gas pressures to 70 MPa at room temperature. Cables approximately 1 meter in length have been inserted into stainless steel capillaries (1.07 mm outside diameter  $\times$  0.66 mm inside diameter) that extend from inside the sample cell to a position above the top of the cryostat where the coaxial cables are soldered into the capillaries. This means that continuous lengths of the coaxial cables extend from inside the sample cell to a region in which the cables are leak-tight. At low temperatures, the cables do not seal because of the relatively large difference in the thermal expansion coefficients of stainless steel and polytetrafluoroethylene. The stainless steel capillaries are soldered into collars in the lid of the cell and at the top of the cryostat.

### 3.3 Magnetic Suspension System

The magnetic suspension system, employed here in the density determination, uses some components from the previous densimeter [1]. The magnetic buoy, with its well-characterized properties deduced from the earlier work, has been described in detail. The buoy is a barium ferrite magnet in the shape of a right circular cylinder (0.51 cm diameter  $\times$  0.64 cm length) magnetized along its cylindrical axis. Barium ferrite is a magnetically hard, ceramic material with a density of approximately  $5 \times 10^3 \text{ kg/m}^3$ . Since barium ferrite is porous, the buoy was plated with copper to a thickness of approximately 0.06 mm. A thin ( $10^{-3} \text{ mm}$ ) protective coating of gold was flashed over the copper. No problems were encountered with fluids penetrating the copper layer at pressures to 35 MPa.

Barium ferrite was selected as the buoy material since its magnetic properties are consistent with absolute density measurements [2]. Over the range of magnetic fields needed to support the buoy, the magnetic moment of the barium ferrite buoy had been found to be independent of the magnetic field intensity.

The densimeter described here included a single solenoid that supplied the force required to lift the buoy. The simplification in the densimeter design in going from a three-coil to a one-coil system, which resulted from a determination of the magnetic properties of barium ferrite, has been discussed in detail in an earlier paper [2]. (Although no further use of a three-coil arrangement with gradient coils was anticipated, the outside diameter of the new support coil was made less than the inside diameter of the gradient coils used in the previous work [1] in the eventuality that a need for tests on new buoy materials ensued.)

The new support coil is composed of two separate coils of 2275 turns each of epoxy-coated aluminum foil of approximately 0.025 mm thickness and 2.5 cm width. Each of the two coils, epoxied to a central quartz tube at a separation distance of 1.3 cm, has an inside diameter of 10.16 cm and an outside diameter of roughly 22.2 cm. To be compatible with the new higher-pressure cell, the inside diameter of the new coil is somewhat larger than that used previously [1]. The quartz tube is attached to a fiberglass plate supported by three quartz rods (2.54 cm diameter) that extend to another fiberglass plate resting on a part of the concrete block structure, used for rigid support of the entire apparatus. Water-cooled copper plates, insulated with thin mylar sheets, have been placed in close thermal contact with all faces of the two coils. No problems have been encountered with this arrangement for mounting and cooling the coils for use at currents to 1.5 A, which corresponds to 270 W heat dissipation in the coils.

The servocircuit is essentially the same as that used before [1] except for a new type of sensor for detecting the position of the buoy. Some problems had been encountered with the earlier densimeter [1] with pressurized fluid slowly penetrating into the coil windings of an inductance sensor, resulting in a slow change in the position of the suspended buoy. Thus, a differential capacitance sensor [13], a solid monolithic structure, has been developed for position detection in the present work that entails measurements in fluids at pressures to 35 MPa. The sensitivity of the capacitance sensor was at least equivalent to that of the linear differential transformer used previously. By balancing a bridge of which the sensor is a part, the

position of the buoy can be made insensitive to the dielectric constant of the sample fluid. For a detailed description of the capacitance sensor, see reference [13].

The previous densimeter [1] included mechanical means for fine adjustment of the position of the buoy in going from vacuum-to-liquid measurements. The new system does not incorporate this feature. Small changes in the buoy position are accomplished electronically in the new system by adjusting the offset voltage of the integrator amplifier in the servocircuit. A calibrated 0.5- $\Omega$  standard resistor, placed in series with the support coil, can handle the relatively large currents needed to lift the buoy in the present work. The measurement of the voltage drop across this resistor, which is immersed in an oil bath, enters directly into the density determination.

A 125x filar micrometer microscope is used to determine the position of the buoy. A new lens combination, which includes an objective lens (38 mm) with a larger working distance (less power) and a higher-power (14x) eyepiece, gives approximately the same magnification as with the earlier apparatus [1]. The microscope is rigidly mounted on an aluminum support table, adjustable in three dimensions. The entire assembly is secured firmly with bolts to the massive concrete block structure.

### 3.4 Concentric Cylinder Capacitor

The capacitor for dielectric constant measurements was located in the top portion of the sample space, as seen in figure 2. The central support mandrel of the capacitor was connected rigidly to the sample cell lid using a slotted brass tube, crimped at its ends, that clamped tightly over mating surfaces on the mandrel and the lid. The same type of brass tube was used to connect the differential capacitance sensor to a nut at the bottom of the capacitor. The use of the brass tubes for support of the components inside the cell resulted in an extremely rigid assembly that provided means for independent rotational orientation of each component. The coaxial leads to the differential capacitance sensor located below the capacitor passed through the brass tubes and a slot in the central support mandrel of the capacitor.

The concentric cylinder capacitor design used in the present work was based on that developed by Younglove and Straty [23]. Two slightly different capacitors are used with the present apparatus, depending on whether the measurements are for mixtures or for pure fluids. For mixture measurements, slots are cut into the cylinders parallel to the

cylindrical axes, similar to the ring and bar design of Pan et al. [24]. This modification was made to minimize the chances for composition gradients in the cell by allowing free passage of fluid mixtures between the electrodes. The vacuum capacitance of the capacitor with slotted cylinders was approximately 20 pF, while that for the one with solid cylinders was about 33 pF.

The dimensions of the capacitors used here were proportionally the same as those of Younglove and Straty [23]; however, the overall size was significantly smaller. The overall external dimensions of each capacitor were 6.4 cm length  $\times$  1.77 cm diameter. For the capacitor with slots, the widths of the five slots in each cylinder were 0.32 cm, while the slot lengths in the outer cylinder were 4.1 cm and those in the inner cylinder were 1.9 cm. The outside diameter of the inner cylinder was 1.06 cm. The outer cylinder had a thickness of 0.32 cm, while that of the inner cylinder was 0.24 cm. There was a separation distance of 0.38 mm between the cylindrical electrodes. Small pieces of Kapton<sup>2</sup> film (0.05 mm thickness) were used to insulate the electrodes from the support assembly. Both of the capacitors were fabricated from copper. A thin protective coating of gold was flashed over the surfaces.

## 4. Measurements

### 4.1 Temperature and Pressure

The primary temperature sensor, calibrated on the IPTS-68, is a platinum resistance thermometer, which had been used with the previous densimeter [1]. The uncertainty of the calibration is approximately 0.002 K. The potentiometric system for temperature measurements gives uncertainties that range from approximately 0.010 K at 100 K to 0.030 K at 300 K. The temperature of the sample space is regulated within a few mK, approximately the same as the reproducibility of the temperature measurements. A current of 1 mA for the thermometer, supplied by an electronic constant current source, is determined to an uncertainty of approximately 0.002%. The total uncertainty in the measured temperatures is estimated to be less than 0.03 K.

<sup>2</sup>In order to describe materials and experimental procedures adequately, it is occasionally necessary to identify commercial products by manufacturers' or trade names. In no instance does such identification imply endorsement by the National Bureau of Standards, nor does it imply that the particular product is necessarily the best available for that purpose.

Vapor pressure measurements on liquid nitrogen, methane, ethane, and propane at temperatures from 100–290 K have been used to check the calibration of the thermometer. Temperatures from vapor pressure measurements, using selected data from the literature, generally agreed with measured temperatures (platinum resistance thermometer) to better than 0.02 K. Further details on temperature measurements are presented in reference [1].

Temperature differences between the ends of the cell are monitored with vapor pressure bulbs located at the ends of the cell. The bulbs have been filled with the fluids mentioned above, the selected fluid depending on the temperature range needed. With the reflux tube evacuated, overall temperature differences were typically less than 0.01 K, or within the precision of the vapor pressure measurements. Thus, a differential thermocouple, with junctions placed near the vapor pressure bulbs, was not needed as part of a control loop to regulate the temperature distribution along the length of the cell.

A third vapor pressure bulb was soldered in close thermal contact with the guard ring. This vapor pressure bulb was used to check a differential thermocouple between the guard ring and the cell. This thermocouple was part of a control circuit to maintain the temperature of the guard ring approximately equal to that of the sample cell. The guard ring was connected to a copper radiation shield that surrounded the cell to provide an approximately isothermal environment for the sample space.

The techniques and instrumentation for control of the temperature of the cell are standard. Four independent heaters along the length of the cell are available, if needed, to minimize temperature gradients. Only the middle two heaters have been used in the control circuit. It should also be noted that temperature gradients along the length of the cell can be monitored by observing the vapor pressure of the liquid inside the cell as a function of the liquid level.

Pressures of the fluid under test are usually measured with a dual-range, precision oil dead-weight gauge. Its sensitivity ranges from  $2 \times 10^{-4}$  MPa at 3 MPa to  $2 \times 10^{-3}$  MPa at 35 MPa. The overall uncertainty in pressure is approximately 0.01%, increasing somewhat at lower pressure. With the high range piston, this gauge cannot be used for pressures less than 0.2 MPa; with the low range piston, the lowest pressure is approximately 0.04 MPa.

A spiral quartz Bourdon-tube gauge with a range of 0–1.38 MPa is normally used for vapor pressure measurements. It has been calibrated against an air dead-weight gauge; maximum uncertainty in the

calibration was 70 Pa. The resolution of this gauge is better than 20 Pa.

Both pressure gauges are characterized by relatively small free volumes, approximately 0.5 cm<sup>3</sup> for each. This is an important consideration when performing mixture (phase equilibria) measurements with this apparatus, e.g., to minimize vapor space corrections.

## 4.2 Density

The accuracy and precision of density measurements with the magnetic suspension technique used here depend on a knowledge of the mass and volume of the buoy, along with the capability to determine the position of the buoy with high resolution independent of the medium in which the buoy is suspended. The same barium ferrite buoy as used with the previous densimeter was employed here; its properties have been well characterized and are discussed elsewhere [1]. The mass of the buoy is 0.73706 g and its volume at 300 K is 0.13485 cm<sup>3</sup>. Thermal expansion data [25] for barium ferrite were previously obtained to calculate the volume of the buoy at low temperatures. The change in the volume of the buoy for a temperature change from 100–300 K is approximately 0.4%.

The earlier densimeter was used at relatively low pressures compared to those used now. Based on the properties of similar materials, it was estimated that the effect of pressure on the volume of the barium ferrite buoy was negligible (<0.001%) for the highest pressures (2.5 MPa) encountered with the previous densimeter. Since the new apparatus is used at pressures up to 35 MPa, bulk modulus measurements [26] have been carried out on a sample of barium ferrite, the buoy material. Bulk modulus ( $B_T$ ) data (in units of MPa) from 75–295 K are represented as a function of temperature ( $T$  in units of K) by the expression,

$$B_T = B_{295} \left( 1.01629 - \frac{0.0206014}{e^{\frac{175.15}{T-75}} - 1} \right), \quad (3)$$

where  $B_{295} = 1.3030 \times 10^5$  MPa, the bulk modulus at 295 K. Coefficients were determined from nonlinear least squares. The correction to the volume of the buoy at room temperature for a pressure of 35 MPa amounts to 0.027%.

For density measurements, it is necessary to suspend the buoy at the same position relative to the support

coil in vacuum and in the test fluid at the same temperature. Although the microscope lens combination (sec. 3.3) used here is different from that of the previous densimeter, the present arrangement results in position measurements of the same quality. The maximum error in the position determination is  $2 \times 10^{-3}$  mm, which corresponds to an error in density of less than 0.03% for a density of  $5 \times 10^2$  kg/m<sup>3</sup>, or larger.

The position of the buoy is observed through a 0.63 cm thick sapphire window in the cell. It has been observed that the apparent position of the buoy changes slowly with the pressure inside the cell; as the cell volume expands, the angle of the sapphire window changes. The magnitude of this effect has been determined as follows. First, the microscope is adjusted so that the position of the buoy is independent of the index of refraction of the fluid inside the cell. This procedure is accomplished by observing the buoy resting at a stationary position on the capacitance sensor assembly as the cell is alternately filled with gas and liquid at a pressure slightly greater than 0.1 MPa; e.g., methane at 120 K. The temperature of the cell is maintained during these tests. Then, the cell is filled with liquid at a pressure less than 0.1 MPa; either propane, isobutane, or normal butane have proved ideal for these tests at temperatures between 100 and 300 K. Then, the pressure inside the cell is increased to greater than 35 MPa while observing the buoy at rest on the sensor assembly. The change in the index of refraction for a 35-MPa change in pressure along an isotherm for liquid propane, isobutane, or normal butane is negligible compared to the change in refractive index in going from vapor-to-liquid for methane at 120 K. The change in position with pressure corresponds to a change in density with pressure of less than  $5 \times 10^{-2}$  kg/(m<sup>3</sup>·MPa) for liquid methane at 120 K.

The currents in the support coil needed to suspend the buoy in vacuum and in the fluid of interest (see eq (1)) are determined by measuring the voltage drops across a 0.5- $\Omega$  standard resistor in series with the support coil. The voltages were routinely measured to  $5 \times 10^{-6}$  V with a high resolution differential-type voltmeter, which corresponds to a change in density of less than 0.01% for a density of  $5 \times 10^2$  kg/m<sup>3</sup>.

## 4.3 Dielectric Constant

The dielectric constant is determined from a measurement of the ratio of the capacitance of the concentric cylinder capacitor with fluid between the electrodes to the capacitance under vacuum. The capacitances are measured with a three-terminal ac

bridge operated at an oscillator frequency of 5 kHz. Measurements to a resolution of  $10^{-6}$  can be obtained with little difficulty with this bridge.

Both capacitors used in this work yielded equal results within the precision of the measurements in tests on liquid methane. Measurements on mixtures are inherently more difficult and are generally characterized by greater scatter because of the difficulties associated with obtaining homogeneous liquid mixtures in the sample space. Examples of dielectric constant measurements on pure fluids and mixtures with the apparatus described here are given in references [7,19-22,27].

Measurements of the vacuum capacitance are normally obtained just before or just after fluid measurements are performed. Since vacuum measurements are required for each run in the density measuring technique used here, there was no reason vacuum capacitances should not be recorded at the same time. Thus, there was no reason to acquire a calibration curve representing the vacuum capacitance as a function of temperature. Vacuum measurements can be made to a precision of  $10^{-4}$  pF and are usually stable within 0.0002 pF when the sample cell is cycled between low temperature and room temperature. (Vacuum capacitances have been observed to be stable to better than  $10^{-3}$  pF for more than 20 temperature cycles over a period of several months.) The total change in the vacuum capacitance from 300-100 K is approximately 0.3%. Based on tests by Younglove and Straty [23] on a similar cylindrical capacitor, the effect of pressure on the capacitor was sufficiently small to neglect. It is estimated that, based on the resolution of the capacitance measurements and the stability of the capacitor design, the total uncertainty in the dielectric constant measurements is approximately 0.01%.

## 5. Performance of Apparatus

### 5.1 Results and Discussion

Before completing measurements for the LNG density project, it was necessary to ensure that the new densimeter yielded results consistent with those from the previous densimeter. First, density data were obtained for several components of LNG (e.g., methane, ethane, etc.); the data obtained with the new apparatus agreed to better than 0.02% with the results [1,3,4] determined at the onset of the LNG density project with the earlier version [1] of the magnetic suspension densimeter. As mentioned earlier, measurements on saturated liquid methane were used as a check on the measurement process during the entirety of the LNG density project. Dielectric

constant data for liquid methane exhibited differences of  $<0.01\%$  when compared with the data of Straty and Goodwin [28].

Next, data were obtained for a binary mixture of methane and ethane, a system that had been extensively investigated with the earlier densimeter. The data for three mixtures of methane and ethane had been used to optimize several mathematical models [15-18] developed for prediction of LNG densities. The most accurate and versatile of these models was the extended corresponding states method [15-17]. The new data for a methane+ethane mixture would be compared with predictions from this model. The mixture, for which data are reported here, had also been used to cross-check results from this laboratory obtained with the magnetic suspension densimeter with those from another laboratory that employed an entirely different technique for determining density [29]. The experimental density of Miller and Hiza [29] for this methane+ethane mixture at 110.08 K differed by 0.01% from that calculated from the extended corresponding states model [16].

The experimental orthobaric liquid densities, vapor pressures, and dielectric constants of a 0.85147  $\text{CH}_4$ +0.14853  $\text{C}_2\text{H}_6$  mixture are presented as a function of temperature in table 1. Excess volumes and values for the Clausius-Mossotti (CM) function, as well as values for the excess function, are also given in table 1. The excess volume ( $V^E$ ) is defined by the relation,

$$V^E = V - \sum_i x_i V_i [1 + \beta_i (p_i - p)], \quad (4)$$

where  $V$  is the molar volume of the mixture at a given temperature at saturation pressure  $p$ ,  $V_i$  is the molar volume of component  $i$  at the same temperature at saturation pressure  $p_i$ ,  $x_i$  is the mole fraction of component  $i$ , and  $\beta_i$  is the isothermal compressibility of component  $i$ . The CM function is defined by the expression,

$$\text{CM} = \frac{1}{\rho} \left( \frac{\epsilon - 1}{\epsilon + 2} \right), \quad (5)$$

where  $\rho$  is the density and  $\epsilon$  is the dielectric constant. Then the excess Clausius-Mossotti function ( $\text{CM}^E$ ) for a liquid mixture is defined, analogous to  $V^E$ , by the relation,

$$\text{CM}^E = \text{CM} - \sum_i x_i \text{CM}_i, \quad (6)$$

**Table 1.** Orthobaric liquid densities ( $\rho$ ) and dielectric constants ( $\epsilon$ ) of 0.85147 CH<sub>4</sub>+0.14853 C<sub>2</sub>H<sub>6</sub> mixture (molecular weight = 18.1265 g·mol<sup>-1</sup>) as a function of temperature ( $T$ ) and pressure ( $P$ ).  $\rho_{\text{CSM}}$ , density calculated from extended corresponding states model;  $V^E$ , excess volume; CM, Clausius-Mossotti function;  $\text{CM}^E$ , excess Clausius-Mossotti function.

$T$ K	$P$ MPa	$\rho$ mol·dm <sup>-3</sup>	$\frac{10^3(\rho_{\text{CSM}}-\rho_{\text{CSM}})}{\rho_{\text{CSM}}}$	$V^E$ cm <sup>3</sup> ·mol <sup>-1</sup>	$\epsilon$	CM cm <sup>3</sup> ·mol <sup>-1</sup>	$\text{CM}^E$ cm <sup>3</sup> ·mol <sup>-1</sup>
115.00	0.116	25.3618	-0.059	-0.410	1.67297	7.2243	0.005
120.00	0.166	24.9911	-0.013	-0.493	1.66070	7.2220	0.000
125.00	0.232	24.5983	-0.045	-0.567	1.64828	7.2239	-0.001
130.00	0.316	24.1950	-0.036	-0.655	1.63561	7.2258	-0.003

where CM refers to the Clausius-Mossotti function of the mixture at a given temperature at the saturation pressure of the mixture, and  $\text{CM}_i$  is the Clausius-Mossotti function of pure component  $i$  at the same temperature and pressure as the mixture. Adjustments of the pure component  $\text{CM}_i$ 's to the saturation pressure of the mixture are sufficiently small to neglect.

In the calculation of  $V^E$  and  $\text{CM}_i$ , the pure component molar volumes of methane and ethane were calculated from equations in references [1,3] obtained from fitting experimental orthobaric liquid densities determined with the earlier version of the magnetic suspension densimeter used in the LNG density project. Vapor pressures for methane and ethane were taken from Goodwin [30] and from Goodwin et al. [31], respectively. Isothermal compressibilities for methane were taken from Rowlinson [32]; those for ethane from Miller [33]. The dielectric constants of Straty and Goodwin [28] were used for methane, while those of Weber [34] were used for ethane.

Also presented in table 1 are comparisons between the experimental densities ( $\rho_{\text{exp}}$ ) from this work and densities ( $\rho_{\text{CSM}}$ ) calculated from the extended corresponding states model [15-17]. The average absolute deviation is 0.038%. This result, combined with the pure fluid comparisons, demonstrates that data obtained with the new densimeter are consistent with data taken with the previous instrument. The total uncertainty of a single density measurement for these binary mixture data is estimated to be  $\pm 0.1\%$ . The present results are also consistent within experimental error with the data point of Miller and Hiza [29] for the same mixture.

The calculated excess Clausius-Mossotti values were less than 0.07% of the mixture CM values for the methane+ethane mixture data presented here. This result was expected based on dielectric constant and density measurements on other mixtures containing nonpolar constituents [7,9,24]. It appears that the excess CM values show a slow decrease with

increasing temperature.

After the new apparatus had been thoroughly tested, it was used to complete the measurements for the LNG density project [7,9]. Next, the apparatus was used to obtain data for propane [19-20], isobutane [19,21], and normal butane [19,22] at pressures up to 35 MPa. The performance of the apparatus at high pressures is demonstrated by these pure fluid data.

## 5.2 Error Analysis

Detailed discussions of the systematic and random errors involved in measurements with the magnetic suspension densimeter used in the present work have been presented elsewhere [1,3-9, 19-22]. The uncertainty in the density measurements depends primarily on the uncertainties in the determination of the volume of the buoy, of the relative position of the buoy and the support coil, and of the temperature of the sample fluid. With the new apparatus, designed for higher pressures than the previous one, the effect of pressure on the apparent position of the buoy, resulting from slight movement of the cell window, must now be included. Maximum uncertainty in the density determination resulting from this effect is 0.02%.

The effect of pressure on the volume of the buoy, which is extremely small at maximum design pressure of the cell, must also be considered. As discussed in section 3.3, the reduction in the buoy volume for a pressure of 35 MPa is 0.027%. The uncertainty involved in this adjustment is negligible.

As discussed [1], the total uncertainty of a single density measurement is taken as the square root of the sum of the squares of the systematic errors plus an allowance of three times the standard deviation for random error. The imprecision of measurement (or standard deviation) is typically less than 0.02%. Both the precision and accuracy of density measurements with a magnetic suspension densimeter depend on the difference between the density of the buoy and the

density of the fluid. For the present arrangement, where the density of the buoy is significantly larger (typically an order of magnitude) than the density of the fluids, the precision and total uncertainty change slowly with fluid density. The total systematic error in the measurement process from known sources is approximately 0.05% at low temperatures, decreasing to approximately 0.03% at room temperature. This results in an estimated total uncertainty in the density of approximately 0.1% at low temperatures and 0.06% at room temperature. (Of course, the uncertainty in the density determination also depends on the values of the derivatives,  $(\partial\rho/\partial P)_T$  and  $(\partial\rho/\partial T)_P$ , for the particular region of the PVT surface for the fluid under investigation.)

The uncertainties in the dielectric constant determination have been discussed in detail (sec. 4.3 and refs. [7,9,19-22]). The total uncertainty in the dielectric constant measurement is estimated to be approximately 0.01%.

The estimates of the uncertainties in the density and dielectric constant measurements can be tested to some degree by making comparisons with reliable data from independent sources. Such comparisons have been made for many fluids over wide ranges of experimental parameters (such as temperature, pressure, density, etc.) [7,9,19-22]. In general, these comparisons have confirmed the estimates of the uncertainty levels.

There has been little information presented in this paper concerning the problems associated with mixture measurements compared to pure fluid measurements. The uncertainties involved in the determination of the composition of mixtures have been discussed in detail in previous papers [1,5-9].

---

The authors are grateful to the following individuals who made significant contributions in the development of this apparatus. W. R. Bjorklund, A. N. DiSalvo, W. G. Layne (deceased), and D. L. Smith assisted in the fabrication of the apparatus. M. J. Hiza participated in many fruitful discussions. H. M. Ledbetter provided prepublished bulk modulus data for barium ferrite.

## 6. References

- [1] Haynes, W. M.; Hiza, M. J.; Frederick, N. V. Magnetic suspension densimeter for measurements on fluids of cryogenic interest. *Rev. Sci. Instrum.* **47**(10): 1237-1250; 1976 October.
- [2] Haynes, W. M. Simplified magnetic suspension densimeter for absolute density measurements. *Rev. Sci. Instrum.* **48**(1): 39-41; 1977 January.
- [3] Haynes, W. M.; Hiza, M. J. Measurements of the orthobaric liquid densities of methane, ethane, propane, isobutane, and normal butane, *J. Chem. Thermodyn.* **9**(2): 179-187; 1977 February.
- [4] Haynes, W. M.; Hiza, M. J. Orthobaric liquid densities of normal butane from 135 to 300 K as determined with a magnetic suspension densimeter. *Advances in Cryogenic Engineering*, Vol. 21. Timmerhaus, K. D.; Weitzel, D. H., ed. New York, NY: Plenum Press; 1976 516-521.
- [5] Hiza, M. J.; Haynes, W. M.; Parrish, W. R. Orthobaric liquid densities and excess volumes for binary mixtures of low molar-mass alkanes and nitrogen between 105 and 140 K. *J. Chem. Thermodyn.* **9**(9): 873-896; 1977 September.
- [6] Hiza, M. J.; Haynes, W. M. Liquid mixture excess volumes and total vapor pressures using a magnetic suspension densimeter with compositions determined by chromatographic analysis: methane plus ethane. *Advances in Cryogenic Engineering*, Vol. 23. Timmerhaus, K. D., ed. New York, NY: Plenum Press; 1976; 594-601.
- [7] Haynes, W. M. Orthobaric liquid densities and dielectric constants of (methane+isobutane) and (methane+normal butane) at low temperatures. *J. Chem. Thermodyn.* to be published.
- [8] Hiza, M. J.; Haynes, W. M. Orthobaric liquid densities and excess volumes for multicomponent mixtures of low molar-mass alkanes and nitrogen between 105 and 125 K. *J. Chem. Thermodyn.* **12**(1): 1-10; 1980 January.
- [9] Haynes, W. M. Measurements of orthobaric-liquid densities of multicomponent mixtures of LNG components ( $N_2$ ,  $CH_4$ ,  $C_2H_6$ ,  $C_3H_8$ ,  $CH_3CH(CH_3)CH_3$ ,  $C_4H_{10}$ ,  $CH_3CH(CH_3)C_2H_5$ , and  $C_5H_{12}$ ) between 110 and 130 K. *J. Chem. Thermodyn.* **14**(7): 603-612; 1982 July.
- [10] Goodwin, R. D. Apparatus for determination of pressure-density-temperature relations and specific heats of hydrogen to 350 atmospheres at temperatures above 14 K. *J. Res. Natl. Bur. Stand. (U.S.)* **65C**(4): 231-243; 1961 October-December.
- [11] Prydz, R.; Straty, G. C. The thermodynamic properties of compressed gaseous and liquid fluorine. *Natl. Bur. Stand. (U.S.) Tech. Note* 392; 1970 October; 182 p.
- [12] Straty, G. C.; Prydz, R. Fluorine compatible apparatus for accurate PVT measurements. *Rev. Sci. Instrum.* **41**(8): 1223-1227; 1970 August.
- [13] Straty, G. C. ( $p, V, T$ ) of compressed fluid ethene. *J. Chem. Thermodyn.* **12**(8): 709-716; 1980 August.
- [14] Frederick, N. V.; Haynes, W. M. Differential capacitance sensor as position detector for a magnetic suspension densimeter. *Rev. Sci. Instrum.* **50**(9): 1154-1155; 1979 September.
- [15] McCarty, R. D. A comparison of mathematical models for the prediction of LNG densities. *Natl. Bur. Stand. (U.S.) NBSIR* 77-867; 1977 October. 60 p.

- [16] McCarty, R. D. Four mathematical models for the prediction of LNG densities. *Natl. Bur. Stand. (U.S.) Tech. Note* 1030; 1980 December. 76 p.
- [17] McCarty, R. D. Mathematical models for the prediction of liquefied-natural-gas densities. *J. Chem. Thermodyn.* 14(9): 837-854; 1982 September.
- [18] Hiza, M. J. An empirical excess volume model for estimating liquefied natural gas densities. *Fluid Phase Equilibria* 2(2): 27-38; 1978 August.
- [19] Haynes, W. M.; Younglove, B. A. Dielectric constants of saturated liquid propane, isobutane, and normal butane. *Advances in Cryogenic Engineering*, Vol. 27. Fast, R. W., ed. New York, NY: Plenum Press; 1982. 883-891.
- [20] Haynes, W. M. Measurements of densities and dielectric constants of liquid propane from 90 to 300 K at pressures to 35 MPa. *J. Chem. Thermodyn.* to be published.
- [21] Haynes, W. M. Measurements of densities and dielectric constants of liquid isobutane from 120 to 300 K at pressures to 35 MPa. *J. Chem. Eng. Data.* to be published.
- [22] Haynes, W. M. Measurements of densities and dielectric constants of liquid normal butane from 140 to 300 K at pressures to 35 MPa. *J. Chem. Thermodyn.* to be published.
- [23] Younglove, B. A.; Straty, G. C. A capacitor for accurate wide range dielectric constant measurements on compressed fluids. *Rev. Sci. Instrum.* 41(7): 1087-1089; 1970 July.
- [24] Pan, W. P.; Mady, M. H.; Miller, R. C. Dielectric constants and Clausius-Mossotti functions for simple liquid mixtures: systems containing nitrogen, argon and light hydrocarbons. *AIChE J.* 21(2): 283-289; 1975 March.
- [25] Clark, A. F.; Haynes, W. M.; Deason, V. A.; Trapani, R. J. Low temperature thermal expansion of barium ferrite. *Cryogenics* 16(3): 267-270; 1976 May.
- [26] Ledbetter, H. M. Fracture and Deformation Division, National Engineering Laboratory, National Bureau of Standards, Boulder, CO 80303. private communication.
- [27] Haynes, W. M.; McCarty, R. D. Prediction of liquefied-natural-gas (LNG) densities from dielectric constant measurements. *Cryogenics.* to be published.
- [28] Straty, G. C.; Goodwin, R. D. Dielectric constant and polarizability of saturated and compressed fluid methane. *Cryogenics* 13(12): 712-715; 1973 December.
- [29] Miller, R. C.; Hiza, M. J. Experimental molar volumes for some LNG-related saturated liquid mixtures. *Fluid Phase Equilibria* 2(1): 49-57; 1978 August.
- [30] Goodwin, R. D. The thermophysical properties of methane, from 90 to 500 K at pressures to 700 bar. *Natl. Bur. Stand. (U.S.) Tech. Note* 653; 1974 April; 274 p.
- [31] Goodwin, R. D.; Roder, H. M.; Straty, G. C. Thermophysical properties of ethane, from 90 to 600 K at pressures to 700 bar. *Natl. Bur. Stand. (U.S.) Tech. Note* 684; 1976 August. 319 p.
- [32] Rowlinson, J. S. *Liquid and Liquid Mixtures*. 2nd Ed. London: Butterworths; 1969. 51.
- [33] Miller, R. C. Estimating the densities of natural gas mixtures. *Chem. Eng.* 81(23): 134-135; 1974 October.
- [34] Weber, L. A. Dielectric constant data and the derived Clausius-Mossotti function for compressed gaseous and liquid ethane. *J. Chem. Phys.* 65(1): 446-449; 1976 July.

M-700

J. Chem. Thermodyn. Vol 9, No. 2, 179-87 (Feb 1977)

## Measurements of the orthobaric liquid densities of methane, ethane, propane, isobutane, and normal butane<sup>a</sup>

W. M. HAYNES and M. J. HIZA

*Cryogenics Division, National Bureau of Standards,  
Institute for Basic Standards, Boulder, Colorado 80302, U.S.A.*

*(Received 9 August 1976)*

The orthobaric liquid densities of the major components of natural gas have been determined with a magnetic suspension densimeter. This paper reports results for methane (105 to 160 K), ethane (100 to 270 K), propane (100 to 288 K), isobutane (115 to 300 K), and normal butane (135 to 300 K). The imprecision of the measured densities is approximately 0.015 per cent; the estimated overall uncertainty is 0.1 per cent at low temperatures and decreases to 0.06 per cent at 300 K. A simple expression has been used to represent the densities as a function of temperature. Comprehensive comparisons with the experimental results of other investigators are presented.

### 1. Introduction

Liquefied natural gas (LNG) is expected to become an increasingly important commodity on the world energy market. The basis for sale of LNG is its total heating value, which requires a knowledge of both density and composition. A project was initiated at this laboratory to provide orthobaric (saturated) liquid densities for the major components of LNG, and for mixtures of these components. The densities will be used to develop a mathematical model or correlation that predicts the density of LNG type mixtures with an inaccuracy of 0.1 per cent, given a knowledge of the composition and temperature of the liquid. In the development of an accurate mathematical model (correlation), it is important to have both an accurate and an internally consistent set of density data.

Before this project was started there were significant temperature ranges for which saturated (orthobaric) liquid density data did not exist for some of the major components of LNG. For nitrogen and methane there were discrepancies as large as 0.5 per cent between different sets of data. Not only was it important to fill in

<sup>a</sup> This work was carried out at the National Bureau of Standards under the sponsorship of British Gas Corp., Chicago Bridge and Iron Co., Columbia Gas Service Corp., Distrigas Corp., Easco Gas LNG, Inc., El Paso Natural Gas, Gaz de France, Marathon Oil Co., Mobil R&D Corp., Natural Gas Pipeline Co., Phillips Petroleum Co., Shell International Gas, Ltd., Sonatrach, Southern California Gas Co., Tennessee Gas Pipeline, Texas Eastern Transmission Co., Tokyo Gas Co., Ltd., and Transcontinental Gas Pipe Line Corp., through a grant administered by the American Gas Association, Inc.

gaps, but also to provide new independent measurements of sufficient accuracy to help resolve inconsistencies.

In this paper orthobaric liquid densities for methane, ethane, propane, isobutane, and normal butane are reported. Results for nitrogen were presented in an earlier paper.<sup>(1)</sup> Major emphasis has been placed on the low temperature region of 105 to 140 K; however, measurements have been carried out to 160 K for methane, to 270 K for ethane, to 288.7 K for propane, and to 300 K for isobutane and normal butane. The densities have been represented as a function of temperature with an expression that is used to facilitate comparisons with other measurements.

The present measurements were carried out with a magnetic suspension densimeter.<sup>(1)</sup> In this method a magnetic buoy is freely suspended in the liquid of interest by the force generated from the axial magnetic fields of air-core solenoids. The motion of the buoy is controlled by the automatic regulation of a servo-circuit. The magnetic force necessary to maintain the buoy at a given position is inversely proportional to the buoyant force on the buoy. Thus, using Archimedes' principle, along with measurements of the mass and volume of the buoy, the density of the liquid is obtained.

## 2. Experimental

The experimental apparatus and its operation have been described in detail elsewhere.<sup>(1)</sup> At low temperatures the experimental procedures for the measurements on the hydrocarbons other than methane differed significantly from those for nitrogen and methane. The density of a given fluid is determined from measurements of the magnetic force necessary to support a barium ferrite buoy in a vacuum and in the fluid at the same position and temperature. For nitrogen and methane the vacuum measurements were performed immediately before or after the liquid measurements. At low temperatures it has been found impossible to evacuate the sample cell within a reasonable time after it has been filled with one of the heavier hydrocarbons. Most of the liquid can be removed by pressurizing with helium gas; however, a liquid film is left on the surfaces, including those of the buoy, inside the cell. The buoy cannot be brought into support until the film is removed. Thus, for the heavy hydrocarbons at low temperatures, the vacuum points must be obtained before the liquid measurements.

So that more than one point could be obtained in a given day for a heavy hydrocarbon at low temperatures, vacuum points were obtained at two temperatures separated by 5 K before liquid was condensed into the cell. Then the liquid measurements were performed at each of these temperatures. Performance tests had demonstrated that the barium ferrite buoy does not exhibit any detectable hysteresis at low temperatures within the precision of the current measurements for a temperature range of, at least, 20 K. After the vacuum and liquid measurements were performed for one of the heavy hydrocarbons at low temperatures the cell was warmed to a temperature above the normal boiling temperature of the test fluid for evacuation.

Methane was used as a control fluid during the heavy-hydrocarbon measurements at low temperatures. Each day a new methane point was taken to insure that the

warm-up and cool-down of the apparatus did not affect the apparent position of the buoy from liquid-to-vacuum measurements. The position of the buoy was determined with a high-powered microscope that had been adjusted initially so that the apparent position of the buoy did not depend on the index of refraction of the fluid inside the cell. It was found that the temperature cycling of the cell had no detectable effect on the apparent buoy position.

Some of the results presented in this paper were taken with a one-coil system instead of the three-coil arrangement described in the apparatus paper.<sup>(1)</sup> The evolution to the use of only one coil is discussed in reference 2.

All of the gases were of research grade quality. The minimum purities as specified by the suppliers were 99.9 moles per cent for isobutane and normal butane and 99.99 moles per cent for methane, ethane, and propane. The gases were analyzed chromatographically with a thermal-conductivity detector and found to be within the specified purities except for isobutane. It was found that the isobutane contained approximately 0.15 per cent of normal butane. This relatively large amount of normal-butane impurity has a negligible effect (< 0.01 per cent) on the density results.

The methane gas was passed through a room-temperature molecular-sieve trap to remove moisture and any heavy contaminants not detected by analysis. The other hydrocarbon gases were normally not passed through a molecular-sieve trap.

### 3. Results

The experimental orthobaric liquid densities of methane, ethane, propane, isobutane, and normal butane are presented as a function of temperature (IPTS-68) in tables 1 to 5. The relatively large number of points for methane at any given temperature resulted from the use of methane as a control fluid throughout the project. Although the mean experimental densities of methane have been given in an earlier paper<sup>(1)</sup> they are presented again here, along with other information (calculated densities, etc.), so that the orthobaric liquid densities of all the low molecular-weight alkanes

TABLE 1. Orthobaric liquid densities of methane, where  $T$  is the temperature (IPTS-68),  $\rho_{\text{expt}}$  is the mean experimental density for  $n$  observations at a given temperature,  $\rho_{\text{calc}}$  is the density calculated from equation (1) and  $\Delta_{\text{max}}$  is the largest value of  $(\rho_{\text{expt}} - \rho_{\text{calc}})/\rho_{\text{calc}}$

$T/K$	$\rho_{\text{expt}}/\text{mol dm}^{-3}$	$n$	$\rho_{\text{calc}}/\text{mol dm}^{-3}$	$10^2 \Delta_{\text{max}}$
105.000	26.9458	12	26.9456	0.030
110.000	26.4985	11	26.5005	0.035
115.000	26.0443	12	26.0429	0.028
120.000	25.5721	17	25.5712	0.036
125.000	25.0845	18	25.0839	0.037
130.000	24.5775	16	24.5790	0.036
135.000	24.0540	23	24.0540	0.031
140.000	23.5067	5	23.5060	0.024
145.000	22.9312	5	22.9311	0.024
150.000	22.3218	2	22.3243	0.014
160.000	20.9876	2	20.9857	0.037

TABLE 2. Orthobaric liquid densities of ethane, where  $T$  is the temperature (IPTS-68),  $\rho_{\text{expt}}$  is the experimental density,  $\rho_{\text{calc}}$  is the density calculated from equation (1), and  $\Delta$  is the value of  $(\rho_{\text{expt}} - \rho_{\text{calc}})/\rho_{\text{calc}}$

$T$ K	$\rho_{\text{expt}}$ mol dm <sup>-3</sup>	$\rho_{\text{calc}}$ mol dm <sup>-3</sup>	$10^2\Delta$	$T$ K	$\rho_{\text{expt}}$ mol dm <sup>-3</sup>	$\rho_{\text{calc}}$ mol dm <sup>-3</sup>	$10^2\Delta$
100.000	21.3408	21.3388	0.009	170.000	18.6867	18.6869	-0.001
105.000	21.1585	21.1568	0.008	180.000	18.2793	18.2787	0.003
110.000	20.9746	20.9742	0.002	190.000	17.8612	17.8586	0.015
115.000	20.7927	20.7907	0.010	200.000	17.4289	17.4240	0.028
120.000	20.6022	20.6063	-0.020	210.000	16.9713	16.9720	-0.004
125.000	20.4186	20.4208	-0.011	220.000	16.4988	16.4989	-0.001
130.000	20.2317	20.2343	-0.013	230.000	15.9973	15.9994	-0.013
135.000	20.0461	20.0466	-0.002	240.000	15.4642	15.4670	-0.018
140.000	19.8566	19.8575	-0.005	250.000	14.8899	14.8919	-0.013
150.000	19.4751	19.4748	0.002	260.000	14.2610	14.2598	0.008
160.000	19.0857	19.0850	0.004	270.000	13.5493	13.5477	0.012

TABLE 3. Orthobaric liquid densities of propane, where  $T$  is the temperature (IPTS-68),  $\rho_{\text{expt}}$  is the experimental density,  $\rho_{\text{calc}}$  is the density calculated from equation (1), and  $\Delta$  is the value of  $(\rho_{\text{expt}} - \rho_{\text{calc}})/\rho_{\text{calc}}$

$T$ K	$\rho_{\text{expt}}$ mol dm <sup>-3</sup>	$\rho_{\text{calc}}$ mol dm <sup>-3</sup>	$10^2\Delta$	$T$ K	$\rho_{\text{expt}}$ mol dm <sup>-3</sup>	$\rho_{\text{calc}}$ mol dm <sup>-3</sup>	$10^2\Delta$
100.075	16.3065	16.3048	0.011	140.075	15.3751	15.3755	-0.002
105.075	16.1872	16.1885	-0.008	145.075	15.2588	15.2590	-0.002
110.075	16.0718	16.0723	-0.003	150.075	15.1400	15.1424	-0.016
115.075	15.9557	15.9562	-0.003	200.000	13.9560	13.9524	0.026
120.075	15.8411	15.8401	0.006	240.000	12.9271	12.9285	-0.010
125.075	15.7250	15.7241	0.006	270.000	12.0733	12.0742	-0.008
130.075	15.6085	15.6080	0.003	280.000	11.7622	11.7631	-0.008
135.075	15.4910	15.4918	-0.005	288.706	11.4790	11.4775	0.013

TABLE 4. Orthobaric liquid densities of isobutane, where  $T$  is the temperature (IPTS-68),  $\rho_{\text{expt}}$  is the experimental density,  $\rho_{\text{calc}}$  is the density calculated from equation (1), and  $\Delta$  is the value of  $(\rho_{\text{expt}} - \rho_{\text{calc}})/\rho_{\text{calc}}$

$T$ K	$\rho_{\text{expt}}$ mol dm <sup>-3</sup>	$\rho_{\text{calc}}$ mol dm <sup>-3</sup>	$10^2\Delta$	$T$ K	$\rho_{\text{expt}}$ mol dm <sup>-3</sup>	$\rho_{\text{calc}}$ mol dm <sup>-3</sup>	$10^2\Delta$
115.075	12.7305	12.7313	-0.006	145.075	12.2353	12.2372	-0.015
120.075	12.6489	12.6491	-0.001	150.075	12.1534	12.1544	-0.008
125.075	12.5687	12.5669	0.015	228.000	10.8273	10.8263	0.009
130.075	12.4850	12.4846	0.003	288.706	9.6676	9.6687	-0.012
135.075	12.4015	12.4022	-0.005	290.000	9.6411	9.6417	-0.007
140.075	12.3215	12.3197	0.014	300.000	9.4300	9.4287	0.014

TABLE 5. Orthobaric liquid densities of normal butane, where  $T$  is the temperature (IPTS-68),  $\rho_{\text{expt}}$  is the experimental density,  $\rho_{\text{calc}}$  is the density calculated from equation (1), and  $\Delta$  is the value of  $(\rho_{\text{expt}} - \rho_{\text{calc}})/\rho_{\text{calc}}$ 

$T$ K	$\frac{\rho_{\text{expt}}}{\text{mol dm}^{-3}}$	$\frac{\rho_{\text{calc}}}{\text{mol dm}^{-3}}$	$10^2\Delta$	$T$ K	$\frac{\rho_{\text{expt}}}{\text{mol dm}^{-3}}$	$\frac{\rho_{\text{calc}}}{\text{mol dm}^{-3}}$	$10^2\Delta$
135.075	12.6517	12.6524	-0.005	165.075	12.1634	12.1659	-0.020
140.075	12.5706	12.5714	-0.006	170.075	12.0839	12.0846	-0.005
145.075	12.4920	12.4904	0.013	230.000	11.0911	11.0905	0.005
150.075	12.4089	12.4093	-0.003	288.706	10.0325	10.0324	0.001
155.075	12.3299	12.3283	0.014	290.000	10.0067	10.0073	-0.007
160.075	12.2484	12.2471	0.010	300.000	9.8103	9.8099	0.004

investigated in the present work are included in a single paper. All of the experimental points for methane will be presented in a future report.<sup>(3)</sup> Each methane point was taken from a new filling of the cell. For the other hydrocarbons no more than two points were taken from a single filling.

The experimental densities  $\rho$  have been fitted as a function of temperature  $T$  to the expression:

$$(\rho - \rho_c)/\text{mol dm}^{-3} = a(1 - T/T_c)^{0.35} + \sum_{i=1}^3 b_i(1 - T/T_c)^{(1+(i-1)/3)}, \quad (1)$$

which incorporates a scaling-law modification<sup>(4)</sup> to a generalized Guggenheim equation.<sup>(5)</sup> The coefficients  $a$ ,  $b_i$  determined by least squares, and selected values of the critical temperature  $T_c$  and density  $\rho_c$  for each fluid are given in table 6.<sup>(6-11)</sup> Only three coefficients were needed to fit the results for methane, which covered a relatively small temperature range compared with that for the other fluids.

The residual standard deviations of the fit to equation (1) for each fluid are given in table 6. These values substantiate the estimate of the imprecision of the density measurements, which is approximately 0.015 per cent. The estimated inaccuracy in

TABLE 6. Parameters of equation (1),

$$(\rho - \rho_c)/\text{mol dm}^{-3} = a(1 - T/T_c)^{0.35} + \sum_{i=1}^3 b_i(1 - T/T_c)^{(1+(i-1)/3)}$$

where  $T_c$  and  $\rho_c$  are the critical temperature and density. The coefficients  $a$ ,  $b_1$ ,  $b_2$ ,  $b_3$  were obtained from a least-squares program in which the experimental mass densities to five digits were converted to molar densities within the program. The standard deviations  $\sigma$  and molar masses  $M$  are also given

	Methane	Ethane	Propane	Isobutane	Normal butane
$a$	18.65812	12.55205	8.684459	7.657535	7.286063
$b_1$	6.712030	13.43284	18.04086	8.145251	11.96308
$b_2$	-0.9472020	-19.00461	-29.46261	-13.10582	-19.87592
$b_3$		11.07716	16.43559	8.145894	11.60211
$T_c/\text{K}$	190.555 <sup>(6)</sup>	305.33 <sup>(8)</sup>	369.82 <sup>(9)</sup>	408.13 <sup>(10)</sup>	425.16 <sup>(11)</sup>
$\rho_c/\text{mol dm}^{-3}$	10.16 <sup>(7)</sup>	6.86 <sup>(8)</sup>	5.00 <sup>(9)</sup>	3.80 <sup>(10)</sup>	3.92 <sup>(11)</sup>
$10^2\sigma/\langle\rho\rangle$	0.016	0.012	0.011	0.013	0.012
$M/\text{g mol}^{-1}$	16.04303	30.07012	44.09721	58.1243	58.1243

the densities is 0.1 per cent at low temperatures and decreases to 0.06 per cent at 300 K. The total uncertainty in the reported temperatures is estimated to be less than 30 mK at 100 K and less than 40 mK at 300 K. These uncertainty limits in the temperature correspond to a maximum uncertainty of 0.02 per cent in the density for the results reported in this paper. A detailed error analysis of the magnetic suspension densimeter used in the present work has been given elsewhere.<sup>(1)</sup>

Equation (1), along with the parameters given in table 6, has been used for comparisons of the present results with independent experimental data.<sup>(8, 12-25)</sup> Deviation plots for ethane, propane, isobutane, and normal butane are presented in figures 1

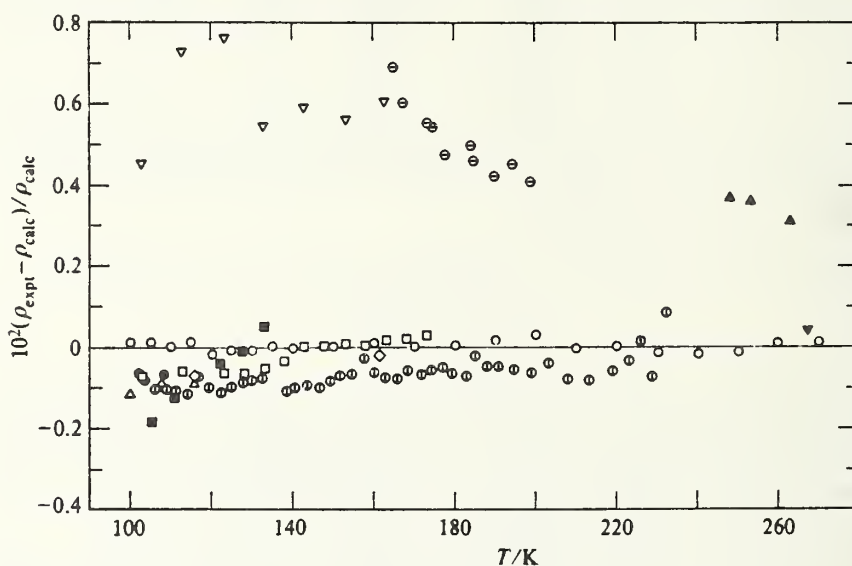


FIGURE 1. Deviation plot of experimental orthobaric liquid densities of ethane compared with values calculated from equation (1) using parameters from table 6.  $\circ$ , present results;  $\bullet$ , Shana'a and Canfield;<sup>(12)</sup>  $\diamond$ , Chui and Canfield;<sup>(13)</sup>  $\odot$ , Orrit and Olives;<sup>(14)</sup>  $\triangle$ , Rodosevich and Miller;<sup>(15)</sup>  $\square$ , McClune;<sup>(16)</sup>  $\blacksquare$ , Klosek and McKinley;<sup>(17)</sup>  $\blacktriangle$ , Douslin and Harrison;<sup>(18)</sup>  $\ominus$ , Maass and Wright;<sup>(19)</sup>  $\nabla$ , Jensen and Kurata;<sup>(20)</sup>  $\blacktriangledown$ , Kahre.<sup>(21)</sup>

through 4. The deviation plot for methane was presented in an earlier paper;<sup>(1)</sup> thus, it is not included here.

In comparing the results of other investigators with equation (1) some general trends are observed. Below 140 K the densities of Shana'a and Canfield,<sup>(12)</sup> Chui and Canfield,<sup>(13)</sup> Orrit and Olives,<sup>(14)</sup> Rodosevich and Miller,<sup>(15)</sup> McClune,<sup>(16)</sup> and Klosek and McKinley<sup>(17)</sup> are generally lower than the present results by 0.05 to 0.1 per cent. Exceptions to this trend are: for isobutane the densities of Rodosevich and Miller<sup>(15)</sup> between 114 and 120 K are larger (maximum of 0.1 per cent) than the present results and exhibit a significantly different temperature dependence; and for ethane the change in density with temperature reported by Klosek and McKinley<sup>(17)</sup> is appreciably larger than that observed in the present work.

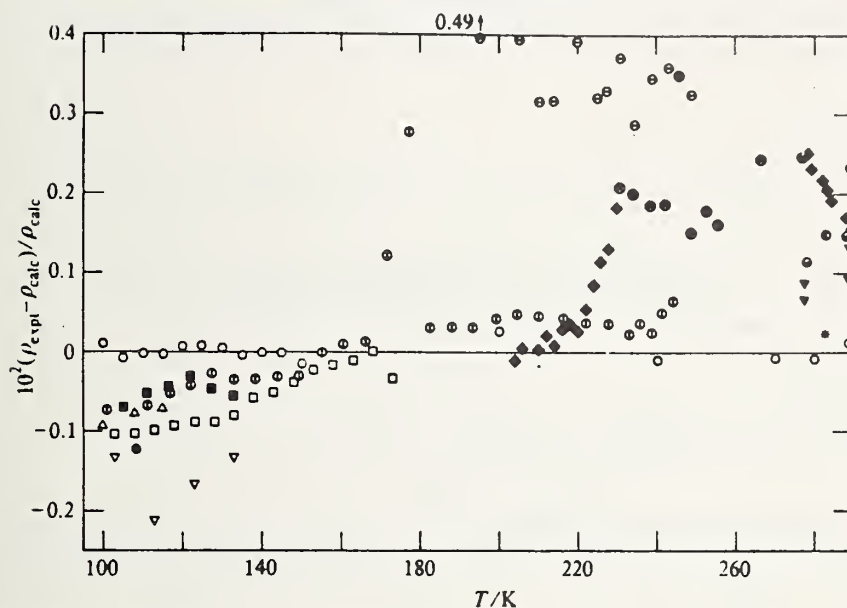


FIGURE 2. Deviation plot of experimental orthobaric liquid densities of propane compared with values calculated from equation (1) using parameters from table 6.  $\circ$ , present results;  $*$ , Sliwinski;<sup>(6)</sup>  $\bullet$ , Shana'a and Canfield;<sup>(12)</sup>  $\oplus$ , Orrit and Olives;<sup>(14)</sup>  $\triangle$ , Rodosevich and Miller;<sup>(15)</sup>  $\square$ , McClune;<sup>(16)</sup>  $\blacksquare$ , Klosek and McKinley;<sup>(17)</sup>  $\ominus$ , Maass and Wright;<sup>(19)</sup>  $\nabla$ , Jensen and Kurata;<sup>(20)</sup>  $\blacktriangledown$ , Kahre;<sup>(21)</sup>  $\odot$ , Tomlinson;<sup>(22)</sup>  $\blacklozenge$ , Seeman and Urban;<sup>(23)</sup>  $\otimes$ , NGAA;<sup>(24)</sup>  $\bullet$ , Van der Vet.<sup>(25)</sup>

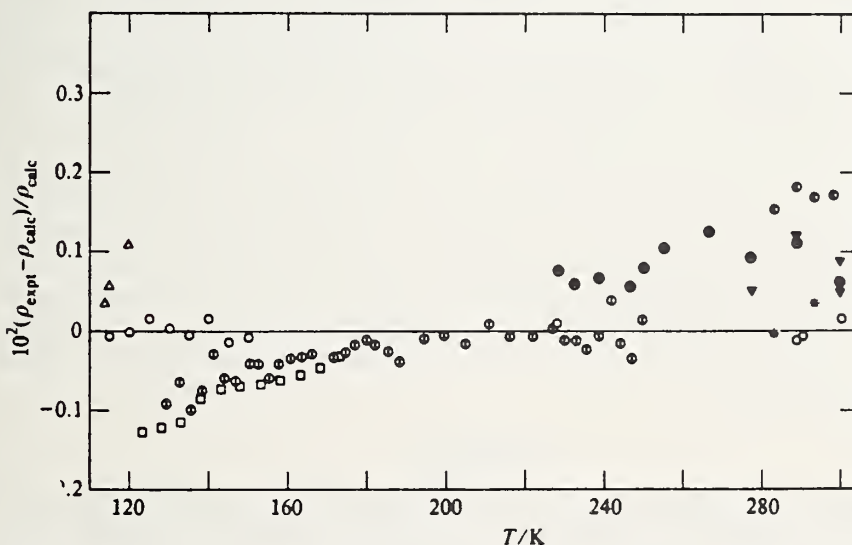


FIGURE 3. Deviation plot of experimental orthobaric liquid densities of isobutane compared with values calculated from equation (1) using parameters from table 6.  $\circ$ , present results;  $*$ , Sliwinski;<sup>(6)</sup>  $\oplus$ , Orrit and Olives;<sup>(14)</sup>  $\triangle$ , Rodosevich and Miller;<sup>(15)</sup>  $\square$ , McClune;<sup>(16)</sup>  $\blacktriangledown$ , Kahre;<sup>(21)</sup>  $\otimes$ , NGAA;<sup>(24)</sup>  $\bullet$ , Van der Vet.<sup>(25)</sup>

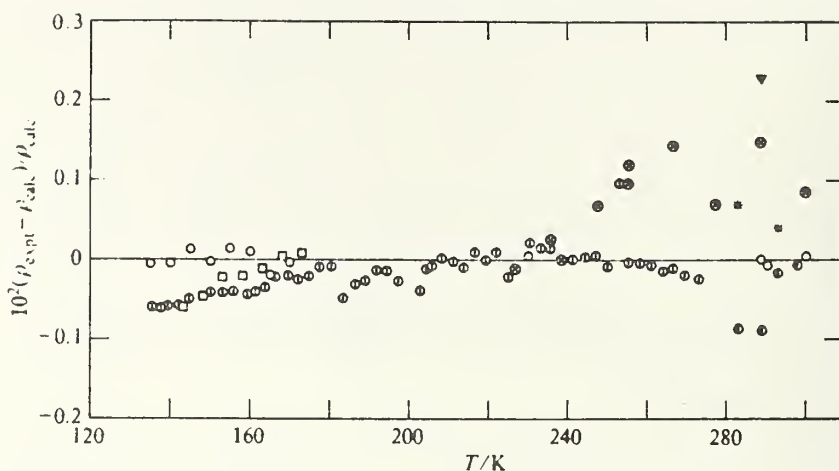


FIGURE 4. Deviation plot of experimental orthobaric liquid densities of normal butane compared with values calculated from equation (1) using parameters from table 6.  $\circ$ , present results;  $*$ , Sliwinski;<sup>(6)</sup>  $\oplus$ , Orrit and Olives;<sup>(14)</sup>  $\square$ , McClune;<sup>(16)</sup>  $\blacktriangledown$ , Kahre;<sup>(21)</sup>  $\otimes$ , NGAA;<sup>(24)</sup>  $\bullet$ , Van der Vet.<sup>(25)</sup>

Above 140 K the data of Chui and Canfield,<sup>(13)</sup> Orrit and Olives,<sup>(14)</sup> and McClune<sup>(16)</sup> differ from the present results by less than 0.05 per cent. At higher temperatures (above 280 K) the data of Sliwinski<sup>(6)</sup> for propane, isobutane, and normal butane generally differ from the present results by less than 0.05 per cent. The orthobaric liquid densities reported by Douslin and Harrison<sup>(18)</sup> for ethane at temperatures between 248 and 263 K were systematically larger than the present results by 0.3 to 0.35 per cent. Some of the older less precise (but frequently used) data have been included on the deviation plots for the sake of completeness.

Although Klosek and McKinley<sup>(17)</sup> give densities for isobutane and normal butane at temperatures between 105 and 133 K, these densities are not experimental, and therefore, are not plotted on figures 3 and 4. A few comments on the reliability of the omitted values are appropriate. Their densities were obtained from the Francis equation.<sup>(26)</sup> For normal butane at temperatures below its triple-point temperature, their results were systematically higher by less than 0.2 per cent than the densities obtained through extrapolation of the present results.<sup>(27)</sup> However, their isobutane densities at temperatures between 116 and 133 K were 1.5 per cent higher than those of the present work.

#### 4. Summary

This research has provided accurate and self-consistent measurements of the orthobaric liquid densities of methane, ethane, propane, isobutane, and normal butane at temperatures down to 100 K. Most of the measurements recently reported by other workers differ from the present results by less than 0.1 per cent. In subsequent papers, density measurements on liquefied mixtures of the major components of liquefied natural gas will be reported.

The authors would like to acknowledge R. D. McCarty and M. J. Brown for assistance with the correlation and reduction of the data.

## REFERENCES

1. Haynes, W. M.; Hiza, M. J.; Frederick, N. V. *Rev. Sci. Instrum.* **1976**, *47*, 1237.
2. Haynes, W. M. *Rev. Sci. Instrum.* In press.
3. Methane data are available from authors upon request and will be published in a Nat. Bur. Stand. (U.S.) report.
4. McCarty, R. D. *Nat. Bur. Stand. (U.S.), Internal Rept.* **1974**, 74-357.
5. Hou, Y. C.; Martin, J. J. *A.I.Ch.E. J.* **1959**, *5*, 125.
6. Goodwin, R. D. *Nat. Bur. Stand. (U.S.), Tech. Note* 653, **1974**.
7. Olson, J. D. *J. Chem. Phys.* **1975**, *63*, 474.
8. Sliwinski, P. Z. *Phys. Chem. (Frankfurt)* **1969**, *63*, 263.
9. Das, T. R.; Eubank, P. T. *Advances in Cryogenic Engineering* Vol. 18. Timmerhaus, K. D.: editor. Plenum Press: New York. **1973**, p. 208.
10. Das, T. R.; Reed, Jr., C. O.; Eubank, P. T. *J. Chem. Eng. Data* **1973**, *18*, 253.
11. Das, T. R.; Reed, Jr., C. O.; Eubank, P. T. *J. Chem. Eng. Data* **1973**, *18*, 244.
12. Shana'a, M. Y.; Canfield, F. B. *Trans. Faraday Soc.* **1968**, *64*, 2281.
13. Chui, C. H.; Canfield, F. B. *Trans. Faraday Soc.* **1971**, *67*, 2933.
14. Orrit, J.; Olives, J. distributed at 4th International Conference on Liquefied Natural Gas, Algeria, **1974**.
15. Rodosevich, J. B.; Miller, R. C. *A.I.Ch.E. J.* **1973**, *19*, 729.
16. McClune, C. R. *Cryogenics* **1976**, *16*, 289.
17. Klosek, J.; McKinley, C. *Proc. 1st Int. Conf. on LNG*, Paper 22, Chicago, **1968**.
18. Douslin, D. R.; Harrison, R. H. *J. Chem. Thermodynamics* **1973**, *5*, 491.
19. Maass, O.; Wright, C. H. *J. Am. Chem. Soc.* **1921**, *43*, 1098.
20. Jensen, R. H.; Kurata, F. *J. Petrol. Technol.* **1969**, *21*, 683.
21. Kahre, L. C. *J. Chem. Eng. Data* **1973**, *18*, 267.
22. Tomlinson, J. R. *Natural Gas Processors Assoc. Tech. Publ.* TP-1, Tulsa, Oklahoma, **1971**.
23. Seeman, F.-W.; Urban, M. *Erdöl und Kohle Erdgas Petrochem.* **1963**, *16*, 117.
24. *Tech. Comm., Natl. Gas. Assoc. Am. Ind. Eng. Chem.* **1942**, *34*, 1240.
25. Van der Vet, A. P. *Congress Mondial du Petrol., Paris*, Vol. II, **1937**, p. 515.
26. Francis, A. W. *Ind. Eng. Chem.* **1957**, *49*, 1779.
27. Haynes, W. M.; Hiza, M. J. *Advances in Cryogenic Engineering* Vol. 21. Timmerhaus, K. D.; Weitzel, D. H.; editors. Plenum Press: New York. **1976**, p. 516.



Advances in Cryogenic Engineering, Vol 21. Plenum Press, New York, 516-21 (1976)

## M-6

# ORTHOBARIC LIQUID DENSITIES OF NORMAL BUTANE FROM 135 TO 300 K AS DETERMINED WITH A MAGNETIC SUSPENSION DENSIMETER\*

W. M. Haynes and M. J. Hiza

*Cryogenics Division, Institute for Basic Standards, Boulder, Colorado*

### INTRODUCTION

Of the principal constituents of natural gas, normal butane is the first in the series of paraffin hydrocarbons that has a triple-point temperature significantly higher than the normal boiling point (112 to 115 K) of methane-rich liquefied natural gas (LNG). Unlike isobutane, with a triple-point temperature (113.6 K) near the normal boiling point of methane-rich LNG, normal butane freezes at the relatively high temperature of 134.8 K. Thus any estimate of the contribution of *n*-butane content to the molar volume (or molar density) of LNG requires a relatively long extrapolation into the subcooled liquid region of *n*-butane. It is also known that *n*-butane is the first in the series of paraffin hydrocarbons exhibiting geometrical isomerism, with nearly instantaneous equilibrium, which contributes to the temperature dependence of the molar density [1-5]. It follows that an analytical expression that provides the most reliable means of extrapolating *n*-butane densities into the subcooled liquid region cannot be based on correspondence alone, but must be based on extensive and accurate data above the triple-point temperature.

Other than references [6,7] that report results of saturated liquid density measurements near room temperature, no references were found that report experimental orthobaric liquid densities of *n*-butane below 283 K. (The results given by Klosek and McKinley [8] at temperatures below the triple-point temperature are probably based on their own data at somewhat higher temperatures.) The purposes of the present study were to obtain orthobaric liquid densities for *n*-butane that cover a relatively large temperature range at low temperatures, as well as some measurements up to ambient temperature, and to provide an analytical representation of these data that is used for extrapolation into the subcooled liquid region to compare with other results [8].

A relatively new technique for determining absolute densities of cryogenic fluids [9] was used in the present work. It is simple in principle and is based on a straightforward application of Archimedes' principle. Using a magnetic suspension

\* This work was carried out at the National Bureau of Standards under the sponsorship of the LNG Density Project Steering Committee, through a grant administered by the American Gas Association, Inc.

technique, a cylinder of magnetic material of known mass and volume is freely suspended by air-core solenoids in a stable configuration in the fluid whose density is to be determined. At such a stable equilibrium position, the upward magnetic force is added to the buoyancy force to balance the gravitational force. Densities of the fluid can be determined directly from the measured currents in the coils necessary to support the magnetic "float" at the same position in vacuum and in the fluid at constant temperature. The vertical position of the float is controlled by the automatic regulation of a servo-circuit, which includes a linear differential transformer for sensing inductively the position of the float. The horizontal position of the float is determined and maintained by the divergence of the magnetic field intensity.

### EXPERIMENTAL

A complete description of the apparatus and a detailed discussion of the performance characteristics are beyond the scope of this paper and will be published elsewhere [<sup>10</sup>]. Only those essentials of the experiment necessary for clarity are included here.

The feasibility of using a magnetic suspension densimeter for measurements on cryogenic fluids had been demonstrated earlier with an absolute density measurement on liquid nitrogen at the normal boiling point [<sup>9</sup>]. The development of the present apparatus, shown in Fig. 1, was based on experience with that apparatus and incorporates a cryostat with continuous wide-range temperature control, a windowed equilibrium cell suitable for studies of the liquids and liquid mixtures of interest here, a new servo-circuit for vertical position control of the magnetic buoy, and a high-powered (125 $\times$ ) microscope for monitoring the position of the magnetic buoy.

The magnetic buoy is a barium ferrite ( $\text{BaFe}_{12}\text{O}_{19}$ ) ceramic magnet in the shape of a right circular cylinder, approximately 5 mm in diameter and 6 mm in length. It has been plated with a thickness of approximately 0.07 mm of copper over its entire surface to prevent fluid from penetrating into the porous ceramic. Gold was flashed over the copper surface. The mass of the buoy was determined to better than 0.002% with an analytical balance. The volume of the buoy was determined within 0.02% at room temperature by using distilled water as a reference fluid of known density. At temperatures below ambient, the change in volume was calculated using recent thermal expansion data obtained for barium ferrite [<sup>11</sup>].

Evaluation of the experimental parameters involved in this method and extensive performance tests indicate that the uncertainty in the density measurements depends primarily on the uncertainty in the determination of the position of the buoy, relative to the main coil, from vacuum to liquid measurements. The position of the float was determined to less than  $10^{-3}$  mm with a 125 $\times$  microscope. The position of the main coil was maintained from vacuum to liquid measurements by supporting the coil at its midplane with quartz rods and by controlling the temperature of the coil with water.

The total uncertainty in the density measurements was estimated to be less than 0.1% at the lower temperatures; near room temperature the absolute error should be less than 0.05%. The imprecision of the density measurements was less than 0.02% over the complete temperature range.

A platinum resistance thermometer calibrated on the International Practical Temperature Scale (1968) was used for the temperature measurements. The uncertainty of the calibration was approximately 0.002 K. Due to the specifications of the

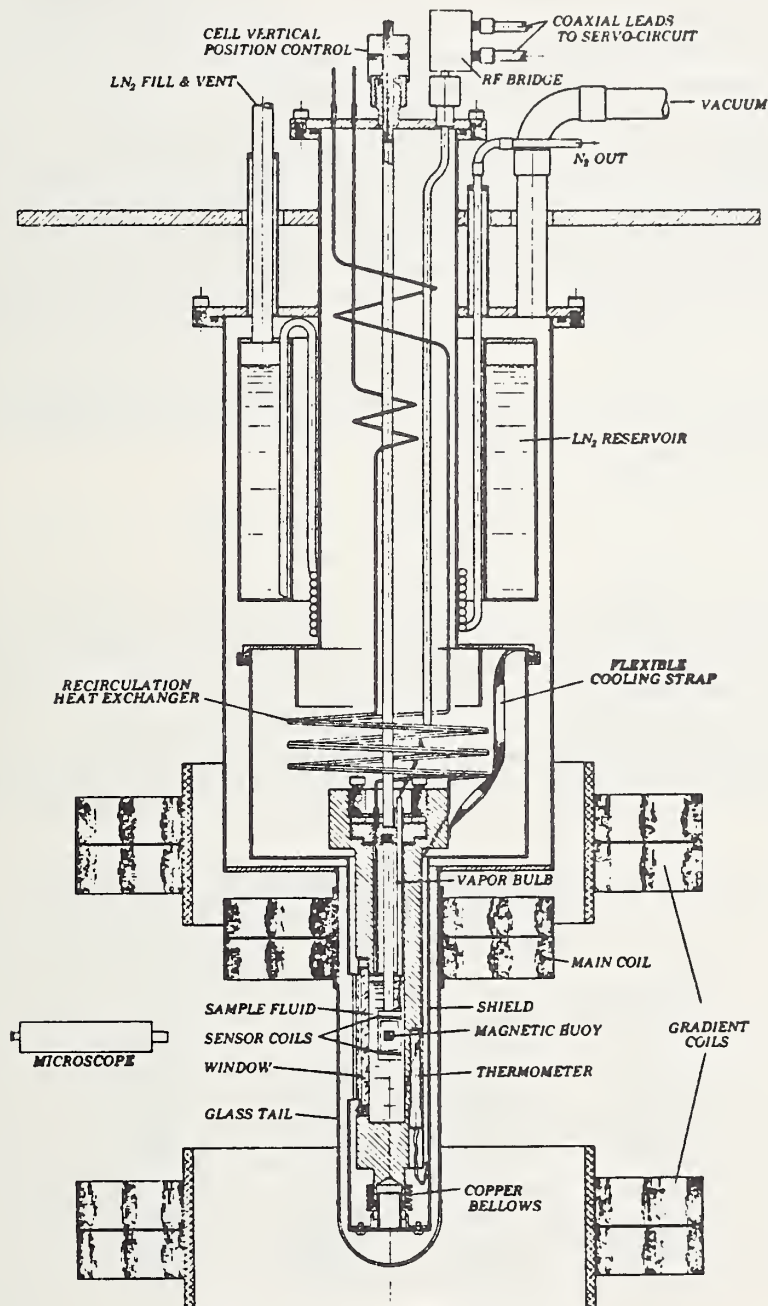


Fig. 1. Magnetic suspension densimeter for cryogenic fluids.

potentiometric measuring system, uncertainties in the temperature amounted to a maximum of 0.0135 K at 135 K, increasing to 0.030 K at 300 K. The temperature of the sample holder was controlled to better than 0.005 K, approximately the same as the reproducibility of the temperature measurements.

The purity of the *n*-butane used in these experiments was determined by chromatographic analysis with thermal conductivity detection. A 7.5-m liquid partition column was used, capable of separating air (or nitrogen) from methane in small concentrations and the paraffinic from olefinic hydrocarbons. The only detectable impurity in this sample was air (or nitrogen) at approximately 25 ppm. The limits of detectability of the analyzer were approximately 20 ppm of air (or nitrogen) and methane and approximately 10 ppm of ethane and the higher hydrocarbons.

## RESULTS

The experimental densities for *n*-butane are given in Table I with the corresponding experimental temperatures. These data were fitted by the method of least squares to an equation of the form

$$\rho - \rho_c = a \left(1 - \frac{T}{T_c}\right)^{0.35} + \sum_{i=1}^3 b_i \left(1 - \frac{T}{T_c}\right)^n \quad (1)$$

where  $\rho$  is the density in moles/liter,  $\rho_c$  is a characteristic density in moles/liter (approximately the critical density),  $T_c$  is a characteristic temperature in kelvin (approximately the critical temperature),  $n$  is defined as  $1 + \frac{1}{3}(i-1)$ , and  $a, b_i$  are coefficients determined by least squares. The parameters of (1) also are given in Table I, as well as the standard deviation and the molecular weight.

The deviations of various experimental results [6,7] and several frequently used literature values [12-14] from the values calculated from (1) are plotted as a function of temperature in Fig. 2. The accuracy with which equation (1), with parameters as

**Table I. Densities of Saturated Liquid Normal Butane and Parameters of Equation (1)**

$\rho_{exp}$ moles/liter	$T$ , K	$\rho_{calc}$ moles/liter	$\frac{100(\rho_{exp} - \rho_{calc})}{\rho_{calc}}$
12.6517	135.075	12.6524	-0.005
12.5706	140.075	12.5714	-0.006
12.4920	145.075	12.4904	0.013
12.4089	150.075	12.4093	-0.003
12.3299	155.075	12.3283	0.014
12.2484	160.075	12.2471	0.010
12.1634	165.075	12.1659	-0.020
12.0839	170.075	12.0846	-0.005
11.0911	230.000	11.0905	0.005
10.0067	290.000	10.0073	-0.006
9.8103	300.000	9.8099	0.005
Standard deviation = 0.013%		$T_c = 425.0$ K	
$a = 7.467330332$		$\rho_c = 3.876$ moles/liter	
$b_1 = 11.25963703$		Molecular weight = 58.12430	
$b_2 = -18.93664709$			
$b_3 = 11.22771351$			

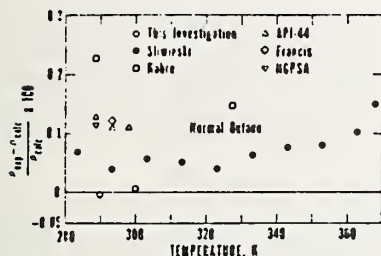


Fig. 2. Deviation plot of densities of saturated liquid normal butane compared with values calculated from equation (1); data from this work and the literature<sup>[6,7,12-14]</sup>. (Note that results from references 12 through 14 are not experimental data.)

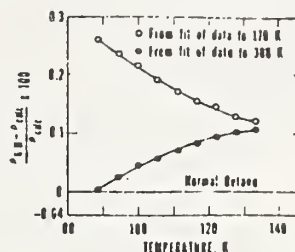


Fig. 3. Deviation plot of densities of liquid normal butane of Klosek and McKinley<sup>[8]</sup> below the triple-point temperature compared with the extrapolated values calculated from equation (1) for two cases: (a) a least squares fit of the data from the present work from 135 to 170 K using two coefficients and (b) a least squares fit of the data from the present work from 135 to 300 K using four coefficients. (Note that the baseline represents two sets of extrapolated results obtained from the present data and that both curves with designated points represent a single set of values from Klosek and McKinley<sup>[8]</sup>.)

given in Table I, can be extrapolated above 300 K has not been investigated, but from the comparisons with the work of Sliwinski<sup>[6]</sup> and Kahre<sup>[7]</sup> it appears that the equation gives reasonably accurate values up to 370 K.

Two different methods of extrapolation to temperatures below 135 K are presented in Fig. 3. First, the present data from 135 to 170 K were fitted to equation (1) using two coefficients ( $a = 7.318406322$  and  $b_1 = 3.479543073$ ) and then densities were calculated for temperatures below the triple point and compared with the values of Klosek and McKinley<sup>[8]</sup>. Next, the present data from 135 to 300 K were fitted, using equation (1) with four coefficients, and again comparisons were made with the values of Klosek and McKinley. The graph demonstrates the significant differences obtained for the two extrapolation methods and also provides comparisons with the only other published density values for normal butane at temperatures below 283 K. It should be noted that no effort has been expended in the present work to produce a "best" method for extrapolation into the subcooled liquid region.

## CONCLUSIONS

The results of this study provide the first set of experimental density data for the orthobaric liquid phase of *n*-butane at temperatures between 135 and 300 K. The

absolute error is estimated to be less than  $\pm 0.1\%$ . The analytical expression selected represents these data with a standard deviation less than the estimated imprecision of measurement, i.e.,  $\pm 0.02\%$ . It is felt that the analytical expression given here provides a reasonable means of extrapolation of *n*-butane densities into the sub-cooled region for liquefied natural gas applications.

### ACKNOWLEDGMENTS

The authors wish to acknowledge the contributions of the LNG Density Project Steering Committee and the financial support of the companies they represent.

### REFERENCES

1. R. A. Bonham and L. S. Bartell, *J. Am. Chem. Soc.* **81**:3491 (1959).
2. R. A. Bonham, L. S. Bartell, and D. A. Kohl, *J. Am. Chem. Soc.* **81**:4765 (1959).
3. A. L. Verma, W. F. Murphy, and H. J. Bernatein, *J. Chem. Phys.* **60**:1540 (1974).
4. M. R. Cines, Phillips Petroleum Co., private communication (January 1974).
5. T. W. Schmidt, Phillips Petroleum Co., private communication (May 1974).
6. P. Sliwinski, *Z. Phys. Chem. (Frankfurt)* **63**:263 (1969).
7. L. C. Kahre, *J. Chem. Eng. Data* **18**:267 (1973).
8. J. Klosek and C. McKinley, in: *Proceedings of First Intern. Conference on LNG*, Chicago, Illinois (1968), Paper 22, Session 5.
9. W. M. Haynes and J. W. Stewart, *Rev. Sci. Instr.* **42**:1142 (1971).
10. W. M. Haynes, N. V. Frederick, and M. J. Hiza, unpublished data.
11. A. F. Clark, W. M. Haynes, V. A. Deason, and R. J. Trapani, *Cryogenics* (to be published).
12. A. W. Francis, *Ind. Eng. Chem.* **49**:1779 (1957).
13. Natural Gas Processors Supplies Association, *Engineering Data Book, Ninth Edition*, NGPA, Tulsa, Oklahoma (1972).
14. American Petroleum Institute, Project 44, *Selected Values of Physical and Thermodynamic Properties of Hydrocarbons and Related Compounds*, Carnegie Press, Pittsburgh, Pennsylvania (1953).

### DISCUSSION

*Question* by R. C. Hendricks, NASA Lewis Research Center: Have you verified the results from your primary platinum temperature sensor by comparison with a second platinum temperature sensor? If not, how did you assure yourself that the temperature values obtained in your study were accurate?

*Answer* by author: No. Vapor pressures of pure methane were measured in the vapor bulb at the top of the cell and in the equilibrium space to determine the reliability of temperature measurement and control, as well as departures from isothermal conditions in the equilibrium cell.

M-754

*J. Chem. Thermodynamics* 1977, 9, 873-896

## Orthobaric liquid densities and excess volumes for binary mixtures of low molar-mass alkanes and nitrogen between 105 and 140 K\*

M. J. HIZA, W. M. HAYNES, and W. R. PARRISH

*Cryogenics Division, Institute for Basic Standards,  
National Bureau of Standards, Boulder, Colorado 80302, U.S.A.**(Received 21 February 1977)*

A magnetic suspension densimeter has been used to determine orthobaric liquid densities of gravimetrically prepared binary mixtures of the major components of liquefied natural gas (LNG) *i.e.* nitrogen, methane, ethane, propane, *i*-butane, and *n*-butane, generally between 105 and 140 K. All binary combinations were included in this study, with the exception of nitrogen + *i*-butane and nitrogen + *n*-butane. Uncertainties in the reported liquid-mixture densities are discussed in detail. Comparisons are made between excess volumes computed from the present results and comparable values from the literature. It was found that the volumetric properties of binary liquid mixtures of the heavy hydrocarbons (those mixtures not containing nitrogen or methane) are closely approximated by ideal mixing. Some observations are included on the use of excess volumes of the heavy hydrocarbon systems to determine effective molar volumes of *n*-butane in liquid mixtures below its triple-point temperature. For mixtures containing nitrogen or methane, approximate total vapor pressures are given.

### 1. Introduction

Custody transfer of liquefied natural gas (LNG) on the world energy market has imposed one of the most stringent requirements for accuracy in the prediction of orthobaric (saturated) liquid mixture densities. Since heating value is directly related to the density and composition of the liquid, it is desirable to be able to predict LNG densities within a small known uncertainty, preferably within  $\pm 0.1$  per cent, for any condition encountered in commerce.

The most promising theoretical methods for predicting the properties of fluid mixtures require that the pure-component characteristic parameters be combined to give the mixture characteristic parameters of the included binary pairs. It is well known that small adjustments to these parameters can significantly affect the difference

\* This work was carried out at the National Bureau of Standards under the sponsorship of British Gas Corp., Chicago Bridge and Iron Co., Columbia Gas Service Corp., Distrigas Corp., Easco Gas LNG, Inc., El Paso Natural Gas, Gaz de France, Marathon Oil Co., Mobil Oil Corp., Natural Gas Pipeline Co., Phillips Petroleum Co., Shell International Gas, Ltd., Sonatrach, Southern California Gas Co., Tennessee Gas Pipeline Co., Texas Eastern Transmission Co., Tokyo Gas Co., Ltd., and Transcontinental Gas Pipe Line Corp., through a grant administered by the American Gas Association, Inc.

between predicted and actual mixture properties. Though reasonable estimates of deviations from the combining rules can be made in special cases,<sup>(1)</sup> the best values for a given application and model must still be derived from accurate and consistent experimental results at several temperatures for the binary mixtures and pure components of interest.

For the development of a model to predict LNG densities reliably, for example, one needs sufficiently accurate densities of uniformly high precision for the pure components and the possible binary combinations, as well as for selected multi-component mixtures, to test and optimize the prediction method. To provide this data base, a comprehensive study was initiated in our laboratory to obtain orthobaric liquid densities of the desired accuracy for the major components of LNG and for their mixtures.

Previously, orthobaric liquid densities were reported for nitrogen<sup>(2)</sup> and the low molecular-weight alkanes—methane,<sup>(2,3)</sup> ethane, propane, *i*-butane, and *n*-butane<sup>(3)</sup>—as determined with a magnetic suspension densimeter.

The present study was conducted with the same apparatus to obtain orthobaric liquid densities for gravimetrically prepared binary mixtures of these components, generally between 105 and 140 K. All of the possible binary systems were studied, with the exception of nitrogen + *i*-butane and nitrogen + *n*-butane. Based on the phase equilibria for nitrogen + ethane<sup>(4)</sup> and nitrogen + propane<sup>(5)</sup> it was estimated that the limits of miscibility for the nitrogen + butane systems would preclude the possibility of obtaining experimental densities for these systems in the temperature range of interest. Where possible, total vapor pressures were also determined, but these are considered approximate since the main focus was to assure the reliability of the density measurements.

Excess volumes, computed for each of the binary mixtures studied, show that mixtures of the heavy hydrocarbons exhibit nearly ideal mixing. Effective liquid-phase molar volumes for *n*-butane below its triple-point temperature were obtained from the ethane + *n*-butane liquid-mixture densities by assuming that the small excess volume remains constant in the temperature range studied.

Only a few sets of orthobaric liquid-mixture densities in the literature<sup>(6)</sup> provide data applicable to the LNG problem discussed above. These data are generally limited in either the temperatures or compositions covered, or have admitted inaccuracies significantly larger than the desired  $\pm 0.1$  per cent. Comparisons are made between excess volumes from the present study and comparable values taken from the literature. Prior to the present study, there were no liquid densities in the temperature range of interest for nitrogen + ethane, nitrogen + propane, ethane + *i*-butane, propane + *i*-butane, propane + *n*-butane, or *i*-butane + *n*-butane.

## 2. Experimental

The magnetic suspension densimeter used in this study was discussed in detail elsewhere.<sup>(2,7)</sup> All of the results reported here were obtained with the one solenoid arrangement.<sup>(7)</sup> With this arrangement a barium ferrite magnetic buoy of known mass and volume is freely suspended, in vacuum and in the liquid, by the force

generated from the axial magnetic field of a single air-core solenoid. The position of the buoy is controlled by automatic regulation of the solenoid current with a radio-frequency servo-circuit. Since the magnetic force necessary to support the buoy at a given position is dependent on the buoyant force, measurement of the solenoid current needed to support the buoy in the liquid relative to vacuum at the same position and temperature yields the liquid density directly.

The relation used to compute the density of the liquid with the one solenoid system is

$$\rho_l = (m_b/V_b)\{1 - (I_l/I_v)\}, \quad (1)$$

where  $\rho_l$  is the mass density of the liquid,  $m_b$  is the mass of the buoy,  $V_b$  is the volume of the buoy, and  $I_l$  and  $I_v$  are the solenoid currents required to support the buoy at the same position in the liquid and vacuum, respectively.

The procedures used in this study were basically the same as those used in measuring liquid densities of the pure fluids.<sup>(2,3,7)</sup> Vacuum measurements were made immediately before or after those for nitrogen + methane liquid-mixture points, and each measurement was made with a separate fill. Since the temperature of the equilibrium cell had to be increased nearly to room temperature for effective removal of the heavy hydrocarbons, it was necessary to make vacuum measurements before introducing mixtures containing the heavy hydrocarbons. Measurements for these mixtures generally were made in pairs at 5 K increments with a single fill. With few exceptions a liquid-methane density measurement was made each day as a control on the measurement parameters. Liquid methane was used as the vapor-bulb fluid to provide the criteria for adjusting the control heat to the top and bottom of the cell to minimize temperature gradients. The heater currents were adjusted so that the methane vapor pressure was consistent with the temperature (IPTS-68) determined with a platinum resistance thermometer mounted near the bottom of the cell. Vapor bulb and equilibrium cell pressures were measured simultaneously with quartz Bourdon-tube pressure gages (0 to 0.69 MPa) calibrated against an air dead-weight gage. The estimated maximum uncertainty in calibration of these gages is about  $\pm 70$  Pa.

Since the uncertainty in the measured density of a binary liquid mixture is inherently larger than for the pure fluids due to the added uncertainty in composition, precautions were taken to assure that the uncertainty in composition was minimized and that the composition in the equilibrium cell was homogeneous.

Basically, there are three options available to fix the composition of a liquid mixture to be studied experimentally. These are (1) liquid-phase sampling and analysis relative to calibration mixtures, (2) introducing known quantities of each pure component and mixing within the experimental chamber, and (3) introducing the desired mixture, prepared under carefully controlled conditions, into the equilibrium chamber in the mixed state. Each method, or the various combinations, requires an exact accounting of the amount of each component at some point in the process. The third method was considered to be the most desirable and potentially the most accurate for this study.

The mixtures were prepared gravimetrically in thoroughly cleaned and dried metal

cylinders, each with a free volume of about 3 dm<sup>3</sup> and a tare mass of about 4 kg. In a few cases, cylinders with about 7 dm<sup>3</sup> free volume and a tare mass of about 12 kg were used. All gases were research grade, and were analyzed chromatographically before use. In addition, nitrogen and methane were passed through room-temperature molecular-sieve adsorption columns to remove moisture and any heavy contaminants not detected by analysis. The amount of each component added to a cylinder was determined by difference weighings using a Class S weight set and a precision equal-arm balance with a capacity of 25 kg. An identical cylinder filled with nitrogen gas at atmospheric pressure was used as ballast on the opposite pan. The standard deviation of 10 repetitive weighings with the balance was determined by the manufacturer to be 0.51 mg. The standard deviation of 11 repetitive weighings as used in the preparation of mixtures in the laboratory was determined to be 0.67 mg. Since the uncertainty in the Class S weights is ten times lower than the standard deviation in the weighings, the uncertainty in the amount of substance of each component in the mixture prepared is dependent only on the random error in the weighing-

TABLE 1. Uncertainty  $\delta x$  in mole fraction of each component in the prepared mixtures based on the total amount of substance  $n$  prepared

Component	$\delta x$	
	$n = 1 \text{ mol}$	$n = 5 \text{ mol}$
N <sub>2</sub>	$\pm 0.00014$	$\pm 0.00003$
CH <sub>4</sub>	$\pm 0.00025$	$\pm 0.00005$
C <sub>2</sub> H <sub>6</sub>	$\pm 0.00013$	$\pm 0.00003$
C <sub>3</sub> H <sub>8</sub>	$\pm 0.00009$	$\pm 0.00002$
C <sub>4</sub> H <sub>10</sub>	$\pm 0.00007$	$\pm 0.00001$

The estimated error in mole fraction of each component is given in table 1 for both 1 and 5 mol of mixture prepared. Since two weighings are required to determine the amount of substance of each component added, the estimated errors are based on 6 times the standard deviation determined in our laboratory.

The composition, molar mass, and the total amount of substance prepared are given in table 2 for each of the binary mixtures included in this study. A comparison of the uncertainties in component composition given in table 1 with the total amount of substance of mixture prepared, given in table 2, is a direct indication of the uncertainty in composition of each mixture. Three of the mixtures given in table 2 (mixtures with  $x \approx 0.5$  of methane + ethane, methane + propane, and ethane + propane) were obtained from the U.S. Bureau of Mines in Amarillo, Texas. The estimated uncertainties in component composition of these gravimetrically prepared mixtures are roughly the same as those given in table 1.<sup>(8)</sup>

A schematic diagram of the apparatus as used to measure liquid mixture densities is given in figure 1. This arrangement incorporates the same capabilities as the closed loop vapor-recirculation apparatus used in liquid-vapor equilibrium measurements<sup>(9, 10)</sup> except for vapor sampling. A window in the equilibrium cell allows visual observation of the liquid sample from about 2 cm above the bottom of the cell cavity

TABLE 2. Prepared binary mixtures:  $M$  denotes molar mass and  $n$  the total amount of substance prepared

Mixture	$M/g\ mol^{-1}$	$n/mol$
0.04752N <sub>2</sub> + 0.95248CH <sub>4</sub>	16.6119	6.30
0.30349N <sub>2</sub> + 0.69651CH <sub>4</sub>	19.6759	4.37
0.49242N <sub>2</sub> + 0.50758CH <sub>4</sub>	21.9375	6.00
0.05933N <sub>2</sub> + 0.94067C <sub>2</sub> H <sub>6</sub>	29.9481	5.42
0.02014N <sub>2</sub> + 0.97986C <sub>3</sub> H <sub>8</sub>	43.7733	1.30
0.03794N <sub>2</sub> + 0.96206C <sub>3</sub> H <sub>8</sub>	43.4870	3.73
0.06740N <sub>2</sub> + 0.93260C <sub>3</sub> H <sub>8</sub>	43.0132	1.23
0.35457CH <sub>4</sub> + 0.64543C <sub>2</sub> H <sub>6</sub>	25.0965	5.04
0.49325CH <sub>4</sub> + 0.50675C <sub>3</sub> H <sub>8</sub> <sup>a</sup>	23.1513	25.56
0.68006CH <sub>4</sub> + 0.31994C <sub>2</sub> H <sub>6</sub>	20.5309	4.87
0.29538CH <sub>4</sub> + 0.70462C <sub>3</sub> H <sub>8</sub>	35.8106	1.27
0.49637CH <sub>4</sub> + 0.50363C <sub>3</sub> H <sub>8</sub> <sup>a</sup>	30.1720	2.19
0.74920CH <sub>4</sub> + 0.25080C <sub>3</sub> H <sub>8</sub>	23.0790	3.54
0.85796CH <sub>4</sub> + 0.14204C <sub>3</sub> H <sub>8</sub>	20.0279	4.79
0.48687CH <sub>4</sub> + 0.51313 <i>i</i> -C <sub>4</sub> H <sub>10</sub>	37.6362	1.63
0.58828CH <sub>4</sub> + 0.41172 <i>n</i> -C <sub>4</sub> H <sub>10</sub>	33.3687	1.92
0.91674CH <sub>4</sub> + 0.08326 <i>n</i> -C <sub>4</sub> H <sub>10</sub>	19.5467	3.85
0.50105C <sub>2</sub> H <sub>6</sub> + 0.49895C <sub>3</sub> H <sub>8</sub> <sup>a</sup>	37.0689	2.23
0.67287C <sub>2</sub> H <sub>6</sub> + 0.32713C <sub>3</sub> H <sub>8</sub>	34.6588	3.04
0.68939C <sub>2</sub> H <sub>6</sub> + 0.31061 <i>i</i> -C <sub>4</sub> H <sub>10</sub>	38.7840	1.21
0.72436C <sub>2</sub> H <sub>6</sub> + 0.27564 <i>i</i> -C <sub>4</sub> H <sub>10</sub>	37.8030	1.78
0.65343C <sub>2</sub> H <sub>6</sub> + 0.34657 <i>n</i> -C <sub>4</sub> H <sub>10</sub>	39.7929	0.83
0.67117C <sub>2</sub> H <sub>6</sub> + 0.32883 <i>n</i> -C <sub>4</sub> H <sub>10</sub>	39.2952	0.96
0.49030C <sub>3</sub> H <sub>8</sub> + 0.50970 <i>i</i> -C <sub>4</sub> H <sub>10</sub>	51.2468	0.74
0.50326C <sub>3</sub> H <sub>8</sub> + 0.49674 <i>i</i> -C <sub>4</sub> H <sub>10</sub>	51.0650	0.75
0.58692C <sub>3</sub> H <sub>8</sub> + 0.41308 <i>n</i> -C <sub>4</sub> H <sub>10</sub>	49.8915	0.53
0.60650C <sub>3</sub> H <sub>8</sub> + 0.39350 <i>n</i> -C <sub>4</sub> H <sub>10</sub>	49.6169	0.54
0.60949C <sub>3</sub> H <sub>8</sub> + 0.39051 <i>n</i> -C <sub>4</sub> H <sub>10</sub>	49.5749	0.58
0.47039 <i>i</i> -C <sub>4</sub> H <sub>10</sub> + 0.52961 <i>n</i> -C <sub>4</sub> H <sub>10</sub>	58.1243	1.03

<sup>a</sup> Obtained from the U.S. Bureau of Mines, Helium Operations, Amarillo, Texas.

up to the base of the vapor bulb. The vapor bulb, attached directly to the closure plug, is a slip fit in the top section of the cell. The vapor leaves the top of cell through a capillary tube passing through the vapor bulb. The density equilibrium system was designed so that the vapor volume, excluding the free volume (65 cm<sup>3</sup>) in the recirculation pump, is extremely small relative to the liquid volume. The vapor volume includes approximately 0.42 cm<sup>3</sup> in the cell, 0.43 cm<sup>3</sup> in the access tubing within the cryostat, and 3.3 cm<sup>3</sup> in the pressure gage and tubing outside the cryostat. The volume occupied by the liquid is approximately 20.5 cm<sup>3</sup>. The vapor volumes were calculated from known dimensions, the liquid volume was determined by filling the cell with water, and the pump volume was determined by gas expansion. Without the pump volume, the effect of the vapor volumes on composition and density of the liquid is quite small and becomes important only at the higher mixture vapor pressures (0.2 to 0.3 MPa).

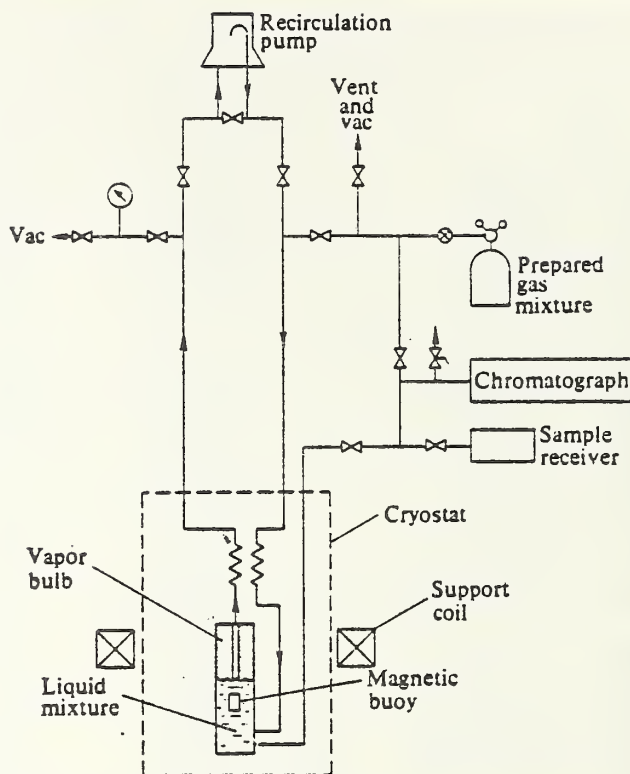


FIGURE 1. Schematic diagram of experimental apparatus.

The prepared gas mixtures were condensed directly and continuously into the equilibrium cell through the capillary vapor inlet tube at the bottom of the cell until the last vapor bubble disappeared below the vapor bulb. This filling method was used to provide continuous mixing of the liquid during the fill, analogous to vapor recirculation. For mixtures containing only the heavy hydrocarbons, the vapor pressures were extremely low, and the amount of vapor space left in the cell was unimportant. Nevertheless, the cell was filled with liquid as discussed above. There were no visible bubbles when filling with these mixtures.

For methane + heavy hydrocarbon mixtures, comparison of the measured densities before and after vapor recirculation provided a simple test of homogeneity of the liquid mixture. For these mixtures, the vapor phase is essentially pure methane at the temperatures included in this study. Ethane, the most volatile of the heavy components, has a vapor pressure of only 0.00383 MPa at 140 K.<sup>(11)</sup> Initially, the recirculation pump was filled with pure methane gas at a pressure equivalent to the vapor pressure of the mixture for the second experimental temperature, and isolated from the system. The solenoid currents for a pure liquid methane point and two vacuum points, separated by 5 K, were taken first. The prepared binary gas mixture to be studied was then condensed into the equilibrium cell in the manner discussed above. Solenoid currents for the two liquid-mixture points were measured at tempera-

tures corresponding to those of the vacuum points, the lower-temperature point generally being taken last. Subsequently, the system was opened to the pump, and vapor was recirculated through the liquid at one to three bubbles per second (probably less than  $1 \text{ cm}^3 \text{ min}^{-1}$ ) for several minutes. A low recirculation rate was used to avoid entrainment. The pump was then turned off, and the solenoid current for the liquid mixture point was remeasured. No change in density could be detected outside the precision of the measurement for any of the reported binary-mixture points thus tested.

For mixtures containing heavy hydrocarbons only, the most direct means to determine that the liquid sample was homogeneous and of the same composition as the prepared mixture was by liquid sampling and analysis. Ethane + propane was selected for this test. Liquid samples were withdrawn under constant helium-gas pressure (about 0.3 MPa) after the density measurements were completed. During sample withdrawal, the solenoid current was monitored to detect any variations in density as a different part of the liquid sample surrounded the magnetic buoy. Due to the extremely low vapor pressures, the compositions of these liquid mixtures are not subject to change by preferential vaporization during sampling. Each liquid sample was analyzed chromatographically using the prepared gas mixture for calibration. For these liquid mixtures, no change in solenoid current could be detected during sample withdrawal, and the composition of the liquid was found to be consistent with that of the prepared mixture within the precision of the gas analysis, *i.e.* within a few hundredths of 1 mole per cent.

Liquid samples of methane + ethane and methane + propane were also withdrawn and analyzed subsequent to the density measurements and recirculation of the vapor. However, it was extremely difficult to obtain samples of consistent composition due to preferential vaporization. At the higher temperatures ( $\geq 135 \text{ K}$ ) samples with compositions consistent with the prepared mixtures could be obtained by using the recirculation-pump volume as pressure ballast during withdrawal. At lower temperatures it was necessary to pressurize the cell with helium gas to obtain samples with compositions equivalent to those of the prepared mixtures. In general, however, analyses of liquid samples of the methane + hydrocarbon mixtures were mainly useful to determine that there were no gross discrepancies (greater than a few tenths of 1 mole per cent) in composition and that the liquid mixtures were not inadvertently contaminated. No attempt was made to recirculate the vapor or to sample and analyze the liquid mixtures containing nitrogen.

### 3. Results and discussion

#### EXPERIMENTAL RESULTS

The experimental orthobaric liquid-mixture amount-of-substance densities are given in table 3 as a function of temperature. The excess volumes  $V^E$ , also given in table 3, were computed from the expression:

$$V^E = V_m - \sum_1 x_1 \{V_1 + \beta_1 V_1 (p_1 - p_m)\}, \quad (2)$$

where  $V_m$  is the molar volume,  $p$  is the saturation pressure,  $x$  is mole fraction, and  $\beta$

TABLE 3. Orthobaric liquid amount-of-substance densities  $\rho$  of binary mixtures of low molar-mass alkanes and nitrogen.  $T$ , temperature (IPTS-68);  $\rho_{\text{calc}}$ ,  $\rho$  calculated from equation (4);  $p$ , pressure;  $V^E$ , excess volume

Mixture	$\frac{T}{\text{K}}$	$\frac{\rho}{\text{mol dm}^{-3}}$	$10^2 \frac{\rho_{\text{expt}} - \rho_{\text{calc}}}{\rho_{\text{calc}}}$	$\frac{p}{\text{MPa}}$	$\frac{V^E}{\text{cm}^3 \text{mol}^{-1}}$
0.04752N <sub>2</sub> + 0.95248CH <sub>4</sub>	105.00	26.8476	-0.006	0.138	-0.144
	110.00	26.4052	0.010	0.199	-0.258
	115.00	25.9374	-0.002	0.263	-0.442
	120.00	25.4522	-0.006	0.350	-0.889
	125.00	24.9496	0.005	0.460	
	130.00	24.4210	0.007	0.583	
	135.00	23.8600	-0.017	0.730	
	140.00	23.2809	0.009	0.920	
0.30349N <sub>2</sub> + 0.69651CH <sub>4</sub>	100.00	26.8735	-0.010	0.345	-0.584
	105.00	26.3393	0.023	0.466	-0.885
	110.00	25.7686	-0.005	0.618	-1.353
	115.00	25.1790	-0.017	0.801	-2.253
	120.00	24.5737	0.010	1.011	-4.510
0.49242N <sub>2</sub> + 0.50758CH <sub>4</sub>	95.00	27.0801	0.006	0.330	-0.541
	100.00	26.4588	0.003	0.465	-0.777
	105.00	25.8106	-0.012	0.637	-1.154
	110.00	25.1387	-0.016	0.844	-1.803
	115.00	24.4431	0.006	1.097	-3.056
	120.00	23.7096	0.017	1.398	-6.110
	125.00	22.9315	0.010	1.731	
	130.00	22.1005	-0.015	2.110	
0.05933N <sub>2</sub> + 0.94067C <sub>2</sub> H <sub>6</sub>	105.00	21.4718		0.385	-0.423
	110.00	21.2912		0.463	-0.590
	115.00	21.0845		0.547	-0.804
	120.00	20.8998		0.638	-1.385
0.02014N <sub>2</sub> + 0.97986C <sub>3</sub> H <sub>8</sub>	110.00	16.2131		0.357	-0.208
	115.00	16.0931		0.471	-0.289
0.03794N <sub>2</sub> + 0.96206C <sub>3</sub> H <sub>8</sub>	105.00	16.4638		0.495	-0.310
	110.00	16.3410		0.671	-0.392
0.06740N <sub>2</sub> + 0.93260C <sub>3</sub> H <sub>8</sub>	100.00	16.8055		0.631	-0.427
	105.00	16.7084		0.880	-0.628
0.35457CH <sub>4</sub> + 0.64543C <sub>2</sub> H <sub>6</sub>	105.00	23.1032	0.002	0.0256	-0.382
	110.00	22.8777	0.009	0.0392	-0.442
	115.00	22.6478	0.007	0.0580	-0.505
	120.00	22.4035	-0.050	0.0826	-0.554
	125.00	22.1872	0.030	0.115	-0.673
	130.00	21.9441	0.002	0.155	-0.798
0.49325CH <sub>4</sub> + 0.50675C <sub>2</sub> H <sub>6</sub>	105.00	23.9619	0.031	0.0325	-0.525
	110.00	23.6937	-0.004	0.0503	-0.569
	115.00	23.4328	0.003	0.0749	-0.639
	120.00	23.1559	-0.047	0.108	-0.697
	125.00	22.8933	-0.024	0.150	-0.801
	130.00	22.6290	0.007	0.205	-0.927
	135.00	22.3581	0.024	0.272	-1.068
	140.00	22.0765	0.009	0.355	-1.223

TABLE 3—continued

Mixture	$\frac{T}{K}$	$\frac{\rho}{\text{mol dm}^{-3}}$	$10^2 \frac{\rho_{\text{expt}} - \rho_{\text{calc}}}{\rho_{\text{calc}}}$	$\frac{p}{\text{MPa}}$	$\frac{V^E}{\text{cm}^3 \text{mol}^{-1}}$
0.68006CH <sub>4</sub> + 0.31994C <sub>2</sub> H <sub>6</sub>	105.00	25.1027	0.002	0.0416	-0.524
	110.00	24.7802	-0.004	0.0645	-0.562
	115.00	24.4612	0.003	0.0963	-0.621
	120.00	24.1402	-0.001	0.138	-0.698
	125.00	23.8212	0.002	0.193	-0.802
	130.00	23.5007	-0.001	0.262	-0.933
0.29538CH <sub>4</sub> + 0.70462C <sub>3</sub> H <sub>8</sub>	105.00	18.5132		0.0270	-0.469
	110.00	18.3624		0.0409	-0.524
0.49637CH <sub>4</sub> + 0.50363C <sub>3</sub> H <sub>8</sub>	105.00	20.4909	0.005	0.0384	-0.727
	110.00	20.3046	-0.002	0.0591	-0.814
	115.00	20.1180	-0.006	0.0874	-0.915
	120.00	19.9311	-0.007	0.125	-1.033
	125.00	19.7471	0.014	0.173	-1.179
	130.00	19.5546	-0.004	0.232	-1.329
0.74920CH <sub>4</sub> + 0.25080C <sub>3</sub> H <sub>8</sub>	105.00	23.4768	0.005	0.0478	-0.700
	110.00	23.2064	-0.009	0.0738	-0.783
	115.00	22.9364	-0.004	0.110	-0.887
	120.00	22.6665	0.017	0.158	-1.014
	125.00	22.3818	-0.010	0.222	-1.141
	130.00	22.1019	0.002	0.303	-1.310
0.85796CH <sub>4</sub> + 0.14204C <sub>3</sub> H <sub>8</sub>	105.00	24.9622	-0.007	0.0516	-0.553
	110.00	24.6331	0.009	0.0801	-0.617
	115.00	24.2941	0.006	0.120	-0.684
	120.00	23.9491	0.002	0.173	-0.764
	125.00	23.5941	-0.021	0.242	-0.855
	130.00	23.2461	0.012	0.330	-0.992
0.48687CH <sub>4</sub> + 0.51313 <i>i</i> -C <sub>4</sub> H <sub>10</sub>	110.00	17.3575		0.0629	-0.803
	115.00	17.2076		0.0938	-0.884
	120.00	17.0639		0.1361	-1.002
	125.00	16.9156		0.1852	-1.125
0.58828CH <sub>4</sub> + 0.41172 <i>n</i> -C <sub>4</sub> H <sub>10</sub>	120.00	18.6495		0.1636	-1.312
	125.00	18.4772		0.2281	-1.466
	125.00	18.4853		0.2281	-1.489
	130.00	18.3058		0.3183	-1.646
0.91674CH <sub>4</sub> + 0.08326 <i>n</i> -C <sub>4</sub> H <sub>10</sub>	105.00	25.1536	0.009		-0.599
	110.00	24.7960	-0.021		-0.638
	115.00	24.4512	0.010		-0.719
	120.00	24.0910	-0.011		-0.797
	125.00	23.7370	0.006		-0.916
	130.00	23.3789	0.018		-1.063
	135.00	23.0110	0.003		-1.234
	140.00	22.6391	-0.015		-1.451
0.50105C <sub>2</sub> H <sub>6</sub> + 0.49895C <sub>3</sub> H <sub>8</sub>	105.00	18.3618	0.021		-0.040
	110.00	18.2169	0.001		-0.036
	115.00	18.0726	-0.012		-0.034
	120.00	17.9282	-0.020		-0.033
	125.00	17.7880	0.000		-0.047

TABLE 3—continued

Mixture	$T$ K	$\rho$ mol dm <sup>-3</sup>	$10^2 \frac{\rho_{\text{expt}} - \rho_{\text{calc}}}{\rho_{\text{calc}}}$	$p$ MPa	$V^E$ cm <sup>3</sup> mol <sup>-1</sup>
0.50105C <sub>2</sub> H <sub>6</sub> + 0.49895C <sub>3</sub> H <sub>8</sub>	130.00	17.6412	-0.011		-0.041
	135.00	17.4988	0.009		-0.051
	140.00	17.3526	0.013		-0.051
0.67287C <sub>2</sub> H <sub>6</sub> + 0.32713C <sub>3</sub> H <sub>8</sub>	125.00	18.6192			-0.044
	130.00	18.4646			-0.053
	135.00	18.3059			-0.052
	140.00	18.1509			-0.065
0.68939C <sub>2</sub> H <sub>6</sub> + 0.31061 <i>i</i> -C <sub>4</sub> H <sub>10</sub>	115.00	17.3716			+0.012
	120.00	17.2344			+0.015
0.72436C <sub>2</sub> H <sub>6</sub> + 0.27564 <i>i</i> -C <sub>4</sub> H <sub>10</sub>	105.00	17.9779			+0.013
	110.00	17.8401			+0.008
	125.00	17.4235			-0.010
	130.00	17.2825			-0.013
0.65343C <sub>2</sub> H <sub>6</sub> + 0.34657 <i>n</i> -C <sub>4</sub> H <sub>10</sub>	115.00	17.2184			-0.055
	120.00	17.0824			-0.045
0.67117C <sub>2</sub> H <sub>6</sub> + 0.32883 <i>n</i> -C <sub>4</sub> H <sub>10</sub>	110.00	17.5047	0.003		-0.045
	115.00	17.3706	-0.000		-0.050
	125.00	17.1031	0.009		-0.060
	130.00	16.9626	-0.020		-0.042
	135.00	16.8285	-0.006		-0.045
	140.00	16.6947	0.014		-0.054
0.49030C <sub>3</sub> H <sub>8</sub> + 0.50970 <i>i</i> -C <sub>4</sub> H <sub>10</sub>	105.00	14.3080	-0.002		+0.086
	110.00	14.2136	-0.007		+0.078
	115.00	14.1219	0.011		+0.056
	120.00	14.0257	0.001		+0.057
	125.00	13.9300	-0.002		+0.054
	130.00	13.8342	-0.002		+0.052
0.50326C <sub>3</sub> H <sub>8</sub> + 0.49674 <i>i</i> -C <sub>4</sub> H <sub>10</sub>	125.00	13.9718			+0.047
	130.00	13.8737			+0.054
0.58692C <sub>3</sub> H <sub>8</sub> + 0.41308 <i>n</i> -C <sub>4</sub> H <sub>10</sub>	110.00	14.6839			-0.034
	135.00	14.1748			+0.021
	140.00	14.0786			+0.006
0.60650C <sub>3</sub> H <sub>8</sub> + 0.39350 <i>n</i> -C <sub>4</sub> H <sub>10</sub>	140.00	14.1343			+0.010
	145.00	14.0333			+0.015
	150.00	13.9346			+0.009
0.60949C <sub>3</sub> H <sub>8</sub> + 0.39051 <i>n</i> -C <sub>4</sub> H <sub>10</sub>	115.00	14.6487			-0.017
	120.00	14.5521			-0.036
0.47039 <i>i</i> -C <sub>4</sub> H <sub>10</sub> + 0.52961 <i>n</i> -C <sub>4</sub> H <sub>10</sub>	125.00	12.6943			+0.016
	130.00	12.6133			+0.013
	135.00	12.5271			+0.048
	140.00	12.4447			+0.053

is the isothermal compressibility. Subscripts *m* and *i* refer to the mixture and to the pure components, respectively. The pure-component molar volumes were calculated from the fit of the experimental results.<sup>(2,3)</sup> Only those for nitrogen, methane, and ethane were adjusted to the mixture pressure where appropriate. Isothermal compressibilities for nitrogen and methane were taken from Rowlinson<sup>(12)</sup> and those for ethane were taken from Miller<sup>(13)</sup> assuming linear temperature dependence. Excess volumes for a few representative methane + ethane points were also computed using isothermal compressibilities derived from the recent methane data of Goodwin.<sup>(14)</sup> The excess volumes using Goodwin's values of  $\beta$  were less than 0.1 per cent different from the excess volumes computed using those of Rowlinson. Rowlinson's values were used here only because excess volumes for methane and nitrogen systems reported in the literature are based on his values. Thus, a direct comparison of excess volumes can be made without assessing the contribution of different compressibility values. The ethane compressibility values of Miller were chosen for the same reason. Vapor pressures for nitrogen, methane, and ethane were taken from Strobridge,<sup>(15)</sup> Goodwin,<sup>(14)</sup> and Goodwin, Roder, and Straty,<sup>(11)</sup> respectively.

Effective molar volumes for *n*-butane below its triple-point temperature (134.8 K) were obtained from equation (2) by assuming that the small negative excess volume of ethane + *n*-butane was constant and equal to the average value of the excess volumes above the triple-point temperature of *n*-butane. These subcooled liquid molar volumes were fitted as a linear function of temperature to obtain the equation:

$$V(n-C_4) = 65.63936 + 0.0992160(T/K). \quad (3)$$

The molar volumes calculated from this expression at 135 and 140 K agree with the experimental values<sup>(3)</sup> within 0.01 per cent. At 105 K, the molar volume of *n*-butane calculated from the equation given in reference 3 fitted to the experimental liquid densities is 0.056 per cent larger than the value given by equation (3). Equation (3) was used to compute the excess volumes given in table 3 for all of the *n*-butane mixtures below 135 K. For *i*-butane, the liquid-phase equation given in reference 3 was used to obtain subcooled liquid molar volumes below the triple-point temperature (113.6 K).

In examining the excess volumes for propane + *n*-butane and *i*-butane + *n*-butane using *n*-butane molar volumes from equation (3), an interesting anomaly was noted. The excess volumes for these systems, as shown in figure 2, appear to have a discontinuity at about the triple-point temperature of *n*-butane. Molar volumes of *n*-butane determined from these systems in the same manner as those determined from ethane + *n*-butane are in good agreement with each other. However, the molar volumes calculated from a linear fit of the values from propane + *n*-butane and *i*-butane + *n*-butane are 0.14 and 0.09 per cent lower than those from equation (3) at 110 and 130 K, respectively, and the extrapolated volumes are about 0.075 per cent lower than the experimental liquid molar volumes at 135 and 140 K.

Though the differences noted are not very large, the imprecision of the density measurements for these heavy hydrocarbons and their mixtures is small enough (see

the ethane + *n*-butane and propane + *i*-butane mixtures in table 3) to suggest that this behavior is real and would be worth investigating in more detail. This behavior might also be important in the development of precise methods to predict densities of mixtures containing *n*-butane.

The pressures listed in table 3 are considered only approximate mixture vapor pressures, and not all of these were directly measured in the present experiment. Pressures are given only for mixtures where sufficient measurements were made to allow either interpolation in temperature or composition for a given system or comparison with existing phase equilibria. For nitrogen + methane, several random pressure measurements were made which were consistent with those interpolated from previous phase-equilibrium measurements in our laboratory.<sup>(16, 17)</sup> As a result, all of the pressures listed for nitrogen + methane were obtained from graphical

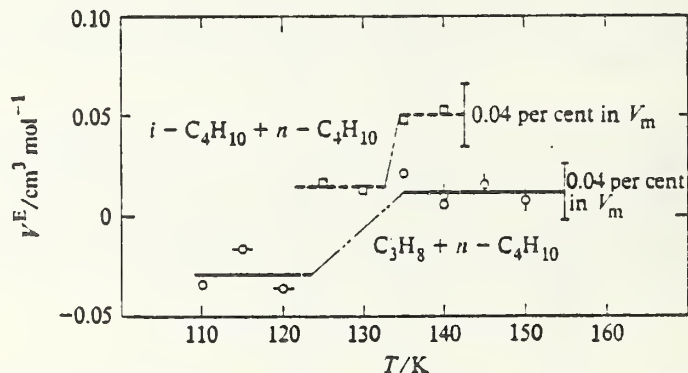


FIGURE 2. Excess volumes of propane + *n*-butane and *i*-butane + *n*-butane from the present study. O, 0.58692C<sub>3</sub>H<sub>8</sub> + 0.41308*n*-C<sub>4</sub>H<sub>10</sub>; ◊, 0.60650C<sub>3</sub>H<sub>8</sub> + 0.39350*n*-C<sub>4</sub>H<sub>10</sub>; ◐, 0.60949C<sub>3</sub>H<sub>8</sub> + 0.39051*n*-C<sub>4</sub>H<sub>10</sub>; ◑, 0.47039*i*-C<sub>4</sub>H<sub>10</sub> + 0.52961*n*-C<sub>4</sub>H<sub>10</sub>.

interpolations of the phase-equilibrium measurements. Pressures for nitrogen + ethane and nitrogen + propane were difficult to measure with any consistency since they are very strong functions of composition. Most of these pressures were estimated by comparison of the present measurements with the phase-equilibrium data of Lu and his colleagues.<sup>(4, 5)</sup> For methane + ethane, the pressure corresponding to the second point from one filling of the equilibrium cell was generally consistent with phase-equilibrium data,<sup>(18, 20)</sup> while the first point was usually high by a few per cent. Pressures for these mixtures were smoothed to the pressures of the second point by comparison with the data of Miller and Staveley<sup>(18)</sup> and of Miller, Kidnay, and Hiza.<sup>(19)</sup> For methane + propane, discrepancies in the pressures between points taken with the same fill were not as apparent, and the values given in table 3 were not smoothed. Comparisons between the ratios of measured to Raoult's law pressures from the present study with those from the measurements of Stoeckli and Staveley,<sup>(21)</sup> Cutler and Morrison,<sup>(22)</sup> and Calado, Garcia, and Staveley<sup>(23)</sup> are shown in figure 3. Pressures given for methane + *i*-butane and methane + *n*-butane, though no phase

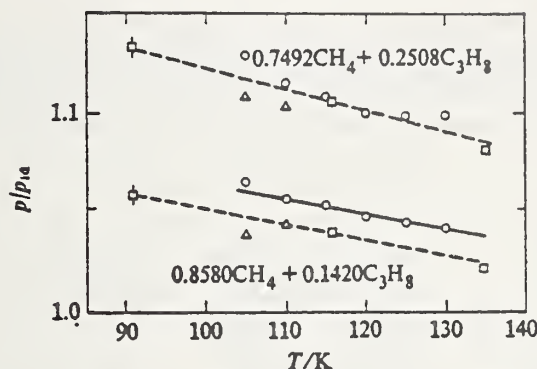


FIGURE 3. Comparison of ratios of actual to ideal total vapor pressures for methane + propane at two compositions.  $\circ$ , present study;  $\square$ , Stoeckli and Staveley;<sup>(21)</sup>  $\triangle$ , Cutler and Morrison;<sup>(22)</sup>  $\square$ , Calado, Garcia, and Staveley.<sup>(23)</sup>

equilibrium measurements are available for comparison, would probably exhibit departures similar to those shown in figure 3.

#### ANALYSIS OF ERRORS IN LIQUID-MIXTURE DENSITIES

Where density measurements were made at five or more temperatures, amount-of-substance densities  $\rho$  at constant composition were fitted as a function of temperature to the expression previously used in representing orthobaric amount-of-substance densities of the pure components:<sup>(2,3)</sup>

$$\rho - \rho_c = a\{1 - (T/T_c)\}^{0.35} + \sum_{i=1}^3 b_i\{1 - (T/T_c)\}^{(1+(i-1)/3)}. \quad (4)$$

The least-squares coefficients  $a$  and  $b_i$ , and the values of the critical temperature  $T_c$  and critical amount-of-substance density  $\rho_c$  for each mixture thus treated are given in table 4. The fourth coefficient  $b_3$  was not statistically significant in the fit of any of these results. Since experimental critical parameters are rarely available for mixtures at the desired composition, those used here were obtained from the correlation of Chueh and Prausnitz.<sup>(24)</sup> The standard deviations from the fit of the experimental densities to equation (4) are also given in table 4 as a percentage of  $\rho$ . The largest standard deviation obtained was 0.029 per cent in  $\rho$  for  $(0.35457CH_4 + 0.64543C_2H_6)$ .

The overall uncertainty in the measured densities of the binary mixtures is slightly larger than for the pure fluids due to the added uncertainty in composition and is dependent on the type of mixture. Estimated uncertainties in the density measurements for three representative mixtures—nitrogen + methane, methane + ethane, and ethane + *n*-butane—are given in table 5. The estimated errors due to mixture preparation were determined from the uncertainty in mole fraction of each component in the mixture for total amount of substance of mixture prepared (tables 1 and 2). The errors due to vapor-volume correction were estimated by assuming a volume uncertainty equivalent to that portion of the vapor volume in the equilibrium cell at the experimental temperature. The sources of the other systematic errors are

TABLE 4. Parameters of equation (4) where  $T_0$  and  $\rho_0$  are the critical temperature and critical amount-of-substance density of the mixture. The coefficients  $a$ ,  $b_1$ , and  $b_2$  were obtained from a least-squares program in which the experimental mass densities to five digits were converted to amount-of-substance densities within the program;  $\sigma$  is the standard deviation

Mixture	$\frac{a}{\text{mol dm}^{-3}}$	$\frac{b_1}{\text{mol dm}^{-3}}$	$\frac{b_2}{\text{mol dm}^{-3}}$	$\frac{T_0}{\text{K}}$	$\frac{\rho_0}{\text{mol dm}^{-3}}$	$10^2 \times \sigma \langle \rho^{-1} \rangle$
0.04752N <sub>2</sub> + 0.95248CH <sub>4</sub>	16.41033	18.47257	-11.57943	188.04	10.258	0.011
0.30349N <sub>2</sub> + 0.69651CH <sub>4</sub>	14.92272	20.19078	-10.85599	173.20	10.747	0.023
0.49242N <sub>2</sub> + 0.50758CH <sub>4</sub>	14.54530	20.60585	-10.07112	161.48	11.018	0.014
0.35457CH <sub>4</sub> + 0.64543C <sub>2</sub> H <sub>6</sub>	13.02060	6.275239		276.40	8.196	0.029
0.49325CH <sub>4</sub> + 0.50675C <sub>2</sub> H <sub>6</sub>	12.99333	7.219530		262.24	8.762	0.028
0.68006CH <sub>4</sub> + 0.31994C <sub>2</sub> H <sub>6</sub>	18.86369	-16.08578	19.91557	239.93	9.482	0.003
0.49637CH <sub>4</sub> + 0.50363C <sub>3</sub> H <sub>8</sub>	9.168092	7.647523		320.33	7.372	0.009
0.74920CH <sub>4</sub> + 0.25080C <sub>3</sub> H <sub>8</sub>	6.367272	24.40468	-11.53932	271.15	9.163	0.013
0.85796CH <sub>4</sub> + 0.14204C <sub>3</sub> H <sub>8</sub>	8.371599	23.49229	-10.69945	241.28	9.836	0.016
0.91674CH <sub>4</sub> + 0.08326 <i>n</i> -C <sub>4</sub> H <sub>10</sub>	8.975024	12.09284		238.92	11.044	0.015
0.50105C <sub>2</sub> H <sub>6</sub> + 0.49895C <sub>3</sub> H <sub>8</sub>	9.598348	5.440200		344.42	6.125	0.015
0.67117C <sub>2</sub> H <sub>6</sub> + 0.32883 <i>n</i> -C <sub>4</sub> H <sub>10</sub>	8.334169	5.886011		359.88	6.082	0.013
0.49030C <sub>3</sub> H <sub>8</sub> + 0.50970 <i>i</i> -C <sub>4</sub> H <sub>10</sub>	7.647038	4.065571		392.63	4.472	0.007

TABLE 5. Estimated uncertainties in density measurements

Source of error	$10^2  \delta\rho /\rho$					
	0.49242N <sub>2</sub> +0.50758CH <sub>4</sub>		0.49325CH <sub>4</sub> +0.50675C <sub>2</sub> H <sub>6</sub>		0.67117C <sub>2</sub> H <sub>6</sub> +0.32883 <i>n</i> -C <sub>4</sub> H <sub>10</sub>	
Systematic errors						
Mass of float	110 K	130 K	110 K	130 K	110 K	130 K
Volume of float at 300 K	0.002	0.002	0.002	0.002	0.002	0.002
Thermal expansion coefficient of barium ferrite	0.020	0.020	0.020	0.020	0.020	0.020
Position of float	0.022	0.020	0.022	0.020	0.022	0.020
Position of main coil, determined from relative measurements	0.012	0.013	0.012	0.012	0.009	0.009
Temperature uncertainty of 0.030 K	0.020	0.020	0.020	0.020	0.020	0.020
Mixture preparation	0.016	0.023	0.007	0.007	0.005	0.005
Vapor volume correction	0.001	0.002	0.001	0.001	0.002	0.002
	0.006	0.020	0.001	0.005	0.000	0.000
Total systematic error <sup>a</sup>	0.042	0.048	0.039	0.038	0.037	0.036
Three times standard deviation <sup>a</sup>	0.042	0.048	0.081	0.084	0.039	0.039
Total uncertainty <sup>a</sup>	0.08	0.10	0.12	0.12	0.08	0.08

<sup>a</sup> The total uncertainty was determined from the square root of the sum of the squares of the systematic errors added to three times the standard deviation from the fit to equation (4).

the same as those discussed earlier<sup>(2)</sup> for pure-fluid measurements. The total uncertainty was taken as the square root of the sum of the squares of the systematic errors plus three times the standard deviation for random error. The standard deviations are those obtained from the fit of the results to equation (4) taken as a percentage of the mixture amount-of-substance density at the specified temperature. For the estimate of random errors for pure-fluid measurements given in reference 2, the standard deviation of a single density measurement was computed relative to the density and temperature of methane at 105 K for which repetitive measurements had been obtained. This method of assessing random error could not be used here. Since the standard deviation for methane obtained from equation (4)<sup>(2)</sup> was in good agreement with that computed from repetitive measurements, standard deviations for the binary mixtures obtained with equation (4) are considered a reasonable basis for estimating the random error.

It is probable that the overall uncertainties in the densities for some of the mixtures investigated in this study are larger than those shown in table 5. Uncertainties in the results for nitrogen + ethane and nitrogen + propane could exceed the maximum total uncertainty shown in table 5 by a few hundredths of a per cent. Because of the dew-point limitations on the pressure of the gas mixtures prepared and the high liquid-mixture vapor pressures, it was difficult to maintain adequate driving force during the fill to provide continuous condensation and mixing. Of these two systems, results for nitrogen + propane are considered the least reliable. Also, during the course of this study, difficulties were encountered in attempting to obtain consistent results for methane + *i*-butane where  $x(\text{CH}_4) > 0.9$ . This difficulty could have been due to a problem in the filling procedure or to a dew-point related problem in the prepared gas mixture. Though this problem was not encountered in measurements of the  $(0.91674\text{CH}_4 + 0.08326n\text{-C}_4\text{H}_{10})$  densities, it is quite possible that the overall uncertainties in these results are also larger by a few hundredths of a per cent than the maximum given in table 5.

Fitting the results for mixtures to equation (4) does not allow a test of their consistency as a function of composition. Where densities are available for a given binary system at several temperatures and at three or more compositions, preferably at mole fractions of approximately 0.3, 0.5, and 0.7, excess volumes can be examined for consistency using a temperature-dependent Redlich-Kister expansion. In this study, compositions for methane + ethane and methane + propane were selected to allow this treatment. As shown in table 2, each of these systems also includes one mixture obtained from a laboratory with many years of experience in preparing gravimetric standards. Excess volumes for these systems were fitted to a Redlich-Kister expansion of the form:

$$V^E/\text{cm}^3 \text{ mol}^{-1} = x_1 x_2 \{ [a_0 + a_1(T/K) + a_2(T/K)^2] + \{b_0 + b_1(T/K) + b_2(T/K)^2\} (2x_1 - 1) + \{c_0 + c_1(T/K) + c_2(T/K)^2\} (2x_1 - 1) \} \quad (5)$$

where  $x_1$  is the mole fraction of methane. The least-squares coefficients  $a_i$ ,  $b_i$ , and  $c_i$ , and the standard deviation, in per cent of the average mixture molar volume, for each system are given in table 6. The  $c_i$  coefficients were not statistically significant

TABLE 6. Parameters of equation (5) for methane + ethane and for methane + propane;  $x_1$  is the methane mole fraction and  $\sigma$  the standard deviation

	methane + ethane	methane + propane
$a_0$	-14.22184	-11.96725
$a_1$	0.2649993	0.236748
$a_2$	-0.001419196	-0.001429237
$b_0$	-18.87392	16.59465
$b_1$	0.3108472	-0.3212125
$b_2$	-0.001349755	0.001398221
$c_0$		-52.93613
$c_1$		0.9887147
$c_2$		-0.004667488
$10^2\sigma\langle V^{-1}\rangle$	0.030	0.040

for methane + ethane. The excess volumes calculated from equation (5) are compared in figure 4 with the experimental values at 110 K from the present study.

The standard deviation for methane + ethane obtained with equation (5) is in very good agreement with that obtained with equation (4) for the methane + ethane mixture in table 5. However, the standard deviation for methane + propane obtained with equation (5) is more than a factor of two higher than that obtained with equation (4) for any of the individual mixtures in the set. The higher value from equation (5) is considered to be more indicative of the random error in the results for methane + propane.

The standard deviation given in table 6 for methane + propane was the highest value obtained in the analysis. With a total systematic error of about  $\pm 0.04$  per cent added to three times this standard deviation ( $\pm 0.12$  per cent), the overall uncertainty for methane + propane would be approximately  $\pm 0.16$  per cent. With the possible exceptions noted above (*i.e.* nitrogen + ethane, nitrogen + propane, and methane + *n*-butane), this is believed to be a suitable estimate of the maximum overall uncertainty in the densities of binary liquid mixtures obtained in this study.

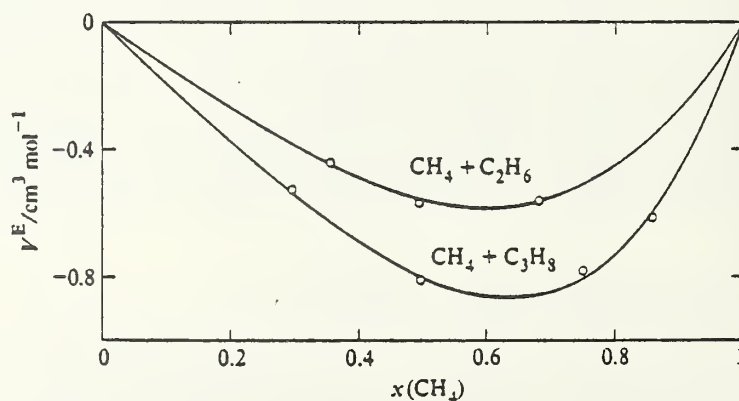


FIGURE 4. Excess volumes for methane + ethane and methane + propane from the present study at 110 K.  $\circ$ , experimental; —, calculated from fit to equation (5).

## COMPARISONS OF EXCESS VOLUMES

Equation (5) has also been used to compare the present results for methane + ethane and methane + propane with those of other investigators at 108.15 K, a temperature approximately common to all of their measurements. The excess volumes were taken directly from the literature where reported, or otherwise were calculated from the pure-fluid molar volumes in their data set. Though some of the results were 0.1 to 0.3 K below 108.15 K, the differences in temperature do not affect the comparisons of excess volumes appreciably. From equation (5), a change in temperature of 0.1 K results in a change in excess volume of  $0.001 \text{ cm}^3 \text{ mol}^{-1}$  for methane + ethane and about  $0.002 \text{ cm}^3 \text{ mol}^{-1}$  for methane + propane.

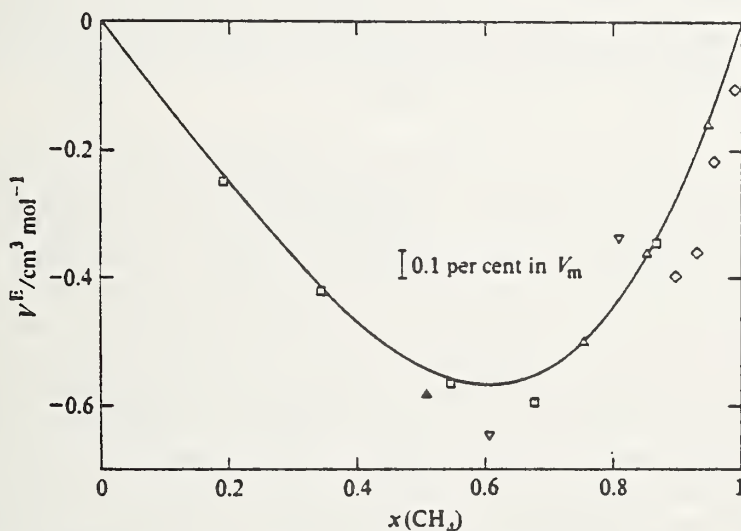


FIGURE 5. Comparison of excess volumes for methane + ethane at 108.15 K. —, Calculated from fit of present results to equation (5); □, Shana'a and Canfield;<sup>(25)</sup> △, Rodosevich and Miller;<sup>(26)</sup> ▲, Pan, Mady, and Miller;<sup>(27)</sup> ▽, Klosek and McKinley;<sup>(28)</sup> ◇, Jensen and Kurata.<sup>(29)</sup>

In figure 5, excess volumes for methane + ethane calculated from equation (5) at 108.15 K are compared with those from the experimental data of Shana'a and Canfield,<sup>(25)</sup> Rodosevich and Miller,<sup>(26)</sup> Pan, Mady, and Miller,<sup>(27)</sup> Klosek and McKinley,<sup>(28)</sup> and Jensen and Kurata.<sup>(29)</sup> The data from references 26 and 27 are at about 108 K and those from reference 28 are at about 107.9 K. The excess volumes from Shana'a and Canfield and from Miller and his colleagues are in excellent agreement with the curve calculated from the present results. With the exception of one point each from Shana'a and Canfield and from Miller and his colleagues, the differences are equivalent to much less than 0.1 per cent in the mixture molar volume. In contrast, the excess volumes from Klosek and McKinley and from Jensen and Kurata are much less consistent with the present results. The differences from the calculated curve are equivalent to 0.15 to 0.3 per cent in the mixture molar volume.

In figure 6, excess volumes for methane + propane calculated from equation (5)

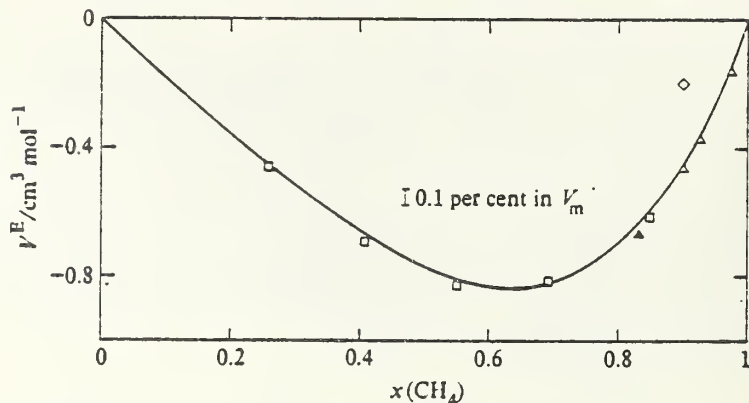


FIGURE 6. Comparison of excess volumes for methane + propane at 108.15 K. —, Calculated from fit of present results to equation (5); □, Shana'a and Canfield;<sup>(25)</sup> △, Rodosevich and Miller;<sup>(26)</sup> ▲, Pan, Mady, and Miller;<sup>(27)</sup> ◇, Jensen and Kurata.<sup>(29)</sup>

at 108.15 K are compared with those from the experimental data of Shana'a and Canfield,<sup>(25)</sup> Rodosevich and Miller,<sup>(26)</sup> Pan, Mady, and Miller,<sup>(27)</sup> and Jensen and Kurata.<sup>(29)</sup> For this system the excess volumes from Shana'a and Canfield and from Miller and his colleagues are also in excellent agreement with the curve from the present results with a maximum difference of about 0.06 per cent in the mixture molar volume. The excess volume from Jensen and Kurata again is not consistent with the present results. The difference is about 0.5 per cent in the average mixture molar volume, in the opposite direction from that found for methane + ethane.

Though there are only a few methane + *n*-butane points reported in the literature, a comparison can be made at 108.15 K in the methane-rich region between the excess volume interpolated from the present results for the (0.91674CH<sub>4</sub> + 0.08326*n*-C<sub>4</sub>H<sub>10</sub>) mixture and excess volumes from the experimental data reported by Shana'a and Canfield<sup>(25)</sup> and by Miller.<sup>(13)</sup> This comparison is given in figure 7. The excess volume from Shana'a and Canfield was computed using their pure methane data and the

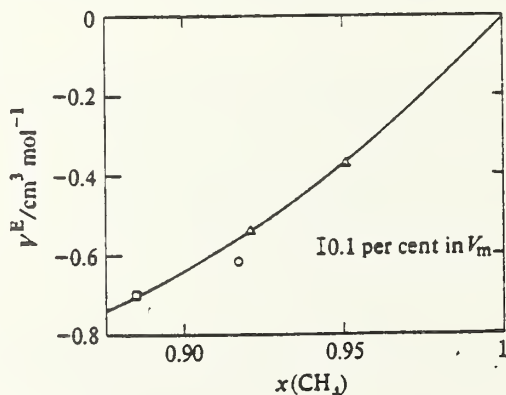


FIGURE 7. Comparison of excess volumes of methane + *n*-butane at 108.15 K. ○, Interpolated from the present study; □, Shana'a and Canfield;<sup>(25)</sup> △, Rodosevich and Miller.<sup>(26)</sup>

molar volume of *n*-butane obtained from equation (3). The excess volumes of Miller are those reported in his paper. The *n*-butane molar volumes used by Miller are within 0.02 per cent of the values given by equation (3). The difference between the excess volume interpolated from the present results and the curve drawn through the excess volumes of Shana'a and Canfield and of Miller is about 0.14 per cent of the mixture molar volume. Since the data from Shana'a and Canfield and from Miller appear to be in as good agreement for methane + *n*-butane as for methane + ethane and methane + propane, it is possible that at least part of the 0.14 per cent difference is due to an unaccounted error in our results for the mixture, as suggested earlier in this paper. Unfortunately, data are not available for comparison with the present results for  $(0.58828\text{CH}_4 + 0.41172n\text{-C}_4\text{H}_{10})$ , the accuracy of which we have no reason to question. Measurements for this mixture could not be made at the lower temperatures since the *n*-butane content is the solid solubility limit at about 116 K.<sup>(30)</sup>

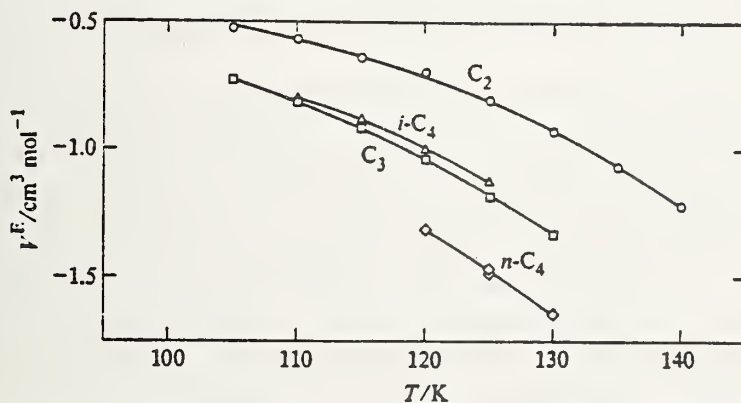


FIGURE 8. Comparison of excess volumes from the present study for methane + heavy hydrocarbon mixtures having  $x \approx 0.5$ ,  $\circ$ ,  $0.49325\text{CH}_4 + 0.50675\text{C}_2\text{H}_6$ ;  $\square$ ,  $0.49637\text{CH}_4 + 0.50363\text{C}_3\text{H}_8$ ;  $\triangle$ ,  $0.48687\text{CH}_4 + 0.51313i\text{-C}_4\text{H}_{10}$ ;  $\diamond$ ,  $0.58828\text{CH}_4 + 0.41172n\text{-C}_4\text{H}_{10}$ .

The only data for methane + *i*-butane in this temperature range are those of Rodosevich and Miller<sup>(26)</sup> for two mixtures with mole fractions 0.9152 and 0.9462 of  $\text{CH}_4$ . The excess volumes they report for these mixtures at 108 K are about half-way between their results for methane + propane and for methane + *n*-butane at the same methane mole fraction. The excess volumes for the mixture of methane + *i*-butane with  $x \approx 0.5$  from the present study are equivalent to those obtained for methane + propane at 110 K and the same composition. Excess volumes from the present study are shown in figure 8 for mixtures with  $x \approx 0.5$  of methane + ethane, + propane, and + *i*-butane. Excess volumes are also included for  $(0.58828\text{CH}_4 + 0.41172n\text{-C}_4\text{H}_{10})$  for comparison. It is clear that more extensive measurements of high precision are needed to describe accurately the composition dependence of the excess volumes for both methane + butane systems.

The small excess volumes given in table 3 for binary mixtures containing the higher molar-mass alkanes—ethane, propane, *i*-butane, and *n*-butane—show that at

cryogenic temperatures the molar volumes for binary mixtures of these components are closely approximated by the assumption of ideal mixing. The only other investigators who report data for binary mixtures of these alkanes at cryogenic temperatures are Shana'a and Canfield.<sup>(25)</sup> They report densities for several mixtures of ethane + propane and for one mixture of ethane + *n*-butane.

For ethane + propane, the excess volume reported by Shana'a and Canfield at 108.15 K for the mixture (0.5852C<sub>2</sub>H<sub>6</sub> + 0.4148C<sub>3</sub>H<sub>8</sub>) is compared in figure 9 with those determined from the present results at two similar compositions. If the excess volumes for ethane + propane exhibit an asymmetry similar to those for methane + ethane (figure 5), the excess volumes for the two ethane + propane mixtures from the present study should be nearly the same, with the excess volume at the higher mole fraction of C<sub>2</sub>H<sub>6</sub> slightly larger. Shana'a and Canfield report a maximum

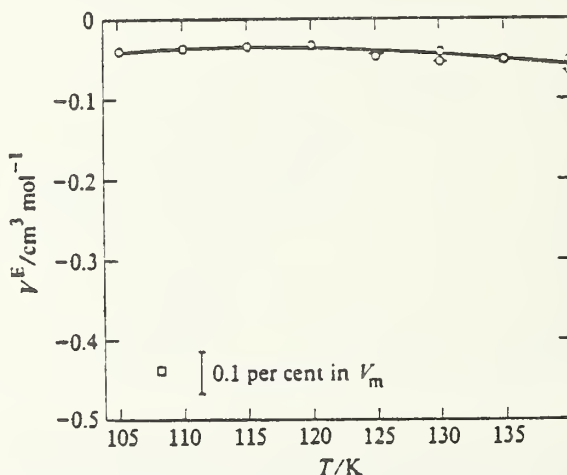


FIGURE 9. Comparison of excess volumes for ethane + propane. ○, ◐, Present study at  $x(\text{C}_2\text{H}_6) = 0.50105$  and  $0.67287$ , respectively; □, Shana'a and Canfield<sup>(25)</sup> at  $x(\text{C}_2\text{H}_6) = 0.5852$ .

excess volume for this system of  $-0.485 \text{ cm}^3 \text{ mol}^{-1}$  for a mixture containing (0.7036C<sub>2</sub>H<sub>6</sub> + 0.2964C<sub>3</sub>H<sub>8</sub>). The difference in excess volumes from the two sets of measurements is surprisingly large, equivalent to approximately 0.8 per cent in the mixture molar volume. Since the pure-fluid molar volumes for ethane and propane from Shana'a and Canfield are only higher than those determined with the present apparatus<sup>(3)</sup> by approximately 0.06 and 0.12 per cent, respectively, it is logical to suspect composition error or incomplete mixing as the source of this disagreement.

To assess the effect of composition uncertainty on the excess volume, it was assumed that the mixture mass density from the present study was exact and that the actual mole fraction of propane was 0.01 larger than the composition of the prepared mixture with  $x = 0.5$ . This results in an error of  $-0.062 \text{ cm}^3 \text{ mol}^{-1}$  in the excess volume. If the excess volume reported by Shana'a and Canfield were assumed to be correct, it would be necessary for the actual mole fraction of ethane in the liquid in the present study to be larger by 0.064 than that of the prepared mixture.

As discussed in the experimental section of this paper, chromatographic comparisons of the compositions of liquid samples for ethane + propane were in agreement with the composition of the prepared mixture within a few hundredths of 1 mole per cent. The fact that no change in density of the mixture could be detected during sample withdrawal is considered evidence that the liquid mixture was homogeneous. The fact that the two mixtures studied were prepared independently in two separate laboratories is also confirmation that there was no significant error in the mixture preparation.

Recent enthalpy of mixing measurements in binary mixtures of methane, ethane, and propane reported by Miller and Staveley<sup>(18)</sup> should also be referred to in regard to the ethane + propane results discussed above. These investigators report that the enthalpy of mixing at 112 K is about  $129 \text{ J mol}^{-1}$  for methane + propane with  $x = 0.5$ , about  $69 \text{ J mol}^{-1}$  for methane + ethane with  $x = 0.5$ , and probably less than  $5 \text{ J mol}^{-1}$  for ethane + propane throughout the composition range. A comparison of ratios of the enthalpies of mixing with ratios of the excess volumes for these systems also tends to support the more ideal excess volumes obtained in the present investigation.

Shana'a and Canfield include a discussion on the invalidity of the principle of congruence based on a comparison of their excess volumes for ethane + propane and methane + ethane with those for methane + propane as a function of the equivalent carbon number. When the excess volumes from the present study are used, methane + ethane shows the same departure as expected, but ethane + propane is in excellent agreement with methane + propane. For a detailed discussion of the method, the reader is referred to Shana'a and Canfield's paper.

In figure 10, the excess volume computed from the molar volume of the  $(0.8833\text{C}_2\text{H}_6 + 0.1167n\text{-C}_4\text{H}_{10})$  mixture reported by Shana'a and Canfield is compared with the excess volumes of this system computed from our results. The excess volume of Shana'a and Canfield was computed using their density for pure ethane and the molar

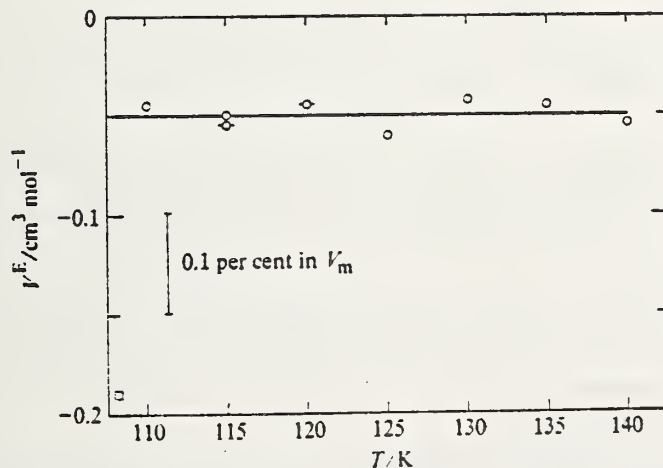


FIGURE 10. Comparison of excess volumes for ethane + *n*-butane. O, ⊙, Present study at  $x(\text{C}_2\text{H}_6) = 0.67117$  and  $0.65343$ , respectively; □, Shana'a and Canfield<sup>(25)</sup> at  $x(\text{C}_2\text{H}_6) = 0.8833$ .

volume of *n*-butane from equation (3). For this system the difference in excess volumes is equivalent to about 0.25 per cent in the mixture molar volume. Since the molar volumes for *n*-butane in the subcooled liquid region given by equation (3) were obtained from the results for this system the lack of temperature dependence is an artificial constraint. For this system, if the actual mole fraction of *n*-butane in the liquid mixture at 110 K was 0.01 larger than the composition of the mixtures prepared for this study, an error of  $-0.119 \text{ cm}^3 \text{ mol}^{-1}$  in the excess volume would result.

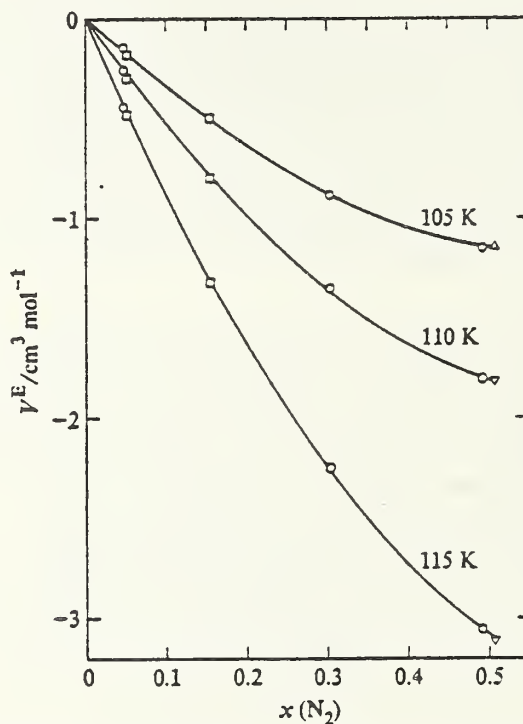


FIGURE 11. Comparison of excess volumes for nitrogen + methane.  $\circ$ , Present study;  $\square$ , Rodosevich and Miller;<sup>(26)</sup>  $\triangle$ , Liu and Miller;<sup>(31)</sup>  $\nabla$ , Massengill and Miller.<sup>(32)</sup>

Of the data available for liquid mixtures of nitrogen + methane,<sup>(6)</sup> the excess volumes reported by Rodosevich and Miller,<sup>(26)</sup> Liu and Miller,<sup>(31)</sup> and Massengill and Miller<sup>(32)</sup> were selected for comparison with excess volumes from the present results. These comparisons are shown in figure 11. The excess volumes of Massengill and Miller are from the data of Liu and Miller adjusted with additional nitrogen measurements. All of the excess volumes of Miller and his colleagues appear to be in agreement with excess volumes from the present results within 0.1 per cent of the mixture molar volumes. The height of the symbols is equivalent to about 0.1 per cent of the mixture molar volumes.

The fact that the nitrogen + methane excess volumes are in good agreement does not mean that the mixture molar volumes are in agreement. It is worth noting that the data reported by Liu and Miller and by Massengill and Miller were obtained with

a calibration based on the molar volumes of saturated liquid argon reported by Terry *et al.*<sup>(33)</sup> while all of the other data of Miller and his colleagues<sup>(13, 26, 27)</sup> referred to here were obtained with a calibration based on molar volumes of saturated liquid methane taken from Goodwin and Prydz.<sup>(34)</sup> From the discussion given earlier,<sup>(2)</sup> the nitrogen + methane molar volumes of Rodosevich and Miller should be higher but consistent with the present results within about 0.1 per cent, while those of Liu and Miller and of Massengill and Miller should be higher than the present results by about 0.4 per cent.

#### 4. Summary

The measurements of the present study provide a set of orthobaric liquid densities for binary mixtures of the major components of LNG which are generally consistent with those for the pure components within the precision of the measurements. The maximum random error in the densities of the binary mixtures is believed to be about  $\pm 0.12$  per cent, roughly twice that for the pure fluid densities. The known systematic errors in the densities for both the pure fluids and the binary mixtures were estimated to be from 0.03 to 0.05 per cent. As noted, the uncertainties in the densities for methane + *n*-butane with  $x(\text{CH}_4) > 0.9$ , and for nitrogen + ethane and nitrogen + propane, could exceed these estimates.

The largest excess volume found was  $-6.11 \text{ cm}^3 \text{ mol}^{-1}$  for nitrogen + methane with  $x = 0.5$  at 120 K. This is equivalent to 13 per cent of the ideal mixture molar volume. In contrast, the present results show that molar volumes of mixtures of the alkanes, excluding methane, are closely approximated by ideal mixing in the temperature range studied. The most significant disagreement between the present results and published data is the 0.8 per cent difference in density for ethane + propane from that of Shana'a and Canfield.

Based on the excess volumes of the alkane mixtures, excluding methane, from the present study, it was shown also that effective molar volumes of subcooled *n*-butane in a binary liquid mixture may differ by a small but significant amount dependent on the other components present. It is suggested that this behavior would be worth investigating in more detail for *n*-butane and other fluids such as *n*-pentane. There is also a definite need for additional measurements on the binary mixtures containing both *n*-butane and *i*-butane with methane.

In subsequent papers, the results of measurements of orthobaric liquid densities of multicomponent mixtures and the ability of theoretical models to predict the measured densities will be reported.

The authors acknowledge the contributions of M. J. Brown, R. C. Miller, and R. D. McCarty to the correlation of the results.

#### REFERENCES

1. Robinson, R. L., Jr.; Hiza, M. J. In *Advances in Cryogenic Engineering*, Vol. 20. Timmerhaus, K. D.: editor. Plenum Press: New York. 1975. p. 218.
2. Haynes, W. M.; Hiza, M. J.; Frederick, N. V. *Rev. Sci. Instrum.* 1976, 47, 1237.
3. Haynes, W. M.; Hiza, M. J. *J. Chem. Thermodynamics* 1977, 9, 179.

4. Yu, P.; Elshayal, I. M.; Lu, B. C.-Y. *Can. J. Chem. Eng.* 1969, 47, 495.
5. Poon, D. P. L.; Lu, B. C.-Y. In *Advances in Cryogenic Engineering*, Vol. 19. Timmerhaus, K. D.: editor. Plenum Press: New York. 1974, p. 292.
6. Hiza, M. J.; Kidnay, A. J.; Miller, R. C. *Equilibrium Properties of Fluid Mixtures, A Bibliography of Data on Fluids of Cryogenic Interest*. NSRDS Bibliographic Series. IFI Plenum: New York. 1975.
7. Haynes, W. M. *Rev. Sci. Instrum.* 1977, 48, 39.
8. Tully, P. C.; Emerson, D. Personal communications. November 1974, August 1976.
9. Duncan, A. G., Hiza, M. J. In *Advances in Cryogenic Engineering* Vol. 15. Timmerhaus, K. D.: editor. Plenum Press: New York. 1970. p. 42.
10. Hiza, M. J.; Duncan, A. G. *Rev. Sci. Instrum.* 1969, 40, 513.
11. Goodwin, R. D.; Roder, H. M.; Straty, G. C. *Nat. Bur. Stand. U.S., Tech. Note* 684, 1976.
12. Rowlinson, J. S. *Liquids and Liquid Mixtures*. 2nd Ed. Butterworths: London. 1969.
13. Miller, R. C. *Chem. Eng.* 1974, 81, 134.
14. Goodwin, R. D. *Nat. Bur. Stand. U.S., Tech. Note* 653, 1974.
15. Strobridge, T. R. *Nat. Bur. Stand. U.S., Tech. Note* 129, 1962.
16. Parrish, W. R.; Hiza, M. J. In *Advances in Cryogenic Engineering* Vol. 19. Timmerhaus, K. D.: editor. Plenum Press: New York. 1974, p. 300.
17. Kidnay, A. J.; Miller, R. C.; Parrish, W. R.; Hiza, M. J. *Cryogenics* 1975, 15, 531.
18. Miller, R. C.; Staveley, L. A. K. In *Advances in Cryogenic Engineering*, Vol. 21. Timmerhaus, K. D. and Weitzel, D. H.: editors. Plenum Press: New York. 1976, p. 493.
19. Miller, R. C.; Kidnay, A. J.; Hiza, M. J. *J. Chem. Thermodynamics* 1977, 9, 167.
20. Wichterle, I.; Kobayashi, R. *J. Chem. Eng. Data* 1972, 17, 9.
21. Stoeckli, H. F.; Staveley, L. A. K. *Helv. Chim. Acta* 1970, 53, 1961.
22. Cutler, A. J. B.; Morrison, J. A. *Trans. Faraday Soc.* 1965, 61, 429.
23. Calado, J. C. G.; Garcia, G.; Staveley, L. A. K. *J. Chem. Soc., Faraday Trans. I*, 1974, 70, 1445.
24. Chueh, P. L.; Prausnitz, J. M. *AIChE J.* 1967, 13, 1107.
25. Shana'a, M. Y.; Canfield, F. B. *Trans. Faraday Soc.* 1968, 64, 2281.
26. Rodosevich, J. B.; Miller, R. C. *AIChE J.* 1973, 19, 729.
27. Pan, W. P.; Mady, M. H.; Miller, R. C. *AIChE J.* 1975, 21, 283.
28. Klosek, J.; McKinley, C. In *Proceedings of the First International Conference on LNG*. White, J. W. and Neumann, A. E. S.: editors. Institute of Gas Technology, Chicago, Illinois. 1968. Paper No. 22.
29. Jensen, R. H.; Kurata, F. *J. Petrol. Technol.* 1969, 21, 683.
30. Kuebler, G. P.; McKinley, C. In *Advances in Cryogenic Engineering* Vol. 21. Timmerhaus, K. D.; Weitzel, D. H.: editors. Plenum Press: New York. 1976, p. 509.
31. Liu, Y.-P.; Miller, R. C. *J. Chem. Thermodynamics* 1972, 4, 85.
32. Massengill, D. R.; Miller, R. C. *J. Chem. Thermodynamics* 1973, 5, 207.
33. Terry, M. J.; Lynch, J. F.; Bunclark, M.; Mansell, K. R.; Staveley, L. A. K. *J. Chem. Thermodynamics* 1969, 1, 413.
34. Goodwin, R. D.; Prydz, R. *J. Res. Nat. Bur. Stand. U.S.* 1972, 76A, 81.

O-37

*J. Chem. Thermodynamics* 1983, 15, 903-911

## Orthobaric liquid densities and dielectric constants of (methane + 2-methylpropane) and (methane + *n*-butane) at low temperatures<sup>a</sup>

W. M. HAYNES

*Thermophysical Properties Division, National Engineering Laboratory,  
National Bureau of Standards, Boulder, Colorado 80303, U.S.A.*

*(Received 12 January 1983)*

Measurements of the orthobaric liquid densities and dielectric constants of methane-rich (methane + 2-methylpropane) and (methane + *n*-butane) have been obtained at temperatures between 110 and 140 K. Densities were determined with a magnetic-suspension densimeter, while a concentric-cylinder capacitor was used for simultaneous measurements of dielectric constant. These measurements were part of an experimental program that has provided a consistent and comprehensive set of densities for the major components of liquefied natural gas (LNG) and their mixtures, which was used to develop mathematical models for the calculation or prediction of LNG densities. Along with the (methane + 2-methylpropane) and (methane + *n*-butane) experimental densities and dielectric constants, are presented experimental vapor pressures, as well as excess volumes, Clausius-Mossotti functions, and excess Clausius-Mossotti functions, derived from the densities and dielectric constants. Comparisons are shown between the excess volumes of the present work and those from independent measurement using an extended corresponding-states model that had been optimized to the results from this work. The total uncertainty of a single density measurement is approximately 0.1 per cent with a precision of a few parts in 10<sup>4</sup>. Dielectric constants are estimated to be accurate to approximately 0.05 per cent. A brief description of the apparatus, experimental method, and procedures is also presented.

### 1. Introduction

An experimental program<sup>(1-8)</sup> has been carried out at this laboratory to measure with an uncertainty of less than 0.1 per cent the orthobaric liquid densities of the major components<sup>(1-3)</sup> of liquefied natural gas (LNG) and mixtures<sup>(4,6,7)</sup> of these components. The pure fluid and binary mixture results have been incorporated into the development of several mathematical models<sup>(9-12)</sup> that can be used to predict within an uncertainty of less than 0.1 per cent the density of any LNG mixture at

<sup>a</sup> This work was carried out at the National Bureau of Standards under the sponsorship of the British Gas Corporation, Chicago Bridge and Iron Co., Columbia Gas Service Corp., Distrigas Corp., Easco Gas LNG, Inc., El Paso Natural Gas, Gaz de France, Marathon Oil Co., Mobil Oil Corp., Natural Gas Pipeline Co., Phillips Petroleum Co., Shell International Gas, Ltd., Sonatrach, Southern California Gas Co., Tennessee Gas Pipeline Co., Texas Eastern Transmission Co., Tokyo Gas Co., Ltd., and Transcontinental Gas Pipe Line Corp., through a grant administered by the American Gas Association, Inc.

saturation from an input of the temperature, composition, and pressure of the liquid mixture. Multicomponent-mixture results have been used to test the models.

Orthobaric liquid densities from this project have been previously reported for nitrogen,<sup>(1)</sup> methane,<sup>(1,3)</sup> ethane,<sup>(3)</sup> propane,<sup>(3)</sup> 2-methylpropane,<sup>(3)</sup> and *n*-butane;<sup>(2,3)</sup> all binary combinations<sup>(4)</sup> of those components except (nitrogen + 2-methylpropane) and (nitrogen + *n*-butane); and selected multicomponent mixtures<sup>(6,7)</sup> with up to eight components that included 2-methylbutane and *n*-pentane in addition to those mentioned above. In an earlier paper<sup>(4)</sup> describing binary-mixture measurements, the need for additional measurements on binary mixtures of methane with either 2-methylpropane or *n*-butane was cited. Experimental problems had been encountered in the earlier study in obtaining consistent results for methane-rich binary mixtures containing 2-methylpropane or *n*-butane. It was conjectured that these difficulties were associated with liquid methane condensing in the narrow annulus around a vapor-pressure bulb that fitted tightly inside the top part of the cell. Thus, the present work was carried out to resolve these inconsistencies and to provide values for these mixtures that would complement and extend the earlier results. The earlier work provided results for  $\{x\text{CH}_4 + (1-x)(\text{CH}_3)_2\text{CHCH}_3\}$  and  $\{x\text{CH}_4 + (1-x)\text{C}_4\text{H}_{10}\}$  with  $x \approx 0.5$  while the present study includes results for methane-rich mixtures ( $x$  from 0.78 to 0.93).

The density results from the present study were obtained using a magnetic-suspension densimeter<sup>(1,5)</sup> that was part of a new apparatus,<sup>(7,8)</sup> which differed significantly from that employed for the previous measurements.<sup>(4)</sup> (The new apparatus<sup>(8)</sup> was developed because a magnetic-suspension densimeter of higher-pressure capability, 35 MPa, was desired for other projects.) Although the new apparatus exploited the same technique for density measurements as that used in the earlier work and gave results that agreed, within experimental precision, with those obtained with the previous apparatus, there were significant new and improved features of the apparatus that were important to the present work. These will be discussed in the next section.

The new apparatus contained a capacitor that was used for obtaining dielectric constants along with the densities. Through the use of the Clausius-Mossotti function, dielectric constant measurements can serve as a simple and reliable substitute for density measurements. In the custody transfer of LNG, densities are determined by direct measurements or indirectly using a calculational technique based on measurements of composition and temperature. One technique for commercially available densimeters is predicated on a density determination through the application of dielectric-constant measurements. Thus both the dielectric constants and densities from this study can contribute to equitable custody transfer of such a valuable commodity as LNG.

## 2. Experimental

The experimental method, apparatus, and procedures for density measurements have been discussed in detail in other papers.<sup>(1-8)</sup> Thus, this section will focus on a description of the technique and procedures for the dielectric-constant

measurements, along with a discussion of those features of the apparatus and procedures that are specific to the present study.

The dielectric-constant measurements were performed with a concentric-cylinder capacitor of a design similar to that of Younglove and Straty.<sup>(13)</sup> There is one major difference between their design and that used here. Instead of solid cylinders, the capacitor in the present work consisted of cylinders with slots cut parallel to the cylindrical axes, similar to the ring-and-bar design of Pan *et al.*<sup>(14)</sup> This modification was carried out for the same reason as that given by Pan *et al.*: to reduce as far as possible the chances for composition gradients in the cell. The copper capacitor was located in the top portion of the cell, while the magnetic buoy and position sensor for the magnetic-suspension densimeter were contained in the lower portion. Assuming the absence of composition and temperature gradients, simultaneous measurements of density and dielectric constant were made on the same liquid samples.

The dielectric constant was determined from measurements of the ratio of the capacitance with liquid between the electrodes to the capacitance *in vacuo*. The capacitance *in vacuo* was approximately 20 pF. The overall external dimensions of the capacitor were 6.4 cm in length by 1.77 cm in diameter. The widths of the five slots in each cylinder were 0.32 cm, while the slot lengths in the outer cylinder were 4.1 cm and those in the inner cylinder were 1.9 cm. Kapton† film insulators of 0.05 mm thickness were used between the cylinders and the support assembly. The entire capacitor assembly was fabricated from copper and subsequently plated with gold. Capacitances were measured with a three-terminal a.c. bridge operated at an oscillator frequency of 5 kHz.

Although the resolution of the measured capacitances was approximately  $10^{-4}$  pF, the overall uncertainty in the dielectric-constant measurements for the mixtures investigated here was approximately 0.05 per cent. The limiting factor was the reproducibility of the measurements, which was based on measurements from several fillings taken from the same cylinder of prepared mixture. The dielectric-constant determination was the most sensitive monitor inside the sample space to indicate the reproducibility of liquid compositions each time the cell was recharged. *In vacuo* capacitances, measured to a precision of approximately  $10^{-4}$  pF, were observed before each run and were stable to better than  $10^{-3}$  pF over the duration of this project.

The densities were determined using a one-solenoid magnetic-suspension densimeter<sup>(5)</sup> with a differential-capacitance sensor<sup>(15)</sup> used to detect the position of the magnetic buoy. The total uncertainty<sup>(1,4)</sup> in the density determination was estimated to be 0.12 per cent, which includes an allowance of three times the standard deviation for random error. As demonstrated in a following section, the precision of measurement was better than  $3 \times 10^{-4}$ .

Procedures for preparing mixtures of LNG components gravimetrically have been

† In order to describe materials and experimental procedures adequately, it is occasionally necessary to identify commercial products by manufacturer's or trade names. In no instance does such identification imply endorsement by the National Bureau of Standards, nor does it imply that the particular product is necessarily the best available for that purpose.

discussed previously.<sup>(4)</sup> For the mixtures investigated here, at least 3.8 mol was prepared for each composition. This corresponds to less than 0.0001 uncertainty in the mole fraction of CH<sub>4</sub> and considerably less uncertainty for either (CH<sub>3</sub>)<sub>2</sub>CHCH<sub>3</sub> or C<sub>4</sub>H<sub>10</sub>.

Vapor pressures were measured with a spiral quartz Bourdon-tube gauge with a range of 0 to 1.38 MPa that had been calibrated against an air dead-weight gauge. Maximum uncertainty in the calibration was 70 Pa. Vapor-pressure measurements were generally reproducible to within  $3 \times 10^{-4}$  MPa for different fillings of the cell with the same mixture.

Prior to the filling of the cell with each new mixture sample, a density measurement was performed on liquid methane to serve as a check on the density-measurement process. The densities were obtained to ensure that the alignment of the cryostat and cell windows had not changed as a result of temperature cycling of the apparatus. The windows had been aligned, along with the microscope, so that the buoy-position determination was independent of the refractive index of the fluid inside the cell. The cell had to be warmed to room temperature to effect complete removal of mixtures containing butanes. Measurements *in vacuo* needed for both density and dielectric-constant determinations were obtained before each new filling of the cell. A maximum of four points at 5 K increments was obtained for each filling.

The mixtures were condensed directly and continuously into the cell at a pressure greater than the vapor pressure of methane either through two capillaries at the bottom of the cell or simultaneously through capillaries at both the top and bottom of the cell. Based on the consistency of the results, it was found that, within the precision of the measurements, the density and dielectric-constant results were independent of the filling routines used.

All of the measurements in this project were made on liquid mixtures in equilibrium with vapor. To minimize composition or density errors, it was of the utmost importance to reduce as much as possible the low-temperature vapor volume in the sample space. The total internal volume of the sample cell was 43 cm<sup>3</sup>, while the low-temperature vapor volume was less than 0.2 cm<sup>3</sup>. Assuming that the vapor composition was pure methane for the mixtures studied here, the maximum adjustment (decrease) to the measured densities because of differences in composition between the prepared mixtures and the mixtures condensed into the cell was 0.045 per cent, which was at 140 K for the mixtures with  $x \approx 0.78$ . This corresponded to a correction of 0.03 per cent in the dielectric constant.

### 3. Results and discussion

The experimental orthobaric liquid densities, vapor pressures, and dielectric constants for (methane + 2-methylpropane) and (methane + *n*-butane) are presented as a function of temperature (IPTS-68) in table 1. Excess molar volumes and Clausius-Mossotti functions, as well as excess Clausius-Mossotti functions, are also given in table 1. The excess molar volume  $V_m^E$  is defined by the relation:

$$V_m^E = V_m - \sum_i x_i V_i^* \{1 + \kappa_i (p_i^* - p)\}, \quad (1)$$

TABLE 1. Orthobaric liquid densities and dielectric constants of  $\{x\text{CH}_4 + (1-x)(\text{CH}_3)_2\text{CHCH}_3\}$  and  $\{x\text{CH}_4 + (1-x)\text{C}_4\text{H}_{10}\}$ .  $M$ , molar mass;  $T$ , temperature (IPTS-68);  $p$ , pressure;  $\rho_n$ , experimental amount-of-substance density;  $\rho_{\text{expt}}$ , experimental density;  $\rho_{\text{calc}}$ , density calculated from equation (4);  $V_m^E$ , excess molar volume;  $\epsilon$ , dielectric constant;  $\phi_{\text{CM}}$ , Clausius-Mossotti function;  $\phi_{\text{CM}}^E$ , excess Clausius-Mossotti function

$T$ K	$p$ MPa	$\rho_n$ $\text{mol} \cdot \text{dm}^{-3}$	$\frac{10^2(\rho_{\text{expt}} - \rho_{\text{calc}})}{\rho_{\text{calc}}}$	$V_m^E$ $\text{cm}^3 \cdot \text{mol}^{-1}$	$\epsilon$	$\phi_{\text{CM}}$ $\text{cm}^3 \cdot \text{mol}^{-1}$	$\phi_{\text{CM}}^E$ $\text{cm}^3 \cdot \text{mol}^{-1}$
<b>0.92044CH<sub>4</sub> + 0.07956(CH<sub>3</sub>)<sub>2</sub>CHCH<sub>3</sub> (<math>M = 19.3910 \text{ g} \cdot \text{mol}^{-1}</math>)</b>							
115.00	0.1254	24.3633	-0.016	-0.547	1.69665	7.7352	0.024
120.00	0.1805	24.0029	-0.006	-0.624	1.68372	7.7326	0.021
125.00	0.2521	23.6403	0.011	-0.726	1.67103	7.7322	0.020
130.00	0.3434	23.2752	0.037	-0.859	1.65838	7.7321	0.018
135.00	0.4567	22.8920	0.004	-1.001	1.64527	7.7326	0.017
140.00	0.5950	22.5037	-0.030	-1.186	1.63196	7.7320	0.015
<b>0.78329CH<sub>4</sub> + 0.21671(CH<sub>3</sub>)<sub>2</sub>CHCH<sub>3</sub> (<math>M = 25.1625 \text{ g} \cdot \text{mol}^{-1}</math>)</b>							
110.00	0.0782	21.9144	0.005	-0.837	1.81689	9.7662	0.050
115.00	0.1164	21.6652	0.001	-0.941	1.80487	9.7639	0.051
120.00	0.1671	21.4136	-0.011	-1.065	1.79271	9.7605	0.050
125.00	0.2329	21.1668	0.006	-1.229	1.78094	9.7581	0.049
130.00	0.3170	20.9125	-0.008	-1.412	1.76906	9.7571	0.049
135.00	0.4208	20.6629	0.006	-1.648	1.75729	9.7543	0.047
140.00	0.5474	20.4082	0.001	-1.925	1.74568	9.7548	0.047
<b>0.92788CH<sub>4</sub> + 0.07212C<sub>4</sub>H<sub>10</sub> (<math>M = 19.0779 \text{ g} \cdot \text{mol}^{-1}</math>)</b>							
120.00	0.1820	24.2615	-0.006	-0.661	1.67289	7.5511	0.007
125.00	0.2547	23.8868	0.005	-0.756	1.66033	7.5524	0.005
130.00	0.3470	23.5047	0.000	-0.872	1.64764	7.5538	0.003
135.00	0.4616	23.1225	0.012	-1.031	1.63477	7.5528	-0.001
140.00	0.6023	22.7284	-0.011	-1.219	1.62190	7.5547	-0.002
<b>0.92780CH<sub>4</sub> + 0.07220C<sub>4</sub>H<sub>10</sub> (<math>M = 19.0813 \text{ g} \cdot \text{mol}^{-1}</math>)</b>							
115.00	0.1270	24.6285		-0.586	1.68465	7.5445	0.002
120.00	0.1824	24.2783		-0.693	1.67243	7.5418	-0.003
125.00	0.2549	23.8999		-0.782	1.65994	7.5446	-0.003
<b>0.77982CH<sub>4</sub> + 0.22018C<sub>4</sub>H<sub>10</sub> (<math>M = 25.3085 \text{ g} \cdot \text{mol}^{-1}</math>)</b>							
120.00	0.1702	21.6066	0.003	-1.288	1.78385	9.5877	0.006
125.00	0.2369	21.3549	-0.002	-1.444	1.77286	9.5925	0.007
130.00	0.3228	21.1020	-0.010	-1.633	1.76202	9.5989	0.009
135.00	0.4291	20.8555	0.016	-1.879	1.75113	9.6013	0.008
140.00	0.5576	20.5978	-0.007	-2.151	1.73990	9.6049	0.007
<b>0.77762CH<sub>4</sub> + 0.22238C<sub>4</sub>H<sub>10</sub> (<math>M = 25.4011 \text{ g} \cdot \text{mol}^{-1}</math>)</b>							
115.00	0.1179	21.8054	-0.027	-1.135	1.79554	9.6122	0.005
120.00	0.1699	21.5601	-0.001	-1.273	1.78485	9.6180	0.007
125.00	0.2372	21.3164	0.037	-1.444	1.77382	9.6193	0.004
130.00	0.3230	21.0605	0.021	-1.623	1.76272	9.6249	0.005
135.00	0.4291	20.8011	-0.009	-1.836	1.75139	9.6291	0.005
140.00	0.5579	20.5448	-0.021	-2.107	1.74020	9.6328	0.004

where  $V_m$  is the molar volume of the mixture at a given temperature at saturation pressure  $p$ ,  $V_i^*$  is the molar volume of pure component  $i$  at the same temperature at saturation pressure  $p_i^*$ ,  $x_i$  is the mole fraction of component  $i$ , and  $\kappa_i$  is the isothermal compressibility of component  $i$ . The Clausius-Mossotti function  $\phi_{CM}$  is defined by the expression:

$$\phi_{CM} = (\epsilon - 1)/(\epsilon + 2)\rho_n \quad (2)$$

where  $\rho_n$  is the amount-of-substance density and  $\epsilon$  is the dielectric constant. Then the excess Clausius-Mossotti function  $\phi_{CM}^E$  for a liquid mixture is defined, analogously to  $V_m^E$ , by the relation:

$$\phi_{CM}^E = \phi_{CM} - \sum_i x_i \phi_{CM,i}^* \quad (3)$$

where  $\phi_{CM}$  refers to the Clausius-Mossotti function of the mixture at a given temperature at saturation pressure and  $\phi_{CM,i}^*$  is the Clausius-Mossotti function of pure component  $i$  at the same temperature and pressure as the mixture. Along an isotherm, the Clausius-Mossotti function is a very slowly varying function; therefore, adjustments of saturated-liquid pure-component Clausius-Mossotti values to the saturation pressure of the mixture are sufficiently small to neglect.

In the calculation of  $V_m^E$  and  $\phi_{CM,i}^*$ , the pure-component molar volumes of  $\text{CH}_4$ ,  $(\text{CH}_3)_2\text{CHCH}_3$ , and  $\text{C}_4\text{H}_{10}$  were calculated from equations<sup>(3)</sup> used to fit the experimental orthobaric liquid densities obtained with the first version of the magnetic-suspension densimeter used in the LNG density project. For 2-methylpropane and  $n$ -butane, the equations were used for extrapolation below their triple-point temperatures. The molar volumes of  $\text{CH}_4$  were adjusted to the mixture pressure using vapor pressures from Goodwin<sup>(16)</sup> and isothermal compressibilities from Rowlinson.<sup>(17)</sup> The compressibility corrections for 2-methylpropane and  $n$ -butane were sufficiently small to disregard. The dielectric constants of the pure components, used in the calculation of  $\phi_{CM,i}^*$ , were taken from Straty and Goodwin<sup>(18)</sup> for  $\text{CH}_4$  and from Haynes and Younglove<sup>(19)</sup> for  $(\text{CH}_3)_2\text{CHCH}_3$  and  $\text{C}_4\text{H}_{10}$ .

The binary-mixture results presented in this paper, along with the previous pure-fluid and binary-mixture results from the LNG density project, have been used to optimize several mathematical models<sup>(9-12)</sup> for the prediction of LNG densities. The most accurate and versatile of the models is the extended corresponding-states model,<sup>(9-11)</sup> which will be utilized here to demonstrate the consistency of the results for (methane + 2-methylpropane) and (methane +  $n$ -butane) from the LNG density project at this laboratory and to make comparisons with values for these mixtures from other sources.

In figure 1 the experimental results for  $\{x\text{CH}_4 + (1-x)(\text{CH}_3)_2\text{CHCH}_3\}$  from the LNG density project and from Rodosevich and Miller<sup>(20)</sup> are compared with values calculated from the extended corresponding-states method. The differences are less than 0.1 per cent for all points, including the values for  $x \approx 0.5$  obtained earlier<sup>(4)</sup> in the LNG density project. Figure 2 shows comparisons of experimental results for  $\{x\text{CH}_4 + (1-x)\text{C}_4\text{H}_{10}\}$  from the LNG density project, from Miller,<sup>(21)</sup> and from Shana'a and Canfield,<sup>(22)</sup> with values predicted from the extended corresponding-

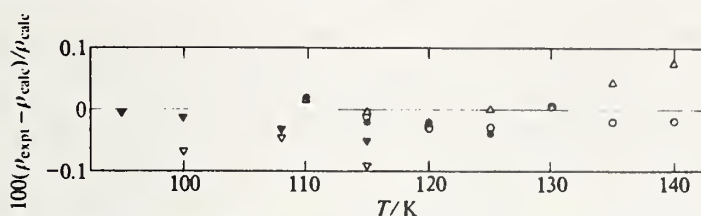


FIGURE 1. Comparison of experimental densities of  $\{x\text{CH}_4 + (1-x)(\text{CH}_3)_2\text{CHCH}_3\}$  from this work, from Hiza *et al.*,<sup>(4)</sup> and from Rodosevich and Miller,<sup>(20)</sup> with values calculated from the extended corresponding-states model.<sup>(9-11)</sup> ○, This work,  $x = 0.92044$ ; △, this work,  $x = 0.78329$ ; \*, Hiza *et al.*,  $x = 0.48687$ ; ▽, Rodosevich and Miller,  $x = 0.9462$ ; ▾, Rodosevich and Miller,  $x = 0.9152$ .

states model. In general, the agreement is good (within  $\pm 0.1$  per cent) except for the results for  $(0.92\text{CH}_4 + 0.08\text{C}_4\text{H}_{10})$ <sup>(4)</sup> obtained with the first version of the magnetic-suspension densimeter used in the LNG density project. As reported earlier in this paper, experimental difficulties were encountered with that apparatus in performing measurements on methane-rich mixtures containing heavy hydrocarbons. Therefore, the results for  $(0.92\text{CH}_4 + 0.08\text{C}_4\text{H}_{10})$  were not included in the development of the LNG mathematical models.<sup>(11)</sup>

The excess molar volume  $V_m^E$  is plotted as a function of  $x$  in figure 3 for isotherms at 115 K for  $\{x\text{CH}_4 + (1-x)(\text{CH}_3)_2\text{CHCH}_3\}$  and  $\{x\text{CH}_4 + (1-x)\text{C}_4\text{H}_{10}\}$ . The smoothed curves represent values calculated from the extended corresponding-states model. The results from the LNG density project are shown on the figure. The maximum excess molar volume for  $\{x\text{CH}_4 + (1-x)\text{C}_4\text{H}_{10}\}$  at 115 K,  $-1.24 \text{ cm}^3 \cdot \text{mol}^{-1}$  at  $x = 0.65$ , was approximately 20 per cent larger than that observed for  $\{x\text{CH}_4 + (1-x)(\text{CH}_3)_2\text{CHCH}_3\}$  at the same temperature.

For those compositions with points at five or more temperatures, the experimental amount-of-substance densities  $\rho_n$  have been fitted as a function of temperature  $T$  to the relation:

$$(\rho_n - \rho_{n,c})/(\text{mol} \cdot \text{dm}^{-3}) = a(1 - T/T_c)^{0.35} + \sum_{i=1}^3 b_i(1 - T/T_c)^{1+(i-1)/3}, \quad (4)$$

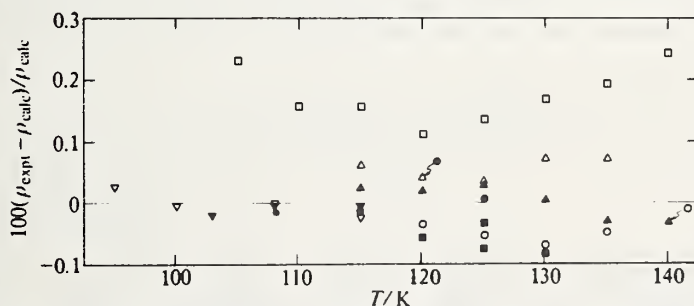


FIGURE 2. Comparison of experimental densities of  $\{x\text{CH}_4 + (1-x)\text{C}_4\text{H}_{10}\}$  from this work, from Hiza *et al.*,<sup>(4)</sup> from Miller,<sup>(21)</sup> and from Shana'a and Canfield,<sup>(22)</sup> with values calculated from the extended corresponding-states model.<sup>(9-11)</sup> ○, This work,  $x = 0.92788$ ; ●, this work,  $x = 0.92780$ ; △, this work,  $x = 0.77982$ ; ▲, this work,  $x = 0.77762$ ; □, Hiza *et al.*,  $x = 0.91674$ ; ■, Hiza *et al.*,  $x = 0.58828$ ; ▽, Miller,  $x = 0.9506$ ; ▾, Miller,  $x = 0.9206$ ; \*, Shana'a and Canfield,  $x = 0.8843$ .

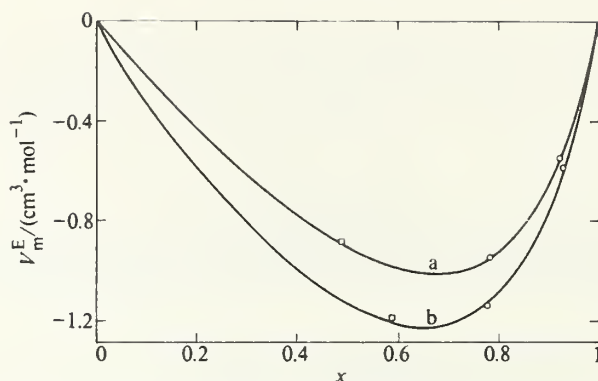


FIGURE 3. Excess molar volumes of (a),  $\{x\text{CH}_4 + (1-x)(\text{CH}_3)_2\text{CHCH}_3\}$  and (b),  $\{x\text{CH}_4 + (1-x)\text{C}_4\text{H}_{10}\}$  as a function of  $x$ . Smoothed curves represent values calculated from the extended corresponding-states model.<sup>(9-11)</sup> Points from the LNG density project are shown: O, This work; □, Hiza *et al.*<sup>(4)</sup>

where  $T_c$  and  $\rho_{n,c}$  are the critical temperature and the critical amount-of-substance density;  $a$  and  $b_i$  are coefficients determined by least squares. (This equation had been used previously<sup>(3)</sup> to represent the orthobaric liquid densities of the pure components<sup>(3)</sup> of LNG and selected binary mixtures<sup>(4)</sup> of these components.) For the results presented here, only two coefficients were statistically significant in the fits. The critical temperatures and densities were obtained from Chueh and Prausnitz<sup>(2,3)</sup> using the pure-component critical-point values given in reference 3. These fits were relatively insensitive to the selected critical-point values. The results of the fits are given in table 2. The maximum standard deviation was 0.028 per cent in the density, which agrees with that observed in the other binary mixture measurements reported earlier<sup>(4)</sup> for the LNG density project. Deviations of the experimental densities from values calculated from equation (4) are given in table 1.

The systematic errors involved in density measurements on mixtures with the magnetic-suspension technique used here have been discussed in detail elsewhere.<sup>(1,4)</sup> The total uncertainty is taken as the square root of the sum of the squares of the systematic errors plus an allowance of three times the standard

TABLE 2. Parameters of equation (4) where  $T_c$  and  $\rho_{n,c}$  are the critical temperature and critical amount-of-substance density of the mixture<sup>a</sup>

Mixture	$a$	$b_1$	$\frac{T_c}{K}$	$\frac{\rho_{n,c}}{\text{mol} \cdot \text{dm}^{-3}}$	$10^2 \langle (\delta\rho/\rho)^2 \rangle^{1/2}$
$0.92044\text{CH}_4 + 0.07956(\text{CH}_3)_2\text{CHCH}_3$	11.21295	10.64118	232.19	10.17	0.026
$0.78329\text{CH}_4 + 0.21671(\text{CH}_3)_2\text{CHCH}_3$	6.265006	11.14928	285.80	9.77	0.007
$0.92788\text{CH}_4 + 0.07212\text{C}_4\text{H}_{10}$	9.448745	12.23371	233.14	10.99	0.010
$0.77982\text{CH}_4 + 0.22018\text{C}_4\text{H}_{10}$	4.436119	12.72402	297.59	10.31	0.012
$0.77762\text{CH}_4 + 0.22238\text{C}_4\text{H}_{10}$	4.238446	12.93083	298.37	10.29	0.028

<sup>a</sup> The coefficients ( $a, b_1$ ) were obtained from a least-squares program in which the experimental mass densities to five digits were converted to amount-of-substance densities within the program.

deviation for random error. The justification for using the standard deviation from equation (4) as the basis for estimating the random error was discussed in detail in references 3 and 4. Combining the maximum standard deviation of 0.028 per cent from the fits to equation (4) with the systematic errors from references 1 and 4, the total uncertainty of a single density measurement for the mixtures studied here was estimated to be  $\pm 0.12$  per cent.

As noted, computed values of the excess Clausius–Mossotti function, as defined in equations (2) and (3), are given in table 1. A distinct difference was observed in the behavior of  $\phi_{\text{CM}}^{\text{E}}$  for the two mixtures investigated here. For  $\{x\text{CH}_4 + (1-x)\text{C}_4\text{H}_{10}\}$ , both nonpolar species, the calculated  $\phi_{\text{CM}}^{\text{E}}$  values were less than 0.1 per cent of the mixture  $\phi_{\text{CM}}$  values. Within the precision of the measurements for  $\{x\text{CH}_4 + (1-x)\text{C}_4\text{H}_{10}\}$ , there was little, if any, evidence of a relation between the  $\phi_{\text{CM}}^{\text{E}}$  values and the composition. There was some indication that the  $\phi_{\text{CM}}^{\text{E}}$  values decreased with temperature for the mixture with  $x = 0.93$ .

For  $\{x\text{CH}_4 + (1-x)(\text{CH}_3)_2\text{CHCH}_3\}$ , in which 2-methylpropane has a small dipole moment, the  $\phi_{\text{CM}}^{\text{E}}$  values were more than 0.2 per cent of  $\phi_{\text{CM}}$  for  $x = 0.92$  and as large as 0.5 per cent of  $\phi_{\text{CM}}$  for  $x = 0.78$ . The large  $\phi_{\text{CM}}^{\text{E}}$  values observed for binary mixtures containing a species with a small dipole moment compared with mixtures of nonpolar species exemplified the behavior observed by Pan *et al.*<sup>(14)</sup> in dielectric-constant measurements on mixtures of LNG components, including their results for  $\{0.91\text{CH}_4 + 0.09(\text{CH}_3)_2\text{CHCH}_3\}$  and  $\{0.95\text{CH}_4 + 0.05\text{C}_4\text{H}_{10}\}$ .

The contribution of M. J. Hiza in the preparation of mixtures is gratefully acknowledged.

## REFERENCES

- Haynes, W. M.; Hiza, M. J.; Frederick, N. V. *Rev. Sci. Instrum.* 1976, 47, 1237.
- Haynes, W. M.; Hiza, M. J. *Advances in Cryogenic Engineering*, Vol. 21. Timmerhaus, K. D.; Weitzel, D. H.: editors. Plenum Press: New York, 1976, p. 516.
- Haynes, W. M.; Hiza, M. J. *J. Chem. Thermodynamics* 1977, 9, 179.
- Hiza, M. J.; Haynes, W. M.; Parrish, W. R. *J. Chem. Thermodynamics* 1977, 9, 873.
- Haynes, W. M. *Rev. Sci. Instrum.* 1977, 48, 39.
- Hiza, M. J.; Haynes, W. M. *J. Chem. Thermodynamics* 1980, 12, 1.
- Haynes, W. M. *J. Chem. Thermodynamics* 1982, 14, 603.
- Haynes, W. M. *J. Res. Nat. Bur. Stand. (U.S.)*, in press.
- McCarty, R. D. *Nat. Bur. Stand. (U.S.), Interagency Report NBSIR 77-867*. 1977.
- McCarty, R. D. *Nat. Bur. Stand. (U.S.), Tech. Note 1030*. 1980.
- McCarty, R. D. *J. Chem. Thermodynamics* 1982, 14, 837.
- Hiza, M. J. *Fluid Phase Equilibria* 1978, 2, 27.
- Younglove, B. A.; Straty, G. C. *Rev. Sci. Instrum.* 1970, 41, 1087.
- Pan, W. P.; Mady, M. H.; Miller, R. C. *AIChE J.* 1975, 21, 283.
- Frederick, N. V.; Haynes, W. M. *Rev. Sci. Instrum.* 1979, 50, 1154.
- Goodwin, R. D. *Nat. Bur. Stand. (U.S.), Tech. Note 653*. 1974.
- Rowlinson, J. S. *Liquids and Liquid Mixtures*. 2nd edition. Butterworths: London, 1969.
- Straty, G. C.; Goodwin, R. D. *Cryogenics* 1973, 13, 712.
- Haynes, W. M.; Younglove, B. A. *Advances in Cryogenic Engineering* Vol. 27. Fast, R. W.: editor. Plenum Press: New York, 1982, p. 883.
- Rodosevich, J. B.; Miller, R. C. *AIChE J.* 1973, 19, 729.
- Miller, R. C. *Chem. Eng.* 1974, 81, 134.
- Shana'a, M. Y.; Canfield, F. B. *Trans. Faraday Soc.* 1968, 64, 2281.
- Chueh, P. L.; Prausnitz, J. M. *AIChE J.* 1973, 19, 729.



ADVANCES IN CRYOGENIC ENGINEERING, Proc. Cryogenic Engineering Conf. (Boulder, Colo., Aug 2-5, 1977) Vol 23, K. D. Timmerhaus, Editor. Plenum Press, New York (1978)

## M-6

# LIQUID MIXTURE EXCESS VOLUMES AND TOTAL VAPOR PRESSURES USING A MAGNETIC SUSPENSION DENSIMETER WITH COMPOSITIONS DETERMINED BY CHROMATOGRAPHIC ANALYSIS: METHANE PLUS ETHANE\*

M. J. Hiza and W. M. Haynes

*National Bureau of Standards, Boulder, Colorado*

## INTRODUCTION

The measurements discussed in this paper are part of a comprehensive experimental program to obtain orthobaric liquid densities for the major components of LNG and their mixtures using a magnetic suspension densimeter. The present measurements on methane plus ethane were made to evaluate vapor recirculation as a method of liquid mixing and the consistency of liquid-phase compositions determined by analysis of liquid samples. The results demonstrate the feasibility of using a magnetic suspension densimeter to obtain accurate isothermal phase equilibria and liquid density data simultaneously, with compositions determined by chromatographic analysis.

The magnetic suspension densimeter, developed for absolute measurements of cryogenic liquid and liquid mixture densities, [1,2] is a sophisticated but straightforward application of Archimedes' principle. Owing to the experimental procedures involved in the determination of temperature-dependent parameters, this instrument is particularly suited for efficient use in isothermal density measurements as a function of either pressure or composition.

In measurements of orthobaric liquid densities reported elsewhere for the major components of LNG [1,3,4] and their binary mixtures [5], the potential for efficient use of the densimeter at constant temperature was not utilized. In the binary mixtures study [5] for example, measurements were made on gravimetrically prepared mixtures as a function of temperature to minimize the uncertainty in composition of the liquid mixture. Vapor recirculation was used only as a test for nonhomogeneity of the liquid mixture. In that study, measurements were made on

---

\* Work carried out at the National Bureau of Standards under the sponsorship of British Gas Corp.; Chicago Bridge and Iron Co.; Columbia Gas Service Corp.; Distrigas Corp.; Easco Gas LNG, Inc.; El Paso Natural Gas; Gaz de France; Marathon Oil Co.; Mobil Oil Corp.; Natural Gas Pipeline Co.; Phillips Petroleum Co.; Shell International Gas, Ltd.; Sonatrach; Southern California Gas Co.; Tennessee Gas Pipeline Co.; Texas Eastern Transmission Co.; Tokyo Gas Co., Ltd.; and Transcontinental Gas Pipe Line Corp., through a grant administered by the American Gas Association, Inc.

methane plus ethane mixtures at about 35 and 68 mole % methane from 105 to 130 K and at about 49 mole % methane from 105 to 140 K. Times involved in the steps of the procedure restricted measurements to two data points per day. A vacuum point at each experimental temperature was taken prior to measurements on the liquid mixture, since the equilibrium cell had to be warmed nearly to room temperature for effective removal of the heavy component from surfaces within the cell. Thermal hysteresis of the magnetic moment of the buoy, although very small, dictates that, for the most precise density measurement [2] large thermal cycles (e.g., from 100 to 300 K) should be avoided between the vacuum and liquid points. Since the position of the buoy (which must be the same within about 0.002 mm for the vacuum and liquid points) is determined with a 125 $\times$  microscope, ambient temperature must remain constant during these measurements. If a series of density measurements can be made (at least within a single day) without changing the experimental temperature, only one vacuum point would be required for the series, and the experimental time per data point would be reduced significantly.

The results of isothermal measurements of liquid mixture densities and the corresponding total vapor pressures are reported for the methane plus ethane system at 125 and 135 K with liquid-phase compositions determined by chromatographic analysis. Excess volumes, computed for the mixtures studied, are compared with those obtained from the densities of gravimetrically prepared mixtures and with values calculated from a temperature-dependent Redlich-Kister equation fitted to all the methane plus ethane data obtained with this apparatus. Excess pressures, derived from the total vapor pressures, are compared with values from the prepared mixtures and from phase equilibria data in the literature. In this discussion, total vapor pressure is used interchangeably with mixture vapor pressure and equilibrium pressure.

## EXPERIMENTAL

A schematic diagram of the apparatus as used in the present study is given in Fig. 1. It incorporates an equilibrium system patterned after the closed-loop vapor recirculation apparatus used for liquid-vapor equilibria measurements [6,7] and the simplified one-coil magnetic suspension densimeter [2]. A window in the equilibrium cell provides visual observation of the magnetic buoy and the liquid sample.

With the simplified version of the densimeter, a barium ferrite magnetic buoy of known density is freely suspended by the force generated from the axial field of a single air core solenoid. Measurement of the solenoid current needed to support the buoy in liquid relative to that in vacuum at the same position and temperature yields the liquid density directly. The relationship used to compute the liquid density is

$$\rho_l = \rho_b [1 - (I_l/I_v)] \quad (1)$$

where  $\rho_l$  and  $\rho_b$  are the mass densities of the liquid and the magnetic buoy, and  $I_l$  and  $I_v$  are the solenoid currents required to support the buoy in the liquid and vacuum at constant temperature and at the same position relative to the support coil.

The procedures used in this study were basically the same as those followed in measuring the liquid densities of gravimetrically prepared binary mixtures [5]. Solenoid currents were measured first with pure liquid methane in the cell and then

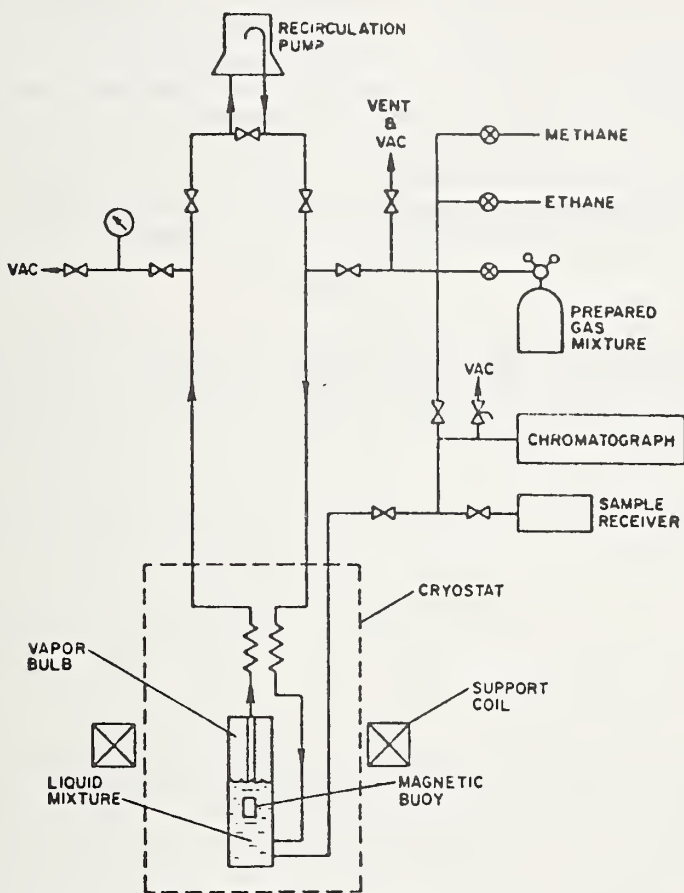


Fig. 1. Schematic of experimental apparatus.

with the cell evacuated at the temperature of interest. (A methane point was taken each day as a control on the measurement process, and these were used in a statistical analysis of the data.) Then the mixture to be studied was introduced into the cell, and the desired density and pressure measurements were made.

For measurements on the prepared binary mixtures [5], an effort was made to reduce the vapor volume to a minimum. A 0 to 100 psi (0 to 0.69 MPa) quartz Bourdon tube gauge with a free volume of approximately  $0.5 \text{ cm}^3$  was used for equilibrium pressure measurements. The recirculation pump, with a free volume of approximately  $65 \text{ cm}^3$ , was isolated during the time the cell was being completely filled and during the density measurements. For binary mixtures containing methane plus ethane, the pump was filled with pure methane gas at the mixture vapor pressure so that the liquid sample could be mixed by vapor recirculation, without significant pressure change, while monitoring the density. This procedure was used as a test for nonhomogeneity of the liquid sample.

In contrast, for measurements on mixtures with compositions determined from liquid sample analysis, a large vapor volume is desirable. A large vapor volume minimizes pressure changes in the equilibrium cell during liquid sample withdrawal, and thus reduces changes in the liquid composition due to preferential vaporiza-

tion. In the present study, equilibrium pressures were measured with a 0 to 100 psi (0 to 0.69 MPa) quartz Bourdon tube gauge with an estimated free volume of 80 cm<sup>3</sup>. In addition, the recirculation pump was in communication with the equilibrium system at all times, and only enough liquid was added to the cell to raise the liquid level at least 1 cm above the top of the magnetic buoy when in suspension, which allowed about 6 cm<sup>3</sup> of vapor space in the cell.

At 135 K, data were obtained at four compositions between 35 and 75 mole % methane by starting with pure liquid ethane in the cell and adding incremental amounts of pure liquid methane. At 125 K, data for an approximately equimolar mixture were obtained by adding pure liquid methane to the cell subsequent to measurements on a gravimetrically prepared mixture at 35 mole % methane. A sufficient amount of the prepared mixture was removed through the liquid sample line so that the liquid level, after adding methane, was a centimeter or so above the suspended buoy. In each case the liquid sample was mixed by vapor recirculation.

The liquid sample line consists of a 25-cm length of 0.028-cm-ID tubing exiting the bottom of the equilibrium cell and about 2 m of 0.048-cm-ID tubing leading out of the cryostat to a small volume valve. The line to the chromatograph consists of about 5 m of 0.159-cm-ID tubing. The sample receiver shown in Fig. 1 was sized to hold the gas equivalent of 1 cm<sup>3</sup> of liquid sample. This receiver provides a sufficient volume of sample for several repetitive analyses and a method of averaging composition variations which might occur during liquid sample withdrawal. If vapor samples had been analyzed in this study, these would have been withdrawn directly from the recirculation pump. Additional vapor volume probably would have been necessary to provide sufficient sample for purging and analysis.

Different liquid sampling and analysis procedures were used at the two temperatures of this study. At 135 K, before a sample was taken for analysis, the line from the densimeter to the chromatograph and the sample valve were evacuated and then purged with sample continuously for 6 min at a flow rate of approximately 120 stp cm<sup>3</sup>/min. For the first data point, with sample line initially containing nearly pure ethane, it was necessary to repeat the density and pressure measurement and sampling procedure to flush the residual ethane from the lines. For these analyses, the sample receiver was not used, and the chromatograph, with a 9-m liquid partition column, was calibrated with an equimolar methane plus ethane standard. At 125 K, the same purging procedure was used, but the sample was then introduced into the sample receiver which had been maintained under vacuum. A recirculation pump [7] attached to the receiver was used to stir the sample before analysis. Two analyses were made which were in agreement within 0.02 mole % of the composition of each component. In this case, the chromatograph with a 4-m silica gel column was calibrated with a 68 mole % methane plus ethane standard.

The imprecision in measurement of component concentration was determined to be about  $\pm 0.03$  mole % with either separation column. The uncertainty in component concentration due only to errors in analyzer calibration is estimated to be about  $\pm 0.05$  mole %. Considering all other known sources of systematic error in the density measurements [1,5] for methane plus ethane mixtures of the compositions studied here, an uncertainty of  $\pm 0.05$  mole % in component concentration combined with the other systematic errors would result in an estimated total systematic error of about  $\pm 0.05$  % in the mixture density. This was determined from the square root of the sum of the squares of the systematic errors. Similarly, the estimated total systematic error in the mixture vapor pressure measurement

due to errors in component concentration, gauge calibration, and temperature uncertainty is approximately  $\pm 0.01 \times 10^5$  Pa.

Owing to the small number of data points obtained, it is not possible to make an estimate of the random error in these measurements. In attempting to establish reliable liquid sampling procedures for these measurements, it was quite apparent that obtaining representative samples is not easily accomplished for systems of this type, particularly at lower temperatures. Problems were encountered when there was inadequate vapor volume to prevent preferential vaporization, low sample driving force, and insufficient purging of the sample lines to the analyzer.

## RESULTS

The methane plus ethane total vapor pressures,  $P_m$ , and molar volumes,  $V_m$ , obtained in this study are given in Table I. Also given are the corresponding excess values,  $P^E$  and  $V^E$ , determined from the difference between the actual mixture value and the mole fraction average of the pure component values at the conditions of the mixture. The pure component properties used by Hiza *et al.* [5] were also used here.

The excess volumes in Table I and those obtained from measurements on the gravimetrically prepared mixtures [5] were fitted to a Redlich-Kister expansion of the form

$$V^E = x_1 x_2 [(a_0 + a_1 T + a_2 T^2) + (b_0 + b_1 T + b_2 T^2)(2x_1 - 1) + (c_0 + c_1 T + c_2 T^2)(2x_1 - 1)^2] \quad (2)$$

where  $x_1$  and  $x_2$  are the mole fractions of methane and ethane, respectively. The least-squares coefficients ( $a_i$  and  $b_i$ ) are given in Table II. The  $c_i$  coefficients were not statistically significant in representing excess volumes for this system. The standard deviation, given in Table II in percent of the average mixture molar volume (0.035%), is slightly higher than the comparable value, 0.030%, obtained in fitting excess volumes from the data on prepared mixtures only [5]. The differences between excess volumes obtained in the present study and values calculated with the coefficients from Table II, in percent of the molar volumes, are also given in Table I.

**Table I. Orthobaric Liquid Molar Volumes, Total Vapor Pressures, and Corresponding Excess Functions for Methane Plus Ethane with Compositions Determined by Chromatographic Analysis**  
[ $V_{\text{calc}}^E$  from equation (2) with coefficients given in Table II]

$T$ , K	$x_1$ , CH <sub>4</sub>	$x_2$ , C <sub>2</sub> H <sub>6</sub>	$P_m$ , Pa $\times 10^{-5}$ *	$P^E$ , Pa $\times 10^{-5}$ *	$V_m$ , cm <sup>3</sup> /mole	$V^E$ , cm <sup>3</sup> /mole	$\frac{V_{\text{exp}}^E - V_{\text{calc}}^E}{V_m} \times 100$
135.00	0.3563	0.6437	2.043	+0.280	46.056	-0.876	-0.020
	0.4447	0.5553	2.505	+0.310	45.171	-1.026	-0.018
	0.5934	0.4066	3.150	+0.229	43.836	-1.126	+0.021
	0.7415	0.2585	3.743	+0.099	42.690	-1.040	-0.066
125.00	0.5014	0.4986	1.515	+0.162	43.573	-0.835	-0.032

\*  $1 \times 10^5$  Pa = 1 bar.

**Table II. Coefficients for Equation (2) from a Least-Squares Fit of all Excess Volumes for Methane Plus Ethane Obtained from Measurements with the Magnetic Suspension Densimeter**

$a_0$	-14.89469
$a_1$	0.2770596
$a_2$	-0.001473116
$b_0$	-37.98245
$b_1$	0.6427122
$b_2$	-0.002783724
$100\sigma/V_m$	0.035%

In Fig. 2, the excess volumes are compared with those obtained from measurements on prepared mixtures at 125 and 135 K and curves showing the composition dependence of excess volumes calculated with the coefficients in Table II. At 135 K, the two prepared mixture points shown at about 35 and 68 mole % methane were obtained by extrapolation from a least-squares fit of the densities of these mixtures as a function of temperature [5]. All others are experimental data.

From the several sources of methane plus ethane liquid-vapor equilibria data listed in a recent survey of the literature [6], excess pressures were taken from the measurements of Miller and Staveley [9] at 115.77 K and of Wichterle and Kobayashi [10] at 130.37 K for comparison with excess pressures given here. This comparison is given in Fig. 3. Miller and Staveley measured total vapor pressures of prepared mixtures, while Wichterle and Kobayashi analyzed the liquid and vapor

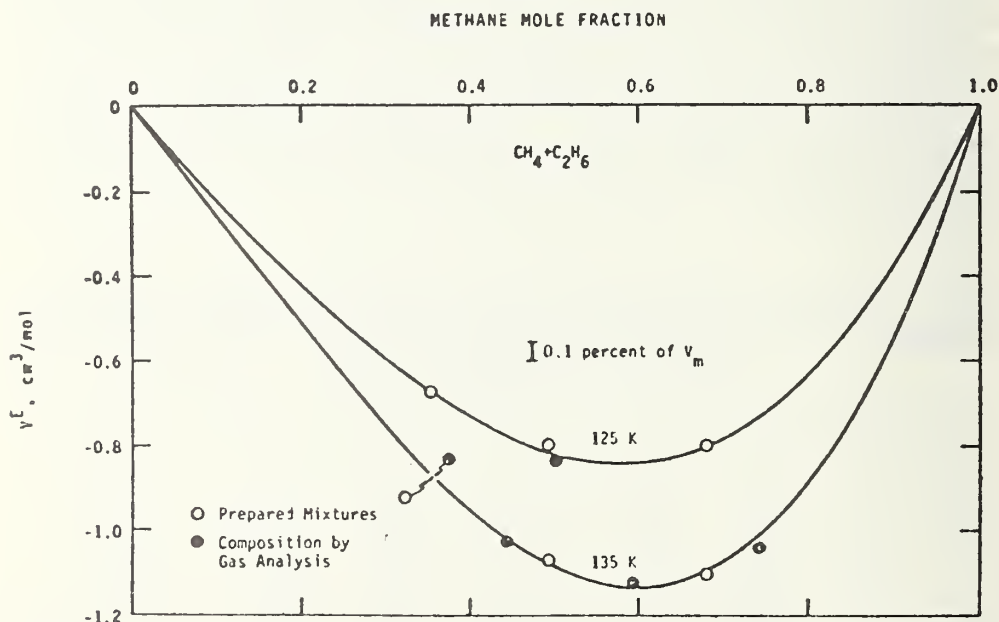


Fig. 2. Comparison of excess volumes for methane plus ethane from the present study with those from measurements on prepared mixtures and with curves calculated from eq. (2).

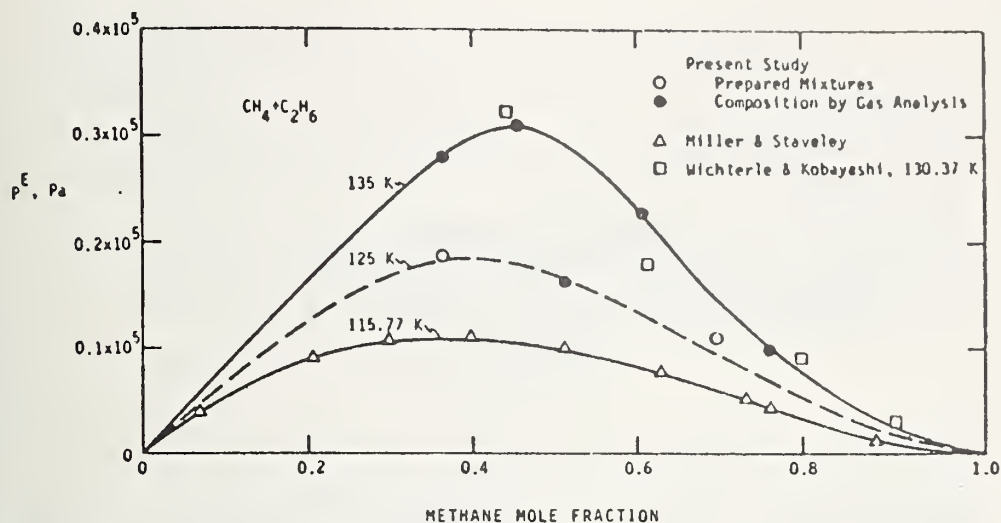


Fig. 3. Comparisons of excess pressures for methane plus ethane from the present study with those from measurements on prepared mixtures and with values obtained from the literature.

compositions at the equilibrium pressure of the mixture. Two points from vapor-pressure measurements at 125 K on prepared mixtures in the densimeter are also shown. There appears to be a discrepancy between the present data and those of Wichterle and Kobayashi. To be consistent, excess pressures at 130.37 K should fall between the values at 125 and 135 K, while those of Wichterle and Kobayashi are predominantly higher than the present values at 135 K. However, a data point of the latter authors at about 60 mole % methane, when plotted with these new values and that of Miller and Staveley at the same composition, produces a smooth curve of excess pressure as a function of temperature.

### SUMMARY

The experimental results given here demonstrate the feasibility of efficiently utilizing the magnetic suspension densimeter to obtain both isothermal phase equilibria and liquid mixture density data, with compositions of the equilibrium phases determined by chromatographic analysis. A more complete evaluation of sampling procedures is needed to determine the best procedure to obtain representative liquid mixture samples reliably. Although vapor-phase compositions were not analyzed in the present study, obtaining representative samples of the equilibrium vapor would not present a difficult problem. Using excess volumes from liquid density data on accurately prepared mixtures as a reference, measurement of the liquid mixture densities along with liquid-vapor equilibria measurements provides an excellent means of assessing the reliability of liquid-phase compositions obtained in the phase equilibria measurements.

### REFERENCES

1. W. M. Haynes, M. J. Hiza, and N. V. Frederick, *Rev. Sci. Instr.* 47:1237 (1976).
2. W. M. Haynes, *Rev. Sci. Instr.* 48:39 (1977)
3. W. M. Haynes and M. J. Hiza, *J. Chem. Thermodynamics* 9:179 (1977).

4. W. M. Haynes and M. J. Hiza, in: *Advances in Cryogenic Engineering, Vol. 21*, Plenum Press, New York (1976), p. 516.
5. M. J. Hiza, W. M. Haynes, and W. R. Parrish, *J. Chem. Thermodynamics* 9:873 (1977).
6. A. G. Duncan and M. J. Hiza, in: *Advances in Cryogenic Engineering, Vol. 15*, Plenum Press, New York (1970), p. 42.
7. M. J. Hiza and A. G. Duncan, *Rev. Sci. Instr.* 40:513 (1969).
8. A. J. Kidnay, M. J. Hiza, and R. C. Miller, *Cryogenics* 13:575 (1973).
9. R. C. Miller and L. A. K. Staveley, in: *Advances in Cryogenic Engineering, Vol. 21*, Plenum Press, New York (1976), p. 493.
10. I. Wichterle and R. Kobayashi, *J. Chem. Eng. Data* 17:9 (1972).

### DISCUSSION

*Question* by R. Kobayashi, Rice University: Are there any attempts to apply the magnetic densimeter to measure gas densities as well as liquids?

*Answer* by author: The precision and accuracy of a magnetic suspension densimeter, which is a straightforward application of Archimedes' principle, depends on the difference between the density of the float and the density of the fluid. Thus, it is very difficult to make precise density measurements on a low-density gas. It is one of our long-range goals. (We have tried some gas measurements in selected regions.) For the extremely low gas densities you need a low-density float as well as very precise measurements of the position of the float and of the force (current in electromagnetic coils) necessary to support the float.

A-145

*J. Chem. Thermodynamics* 1980, 12, 1-10

## Orthobaric liquid densities and excess volumes for multicomponent mixtures of low molar-mass alkanes and nitrogen between 105 and 125 K<sup>a</sup>

M. J. HIZA and W. M. HAYNES

*Thermophysical Properties Division,  
National Engineering Laboratory,  
National Bureau of Standards,  
Boulder, Colorado 80303, U.S.A.*

(Received 15 March 1979)

A magnetic suspension densimeter has been used to determine orthobaric liquid densities of gravimetrically prepared multicomponent mixtures containing the major components of liquefied natural gas, *i.e.* nitrogen, methane, ethane, propane, isobutane, and normal butane, between 105 and 125 K. These results were obtained to provide a test of the capability of mathematical models to predict the densities of liquefied natural-gas mixtures. Combinations of the subject components were chosen to provide the most severe test of the models and the possibility of using the measured densities to optimize parameters of the models. Deviations are given between the experimental densities for each mixture and values predicted with an extended corresponding-states model optimized to binary-mixture and pure-component orthobaric liquid densities obtained with the same apparatus. Uncertainties of the present results are discussed in relation to the experimental technique, the knowledge of the compositions of the liquid mixtures, and the comparisons between the experimental and predicted results. Approximate total vapor pressures are also given for each mixture at the temperatures studied.

### 1. Introduction

The present study is part of an experimental program to obtain orthobaric liquid densities for the major components of liquefied natural gas (LNG) and their mixtures, primarily in the temperature range from 105 to 140 K. The overall purpose of the program is to provide sufficiently accurate densities ( $\pm 0.1$  per cent) of uniformly high precision ( $\pm 0.02$  per cent) for the pure components, the possible binary combinations, and selected multicomponent mixtures, for optimization and testing of prediction methods.

<sup>a</sup> This work was carried out at the National Bureau of Standards under the sponsorship of British Gas Corp., Chicago Bridge and Iron Co., Columbia Gas Service Corp., Distrigas Corp., Easco Gas LNG, Inc., El Paso Natural Gas, Gaz de France, Marathon Oil Co., Mobil Oil Corp., Natural Gas Pipeline Co., Phillips Petroleum Co., Shell International Gas Ltd., Sonatrach, Southern California Gas Co., Tennessee Gas Pipeline Co., Texas Eastern Transmission Co., Tokyo Gas Co. Ltd., and Transcontinental Gas Pipe Line Corp., through a grant administered by the American Gas Association, Inc.

Previously, orthobaric liquid densities were reported for nitrogen,<sup>(1)</sup> the low molar mass alkanes: methane,<sup>(1,2)</sup> ethane,<sup>(2)</sup> propane,<sup>(2)</sup> isobutane,<sup>(2)</sup> and normal butane;<sup>(2,3)</sup> and their binary mixtures,<sup>(4)</sup> as determined with a magnetic suspension densimeter.

In this paper, orthobaric liquid densities between 105 and 125 K, determined with the same apparatus, are reported for 10 gravimetrically prepared multicomponent mixtures containing methane. Total vapor pressures are also reported, but these are considered approximate since the main focus was to assure the reliability of the density measurements. As an indication of the consistency of the densities of the multicomponent mixtures with those for the pure fluids and binary mixtures reported earlier, deviations are given between the experimental densities for each multicomponent mixture and values predicted with an extended corresponding states LNG density model with parameters determined from the binary mixture and pure-component results only. A brief discussion is also included on the consistency of other multicomponent liquid densities in the literature with the results presented here.

## 2. Experimental

The magnetic suspension densimeter used in this study has been discussed in detail elsewhere.<sup>(1,5)</sup> All of the results reported here were obtained with the one solenoid arrangement<sup>(5)</sup> using the procedures followed in measuring the densities of the binary liquid mixtures.<sup>(4)</sup> The relation used to compute the density of the liquid with the one solenoid arrangement is

$$\rho_l = \rho_b \{1 - (I_l/I_v)\}, \quad (1)$$

where  $\rho_l$  and  $\rho_b$  are the mass densities of the liquid and the buoy, and  $I_l$  and  $I_v$  are the solenoid currents required to support the buoy at the same temperature and at the same position, relative to the solenoid, in the liquid and vacuum, respectively.

The multicomponent mixtures were prepared gravimetrically as gas mixtures in thoroughly cleaned and dried metal cylinders, each with a free volume of about 3.3 dm<sup>3</sup>, using research-grade gases which were analysed chromatographically for impurities before use. In addition, nitrogen and methane were passed through room-temperature molecular-sieve adsorption columns to remove moisture and any heavy hydrocarbon contaminants not detected by analysis. Estimated errors in component mole fractions, based on six times the standard deviation of weighing,<sup>(4)</sup> are given in table 1 for both 1 and 5 mol of mixture prepared.

Composition, molar mass, and the total amount prepared are given in table 2 for each of the multicomponent mixtures included in this study. Compositions given for mixtures containing only hydrocarbons are the same as the prepared compositions. Compositions given for mixtures containing nitrogen have been adjusted slightly (by as much as 0.0005 in the mole fraction of N<sub>2</sub> and CH<sub>4</sub>) to include all or most of the vapor-phase correction at each temperature studied. In making the composition adjustments, the mole fraction of each component was rounded to the nearest 0.0001. These vapor-phase corrections to the compositions were made to reduce the final

TABLE 1. Uncertainty  $\delta x$  in mole fraction of each component in the prepared mixtures based on the total amount of substance  $n$  prepared.

Component	$\delta x$	
	$n = 1 \text{ mol}$	$n = 5 \text{ mol}$
N <sub>2</sub>	$\pm 0.00014$	$\pm 0.00003$
CH <sub>4</sub>	$\pm 0.00025$	$\pm 0.00005$
C <sub>2</sub> H <sub>6</sub>	$\pm 0.00013$	$\pm 0.00003$
C <sub>3</sub> H <sub>8</sub>	$\pm 0.00009$	$\pm 0.00002$
C <sub>4</sub> H <sub>10</sub>	$\pm 0.00007$	$\pm 0.00001$

TABLE 2. Multicomponent mixtures studied:  $x$ , mole fraction;  $M$ , molar mass;  $n$ , the total amount of substance prepared

Mixture	$x(\text{N}_2)$	$x(\text{CH}_4)$	$x(\text{C}_2\text{H}_6)$	$x(\text{C}_3\text{H}_8)$	$x(i\text{-C}_4\text{H}_{10})$	$x(n\text{-C}_4\text{H}_{10})$	$M/\text{g mol}^{-1}$	$n/\text{mol}$
A		0.34242	0.31372	0.34386			30.0903	1.78
B		0.80284	0.09902	0.09814			20.1852	4.93
C		0.85443	0.05042	0.04038	0.02577	0.02901	20.1885	1.89
D	0.3380	0.3414	0.3206				24.5861	4.66
E	0.1635	0.6704	0.1661				20.3301	4.66
F	0.0995	0.7977		0.1028			20.1181	4.67
G	0.0484	0.8526	0.0483	0.0507			18.7223	4.41
H	0.0490	0.8060	0.0468	0.0482	0.0500		20.7423	3.00
I	0.0554	0.7909	0.0560	0.0500		0.0477	20.9017	3.16
J	0.0425	0.8130	0.0475	0.0487	0.0241	0.0242	20.6168	3.09

adjustment of the mixture densities from a maximum of about 0.05 per cent to 0.01 per cent or less.

The prepared gas mixtures were condensed directly and continuously into the windowed equilibrium cell through a capillary tube entering at the bottom until no vapor space could be observed. This filling method provided continuous mixing of the liquid while the gas mixture was being condensed into the cell. For one mixture (mixture C in table 2) a comparison was made between the measured densities at 105 K obtained before and after the vapor phase was recirculated through the liquid for several min at a bubble rate of 1 to 3 s<sup>-1</sup> with an external vapor-recirculation pump. No change in measured density was detected after recirculation. Subsequently, liquid samples were withdrawn, and two comparisons were made chromatographically with the composition of the prepared mixture. During withdrawal of liquid samples, the recirculation pump (with a free volume of about 65 cm<sup>3</sup>) was kept open to the vapor space of the equilibrium system to reduce the amount of CH<sub>4</sub> vaporized from the liquid in the cell. The liquid samples were, nevertheless, lean in CH<sub>4</sub> by about 0.3 mole per cent, and mole fractions of heavy components in the liquid were all higher than those in the prepared mixture. The mole fractions of C<sub>2</sub>H<sub>6</sub> and C<sub>3</sub>H<sub>8</sub> were higher by approximately 0.001, while the mole fractions of (CH<sub>3</sub>)<sub>2</sub>CHCH<sub>3</sub> and C<sub>4</sub>H<sub>10</sub> were higher by approximately 0.0006 and 0.0002, respectively. Since it would be difficult, with this arrangement, to completely avoid

partial vaporization of methane from the liquid samples, the main value of the analysis was in the comparison of the mole fractions of the heavy components in the liquid samples to those in the prepared mixtures on a methane-free basis. On this basis, the variations in the liquid-phase compositions observed for mixture C are not considered unreasonable.

Attempts to study mixtures comparable to mixture C containing only one of the butanes were unsuccessful. Differences between measured and predicted densities were three to four times larger than expected, even after several min of vapor recirculation, and the mole fractions of the heavy components from analysis of liquid samples were inconsistent with those in the prepared mixture. Analysis of a liquid sample for one mixture containing mole fraction approximately 0.05 of  $(\text{CH}_3)_2\text{CHCH}_3$ , without  $\text{C}_4\text{H}_{10}$ , for example, gave mole fractions of  $\text{C}_2\text{H}_6$  and  $\text{C}_3\text{H}_8$  in the liquid approximately 0.002 higher than those in the prepared mixture, and a mole fraction of  $(\text{CH}_3)_2\text{CHCH}_3$  lower than that in the prepared mixture by about 0.0013. This inconsistency in composition could be interpreted as a non-uniform mole fraction of  $(\text{CH}_3)_2\text{CHCH}_3$  in the liquid of up to 0.0033. Since the magnetic buoy is essentially a point sensor relative to the size of the cell, the direction of error in observed density depends on the composition of liquid actually surrounding the buoy. From observations made during the course of this study and in the previous study on binary mixtures,<sup>(4)</sup> it appeared that mixtures which were most likely to present problems in filling the equilibrium cell with a homogeneous liquid sample of the same composition as the prepared gas mixture were those of hydrocarbons only which contain the butanes and mole fraction 0.85 or more of  $\text{CH}_4$ . Though mixture C fits these criteria, we did not detect any abnormalities in the liquid mixture during measurement, as noted above, which we could consider significant.

### 3. Results and discussion

#### EXPERIMENTAL RESULTS

The experimental orthobaric liquid-mixture amount-of-substance densities are given in table 3 as a function of temperature. Pressures listed in table 3 are considered only approximate mixture vapor pressures, and in a few cases, measurements were not made and values given were obtained by interpolation. Based on comparisons of pressures measured for the binary mixtures with reported phase equilibria,<sup>(4)</sup> pressures reported here are thought to be either equal to or slightly higher than the true multicomponent mixture vapor pressures.

Also given in table 3 are the corresponding experimental excess volumes  $V^E$ , computed from

$$V^E = V_m - V_{\text{ideal}}, \quad (2)$$

where

$$V_{\text{ideal}} = \sum_i x_i V_i \{1 + \kappa_{T,i}(p_i - p_m)\}, \quad (3)$$

$V$  is molar volume,  $p$  is saturation pressure,  $x$  is mole fraction, and  $\kappa_T$  is isothermal compressibility. Subscripts  $m$  and  $i$  refer to the mixture and pure components,

TABLE 3. Orthobaric amount-of-substance densities  $\rho_n$  of multicomponent mixtures of low molar-mass alkanes and nitrogen:  $T$ , temperature (IPTS-68);  $p$ , pressure;  $V^E$ , excess volume calculated from equations (2) and (3);  $\rho_{\text{calc}}$ , density calculated from the extended corresponding-states model as given in reference 18

Mixture	$T/\text{K}$	$p/\text{MPa}$	$\rho_n/\text{mol dm}^{-3}$	$V^E/\text{cm}^3 \text{mol}^{-1}$	$10^2(\rho - \rho_{\text{calc}})\rho^{-1}$
A	110.00	0.0427	20.5342	-0.573	-0.03
	115.00	0.0637	20.3497	-0.646	-0.02
	115.00	0.0637	20.3567	-0.663	+0.01
	120.00	0.0914	20.1786	-0.766	+0.06
	120.00	0.0914	20.1803	-0.770	+0.07
	125.00	0.128	19.9858	-0.848	+0.04
B	105.00	0.0477	24.9975	-0.533	+0.02
	110.00	0.0747	24.6696	-0.587	-0.02
	115.00	0.112	24.3515	-0.676	+0.01
	120.00	0.162	24.0335	-0.790	+0.06
C	105.00	0.0515	24.8775	-0.596	+0.18
	110.00	0.0818	24.5382	-0.638	+0.11
	115.00	0.119	24.2083	-0.716	+0.10
	120.00	0.170	23.8859	-0.832	+0.14
D	105.00	0.719	24.9084	-2.108	+0.07
	110.00	0.949	24.5350	-2.764	+0.04
	115.00	1.237	24.1433	-3.816	-0.06
E	105.00	0.369	25.8587	-1.069	-0.00
	110.00	0.481	25.4598	-1.433	-0.01
	115.00	0.618	25.0466	-2.052	-0.05
	120.00	0.773	24.6359	-3.496	-0.04
F	105.00	0.282	25.3950	-0.845	-0.01
	110.00	0.362	25.0153	-1.091	-0.04
	115.00	0.455	24.6465	-1.542	+0.01
	120.00	0.561	24.2667	-2.525	+0.04
G	105.00	0.158	25.8910	-0.513	-0.07
	110.00	0.214	25.5081	-0.656	-0.07
	115.00	0.283	25.1224	-0.900	-0.06
	120.00	0.365	24.7283	-1.425	-0.04
H	105.00	0.204	24.7803	-0.726	+0.03
	110.00	0.255	24.4327	-0.870	-0.03
	115.00	0.314	24.1039	-1.154	+0.00
	120.00	0.379	23.7707	-1.730	+0.05
I	105.00	0.193	24.8080	-0.786	-0.00
	110.00	0.253	24.4664	-0.954	-0.06
J	105.00	0.183	24.8496	-0.717	+0.04
	110.00	0.252	24.5159	-0.870	+0.03
	115.00	0.338	24.1783	-1.109	+0.02
	120.00	0.443	23.8577	-1.634	+0.10

respectively. Pure-component molar volumes were calculated from the fit of the experimental results.<sup>(1,2)</sup> Isothermal compressibilities for nitrogen, methane, and ethane were calculated from the expressions:

$$\kappa_T(\text{N}_2)/\text{MPa}^{-1} = -0.01032 + 0.51368/(126.2 - T/\text{K}), \quad (4)$$

$$\kappa_T(\text{CH}_4)/\text{MPa}^{-1} = -0.001595 + 0.29488/(190.555 - T/\text{K}), \quad (5)$$

and

$$\kappa_T(\text{C}_2\text{H}_6)/\text{MPa}^{-1} = \{(T/250 \text{ K}) + 0.45\} \times 10^{-3}, \quad (6)$$

where  $T$  is thermodynamic temperature. These expressions are considered adequate representation of isothermal compressibilities of nitrogen and methane from Rowlinson,<sup>(6)</sup> those of methane from Goodwin,<sup>(7)</sup> and those for ethane from Miller.<sup>(8)</sup> Isothermal-compressibility corrections were not made for molar volumes of propane, isobutane, and normal butane. Vapor pressures for nitrogen, methane, and ethane were taken from Strobridge,<sup>(9)</sup> Goodwin,<sup>(7)</sup> and Goodwin, Roder, and Straty,<sup>(10)</sup> respectively.

#### UNCERTAINTIES IN MEASURED LIQUID-MIXTURE DENSITIES

The uncertainty in measured density of a liquid mixture is inherently larger than for a pure fluid due to the added uncertainty in composition. Previously, detailed discussions were given on random and systematic errors associated with magnetic suspension densimeter measurements for pure liquids<sup>(1)</sup> and binary liquid mixtures.<sup>(4)</sup> In each case the total uncertainty was taken as the square root of the sum of the squares of known systematic errors plus three times the standard deviation for random error.

For measurements on pure liquid methane, the predominant component in liquefied natural gas, the total uncertainty in density was estimated to be about  $\pm 0.1$  per cent, with approximately equal contributions from random and systematic errors.<sup>(1)</sup> For measurements on (methane + propane) liquid mixtures, which typify the binary liquid mixtures studied, the total uncertainty was estimated to be about  $\pm 0.16$  per cent with approximately the same contribution from known systematic errors as in pure liquid methane measurements.<sup>(4)</sup> The random error in the (methane + propane) density measurements was estimated from the standard deviation obtained by fitting the excess volumes, for the four different compositions studied, to a Redlich-Kister expansion as a function of both composition and temperature. Fitting the results as a function of temperature at constant composition resulted in significantly smaller standard deviations, comparable to that for pure methane. However, it was felt that the evaluation based on both temperature and composition would give a more realistic estimate of the random error.

It is not possible to obtain a standard deviation for the multicomponent-mixture results from which an estimate of random error can be made as a function of both temperature and composition, nor are the results for any mixture sufficient to obtain a meaningful standard deviation as a function of temperature only. However, there is

no reason to believe that the random error in density measurements for the multicomponent liquid mixtures in the present study should be significantly larger than that noted above for the (methane+propane) binary mixtures. Estimated systematic errors are also about the same. The increased uncertainty in composition of prepared mixtures due to the increased number of components present adds very little to the total systematic error.

There is a potential source of error, suggested by our experimental observations, for mixtures containing high mole fractions of  $\text{CH}_4$  with higher molar-mass alkanes including either or both butanes, but with no nitrogen. These are mixtures for which the vapor phase is essentially pure methane. Thus, as the mole fraction of  $\text{CH}_4$  in the liquid mixture is increased, the difference between the mixture vapor pressure and that for pure methane becomes quite small, and the probability increases for condensing pure methane in the vapor space, particularly at the lowest temperatures, while the prepared mixture is being condensed into the equilibrium cell. If methane thus condensed were to accumulate in a location where it could not be readily blended back into the liquid mixture, and if the mixture were homogeneous, analysis of representative liquid samples would indicate the mixture to be lean in methane similar to the effect of partial vaporization during liquid sampling. Consequently, this experimental test alone would not be sufficient to confirm a possible error in measured density due to such an occurrence.

In the top section of the equilibrium cell, the annulus volume (of approximately  $0.3 \text{ cm}^3$ ) between the vapor bulb and the cell wall<sup>(1)</sup> is the only possible location where methane might condense without being in good communication with the bulk of the liquid mixture in the cell. If pure liquid methane (rather than methane vapor) completely filled this annulus when mixture C, for example, was condensed into the cell, the mole fraction of  $\text{CH}_4$  in the liquid mixture would be about 0.0024 lower and the measured mass density would be about 0.2 per cent higher than for the prepared mixture, with a variation in the density error of about 0.015 per cent between 105 and 120 K. For comparison, if methane were to condense in a 20 cm length of the vapor-exit capillary with an internal diameter of 0.048 cm, the error introduced in the densities for mixture C would be about 0.03 per cent, about the same as the imprecision of measurement. Due to vapor-phase enhancement of the mole fraction of  $\text{CH}_4$  in (nitrogen + methane) gas mixtures in equilibrium with the liquid,<sup>(11,12)</sup> the presence of nitrogen in the multicomponent liquid mixture, e.g. mixture J as against mixture C, would reduce the probability of methane condensing out in the vapor space.

#### DEVIATIONS FROM PREDICTED DENSITIES

Comparisons between experimental and predicted liquid densities for multicomponent mixtures of LNG components primarily provide a test of the predictive (or correlative) capability of a proposed LNG density model. However, when the parameters of a model are optimized only to the pure-fluid and binary-mixtures results obtained in the same experimental apparatus, these comparisons also can provide information on the consistency of the results for the multicomponent

mixtures with those for the pure fluids and binary mixtures, within known limitations imposed in the development of the model.

Of several models proposed for the prediction of orthobaric liquid densities of LNG mixtures,<sup>(8,13-17)</sup> the extended corresponding-states model<sup>(15)</sup> appears to be the most general in application. McCarty<sup>(18)</sup> has demonstrated that, when optimized to pure-fluid and binary-mixtures densities obtained with the magnetic suspension densimeter of the present study, all of the pure-fluid and binary-mixtures results are correlated generally within their estimated accuracy, and, in most cases, nearly within the precision of measurement. It was felt that comparisons of the values for multicomponent mixtures with values predicted from this model would be most likely to identify inconsistencies.

Percent deviations of the experimental orthobaric liquid amount-of-substance densities from values predicted with the extended corresponding-states model, without further modification, are also given in table 3. The average deviation or bias is +0.016 per cent, and the average absolute deviation is 0.05 per cent. The maximum deviation is +0.18 per cent for the 105 K point for mixture C. Only the results for mixture C show a systematic bias of 0.1 per cent or larger. Excluding the results for mixture C results in an average deviation or bias of +0.003 per cent, an average absolute deviation of 0.04 per cent, and a maximum deviation of +0.1 per cent.

It is also worth noting the significant results of comparisons made with values predicted from two less complex models, which are more limited in their application. These are both excess-volume models, the empirical model of Hiza<sup>(17)</sup> and the modified hard-sphere model of Rodosevich and Miller,<sup>(16)</sup> with parameters optimized to the same pure-fluid and binary-mixture values. Excluding results outside the applicable range of each model, deviations of experimental from predicted densities are in substantial agreement with those of the extended corresponding-states model. Excluding the results for mixtures D and E and the 120 K point for mixture F, the maximum deviation from values predicted with the empirical excess-volume model is +0.14 per cent for the 105 K point for mixture C. Excluding the results for mixtures containing nitrogen at the highest temperatures, the 120 K points for mixtures E through J and the 115 K point for mixture D, the maximum deviation from values predicted with the hard-sphere model is +0.18 per cent, also for the 105 K point for mixture C. In fact, deviations of the densities for mixture C from values predicted with the hard-sphere model are the same as those given in table 3 for the extended corresponding-states model.

Though the densities for mixture C are systematically larger than the predicted values by 0.1 per cent or more, the deviations given in table 3 generally are random and, for the most part, are significantly smaller than  $\pm 0.1$  per cent.

#### CONSISTENCY OF OTHER MULTICOMPONENT LNG MIXTURE DENSITIES

Orthobaric liquid densities for multicomponent mixtures of LNG components are scarce in the open literature, and only some of those available approach the accuracy goal of the present study. Our primary source of references is a fluid-mixtures bibliography<sup>(19)</sup> current to January 1975 and more recent references from a file

maintained to update that bibliography. A summary of the results of comparisons of literature data with values predicted with the extended corresponding-states model are included here as an indication of the precision and consistency of available values with those of the present study. The values are divided, for purposes of discussion, into two groups: first, those with an apparent imprecision of more than  $\pm 0.3$  per cent, and second, those with an apparent imprecision of less than  $\pm 0.3$  per cent.

In the first group are the results reported by Morlet,<sup>(20)</sup> Gonzalez and Lee,<sup>(21)</sup> Klosek and McKinley,<sup>(13)</sup> and Jensen and Kurata.<sup>(22)</sup> Morlet<sup>(20)</sup> reported results graphically for several ternary mixtures of (methane + ethane + propane) at 90.2 K. These results appear reproducible within about  $\pm 1.0$  per cent, and tabulated densities for three compositions from a fit of them deviate from predicted values by  $-0.5$  to  $-1.1$  per cent. Gonzalez and Lee<sup>(21)</sup> reported bubble-point densities for 10 methane-rich mixtures, simulating natural gas, down to 99.8 K. For the four mixtures not containing helium or hexanes and higher hydrocarbons, comparisons were made with predicted values at the lowest temperature reported. For three of the mixtures at 116.5 K, the densities deviate from predicted values by  $-0.60$  per cent,  $+0.25$  per cent, and  $-26.15$  per cent. The density for the fourth mixture at 144.3 K deviates from the predicted value by  $-12.14$  per cent. Klosek and McKinley<sup>(13)</sup> reported densities for 13 multicomponent mixtures with three to seven components from 94.37 to 125.04 K. Though their values deviate from predicted values by  $\pm 1$  per cent, the average deviation or bias is only  $+0.04$  per cent, the average absolute deviation being 0.36 per cent. Since the values for each mixture generally deviate from predicted values systematically, the variation may be due largely to an uncertainty in composition. Jensen and Kurata<sup>(22)</sup> reported results for essentially three methane-rich mixtures containing nitrogen, ethane, propane, and normal butane from 98.15 to 113.15 K. These values appear to have an imprecision of about  $\pm 0.5$  per cent. From comparisons made at 108.15 and 113.15 K, they deviate from predicted values by  $+1.03$  to  $+2.21$  per cent.

In the second group are the results reported by Shana'a and Canfield,<sup>(23)</sup> Rodosevich and Miller,<sup>(24)</sup> Miller,<sup>(8)</sup> Orrit and Laupretre,<sup>(25)</sup> and Miller and Hiza.<sup>(26)</sup> Shana'a and Canfield<sup>(23)</sup> reported results for two methane + ethane + propane mixtures at 108.15 K. These deviate from predicted values by  $-0.09$  per cent and  $+0.15$  per cent. Rodosevich and Miller<sup>(24)</sup> and Miller<sup>(8)</sup> reported results for three ternary mixtures and one quaternary mixture at 108.00 and 115.00 K. In addition, results included in reference 26 for one ternary mixture obtained by Rodosevich at 108.00, 110.00, and 115.00 K were included here. From predicted values, the average deviation or bias of these is  $-0.03$  per cent, the average absolute deviation is 0.03 per cent, and the maximum deviation is  $-0.06$  per cent. Very recently, Orrit and Laupretre<sup>(25)</sup> reported a sample of their results for five methane-rich mixtures of four to eight components containing nitrogen and hydrocarbons through pentane from 95.50 to 123.61 K. From predicted values, the average deviation or bias of these values is  $-0.10$  per cent, the average absolute deviation is 0.10 per cent, and the maximum deviation is  $-0.175$  per cent.

The last investigation in the second group, that of Miller and Hiza,<sup>(26)</sup> is not completely independent of the present study. Measurements were made between 105

and 115 K at the University of Wyoming with Miller's apparatus calibrated on pure-methane values obtained with the magnetic suspension densimeter of the present study.<sup>(1,2)</sup> Mixtures studied were prepared in our laboratory. These included two mixtures for which results are reported here (mixtures H and I) and two similar four-component mixtures without nitrogen. From predicted values, the average deviation or bias of these values is +0.04 per cent, the average absolute deviation is 0.04 per cent, and the maximum deviation is +0.102 per cent (for mixture I at 105 K). Though there is a slight bias, these deviations are consistent with the accuracy of the calibration.

Additional measurements are now in progress with a new design of the magnetic suspension densimeter, significantly different than that used in the present study. Measurements are being made on both binary and multicomponent mixtures for which the data are insufficient, and for multicomponent mixtures containing the pentanes. These new results will be reported in subsequent papers.

The authors acknowledge the contributions of M. J. Brown and R. D. McCarty during the course of the present study.

#### REFERENCES

1. Haynes, W. M.; Hiza, M. J.; Frederick, N. V. *Rev. Sci. Instrum.* **1976**, *47*, 1237.
2. Haynes, W. M.; Hiza, M. J. *J. Chem. Thermodynamics* **1977**, *9*, 179.
3. Haynes, W. M.; Hiza, M. J. In *Advances in Cryogenic Engineering*, Vol. 21. Timmerhaus, K. D.; Weitzel, D. H.: editors. Plenum Press: New York. **1976**. p. 516.
4. Hiza, M. J.; Haynes, W. M.; Parrish, W. R. *J. Chem. Thermodynamics* **1977**, *9*, 873.
5. Haynes, W. M. *Rev. Sci. Instrum.* **1977**, *48*, 39.
6. Rowlinson, J. S. *Liquids and Liquid Mixtures*. 2nd Ed. Butterworths: London. **1969**.
7. Goodwin, R. D. *Nat. Bur. Stand. U.S., Technical Note* 653, **1974**.
8. Miller, R. C. *Chem. Eng.* **1974**, *81*, 134.
9. Strobridge, T. R. *Nat. Bur. Stand. U.S., Technical Note* 129, **1962**.
10. Goodwin, R. D.; Roder, H. M.; Straty, G. C. *Nat. Bur. Stand. U.S., Technical Note* 684, **1976**.
11. Miller, R. C.; Kidnay, A. J.; Hiza, M. J. *Am. Inst. Chem. Eng. J.* **1973**, *19*, 145.
12. Kidnay, A. J.; Miller, R. C.; Parrish, W. R.; Hiza, M. J. *Cryogenics* **1975**, *15*, 531.
13. Klosek, J.; McKinley, C. In *Proceedings First International Conference on LNG*. White, J. W.; Neumann, A. E. S.: editors. Institute of Gas Technology: Chicago, Ill. **1968**, Paper 22, Session 5.
14. Albright, M. A. *Nat. Gas Proc. Assn. Tech. Publ.* TP-3, **1973**.
15. Mollerup, J.; Rowlinson, J. S. *Chem. Eng. Sci.* **1973**, *29*, 1373.
16. Rodosevich, J. B.; Miller, R. C. In *Advances in Cryogenic Engineering*, Vol. 19. Timmerhaus, K. D.: editor. Plenum Press: New York. **1974**. p. 339.
17. Hiza, M. J. *Fluid Phase Equilibria* **1978**, *2*, 27.
18. McCarty, R. D. *Nat. Bur. Stand. U.S., Interagency Rept.* NBSIR 77-867, **1977**, 60 pp. See also: Haynes, W. M.; Hiza, M. J.; McCarty, R. D. In: *Proceedings Fifth International Conference on LNG*, Vol. 2. White, J. W.; McGrew, W.; Farmer, S.; Hansen, D.; Jacobshagen, H.: editors. Institute of Gas Technology: Chicago, Ill. **1977**, Paper 11, Session III.
19. Hiza, M. J.; Kidnay, A. J.; Miller, R. C. *Equilibrium Properties of Fluid Mixtures, A Bibliography of Data on Fluids of Cryogenic Interest*. NSRDS Bibliographic Series. IFI Plenum: New York. **1975**.
20. Morlet, J. *Rev. Inst. Franc. Petrol.* **1963**, *18*, 127.
21. Gonzalez, M. H.; Lee, A. L. *J. Chem. Eng. Data* **1968**, *13*, 172.
22. Jensen, R. H.; Kurata, F. *J. Petrol. Technol.* **1969**, *21*, 683.
23. Shana'a, M. Y.; Canfield, F. B. *Trans. Faraday Soc.* **1968**, *64*, 2281.
24. Rodosevich, J. B.; Miller, R. C. *Am. Inst. Chem. Eng. J.* **1973**, *19*, 729.
25. Orrit, J. E.; Lauprete, J. M. In *Advances in Cryogenic Engineering*, Vol. 23. Timmerhaus, K. D.: editor. Plenum Press: New York. **1978**, p. 566.
26. Miller, R. C.; Hiza, M. J. *Fluid Phase Equilibria* **1978**, *2*, 49.

A-279

*J. Chem. Thermodynamics* **1982**, *14*, 603-612

**Measurements of orthobaric-liquid densities of multicomponent mixtures of LNG components ( $N_2$ ,  $CH_4$ ,  $C_2H_6$ ,  $C_3H_8$ ,  $CH_3CH(CH_3)CH_3$ ,  $C_4H_{10}$ ,  $CH_3CH(CH_3)C_2H_5$ , and  $C_5H_{12}$ ) between 110 and 130 K<sup>a</sup>**

W. M. HAYNES

*Thermophysical Properties Division, National Engineering Laboratory,  
National Bureau of Standards, Boulder, Colorado 80303, U.S.A.*

(Received 14 September 1981)

A magnetic suspension densimeter has been used to measure the orthobaric-liquid densities of 17 multicomponent mixtures of the major components of liquefied natural gas (LNG) at temperatures from 110 to 130 K. These mixtures ranged from a ternary mixture containing nitrogen, methane, and butane to 4-to-8-component methane-rich (74 to 90 moles per cent) mixtures containing up to 5 moles per cent of nitrogen, 16 moles per cent of ethane, 7 moles per cent of propane, 5 moles per cent of the butanes, and 0.44 mole per cent of the pentanes. Some of the compositions were selected to simulate commercial LNG mixtures. Results of vapor-pressure measurements are also presented. The major purpose of this work was to obtain multicomponent-mixture values that could be used to test mathematical models that have been developed for the prediction of LNG densities. To demonstrate the consistency of the multicomponent-mixture values, comparisons are presented between experimental densities and calculated values from an extended corresponding-states method that was optimized to pure-fluid and binary-mixture results from the LNG density project here. The total uncertainty of a single density measurement is estimated to be approximately 0.1 per cent, which includes an allowance of three times the standard deviation for random error. The imprecision of measurement is a few parts in  $10^4$ .

### 1. Introduction

A project has been carried out at this laboratory to provide one or more mathematical models that can be used to predict the density of a liquefied natural gas (LNG) mixture at saturation within 0.1 per cent of its true value from an input of the

<sup>a</sup> This work was carried out at the National Bureau of Standards under the sponsorship of British Gas Corp., Chicago Bridge and Iron Co., Columbia Gas Service Corp., Distrigas Corp., Easco Gas LNG, Inc., El Paso Natural Gas, Gaz de France, Marathon Oil Co., Mobil Oil Corp., Natural Gas Pipeline Co., Phillips Petroleum Co., Shell International Gas, Ltd., Sonatrach, Southern California Gas Co., Tennessee Gas Pipeline Co., Texas Eastern Transmission Co., Tokyo Gas Co., Ltd., and Transcontinental Gas Pipe Line Corp., through a grant administered by the American Gas Association, Inc.

temperature, composition, and pressure of the liquid mixture. Such a model would serve as a basis for custody transfer of this valuable commodity. In order to develop and test such models, an accurate and consistent set of densities was needed for the major components of LNG and for mixtures of these components. Results from this project have been previously reported for (a) nitrogen,<sup>(1)</sup> methane,<sup>(1,2)</sup> ethane,<sup>(2)</sup> propane,<sup>(2)</sup> isobutane,<sup>(2)</sup> and normal butane<sup>(2,3)</sup> (major components of LNG), (b) binary mixtures<sup>(4,5)</sup> of these components, including all combinations except (nitrogen + isobutane) and (nitrogen + normal butane), and (c) selected multicomponent mixtures<sup>(6)</sup> of these components with an emphasis on ternary mixtures containing methane and binary combinations of nitrogen, ethane, and propane. All of these results were obtained with a magnetic suspension densimeter,<sup>(1)</sup> an instrument based on an application of Archimedes' principle.

In an earlier paper giving results for multicomponent mixtures,<sup>(6)</sup> reference was made to experimental problems that resulted in inconsistencies in densities for methane-rich (80 moles per cent or more) mixtures containing only hydrocarbons with approximately 5 moles per cent of butanes. The resolution of these inconsistencies was one of the major objectives of the present series of measurements. Also, more results were needed for 5- and 6-component LNG-like mixtures containing less than 5 moles per cent of the butanes and/or less than 5 moles per cent of nitrogen, and for 7- and 8-component LNG-like mixtures containing up to 0.44 mole per cent of the pentanes to test and define the limits of the models for prediction of densities for compositions approximating those of commercial LNG. These types of mixtures had not been investigated in the first series of measurements. (In the mathematical models,<sup>(7-9)</sup> results for pentanes were obtained from the literature<sup>(10)</sup> from papers that also included results for the other components of LNG that agreed with results from the present project. The behavior of binary mixtures containing pentanes was predicted by extrapolating the results of binary-mixture measurements on other LNG components.)

The results presented here were obtained with a new magnetic suspension densimeter<sup>(11)</sup> that was significantly different from, and more versatile than, the apparatus<sup>(1)</sup> that was used for most of the previous measurements of this project. However, the new apparatus did employ the same technique for determining densities and gave results for pure fluids and binary mixtures that agreed, within the precision of the measurements, with values obtained with the previous apparatus. [The new apparatus was constructed because there was a need for a higher-pressure capability (35 MPa) for the magnetic suspension densimeter in other research projects.]

New or improved features<sup>(11)</sup> of the new apparatus that were pertinent to the study of multicomponent mixtures here are as follows: (a) improved temperature control and measurements, (b) improved handling of mixtures, especially the filling of the cell so as to obtain homogeneous liquid mixtures of known composition, (c) improved vapor-pressure measurements, and (d) a capacitor for dielectric-constant measurements. (The dielectric constants for the multicomponent mixtures have not been analyzed as yet due to a lack of values for some of the pure components.) The new apparatus was also used for a study of (methane + isobutane) and (methane + normal butane).<sup>(5)</sup>

## 2. Experimental

The method of measurement,<sup>(1,12)</sup> the apparatus,<sup>(11)</sup> and the experimental procedures and measurements<sup>(1,2,4,6,11,12)</sup> have been described in detail elsewhere. Only those details that are different or essential for this paper will be discussed here. A one-solenoid magnetic suspension system<sup>(12)</sup> was used to obtain the results reported here.

Measurements on liquid methane were used as a control on the measurement process during the course of the mixture measurements. A density measurement on liquid methane was performed before each filling of the cell with a new mixture sample. This procedure was followed to insure that the warm-up and cool-down cycles of the apparatus did not affect the apparent position of the buoy from liquid-to-vacuum measurements. After mixture measurements were completed for each sample, the cell was warmed to room temperature to facilitate complete removal of the heavy hydrocarbons. A maximum of four points at 5 K increments was obtained for each sample.

There were a total of four capillaries entering into the cell, two at the top and two at the bottom. A pair of these (one at top and one at bottom) was available for recirculation of the vapor through the liquid. The second capillary into the bottom of the cell was available for liquid sampling. The second line into the top of the cell was used solely for pressure measurements. This was the only capillary not used in the filling process.

The mixtures were condensed directly and continuously into the equilibrium cell either through the two capillaries at the bottom of the cell (analogous to vapor recirculation) or through the recirculation and liquid-sampling capillaries at the top and bottom simultaneously. An effort was made to determine if the homogeneity of the liquid sample in the cell was dependent on the filling procedure. As indicated by the consistency of the densities, it was found that the measured densities were independent of the filling routines attempted.

All measurements were on saturated liquids. In the present work it was impossible, and not essential, to observe the liquid-vapor interface through a small high-pressure sapphire window positioned near the mid-point of the cell along its length. The cell was initially filled with each new sample until the mixture was in the compressed liquid, or at a pressure a few tenths of a MPa above its vapor pressure. Then, small amounts of liquid were withdrawn from the bottom of the cell until the saturation pressure was attained, as denoted by reproducibility of the pressure readings. It was extremely important to have as small vapor volume as possible in the sample space.

As the cell was warmed to the temperature of the next point, the pressure of the mixture was monitored as a function of temperature. This information could be used to calculate the amount of vapor volume in the cell for the prior point and to confirm that the liquid mixture had been at saturation. The vapor volume in the cell was sufficiently small ( $0.2 \text{ cm}^3$ ) so that the liquid went into the compressed state for a temperature change of less than 2 K.

It was thought that the most accurate method to determine the compositions of the liquid mixtures was to prepare them by gravimetric means under carefully controlled conditions and, subsequently, to introduce them in a mixed state into the equilibrium

chamber. The preparation of mixtures of LNG components, with the exception of pentanes, has been described in previous papers.<sup>(4,6)</sup> The pentane fractions were obtained from bottles of commercially available research-grade liquids. The lowest purities, as specified by the supplier from freezing-temperature determinations, were 99.99 and 99.93 moles per cent for isopentane and normal pentane, respectively. The most probable impurity in normal pentane was isopentane while those for isopentane were neopentane and normal pentane.

With one exception (mixture C in table 1, 3.1 mol), at least 4 mol was prepared for each mixture investigated here. This corresponds to less than 0.0001 uncertainty in mole fraction of methane in the prepared mixture and considerably less uncertainty for each of the other components. Due to insufficient mixing in a base mixture, the compositions of three of the mixtures (mixtures m, n, and p) were determined by analyses of samples using a gas chromatograph with a thermal-conductivity detector.<sup>(13)</sup> The uncertainty in the compositions determined in this manner corresponds to an uncertainty of roughly 0.03 per cent in the density. At least six samples, with subsequent analyses, were taken for each mixture. Half of these samples were taken after heating the cylinders, in which the gas mixtures were contained, for approximately 30 min with an infrared lamp. The compositions for the six samples agreed within experimental uncertainty and did not exhibit any dependence on the temperature of the mixture being tested.

The total liquid volume within the cell was approximately 43 cm<sup>3</sup>, as determined by filling the cell with water. The total vapor volume of the sample space was approximately 7.4 cm<sup>3</sup> and can be divided into three parts as follows: (a) inside cell—0.2 cm<sup>3</sup>, (b) access tubing within cryostat—1 cm<sup>3</sup>, and (c) access tubing and pressure gauge outside cryostat—6.2 cm<sup>3</sup>. The volumes of the tubing and pressure gauge were computed from known dimensions. The composition of the liquid in the cell should be slightly different from the prepared mixture composition as a result of the vapor volume. The magnitude of the adjustment to the measured densities to account for this composition change, so that the experimental densities can be assigned to the prepared mixture composition, is discussed in the next section.

For all measurements reported here, the cell was always isolated from a recirculation pump that could be used to mix the liquid inside the cell. Based on the consistency of the densities for different filling procedures and new mixture samples and from comparisons of the experimental densities with predicted values, it was not deemed necessary to recirculate the vapor through the liquid to mix the samples or to take liquid samples and analyze them. There were other means for gaining information on the reproducibility of liquid compositions within the cell for different samples from the same prepared mixture and on the homogeneity of the liquid sample, as discussed below.

Vapor pressures were measured for each of the mixtures investigated here using a spiral quartz Bourdon-tube gauge (0 to 1.38 MPa) calibrated against an air dead-weight gauge. The maximum uncertainty in the gauge calibration was estimated to be approximately 70 Pa. Vapor-pressure measurements for different samples and filling procedures generally agreed within  $3 \times 10^{-4}$  MPa.

A capacitor composed of slotted concentric cylinders located in the top part of the

cell was used for dielectric-constant measurements on the mixtures. The capacitor had a vacuum capacitance of 19.8 pF. Readings could be made routinely to within 0.0001 pF. This device was the most sensitive monitor within the sample space to determine the reproducibility of liquid compositions for different filling procedures and for different samples from the same mixture.

Although the cell was monitored for temperature gradients along its length using vapor bulbs at the top and bottom of the cell in only a few runs, a differential thermocouple with junctions at the same locations as the vapor bulbs was used in all runs. The vapor-bulb measurements were used as a control on the thermocouple measurements. The reflux tube was always evacuated while performing measurements. At temperatures between 110 and 130 K, greatest power input into the cell to balance the cooling was 0.5 W. The guard ring was controlled at a temperature somewhat above the cell temperature. Under the above conditions, no problems were encountered with temperature gradients along the length of the cell within the precision of the vapor-pressure measurements.

The vapor pressures and dielectric constants were obtained for different portions (different heights) of the liquid sample from that of the density determination. Assuming an isothermal sample space, information on composition (or density) gradients along the length of the cell could be gained from the various measurements at different positions within the sample space.

### 3. Results

Experimental orthobaric liquid densities and vapor pressures of mixtures of LNG components are presented in table 1 as a function of temperature (IPTS-68). The compositions presented in this table were determined gravimetrically except those for mixtures m, n, and p. The compositions of these mixtures were determined by analyses of the prepared mixtures using a gas chromatograph with a thermal conductivity detector, as discussed in the preceding section.

Small corrections were made to the measured densities to account for differences in compositions between the prepared mixtures and the liquid mixtures in the equilibrium cell, which resulted from some of the sample space being occupied with vapor. The largest adjustment was less than 0.05 per cent, which was for mixture a at 125 K. All other corrections were less than 0.02 per cent. For all mixtures containing hydrocarbons only, it was assumed that the vapor composition was 100 per cent methane. For those mixtures containing nitrogen, the vapor compositions were estimated from partial-pressure calculations using available phase-equilibria data for (nitrogen + methane).<sup>(14, 15)</sup>

Excess volumes defined by the relation:

$$V^E = V_m - \sum_i x_i V_i \{1 + \kappa_i (p_i - p_m)\}, \quad (1)$$

are also given in table 1. In this expression  $V_m$  is the molar volume of mixture at a given temperature at saturation pressure  $p_m$ ,  $V_i$  is the molar volume of pure

TABLE 1. Orthobaric-liquid densities of multicomponent mixtures of LNG components.  $M$ , Molar mass;  $T$ , temperature (IPTS-68);  $p$ , pressure;  $\rho_{n, \text{expt}}$ , experimental amount-of-substance density,  $\rho_{\text{expt}}$ , experimental density;  $V^E$ , excess volume calculated from equation (1);  $\rho_{\text{csm}}$ , density calculated from the extended corresponding-states method as given in references 7 to 9

$\frac{T}{\text{K}}$	$\frac{p}{\text{MPa}}$	$\frac{\rho_{n, \text{expt}}}{\text{mol} \cdot \text{dm}^{-3}}$	$\frac{V^E}{\text{cm}^3 \cdot \text{mol}^{-1}}$	$\frac{10^2(\rho_{\text{expt}} - \rho_{\text{csm}})}{\rho_{\text{csm}}}$
(a) $(0.05931\text{N}_2 + 0.89071\text{CH}_4 + 0.04998\text{C}_4\text{H}_{10})$ ( $M = 18.8562 \text{ g} \cdot \text{mol}^{-1}$ )				
110.00	0.2400	25.3450	-0.713	+0.03
115.00	0.3145	24.9440	-0.983	+0.01
120.00	0.4082	24.5383	-1.595	+0.00
125.00	0.5196	24.1141		-0.04
(b) $\{0.86040\text{CH}_4 + 0.04600\text{C}_2\text{H}_6 + 0.04790\text{C}_3\text{H}_8 + 0.04570\text{CH}_3\text{CH}(\text{CH}_3)\text{CH}_3\}$ ( $M = 19.9552 \text{ g} \cdot \text{mol}^{-1}$ )				
115.00	0.1186	24.2654	-0.631	-0.03
120.00	0.1710	23.9371	-0.741	+0.01
125.00	0.2387	23.5868	-0.842	-0.01
130.00	0.3248	23.2331	-0.970	-0.02
135.00	0.4320	22.8637	-1.110	-0.07
(c) $\{0.85378\text{CH}_4 + 0.05178\text{C}_2\text{H}_6 + 0.04703\text{C}_3\text{H}_8 + 0.04741\text{CH}_3\text{CH}(\text{CH}_3)\text{CH}_3\}$ ( $M = 20.0838 \text{ g} \cdot \text{mol}^{-1}$ )				
115.00	0.1191	24.2100	-0.640	-0.03
120.00	0.1706	23.8779	-0.739	-0.02
125.00	0.2379	23.5324	-0.843	-0.04
130.00	0.3238	23.1834	-0.975	-0.05
(d) $(0.85133\text{CH}_4 + 0.05759\text{C}_2\text{H}_6 + 0.04808\text{C}_3\text{H}_8 + 0.04300\text{C}_4\text{H}_{10})$ ( $M = 20.0092 \text{ g} \cdot \text{mol}^{-1}$ )				
115.00	0.1180	24.3243	-0.675	-0.01
120.00	0.1700	23.9965	-0.785	+0.03
125.00	0.2374	23.6586	-0.907	+0.05
130.00	0.3232	23.3108	-1.045	+0.05
135.00	0.4301	22.9634	-1.226	+0.09
(e) $(0.84566\text{CH}_4 + 0.07924\text{C}_2\text{H}_6 + 0.05060\text{C}_3\text{H}_8 + 0.02450\text{C}_4\text{H}_{10})$ ( $M = 19.6051 \text{ g} \cdot \text{mol}^{-1}$ )				
115.00	0.1167	24.5569	-0.621	-0.01
120.00	0.1683	24.2126	-0.711	-0.01
125.00	0.2350	23.8698	-0.832	+0.03
130.00	0.3201	23.5204	-0.975	+0.07
(f) $\{0.04801\text{N}_2 + 0.80940\text{CH}_4 + 0.04542\text{C}_2\text{H}_6 + 0.05050\text{C}_3\text{H}_8 + 0.04667\text{CH}_3\text{CH}(\text{CH}_3)\text{CH}_3\}$ ( $M = 20.6355 \text{ g} \cdot \text{mol}^{-1}$ )				
115.00	0.3005	24.1487	-1.129	-0.04
120.00	0.3863	23.8075	-1.679	-0.03
125.00	0.4874	23.4518		-0.05
130.00	0.6125	23.0893		-0.07

TABLE 1—continued

$\frac{T}{K}$	$\frac{p}{\text{MPa}}$	$\frac{\rho_{n,\text{expt}}}{\text{mol} \cdot \text{dm}^{-3}}$	$\frac{V^E}{\text{cm}^3 \cdot \text{mol}^{-1}}$	$\frac{10^2(\rho_{\text{expt}} - \rho_{\text{csm}})}{\rho_{\text{csm}}}$
(g) $(0.02628\text{N}_2 + 0.81249\text{CH}_4 + 0.08484\text{C}_2\text{H}_6 + 0.04931\text{C}_3\text{H}_8 + 0.02708\text{C}_4\text{H}_{10})$ ( $M = 20.0706 \text{ g} \cdot \text{mol}^{-1}$ )				
115.00	0.2214	24.4562	-0.908	-0.02
120.00	0.2874	24.1119	-1.254	-0.01
125.00	0.3768	23.7507		-0.05
130.00	0.4793	23.3954		-0.03
(h) $\{0.85892\text{CH}_4 + 0.11532\text{C}_2\text{H}_6 + 0.01341\text{C}_3\text{H}_8 + 0.00530\text{CH}_3\text{CH}(\text{CH}_3)\text{CH}_3 + 0.00705\text{C}_4\text{H}_{10}\}$ ( $M = 18.5565 \text{ g} \cdot \text{mol}^{-1}$ )				
115.00	0.1185	25.0957	-0.480	-0.03
120.00	0.1706	24.7131	-0.534	-0.07
125.00	0.2372	24.3294	-0.613	-0.08
130.00	0.3225	23.9490	-0.730	-0.06
(i) $\{0.84558\text{CH}_4 + 0.08153\text{C}_2\text{H}_6 + 0.04778\text{C}_3\text{H}_8 + 0.01259\text{CH}_3\text{CH}(\text{CH}_3)\text{CH}_3 + 0.01252\text{C}_4\text{H}_{10}\}$ ( $M = 19.5838 \text{ g} \cdot \text{mol}^{-1}$ )				
115.00	0.1166	24.5586	-0.620	+0.01
120.00	0.1680	24.2180	-0.716	+0.03
125.00	0.2348	23.8688	-0.826	+0.04
130.00	0.3188	23.5154	-0.963	+0.07
(j) $\{0.00601\text{N}_2 + 0.90613\text{CH}_4 + 0.06026\text{C}_2\text{H}_6 + 0.02154\text{C}_3\text{H}_8 + 0.00300\text{CH}_3\text{CH}(\text{CH}_3)\text{CH}_3 + 0.00306\text{C}_4\text{H}_{10}\}$ ( $M = 17.8195 \text{ g} \cdot \text{mol}^{-1}$ )				
115.00	0.1478	25.3834	-0.425	-0.01
120.00	0.2043	24.9894	-0.551	+0.02
125.00	0.2785	24.5702		-0.02
130.00	0.3722	24.1578		+0.02
(k) $\{0.00973\text{N}_2 + 0.88225\text{CH}_4 + 0.07259\text{C}_2\text{H}_6 + 0.02561\text{C}_3\text{H}_8 + 0.00490\text{CH}_3\text{CH}(\text{CH}_3)\text{CH}_3 + 0.00492\text{C}_4\text{H}_{10}\}$ ( $M = 18.3094 \text{ g} \cdot \text{mol}^{-1}$ )				
115.00	0.1639	25.2023	-0.556	-0.04
120.00	0.2247	24.8047	-0.698	-0.00
125.00	0.3022	24.4022		-0.03
(l) $\{0.01383\text{N}_2 + 0.85934\text{CH}_4 + 0.08477\text{C}_2\text{H}_6 + 0.02980\text{C}_3\text{H}_8 + 0.00519\text{CH}_3\text{CH}(\text{CH}_3)\text{CH}_3 + 0.00707\text{C}_4\text{H}_{10}\}$ ( $M = 18.7496 \text{ g} \cdot \text{mol}^{-1}$ )				
115.00	0.1812	25.0384	-0.662	+0.06
120.00	0.2441	24.6661	-0.874	+0.07
125.00	0.3223	24.2880		+0.09
130.00	0.4222	23.8981		+0.10
(m) $0.85341\text{CH}_4 + 0.07898\text{C}_2\text{H}_6 + 0.04729\text{C}_3\text{H}_8 + 0.00854\text{CH}_3\text{CH}(\text{CH}_3)\text{CH}_3 + 0.00992\text{C}_4\text{H}_{10} + 0.00097\text{CH}_3\text{CH}(\text{CH}_3)\text{C}_2\text{H}_5 + 0.00089\text{C}_5\text{H}_{12}\}$ ( $M = 19.3587 \text{ g} \cdot \text{mol}^{-1}$ )				
110.00	0.0787	25.0063	-0.517	-0.01
115.00	0.1172	24.6566	-0.581	-0.03
120.00	0.1686	24.3079	-0.670	-0.02
125.00	0.2351	23.9525	-0.777	-0.01
130.00	0.3210	23.5883	-0.901	0.00

TABLE 1—continued

$T$ K	$p$ MPa	$\rho_{n, \text{expt}}$ $\text{mol} \cdot \text{dm}^{-3}$	$V^E$ $\text{cm}^3 \cdot \text{mol}^{-1}$	$\frac{10^2(\rho_{\text{expt}} - \rho_{\text{CSM}})}{\rho_{\text{CSM}}}$
(n) $\{0.75442\text{CH}_4 + 0.15401\text{C}_2\text{H}_6 + 0.06950\text{C}_3\text{H}_8 + 0.00978\text{CH}_3\text{CH}(\text{CH}_3)\text{CH}_3 + 0.01057\text{C}_4\text{H}_{10}$ $+ 0.00089\text{CH}_3\text{CH}(\text{CH}_3)\text{C}_2\text{H}_5 + 0.00083\text{C}_5\text{H}_{12}\}$ ( $M = 21.1060 \text{ g} \cdot \text{mol}^{-1}$ )				
110.00	0.0723	24.2529	-0.633	-0.05
115.00	0.1081	23.9619	-0.740	+0.01
120.00	0.1549	23.6535	-0.840	+0.01
125.00	0.2153	23.3351	-0.949	-0.01
(o) $\{0.00859\text{N}_2 + 0.75713\text{CH}_4 + 0.13585\text{C}_2\text{H}_6 + 0.06742\text{C}_3\text{H}_8 + 0.01336\text{CH}_3\text{CH}(\text{CH}_3)\text{CH}_3$ $+ 0.01326\text{C}_4\text{H}_{10} + 0.00223\text{CH}_3\text{CH}(\text{CH}_3)\text{C}_2\text{H}_5 + 0.00216\text{C}_5\text{H}_{12}\}$ ( $M = 21.3094 \text{ g} \cdot \text{mol}^{-1}$ )				
110.00	0.1155	24.1809	-0.741	+0.03
115.00	0.1595	23.8731	-0.857	+0.02
120.00	0.2155	23.5709	-1.055	+0.05
125.00	0.2873	23.2644		+0.08
130.00	0.3744	22.9514		+0.11
(p) $\{0.00801\text{N}_2 + 0.74275\text{CH}_4 + 0.16505\text{C}_2\text{H}_6 + 0.06547\text{C}_3\text{H}_8 + 0.00843\text{CH}_3\text{CH}(\text{CH}_3)\text{CH}_3$ $+ 0.00893\text{C}_4\text{H}_{10} + 0.00069\text{CH}_3\text{CH}(\text{CH}_3)\text{C}_2\text{H}_5 + 0.00067\text{C}_5\text{H}_{12}\}$ ( $M = 21.0976 \text{ g} \cdot \text{mol}^{-1}$ )				
110.00	0.1158	24.3141	-0.676	-0.05
115.00	0.1584	24.0160	-0.807	-0.02
120.00	0.2093	23.6937	-0.965	-0.06
125.00	0.2853	23.3804		-0.05
(q) $\{0.00599\text{N}_2 + 0.90068\text{CH}_4 + 0.06537\text{C}_2\text{H}_6 + 0.02200\text{C}_3\text{H}_8 + 0.00291\text{CH}_3\text{CH}(\text{CH}_3)\text{CH}_3$ $+ 0.00284\text{C}_4\text{H}_{10} + 0.00010\text{CH}_3\text{CH}(\text{CH}_3)\text{C}_2\text{H}_5 + 0.00011\text{C}_5\text{H}_{12}\}$ ( $M = 17.9026 \text{ g} \cdot \text{mol}^{-1}$ )				
115.00	0.1456	25.3600	-0.449	+0.02
120.00	0.2024	24.9656	-0.571	+0.03
125.00	0.2762	24.5450		-0.03
130.00	0.3698	24.1289		-0.02

component  $i$  at the same temperature at saturation pressure  $p_i$ ,  $x_i$  is the mole fraction of component  $i$ , and  $\kappa_i$  is the isothermal compressibility of component  $i$ .

The pure-fluid molar volumes were obtained from expressions given in references 1, 2, and 16, while the compressibilities for nitrogen, methane, and ethane were obtained from expressions presented in reference 6. Compressibility corrections for hydrocarbons beyond ethane were sufficiently small to neglect. For those mixtures containing nitrogen, excess volumes were not computed for temperatures above 120 K. (The critical temperature of nitrogen is approximately 126.2 K.) Vapor pressures for nitrogen, methane, and ethane were obtained from references 17 to 19, respectively.

To demonstrate the consistency of the results presented here, table 1 includes comparisons between the experimental densities and the values calculated using an extended corresponding-states method,<sup>(7-9)</sup> which was optimized to only the pure-fluid (except for pentanes) and binary-mixture values from the LNG density project at this laboratory. Of the mathematical models developed at this laboratory<sup>(7-9)</sup> for the prediction of LNG densities, the extended corresponding-states method is probably the most accurate and certainly the most general since it handles the widest ranges of

pressure, temperature, and composition. All other models<sup>(7-9)</sup> developed at this laboratory were characterized by limitations in the ranges of either temperature or composition covered for mixtures containing nitrogen and butanes. The maximum deviation between the experimental and calculated densities using the extended corresponding-states method was 0.11 per cent, while the average absolute deviation was 0.04 per cent.

Comparisons of the present results with other mathematical models optimized to the pure-fluid and binary-mixture values from this project are presented in reference 8. Comparisons of multicomponent mixture values (LNG components) from other sources with those of the present study have been accomplished indirectly in earlier papers.<sup>(6,7)</sup> The results from other work were compared with the calculated values from the extended corresponding-states method that had been optimized to the pure fluid and binary-mixture values from this project.

Detailed descriptions of the random and systematic errors involved in density measurements on liquids and liquid mixtures with a magnetic suspension densimeter have been presented elsewhere.<sup>(1,4,6)</sup> The total systematic error in the measurements on multicomponent mixtures should be little different from that for binary mixtures. The added uncertainty in the composition of the prepared mixtures resulting from the larger number of components is insignificant.

The random error in the multicomponent-mixture measurements was difficult to evaluate since, for most mixtures, there was not a sufficient amount prepared to make a statistically significant number of repetitive measurements on different samples from the same mixture. It is believed that the random error in these multicomponent mixture measurements should not be significantly different from that for (methane + isobutane) and (methane + normal butane) measurements<sup>(5)</sup> (maximum standard deviation of 0.024 per cent) obtained with the same apparatus.

Based on the analysis of errors for density measurements on pure fluids and binary mixtures with a magnetic suspension densimeter, it is believed that the maximum total uncertainty in the densities for the multicomponent mixtures presented in this paper is approximately 0.12 per cent. The total uncertainty has been taken as the root mean square of the known systematic errors added to three times the standard deviation for random error. This estimate was confirmed, to some extent, in the comparisons between the experimental results and the predicted values from the extended corresponding-states method. As reported earlier in this section, the maximum deviation was 0.11 per cent and the average absolute deviation was 0.04 per cent.

The contributions of M. J. Hiza in the preparation of mixtures, R. J. Richards in the analysis of mixtures, and R. D. McCarty and R. G. Sargent in the reduction and analysis of results are gratefully acknowledged.

## REFERENCES

1. Haynes, W. M.; Hiza, M. J.; Frederick, N. V. *Rev. Sci. Instrum.* **1976**, *47*, 1237.
2. Haynes, W. M.; Hiza, M. J. *J. Chem. Thermodynamics* **1977**, *9*, 79.
3. Haynes, W. M.; Hiza, M. J. *Advances in Cryogenic Engineering* Vol. 21. Timmerhaus, K. D.; Weitzel, D. H.; editors. Plenum Press: New York. **1976**, p. 516.

4. Hiza, M. J.; Haynes, W. M.; Parrish, W. R. *J. Chem. Thermodynamics* **1977**, *9*, 873.
5. Haynes, W. M. To be published.
6. Hiza, M. J.; Haynes, W. M. *J. Chem. Thermodynamics* **1980**, *12*, 1.
7. McCarty, R. D. *Natl. Bur. Stand. (U.S.), Interagency Rept NBSIR 77-867*. **1977**.
8. McCarty, R. D. *Natl. Bur. Stand. (U.S.), Tech. Note 1030*. **1980**.
9. McCarty, R. D. to be published.
10. Orrit, J. E.; Laupretre, J. M. *Advances in Cryogenic Engineering* Vol. 23. Timmerhaus, K. D.: editor. Plenum Press: New York. **1978**, p. 573.
11. Haynes, W. M. To be published.
12. Haynes, W. M. *Rev. Sci. Instrum.* **1977**, *48*, 39.
13. Parrish, W. R.; Arvidson, J. M.; LaBrecque, J. F. *Natl. Bur. Stand. (U.S.), Interagency Rept NBSIR 78-887*. **1978**.
14. Parrish, W. R.; Hiza, M. J. *Advances in Cryogenic Engineering* Vol. 19. Timmerhaus, K. D.: editor. Plenum Press: New York. **1974**, p. 300.
15. Kidnay, A. J.; Miller, R. C.; Parrish, W. R.; Hiza, M. J. *Cryogenics* **1975**, *15*, 531.
16. Hiza, M. J. *Fluid Phase Equilibria* **1978**, *2*, 27.
17. Strobridge, T. R. *Natl. Bur. Stand. (U.S.), Tech. Note 129*. **1962**.
18. Goodwin, R. D. *Natl. Bur. Stand. (U.S.), Tech. Note 653*. **1974**.
19. Goodwin, R. D.; Roder, H. M.; Straty, G. C. *Natl. Bur. Stand. (U.S.), Tech. Note 684*. **1976**.

# Four Mathematical Models for the Prediction of LNG Densities

Robert D. McCarty

Thermophysical Properties Division  
National Engineering Laboratory  
National Bureau of Standards  
Boulder, Colorado 80303



---

U.S. DEPARTMENT OF COMMERCE, Philip M. Klutznick, Secretary

Jordan J. Baruch, Assistant Secretary for Productivity, Technology and Innovation

NATIONAL BUREAU OF STANDARDS, Ernest Ambler, Director

Issued December 1980

# CONTENTS

	Page
Abstract . . . . .	1
1. INTRODUCTION . . . . .	1
2. EXTENDED CORRESPONDING STATES . . . . .	3
3. A HARD SPHERE METHOD . . . . .	6
4. A REVISED KLOSEK AND MCKINLEY METHOD . . . . .	11
5. THE CELL MODEL . . . . .	13
6. USE OF THE METHODS . . . . .	15
7. CONCLUSIONS . . . . .	19
8. REFERENCES . . . . .	20
Appendix A. Experimental Data . . . . .	24
Appendix B. Computer Program and Equation Parameters for the Extended Corresponding States Model . . . . .	39
Appendix C. Computer Program and Equation Parameters for the Hard Sphere Model . . . . .	46
Appendix D. Computer Program and Parameters for the Revised Klosek and McKinley Model . . . . .	50
Appendix E. Computer Program for the Cell Model . . . . .	54
Appendix F. Computer Programs . . . . .	55

## FOUR MATHEMATICAL MODELS FOR THE PREDICTION OF LNG DENSITIES\*

Robert D. McCarty

Thermophysical Properties Division  
National Engineering Laboratory  
National Bureau of Standards  
Boulder, Colorado 80303

Four mathematical models of the equation of state for LNG like mixtures are presented. The four models include an extended corresponding states model, a cell model, a hard sphere model and a revised Klosek and McKinley model. Each of the models has been optimized to the same experimental data set which included data for pure nitrogen, methane, ethane, propane, iso and normal butane, iso and normal pentane and mixtures thereof. For LNG like mixtures (mixtures of the orthobaric liquid state at temperatures of 120 K or less and containing at least 60% methane, less than 4% nitrogen, less than 4% each of iso and normal butane and less than 2% total of iso and normal pentane), all of the models are estimated to predict densities to within 0.1% of the true value. The revised Klosek and McKinley model is valid only for mixtures within the range of temperature and composition specified above while the other three models are valid for a broader range of pressure, temperature and composition. The experimental PVTx data set used in the optimization together with comparisons are given and listings of computer programs for each of the models are included.

Key words: Cell model; comparisons; computer programs; corresponding states; equation of state; hard sphere; LNG; mixtures; PVTx data; revised Klosek and McKinley.

### 1. INTRODUCTION

The purpose of this report is to present in final form the four mathematical models which were optimized to the experimentally determined orthobaric liquid

---

\* This work was carried out at the National Bureau of Standards under the sponsorship of British Gas Corp., Chicago Bridge and Iron Co., Columbia Gas Service Corp., Distrigas Corp., Easco Gas LNG, Inc., El Paso Natural Gas, Gaz de France, Marathon Oil Co., Mobil Oil Corp., Natural Gas Pipeline Co., Phillips Petroleum Co., Shell International Gas, Ltd., Sonatrach, Southern California Gas Co., Tennessee Gas Pipeline, Texas Eastern Transmission Co., Tokyo Gas Co., Ltd., and Transcontinental Gas Pipe Line Corp., through a grant administered by the American Gas Association, Inc.

PVTx data of Miller and Hiza [25], Haynes and Hiza [12], Haynes, et al. [11], Hiza, et al. [14], Hiza and Haynes [15] and Haynes [9]. Interim results of the project have been reported by Haynes, et al. [13] and by McCarty [23]. The models reported in these two interim publications differ only slightly from those presented here. A companion archival document, McCarty [24] with the same results but in much less detail has been submitted to the Journal of Chemical Thermodynamics. The intent of the documentation here is more in the vein of a user's handbook. The above experimental data are for the liquid phase of nitrogen, methane, ethane, propane, normal and isobutane and various mixtures thereof.

The goal of the project (the project included the above referenced experimental work) was to produce one or more computer models which would predict the density of LNG to within 0.1% of the true value from a knowledge of the temperature, pressure and composition of the LNG. At the beginning of this study LNG was defined as mixtures of the above components ( $N_2$ ,  $CH_4$ ,  $C_2H_6$ ,  $C_3H_8$ , n and  $iC_4H_{10}$ ) and only the saturated liquid between 95 - 150 K was to be considered. Near the end of the project n and  $iC_5H_{12}$  were added to the list of allowable components but no experimental PVTx of pure n and  $iC_5H_{12}$  or binary systems containing n and  $iC_5H_{12}$  were measured as part of the project. The inclusion of these two components is based on data from Orrit, et al. [29] and Orrit, et al. [30].

Four models were considered: the extended corresponding states model, a hard sphere model, a cell model and a Revised Klosek and McKinley model. With the exception of the Revised Klosek and McKinley model only pure fluid and binary system data were used to optimize the models. In the case of the Revised Klosek and McKinley model multicomponent PVTx data were used in the optimization process.

Over a normal range of LNG composition and temperature all four of the models predict densities which agree to within 0.1% of experiment. This is true of all of the experimental PVTx measurements on LNG like mixtures made as part of this project.

No equation or mathematical model based on experimental data can be more accurate than the original data and therefore the extent to which the original goal of 0.1% accuracy has been met depends entirely upon the accuracy of the experimental data referenced above.

There is no reason to doubt the experimental data and therefore there is every reason to believe that the goal of the project has been achieved.

## 2. EXTENDED CORRESPONDING STATES

The thermodynamic equations for the extended corresponding states method are developed in a paper by Rowlinson and Watson [35] and only a very brief description will be given here. Leach [20] developed transformation functions for hydrocarbons which are called shape factor functions. Mollerup [27] and Mollerup and Rowlinson [26] combined the earlier work with the equation of state for methane by Goodwin [8] to produce a computer program to calculate the density of LNG mixtures, which was further modified by Mollerup [28].

The computer program in Appendix F for the calculation of LNG densities based on the extended corresponding states method is an extensive revision of the Mollerup program. Earlier revisions were reported by McCarty [23] and Haynes, Hiza and McCarty [13].

The extended corresponding states method is defined by the following equations:

$$Z_i[P,T] = Z_o[P h_{ii,o}/f_{ii,o}, T/f_{ii,o}] \quad (1)$$

$$G_i[P,T] = f_{ii,0} G_0[P h_{ii,0}/f_{ii,0}, T/f_{ii,0}] - RT \ln(h_{ii,0}) \quad (2)$$

where  $Z$  is the compressibility factor,  $G$  is the Gibbs free energy,  $P$  is pressure and  $T$  is temperature. The subscript  $0$  denotes the reference fluid and the subscript  $i$  denotes the fluid for which properties are to be obtained via the equation of state for the reference fluid and the transformation functions  $f_{ii,0}$  and  $h_{ii,0}$ . The double subscript  $ii$  is introduced now to allow extension of the method to mixtures. The two defining eqs (1) and (2) are necessary since there are two transformation functions. In this case the equation of state for methane by McCarty [22] was chosen for the reference fluid. During the course of the study it was necessary to modify the equation of state by McCarty [22] to give a realistic vapor liquid phase boundary down to a temperature of 43 K. This modification was necessary to accommodate the very low reduced temperatures of the heavier hydrocarbons and was accomplished without changing the performance of the equation of state above the triple point of methane. The equation of state is given in Appendix B.

The  $f_{ii,0}$  and  $h_{ii,0}$  are defined as

$$f_{ii,0} = (T_{ii}^C/T_0^C) \theta_{ii,0}(T_r, V_r) \quad (3)$$

and

$$h_{ii,0} = (V_{ii,0}^C/V_0^C) \phi_{ii,0}(T_r, V_r) \quad (4)$$

where

$$\theta_{ii,0} = 1 + (w_i - w_0)[n_1 - n_2 \ln T_{r_i} + (n_3 - n_4/T_{r_i})(V_{r_i} - n_5)] \quad (5)$$

and

$$\phi_{ii,0} = \frac{Z_0^C}{Z_i^C} \left[ 1 + (w_i - w_0) [n_6 (V_{r_i} - n_7) - n_8 (V_{r_i} - n_9) \ln T_{r_i}] \right] \quad (6)$$

The  $V_{r_i}$  and  $T_{r_i}$  are reduced temperature and volume, (i.e.,  $T_{r_i} = T/T_{ii}^C$  and  $V_{r_i} = V/V_{ii}^C$ ) each fluid requires a unique  $w_i$  which was estimated using pure fluid experimental data. A single set of the  $n_i$ 's are used for all fluids. The  $n_i$ 's were estimated using all of the pure fluid experimental data from this study. The  $Z_0^C/Z_i^C$  is the ratio of the compressibility factors ( $Z^C = P_c V_c / RT_c$ ) at the critical point. The parameters  $n_j$ ,  $n_j$ ,  $w_i$  and  $Z_{ij}$  are given in Appendix B. All of these parameters were estimated using the experimental PVT data set from this laboratory and least squares estimation techniques.

The extension of the above to mixtures is now accomplished by the following application of the following combining rules:

$$h_{x,0} = \sum_i \sum_j x_i x_j h_{ij,0} \quad (7)$$

$$f_{x,0} h_{x,0} = \sum_i \sum_j x_i x_j f_{ij,0} h_{ij,0} \quad (8)$$

$$f_{ij,0} = \xi_{ij} (f_{ii,0} f_{jj,0})^{1/2} \quad (9)$$

$$h_{ij,0} = \eta_{ij} \left( \frac{1}{2} h_{ii,0}^{1/3} + \frac{1}{2} h_{jj,0}^{1/3} \right)^3 \quad (10)$$

The  $\xi_{ij}$  and the  $\eta_{ij}$  are binary interaction parameters determined by least squares from the PVTx data for binary mixtures. These parameters are given in Appendix B.

This method works quite well as may be seen in the comparisons in Appendix A. It has indeed reproduced all of the present experimental data set to within  $\pm 0.1\%$  except for 14 out of a total of 285 experimental data points. Of these 14 points, 11 are judged to have an uncertainty greater than 0.1%. Figure 1 presents the deviations between the calculated and experimental densities for these 14 points. Appendix A contains comparisons of calculated and experimental densities for the entire data set. This is the best performance of the four models presented here. No pressure, temperature or composition restrictions have been placed on this model.

In the interim publications by McCarty [23] and Haynes, Hiza and McCarty [13] some doubt about the accuracy of the calculated densities was expressed because of the disagreement with a few binary and multicomponent systems containing methane and butane. This disagreement has since been resolved by additional measurements (Haynes [9], Haynes [10] and Miller and Hiza [25] on some of the systems which agree with the predictions of the model but disagree with the previous measurements. The net result of the new measurements is a very slight change in binary interaction coefficients of the methane-butane and nitrogen-butane system. These changes have no practical effect on LNG like mixtures where the concentrations of  $N_2$ ,  $iC_4H_{10}$  and  $nC_4H_{10}$  are individually less than 5%. In other words either the models presented here or those in the interim publications may be used to predict the density of a LNG like mixture to within 0.1% of the true density.

### 3. A HARD SPHERE METHOD

The model of Rodosevich and Miller [33] is one of many modifications of the Longuet-Higgins and Widom [21] model, and was chosen to be included in this study

as a representative example of the application of the hard sphere equation of state concept to the correlation of PVTx data. The equation of state by Rodosevich and Miller [33] is

$$\frac{PV}{RT} = c \frac{1 + y + y^2}{(1 - y)^3} - \frac{a}{RTV} \quad (11)$$

where the  $y = b/4V$  and  $a$ ,  $b$ , and  $c$  are adjustable parameters,  $P$  is pressure,  $V$  is specific volume,  $T$  is temperature and  $R$  is the gas constant. The equation is applied to mixtures by assuming the one-fluid theory and applying the following combining rules.

$$a_m = \sum_i \sum_j a_{ij} x_i x_j \quad (12)$$

$$b_m = \sum_i \sum_j b_{ij} x_i x_j \quad (13)$$

$$c_m = \sum_i \sum_j c_{ij} x_i x_j \quad (14)$$

The mixing rules are:

$$b_{ij} = \left[ \frac{b_{ii}^{1/3} + b_{jj}^{1/3}}{2} (1 - j_{ij}) \right]^3 \quad (15)$$

$$a_{ij} = (a_{ii} a_{jj})^{1/2} \left[ \frac{b_{ij}^2}{b_{ii} b_{jj}} \right]^{1/2} (1 - k_{ij}) \quad (16)$$

$$c_{ij} = \frac{c_{ii} + c_{jj}}{2} \quad (17)$$

The parameters  $j_{ij}$  and  $k_{ij}$  are in this case the binary interaction parameters. The  $a$ 's,  $b$ 's,  $c$ 's,  $j_{ij}$ 's and  $k_{ij}$ 's are given in Appendix B. The excess volume is now calculated using the equation of state and

$$V_E = \tilde{V}_m - \sum_i \tilde{V}_i x_i \quad (18)$$

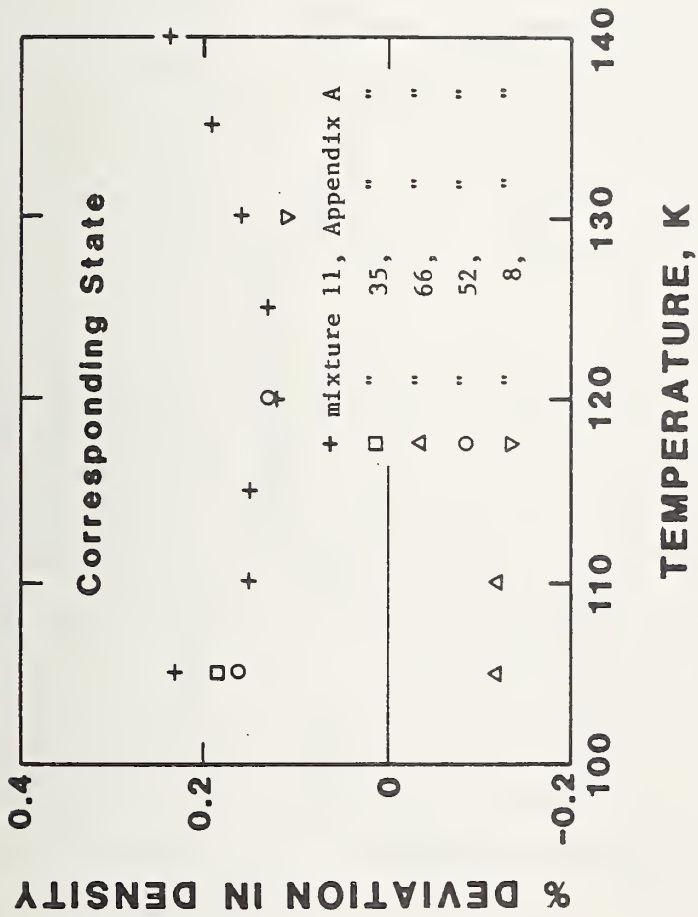
where  $\tilde{V}_m$  and the  $\tilde{V}_i$  are calculated via the eqs 11 through 17 and then

$$V_m = \sum_i V_i x_i + V_E \quad (19)$$

where the  $V_E$  is from eq (18) and the  $V_i$  are from experimental data. The values of  $V_i$  in this case were calculated from the equations for the liquid density of the pure fluids given in Appendix C.

The above equations are those of Rodosevich and Miller [33] and Rodosevich [34] and only the  $j_{ij}$ 's and  $k_{ij}$ 's have been revised on the basis of the present new data set, and only binary systems data were used to estimate via least squares the  $j_{ij}$ 's and  $k_{ij}$ 's.

As the method is used here it is an excess volume method, and consequently when the temperature of the mixture approaches the critical temperature of one of the component fluids, the method fails. Since the critical temperature of nitrogen is about 126 K, this method should not be used for mixtures containing nitrogen at temperatures above 120 K. Eliminating the data points for mixtures which contain nitrogen at temperatures above 120 K reduces the set from 285 to 251 PVTx points. Figure 2 is a percentage deviation plot containing all of the data points from the set of 251 for which densities calculated by the hard sphere method differ from the experimental density by more than 0.1%. Two things are readily seen in comparing figs. 1 and 2; first, even though total number of points has been reduced in the comparison set, the number of points for which deviations exceed 0.1% in the hard sphere comparison, fig. 2, is far more than for the extended corresponding states comparison, fig. 1. Second, the hard sphere method becomes more uncertain for all mixtures, regardless of components as the temperature exceeds 115 K.



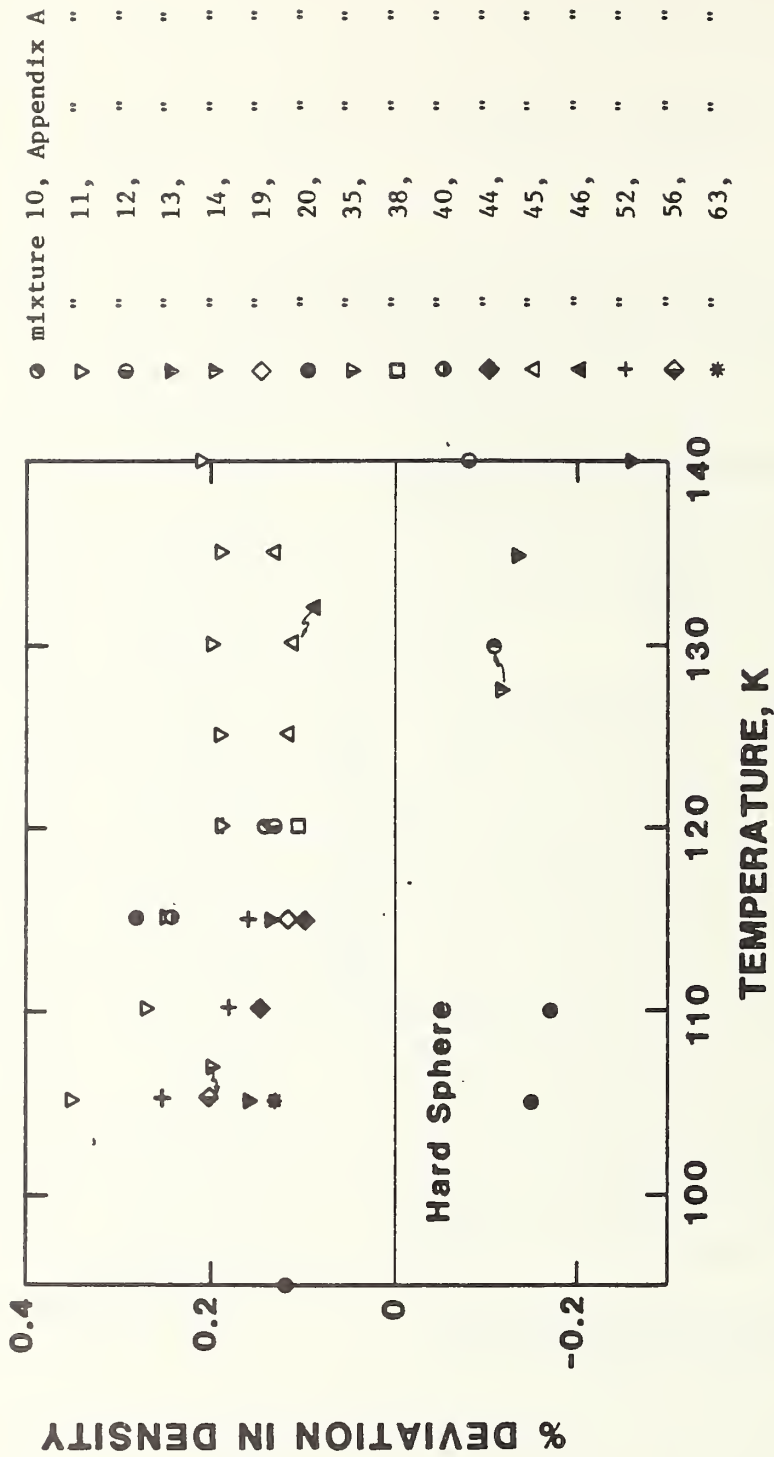


Figure 2. Deviations greater than 0.1% between experimental and calculated densities using the Hard Sphere model. The comparison set is all of the data in Appendix A except those data points for mixtures containing N<sub>2</sub> at temperatures above and including 120 K. (251 data points)

#### 4. A REVISED KLOSEK AND MCKINLEY METHOD

The Klosek and McKinley method [18] is a totally empirical recipe for calculating the density of a LNG-like mixture given the temperature and composition. Pressure is not taken into account. However, this does not seem to be a serious omission. The procedure proposed by Klosek and McKinley [18] is as follows:

$$V_{mix} = \sum X_i V_i - k X_{CH_4} \quad (20)$$

where  $V_{mix}$  is the volume of the mixture,  $X_i$  and  $V_i$  are the mole fraction and volume of the  $i^{th}$  component,  $X_{CH_4}$  is the mole fraction of methane and  $k$  is a correction factor obtained from a table or graph. The  $V_i$  and  $k$  are obviously temperature dependent and in addition  $k$  is dependent upon the molecular weight of the mixture.

Using the present data set  $k$  was calculated for all of the experimental data points where methane was present in the mixture and excluding all data points where  $N_2$  was present in greater than 5% concentration. Figure 3 shows a typical isotherm for  $k$ , with  $N_2$  present (labeled  $k_2$ ) and without  $N_2$  present (labeled  $k_1$ ). All of the isotherms available show similar behavior, i.e., all of the  $k$ 's for mixtures containing nitrogen (of about 5%) fall on one line and all of those for mixtures without nitrogen fall on another. Since all of the mixtures with nitrogen have about the same amount of nitrogen present (about 4.5%), the method was modified by adding a term to take into account the nitrogen when it is present. The equation becomes

$$V_{mix} = \sum X_i V_i - [k_1 + (k_2 - k_1) X_{N_2} / .0425] X_{CH_4} \quad (21)$$

where everything is the same as in eq (20) except that  $k_1$  is read from one

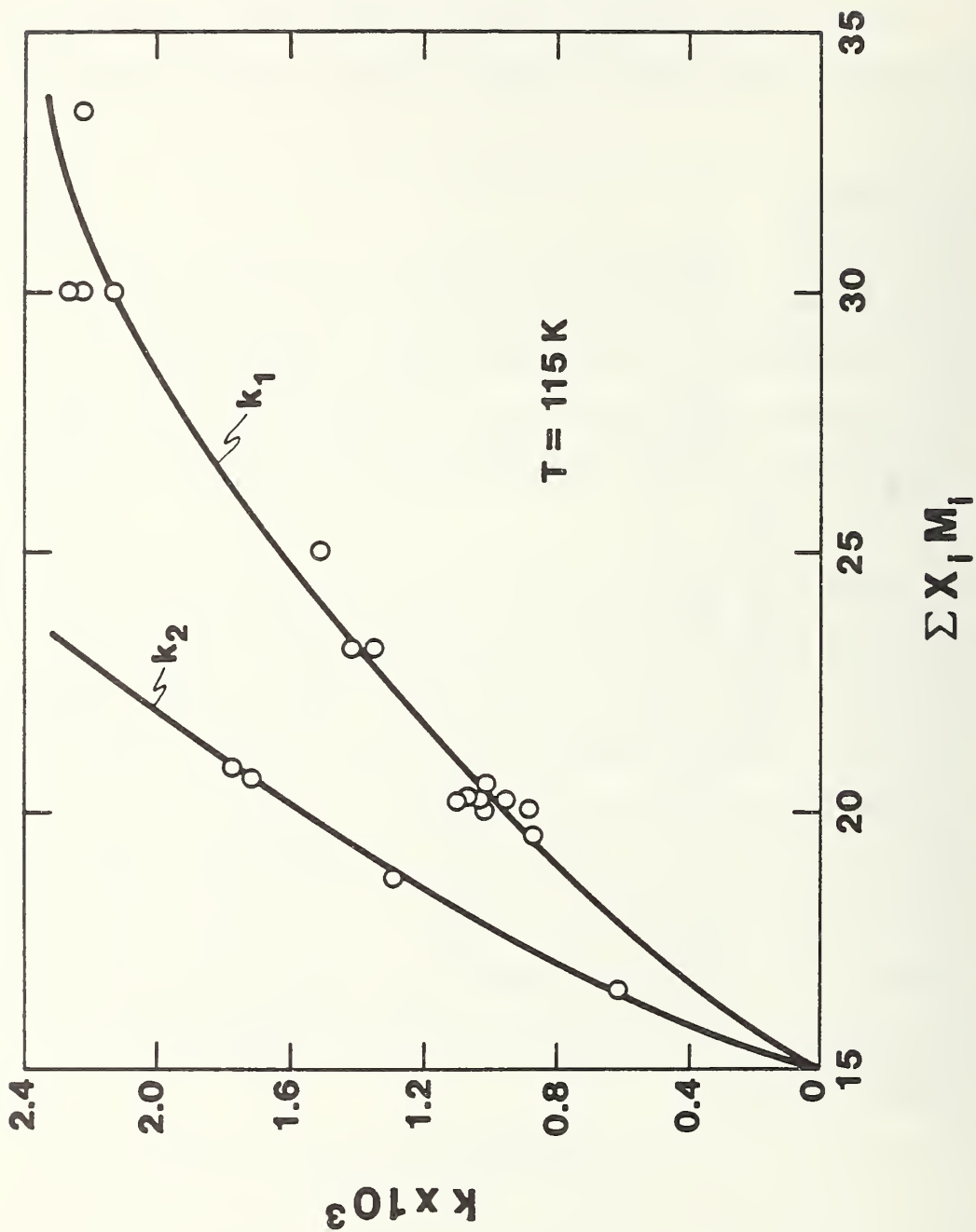


Figure 3. A plot of the correction factors ( $k_1$  and  $k_2$ ) for the 115 kelvin isotherms.

curve and  $k_2$  is read from the other. Appendix D gives tables of values for the  $V_i$ ,  $k_1$  and  $k_2$  which are spaced such that linear interpolation is adequate in both variables (i.e., temperature or molecular weight). The  $k$  factors in Appendix D have been obtained graphically from the multicomponent PVTx data of Hiza and Haynes [15] and Miller and Hiza [25] as well as densities calculated from the extended corresponding states method of section 2.

The limits of compositions of the revised Klosek and McKinley method are the most severe of any of the methods given here. This method should not be used for mixtures other than LNG like mixtures and for LNG like mixtures only when they contain at least 60% methane, less than 4% nitrogen, less than 4% each of  $iC_4H_{10}$   $nC_4H_{10}$  and less than 2% total of  $iC_5H_{12}$  and  $nC_5H_{12}$ .

There are 40 experimental PVTx points from the original set of 285 which may be considered LNG like and fall within the composition limits outlined above. Figure 4 shows all of the deviations between calculated and experimental densities in this 40 point comparison set which exceeds the 0.1% criterion. The deviation trends for the revised Klosek and McKinley method (fig. 4) are very similar to those of the hard sphere method (fig. 2) and in fact all of the deviations in fig. 4 occur at temperatures at or above 115 K, therefore the method can only be considered as accurate as the others for LNG like mixtures at temperatures below 115 K.

## 5. THE CELL MODEL

The cell model considered here was originally proposed by Renon, et al. [32]. In a paper by the same three authors which appeared simultaneously (Eckert, et al. [7]), the cell model was applied to mixtures via Scott's [36] two-fluid theory and a three parameter corresponding states theory. Albright [2] further modified the method by modifying the mixing rules on the basis of a

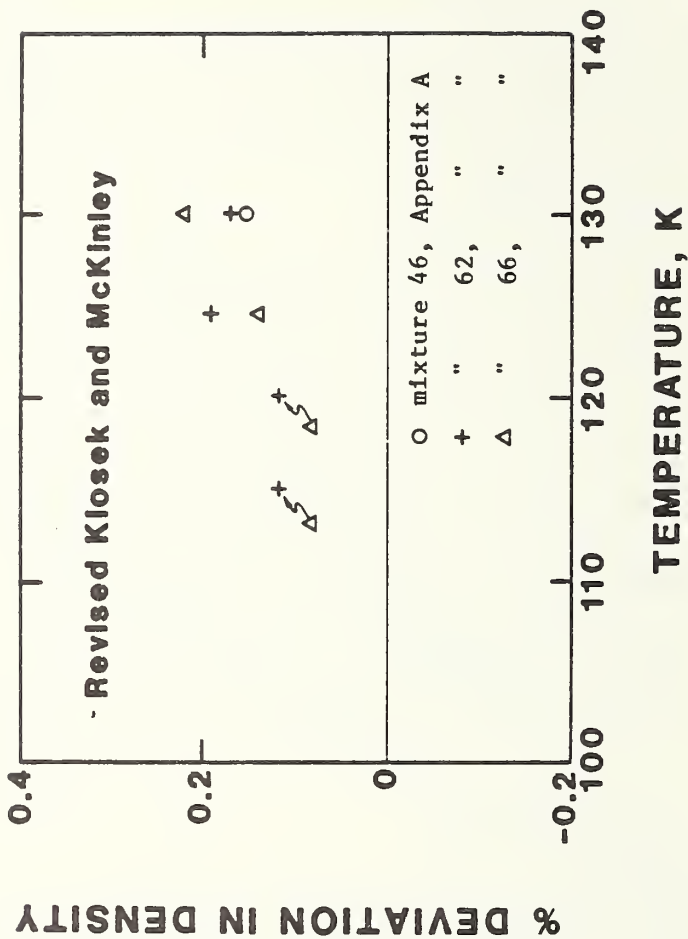


Figure 4. All deviations greater than 0.1% between experimental and calculated densities using the Revised Klosek and McKinley model. The comparison set is all multicomponent mixture data in Appendix A with > 60% CH<sub>4</sub>, < 4% nC<sub>4</sub>H<sub>10</sub>, < 4% iC<sub>4</sub>H<sub>10</sub>, < 4% N<sub>2</sub> and < 2% of n + iC<sub>5</sub>H<sub>12</sub>. (40 data points)

proposal by Yuan [38] and by inserting a pressure dependence based on the experimental liquid ethane data by Pope [31].

The optimization of this method was carried out by M. Albright [1] at Phillips Petroleum Company in Bartlesville, Oklahoma and the details of this work will be published elsewhere. The model is included here because it was optimized to the same data set as the others and therefore the comparisons between experimental and calculated densities given here in fig. 5 together with figs. 1, 2 and 4 provide a common basis of comparison with the other three methods. A listing of the computer program is given in Appendix F.

The same data set as was used in the hard sphere method for comparison has been used here, i.e., all of the data points for mixtures containing nitrogen at temperatures 120 K and above have been taken out of the original 285 points leaving a total of 251 data points.

As in the case of the other methods fig. 5 shows all of the points for which the calculated and experimental densities differ by more than 0.1%.

## 6. USE OF THE METHODS

When the project started in 1972, the atomic weights of nitrogen, carbon and hydrogen were taken from the 1961 carbon 12 scale, IUPAC [16]. During the course of the investigation a revision, Atomic Weights of the Elements [3], to this scale appeared. The revision changed slightly the atomic weights of carbon and hydrogen, but since the changes were small (the maximum difference in any of the densities used here is 0.003%), and because changing the atomic weights would not change the relative results, the changes were not made. Therefore when using the tables and programs in the appendices, the molecular weights given in the tables and programs should be used to maintain consistency.

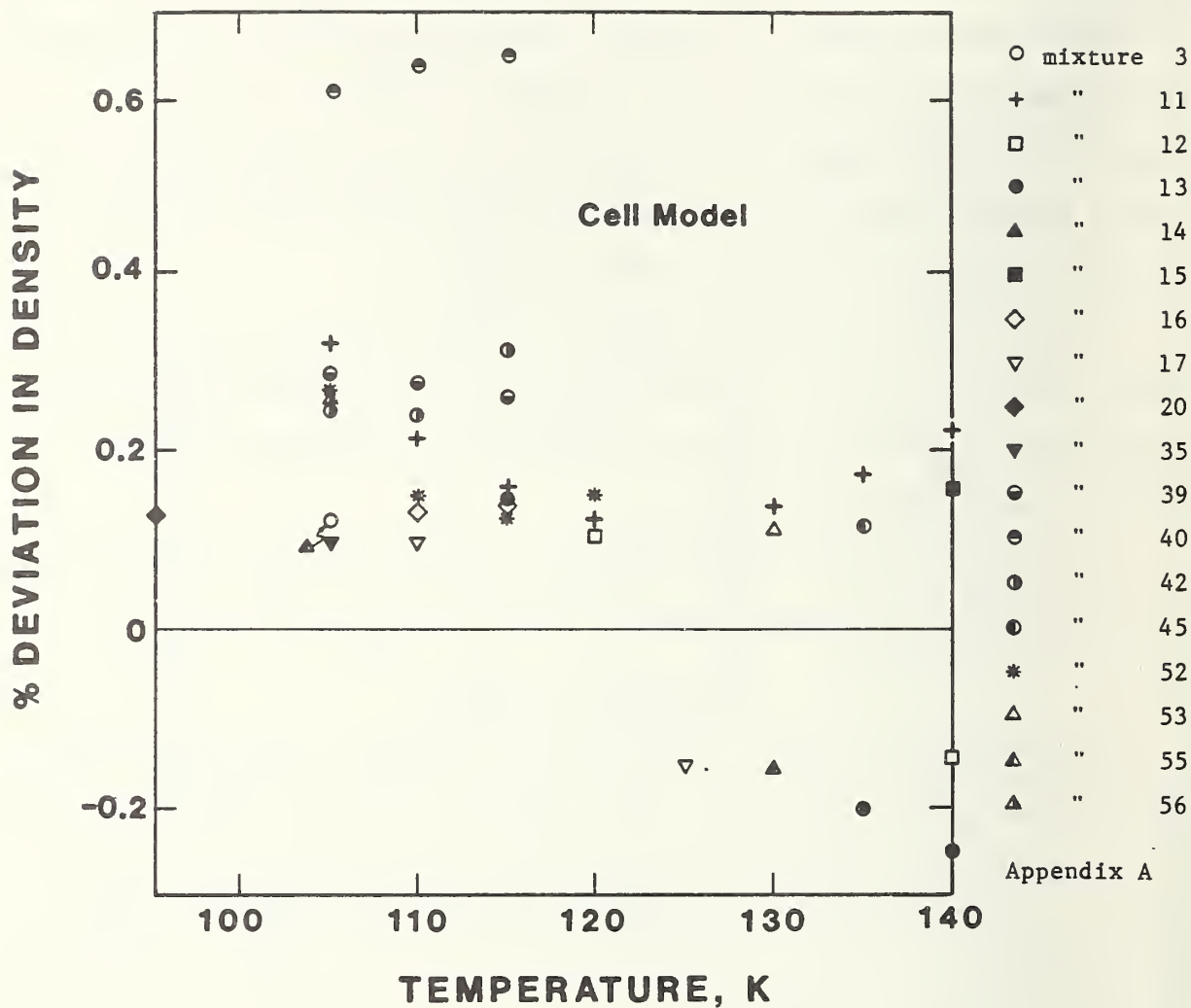


Figure 5. Deviations greater than 0.1% between experimental and calculated densities using the Cell model. The comparison set is all of the data in Appendix A except those data points for mixtures containing N<sub>2</sub> at temperatures above and including 120 K. (251 data points)

The critical parameters used here are from:  $\text{CH}_4$ , McCarty [22];  $\text{C}_2\text{H}_6$ , Sliwinski [37];  $\text{C}_3\text{H}_8$ , Das, et al. [4];  $i\text{C}_4\text{H}_{10}$ , Das, et al. [5];  $n\text{C}_4\text{H}_{10}$ , Das, et al. [6];  $i\text{C}_5\text{H}_{12}$ , Kudchadker, et al. [19]; and  $\text{N}_2$ , Jacobsen, et al. [17].

Errors in the input variables will of course, cause errors in the density predicted by the models. In general, the error in density caused by an error in the input variables is a function of those input variables, and must be treated on an individual basis. However, for LNG like mixtures certain general trends are found. An error in the pressure must be at least 50% before it will have any effect at all on the resulting density. An error in composition, unless it is of the order of several percent, will cause the same relative error in density as it will cause in the molecular weight of the mixture, i.e., if an error in composition causes a 0.1% error in the resulting molecular weight, it will also cause a 0.1% error in the predicted density.

The error in the calculated density due to an error in the input temperature is a function of the composition and the temperature. Table 1 gives resulting errors in density for a 1% error in temperature, for three hypothetical LNG like mixtures.

In general the errors in density caused by an error in temperature are the largest for mixtures containing a high concentration of the most volatile fluids,  $\text{CH}_4$  and  $\text{N}_2$ , and correspondingly the errors decrease as the concentration of the heavier hydrocarbons increases in the mixture. These errors are not a function of which model is being used.

When using the extended corresponding states method, one should keep in mind that twelve significant figures are required by the methane equation of state. The hard sphere model also uses the methane equation from McCarty [22] and the nitrogen equation of Jacobsen, et al. [17] to calculate compressibilities and

TABLE 1. Errors in Density Caused by an Error in the Input Temperature of 1%.

Temperature K	% Error in Density		
	Mix A <sup>*</sup>	Mix B <sup>*</sup>	Mix C <sup>*</sup>
95	0.28	0.25	0.20
100	0.30	0.27	0.22
105	0.32	0.29	0.24
110	0.35	0.32	0.29
115	0.39	0.34	0.31

Mix A<sup>\*</sup> = 0.95 CH<sub>4</sub>, 0.05 N<sub>2</sub>

Mix B<sup>\*</sup> = 0.9 CH<sub>4</sub>, 0.02 C<sub>2</sub>H<sub>6</sub>, 0.02 C<sub>3</sub>H<sub>8</sub>, 0.02 iC<sub>4</sub>H<sub>10</sub>, 0.02 nC<sub>4</sub>H<sub>10</sub>, 0.02 N<sub>2</sub>

Mix C<sup>\*</sup> = 0.6 CH<sub>4</sub>, 0.3 C<sub>2</sub>H<sub>6</sub>, 0.02 C<sub>3</sub>H<sub>8</sub>, 0.02 iC<sub>4</sub>H<sub>10</sub>, 0.02 nC<sub>4</sub>H<sub>10</sub>, 0.02 N<sub>2</sub>,  
0.02 iC<sub>5</sub>H<sub>12</sub>.

\*Arbitrary LNG like compositions assumed for the purpose of illustrating the effect of an error in the input temperature.

therefore requires twelve significant figures to insure the accuracy of the calculated density. The other two models require only eight significant figures to be carried along in the calculations.

## 7. CONCLUSIONS

On the basis of the performance of the four models given here and subject to the composition and temperature restrictions already noted, it is estimated that given the pressure, temperature and composition of LNG, any one of the four models may be used to predict the density to within 0.1% of the true value. As has already been mentioned (see section 1) the above accuracy statement is dependent entirely upon the accuracy of the experimental data in Haynes, et al. [11], Haynes, et al. [13], Hiza, et al. [14], Haynes [9], Hiza and Haynes [15], Miller and Hiza [25] and Haynes [10]. These data have been estimated by the authors to be accurate to within 0.1% of the true value with a precision of a few hundredths of a percent. The work on the models given here have provided no basis for questioning the claims of the experimenters, in fact the ability of the models to predict the densities of the multicomponent mixtures to within 0.1% of the measured values tends to support the accuracy claims of the experimenters.

Interim results of this study were reported by Haynes, et al. [13] and McCarty [23], both of which contain earlier versions of the mathematical models given here. These earlier versions are only slightly different than the final ones and for the purposes of calculating LNG densities either of the versions may be used. The reader is, however, cautioned to read the limitations of each model as defined in the earlier sections.

Computer programs for the four models are available at the Thermophysical Properties Division of the National Bureau of Standards in Boulder, Colorado.

## 8. REFERENCES

- [1] Albright, M. A., Private communication (1976).
- [2] Albright, M. A., A Model for the Precise Calculation of Liquefied Natural Gas Densities, NGPA Technical Publication TP-3 (1973).
- [3] Atomic Weights of the Elements 1973, Pure and Applied Chemistry, Vol 37, 589-603 (1974).
- [4] Das, T. R., Eubank, P. T., Advances in Cryogenic Engineering Vol 18, Plenum Press, New York (1973), p. 208.
- [5] Das, T. R., Eubank, P. T., Advances in Cryogenic Engineering Vol 18, Plenum Press, New York (1973), p. 253.
- [6] Das, T. R., Eubank, P. T., Advances in Cryogenic Engineering Vol 18, Plenum Press, New York (1973), p. 244.
- [7] Eckert, C. A., Renon, H. and Prausnitz, J. M., Molecular Thermodynamics of Simple Liquids, IEC Fund 6, 58 (1967).
- [8] Goodwin, R. D., The Thermophysical Properties of Methane, from 90 to 500 K at Pressures up to 700 Bars, Nat. Bur. Stand. (U.S.), Tech. Note 653 (1974).
- [9] Haynes, W. M., Orthobaric Liquid Densities of Methane + Isobutane and Methane + Normal Butane Mixtures at Low Temperatures (to be published).
- [10] Haynes, W. M., Measurements of Orthobaric Liquid Densities of Multicomponent Mixtures of LNG Components ( $N_2$ ,  $CH_4$ ,  $C_2H_6$ ,  $C_3H_8$ ,  $iC_4H_{10}$ ,  $nC_4H_{10}$ ,  $iC_5H_{12}$ ,  $nC_5H_{12}$ ) Between 110 and 130 K, to be published.
- [11] Haynes, W. M., Hiza, M. J. and Frederick, N. V., A Magnetic Suspension Densimeter for Measurements on Fluids of Cryogenic Interest, Review of Scientific Instruments 47, No. 10, 1237-50 (Oct 1976).
- [12] Haynes, W. M. and Hiza, M. J., Measurements of the Orthobaric Liquid Densities of Methane, Ethane, Propane, Isobutane, and Normal Butane, J. Chem. Thermodyn., 9, 179 (1977).

- [13] Haynes, W. M., Hiza, M. J. and McCarty, R. D., Densities of LNG for Custody Transfer, (Proc. Fifth International Conference of LNG, Dusseldorf, Germany), J. W. White, W. McGrew, S. Farmer, D. Hansen, H. Jacobshagen, editors; Institute of Gas Technology, Chicago, Ill., Vol. 2, Paper II, Section III (1977).
- [14] Hiza, M. J., Haynes, W. M. and Parrish, W. R., Orthobaric Liquid Densities and Excess Volumes for Binary Mixtures of Low Molecular Weight Alkanes and Nitrogen Between 105 and 140 K, *J. Chem. Thermodyn.* 9, 873 (1977).
- [15] Hiza, M. J. and Haynes, W. M., Orthobaric Liquid Densities and Excess Volumes for Multicomponent Mixtures of Low Molar Mass Alkanes and Nitrogen Between 105 and 125 K, *J. Chem. Thermodyn.* 12, 1 (1980).
- [16] International Union of Pure and Applied Chemistry, 1961 Carbon 12 Scale.
- [17] Jacobsen, R. T., Stewart, R. B., McCarty, R. D. and Hanley, H. J. M., Thermophysical Properties of Nitrogen from the Fusion Line to 3500 R (1944 K) for Pressures to 150,000 psia ( $10342 \times 10^5 \text{ N/m}^2$ ), Nat. Bur. Stand. (U.S.), Technical Note No. 648 (Dec 1973).
- [18] Klosek, J. and McKinley, C., Densities of Liquefied Natural Gas and of Low Molecular Weight Hydrocarbons, Proc. First Int. Conf. on LNG, IGT, Chicago (1968).
- [19] Kudchadker, A. P., Alani, G. H. and Zwolinski, B. J., The Critical Constants of Organic Substances, *Chem. Rev.* 68, 659-735 (1968).
- [20] Leach, J. W., Molecular Structure Correction for Applying the Theory of Corresponding States to Non-Spherical Pure Fluids and Mixtures, Ph.D. Thesis, Rice University (1967).
- [21] Longuet-Higgins, H. C. and Widom, B., A Rigid Sphere Model for Melting of Argon, *Mol. Phys.* 8, 549 (1964).

- [22] McCarty, R. D., A Modified Benedict-Webb-Rubin Equation of State for Methane Using Recent Experimental Data, *Cryogenics* 14, No. 5, 276-80 (May 1974).
- [23] McCarty, R. D., A Comparison of Mathematical Models for the Prediction of LNG Densities, Nat. Bur. Stand. (U.S.), Interagency Report NBSIR 77-867 (Oct 1977).
- [24] McCarty, R. D., Optimization and Comparisons of Mathematical Models for the Prediction of Liquefied Natural Gas Densities, *J. Chem. Thermodyn.* (to be published, 1980).
- [25] Miller, R. C. and Hiza, M. J., Experimental Molar Volumes for Some LNG Related Saturated Liquid Mixtures, *Fluid Phase Equilibria* 2, 49-57 (1978).
- [26] Mollerup, J. and Rowlinson, J. S., The Prediction of Densities of Liquefied Natural Gas and of Lower Molecular Weight Hydrocarbons, *Chem. Engng. Sci.* 29 (1973).
- [27] Mollerup, J., Correlated and Predicted Thermodynamic Properties of LNG and Related Mixtures in the Normal and Critical Region, *Adv. Cryog. Eng.* 20, 172 (K. D. Timmerhaus, editor, Plenum Press, New York, 1975).
- [28] Mollerup, J., Thermodynamic Properties of Natural Gas, Petroleum Gas, and Related Mixtures Enthalpy Predictions, *Adv. Cryog. Eng.* 23, 550 (K. D. Timmerhaus, editor, Plenum Press, New York, 1978).
- [29] Orrit, J. and Olives, J. F., Density of Liquefied Natural Gas and Its Components, Distributed at the 4th International Conference on Liquefied Natural Gas, Algeria (1974).
- [30] Orrit, J. E. and Laupretre, T. M., Density of Liquefied Natural Gas Components, *Adv. Cryog. Eng.* 23, 573 (K. D. Timmerhaus, editor, Plenum Press, New York, 1978).

- [31] Pope, G. A., Calculation of Argon, Methane and Ethane Virial Coefficients at Low Reduced Temperature, Ph.D. Thesis, Rice University (1971).
- [32] Renon, H., Eckert, C. A. and Prausnitz, J. M., Molecular Thermodynamics of Simple Liquids, IEC Fund. 6, 52 (1967).
- [33] Rodosevich, J. B. and Miller, R. C., Calculation of LNG Excess Volumes by a Modified Hard-Sphere Model, Adv. Cryog. Eng. 19, 339 (1974).
- [34] Rodosevich, J. B., Measurements and Prediction of Liquefied Natural Gas Densities, M.Sc. Thesis, Univ. Wyoming (1973).
- [35] Rowlinson, J. S. and Watson, I. D., The Prediction of the Thermodynamic Properties of Fluids and Fluid Mixtures - I. The Principle of Corresponding States and Its Extensions, Chem. Engng. Sci. 24, 1565 (1969).
- [36] Scott, R. L., J. Chem. Phys. 25, 193 (1956).
- [37] Sliwinski, P. Z., Die Lorentz-Lorenz Funktion Von Dampfformigem und Fluessiyem Athan, Propan and Butan, Phys. Chem. (Frankfurt) 63, 263 (1969).
- [38] Yuan, I. C., Correlation and Prediction of Excess Properties for Selected Binaries in the C<sub>6</sub>-C<sub>7</sub> Hydrocarbon Boiling Range of Conformal Solution Theory, D.Sc. Dissertation, Washington University (1971).

## Appendix A. Experimental Data

The following is a list of all of the experimental PVTx mixtures data which were measured during the course of this project. The data are from Miller and Hiza [25]; Haynes and Hiza [12]; Haynes, et al. [11]; Hiza, et al. [14]; Hiza and Haynes [15] and Haynes [9,10).

All of the data are for the orthobaric liquid except for the data of Miller and Hiza [25] which are for the single phase liquid phase, very close to the orthobaric conditions. The units of the data are bars, moles per liter and kelvin. The columns labeled RKM, HS, CELL and CS correspond to percentage derivations between experimental and predicted densities by the Revised Klosek and McKinley, hard sphere, cell and extended corresponding states models respectively. The derivations are always calculated using experimental-calculated densities.

MIXTURE NO 1 (Miller and Hiza [25])

0.85147 CH<sub>4</sub> + 0.14853 C<sub>2</sub>H<sub>6</sub>

P	D	T	MM	RKM	HS	CELL	CS
.977	25.7499	110.08	18.1265	.13	- .02	.02	.01

MIXTURE NO 2 (Hiza, et al. [14])

0.68006 CH<sub>4</sub> + 0.31994 C<sub>2</sub>H<sub>6</sub>

.416	25.1027	105.00	20.5309	.14	.05	.10	.07
.645	24.7802	110.00	20.5309	.07	- .01	.02	.01
.961	24.4612	115.00	20.5309	.05	- .04	-.03	-.03
1.380	24.1402	120.00	20.5309	.06	- .06	-.06	-.05
1.930	23.8212	125.00	20.5309	.08	- .05	-.04	-.05
2.620	23.5007	130.00	20.5309	.12	- .01	.00	-.02

MIXTURE NO 3 (Hiza, et al. [14])

0.49325 CH<sub>4</sub> + 0.50675 C<sub>2</sub>H<sub>6</sub>

.325	23.9619	105.00	23.1513	.14	.07	.11	.07
.503	23.6937	110.00	23.1513	.09	.03	.03	.03
.749	23.4328	115.00	23.1513	.11	.03	.01	.03
1.080	23.1559	120.00	23.1513	.07	- .02	-.06	-.03
1.500	22.8933	125.00	23.1513	.08	.00	-.05	.00
2.050	22.6290	130.00	23.1513	.14	.04	-.02	.03
2.720	22.3581	135.00	23.1513	.19	.06	.01	.05
3.550	22.0765	140.00	23.1513	.25	.05	.02	.04

MIXTURE NO 4 (Hiza, et al. [14])

0.35457 CH<sub>4</sub> + 0.64543 C<sub>2</sub>H<sub>6</sub>

.256	23.1033	105.00	25.0965	- .04	- .07	-.04	-.07
.397	22.8777	110.00	25.0965	- .01	- .04	-.05	-.05
.580	22.6478	115.00	25.0965	.03	- .02	-.06	-.03
.826	22.4035	120.00	25.0965	.00	- .06	-.11	-.07
1.146	22.1872	125.00	25.0965	.10	.04	-.03	.03
1.550	21.9441	130.00	25.0965	.10	.03	-.04	.02

## MIXTURE NO 5 (Hiza, et al. [14])

0.85796 CH<sub>4</sub> + 0.14204 C<sub>3</sub>H<sub>8</sub>

P	D	T	MW	RKM	HS	CELL	CS
.517	24.9622	105.00	20.0279	.01	.10	.10	.07
.817	24.6332	110.00	20.0279	- .02	.08	.07	.06
1.199	24.2942	115.00	20.0279	- .04	.04	.03	.03
1.785	23.9492	120.00	20.0279	- .07	.00	.00	.00
2.415	23.5942	125.00	20.0279	- .09	- .06	-.04	-.05
3.290	23.2461	130.00	20.0279	- .11	- .06	-.01	-.04

## MIXTURE NO 6 (Hiza, et al. [14])

0.74920 CH<sub>4</sub> + 0.25080 C<sub>3</sub>H<sub>8</sub>

.478	23.4767	105.00	23.0790	.01	.02	.03	-.02
.738	23.2064	110.00	23.0790	- .03	.00	-.01	-.03
1.099	22.9364	115.00	23.0790	- .01	.00	-.02	-.02
1.582	22.6665	120.00	23.0790	.02	.01	-.01	.01
2.216	22.3818	125.00	23.0790	- .03	- .04	-.04	-.01
3.029	22.1019	130.00	23.0790	.02	- .05	-.02	.01

## MIXTURE NO 7 (Hiza, et al. [14])

0.49637 CH<sub>4</sub> + 0.50363 C<sub>3</sub>H<sub>8</sub>

.384	20.4909	105.00	30.1720	- .05	.01	.04	-.03
.591	20.3046	110.00	30.1720	- .08	.01	.01	-.02
.874	20.1180	115.00	30.1720	- .06	.01	-.02	-.02
1.250	19.9311	120.00	30.1720	.00	.01	-.03	.00
1.730	19.7471	125.00	30.1720	.04	.03	-.01	.04
2.320	19.5546	130.00	30.1720	- .01	.01	-.03	.05

## MIXTURE NO 8 (Hiza, et al. [14])

0.29538 CH<sub>4</sub> + 0.70462 C<sub>3</sub>H<sub>8</sub>

.271	18.5132	105.00	35.8106	- .19	- .08	-.05	-.12
.409	18.3624	110.00	35.8106	- .24	- .09	-.10	-.12

## MIXTURE NO 9 (Haynes [10])

0.92788 CH <sub>4</sub> + 0.07212 nC <sub>4</sub> H <sub>10</sub>							
P	D	T	MW	RKM	HS	CELL	CS
1.820	24.2615	120.00	19.0779	.00	.04	-.04	-.04
2.547	23.8868	125.00	19.0779	.00	.00	-.07	-.05
3.470	23.5047	130.00	19.0779	-.01	-.03	-.09	-.07
4.616	23.1225	135.00	19.0779	.04	-.03	-.06	-.05
6.023	22.7284	140.00	19.0779	.16	-.04	-.03	-.03

## MIXTURE NO 10 (Haynes [10])

0.92780 CH <sub>4</sub> + 0.07220 nC <sub>4</sub> H <sub>10</sub>							
P	D	T	MW	RKM	HS	CELL	CS
1.270	24.6285	115.00	19.0813	.01	.08	.01	-.01
1.824	24.2783	120.00	19.0813	.07	.11	.03	.04
2.549	23.8999	125.00	19.0813	.06	.07	-.01	.01

## MIXTURE NO 11 (Hiza, et al. [14])

0.91674 CH <sub>4</sub> + 0.08326 nC <sub>4</sub> H <sub>10</sub>							
P	D	T	MW	RKM	HS	CELL	CS
.521	25.1536	105.00	19.5467	.21	.35	.33	.22
.810	24.7960	110.00	19.5467	.12	.26	.21	.15
1.216	24.4512	115.00	19.5467	.14	.24	.18	.15
1.753	24.0889	120.00	19.5467	.10	.19	.11	.11
2.472	23.7370	125.00	19.5467	.15	.18	.10	.13
3.374	23.3789	130.00	19.5467	.17	.19	.12	.16
4.509	23.0110	135.00	19.5467	.21	.19	.15	.18
5.887	22.6391	140.00	19.5467	.35	.20	.22	.23

## MIXTURE NO 12 (Haynes [10])

0.77982 CH <sub>4</sub> + 0.22018 nC <sub>4</sub> H <sub>10</sub>							
P	D	T	MW	RKM	HS	CELL	CS
1.702	21.6066	120.00	25.3805	.12	.14	.11	.06
2.369	21.3549	125.00	25.3805	.11	.08	.02	.04
3.228	21.1020	130.00	25.3805	.09	.00	-.07	.03
4.291	20.8555	135.00	25.3805	.12	-.03	-.10	.07
5.576	20.5978	140.00	25.3805	.20	-.13	-.15	.07

MIXTURE NO 13 (Haynes [10])

0.77762 CH<sub>4</sub> + 0.22238 nC<sub>4</sub>H<sub>10</sub>

P	D	L	T	MW	RKM	HS	CEL	CS
1.179	21.8054	115.00	25.4011	.07	.15	.16	.02	.02
1.699	21.5601	120.00	25.4011	.07	.10	.07	.02	.02
2.372	21.3164	125.00	25.4011	.10	.06	.01	.03	.03
3.230	21.0605	130.00	25.4011	.06	-.03	-.10	.00	.00
4.291	20.8011	135.00	25.4011	.02	-.14	-.20	-.03	-.03
5.579	20.5448	140.00	25.4011	.09	-.23	-.26	-.03	-.03

MIXTURE NO 14 (Hiza, et al. [14])

0.58828 CH<sub>4</sub> + 0.41172 nC<sub>4</sub>H<sub>10</sub>

3.183	18.3058	130.00	33.3687	-.32	-.11	-.15	-.08	-.08
2.342	18.4853	125.00	33.3687	-.17	.00	.00	-.03	-.03
2.281	18.4772	125.00	33.3687	-.21	-.05	-.04	-.08	-.08
1.636	18.6495	120.00	33.3687	-.18	.02	.07	-.06	-.06

MIXTURE NO 15 (Haynes [10])

0.92044 CH<sub>4</sub> + 0.07956 iC<sub>4</sub>H<sub>10</sub>

1.254	24.3633	115.00	19.3910	-.21	.05	.06	-.01	-.01
1.805	24.0029	120.00	19.3910	-.24	.02	.03	-.03	-.03
2.521	23.6403	125.00	19.3910	-.22	.01	.04	-.03	-.03
3.434	23.2752	130.00	19.3910	-.21	.03	.08	.00	.00
4.567	22.8920	135.00	19.3910	-.22	.00	.09	-.02	-.02
5.950	22.5037	140.00	19.3910	-.14	-.02	.14	-.02	-.02

MIXTURE NO 16 (Haynes [10])

0.78329 CH<sub>4</sub> + 0.21671 iC<sub>4</sub>H<sub>10</sub>

.782	21.9144	110.00	25.1625	-.33	.10	.15	.01	.01
1.164	21.6652	115.00	25.1625	-.33	.05	.07	-.01	-.01
1.671	21.4136	120.00	25.1625	-.35	.01	.00	-.02	-.02
2.329	21.1668	125.00	25.1625	-.34	.00	-.03	.00	.00
3.170	20.9125	130.00	25.1625	-.35	-.04	-.07	.00	.00
4.208	20.6629	135.00	25.1625	-.33	-.06	-.06	.04	.04
5.474	20.4082	140.00	25.1625	-.23	-.09	-.04	.07	.07

## MIXTURE NO 17 (Hiza, et al. [14])

0.48687 CH<sub>4</sub> + 0.51313 iC<sub>4</sub>H<sub>10</sub>

P	D	T	MW	RKM	HS	CELL	CS
.629	17.3575	110.00	37.6362	- .62	.05	.11	.02
.938	17.2076	115.00	37.6362	- .70	.00	-.01	-.02
1.361	17.0639	120.00	37.6362	- .64	-.02	-.08	-.02
1.852	16.9156	125.00	37.6362	- .69	-.07	-.17	-.04

## MIXTURE NO 18 (Hiza, et al. [14])

0.95248 CH<sub>4</sub> + 0.04752 N<sub>2</sub>

1.380	26.8476	105.00	16.6119	- .05	-.04	-.04	-.02
1.990	26.4052	110.00	16.6119	.06	.00	.00	.04
2.634	25.9374	115.00	16.6119	.20	.01	.02	.06
3.500	25.4522	120.00	16.6119	.26	*	.03	.07
4.600	24.9496	125.00	16.6119	.54	*	.04	.07
5.830	24.4210	130.00	16.6119	.69	-5.69	.03	.05
7.300	23.8600	135.00	16.6119	.77	-3.99	-.01	-.03
9.200	23.2809	140.00	16.6119	1.09	-2.69	-.02	-.07

## MIXTURE NO 19 (Hiza, et al. [14])

0.69651 CH<sub>4</sub> + 0.30349 N<sub>2</sub>

3.450	26.8735	100.00	19.6759	- .39	.06	.09	.00
4.661	26.3393	105.00	19.6759	- .56	.02	.07	.04
6.181	25.7686	110.00	19.6759	- .92	-.05	-.02	.00
8.010	25.1790	115.00	19.6759	-1.28	.13	-.08	-.03
10.112	24.5737	120.00	19.6759	-1.56	1.88	-.07	-.04

## MIXTURE NO 20 (Hiza, et al. [14])

0.50758 CH<sub>4</sub> + 0.49242 N<sub>2</sub>

3.303	27.0801	95.00	21.9375	-2.16	.11	.14	.06
4.468	26.4588	100.00	21.9375	-1.92	-.01	.05	.04
6.383	25.8106	105.00	21.9375	-1.56	-.15	-.05	-.01
8.461	25.1387	110.00	21.9375	-1.29	-.17	-.09	-.03
10.740	24.4431	115.00	21.9375	1.12	.28	-.04	-.01
13.983	23.7096	120.00	21.9375	-1.79	3.41	.07	-.01
17.529	22.9315	125.00	21.9375	-1.14	*	.26	.00
21.076	22.1005	130.00	21.9375	-.72	-2.84	.05	.10

\* The hard sphere solution for the density of N<sub>2</sub> failed.

## MIXTURE NO 21 (Hiza, et al. [14])

0.67287 C <sub>2</sub> H <sub>6</sub> + 0.32713 C <sub>3</sub> H <sub>8</sub>		P	D	T	MW	RKM	HS	CELL	CS
			18.6192	125.00	34.6588	.00	.02	-.02	.00
			18.4648	130.00	34.6588	.00	.02	.00	.01
			18.3059	135.00	34.6588	.00	.00	.00	.00
			18.1509	140.00	34.6588	.00	.01	.04	.02

## MIXTURE NO 22 (Hiza, et al. [14])

0.50105 C <sub>2</sub> H <sub>6</sub> + 0.49895 C <sub>3</sub> H <sub>8</sub>		P	D	T	MW	RKM	HS	CELL	CS
			18.3618	105.00	37.0689		.02	.04	.02
			18.2169	110.00	37.0689		.01	.00	.00
			18.0726	115.00	37.0689		.00	-.03	-.01
			17.9282	120.00	37.0689		- .01	-.05	-.01
			17.7880	125.00	37.0689		.00	-.03	.00
			17.6412	130.00	37.0689		- .02	-.04	-.02
			17.4988	135.00	37.0689		- .01	-.01	-.01
			17.3526	140.00	37.0689		- .03	.00	-.01

## MIXTURE NO 23 (Hiza, et al. [14])

0.67117 C <sub>2</sub> H <sub>6</sub> + 0.32883 nC <sub>4</sub> H <sub>10</sub>		P	D	T	MW	RKM	HS	CELL	CS
			17.5047	110.00	39.2952		.00	.02	.00
			17.3706	115.00	39.2952		.01	.00	.00
			17.1031	125.00	39.2952		.02	.00	.02
			16.9626	130.00	39.2952		- .01	-.03	-.02
			16.8285	135.00	39.2952		.00	-.01	-.01
			16.6947	140.00	39.2952		.00	.03	.01

## MIXTURE NO 24 (Hiza, et al. [14])

0.65343 C <sub>2</sub> H <sub>6</sub> + 0.34657 nC <sub>4</sub> H <sub>10</sub>		P	D	T	MW	RKM	HS	CELL	CS
			17.2184	115.00	39.7929		.00	.00	.00
			17.0824	120.00	39.7929		- .02	-.03	-.02

## MIXTURE NO 25 (Hiza, et al. [14])

0.72436 C <sub>2</sub> H <sub>6</sub> + 0.27564 iC <sub>4</sub> H <sub>10</sub>		P	D	T	MW	RKM	HS	CELL	CS
			17.9779	105.00	37.8030		.01	.01	.01
			17.8401	110.00	37.8030		.01	.00	.01
			17.4235	125.00	37.8030		.01	.00	.01
			17.2825	130.00	37.8030		.00	.01	.01

## MIXTURE NO 26 (Hiza, et al. [14])

0.68939 C<sub>2</sub>H<sub>6</sub> + 0.31061 iC<sub>4</sub>H<sub>10</sub>

P	D	T	MW	RKM	HS	CELL	CS
	17.3716	115.00	38.7840		.00	-.03	.00
	17.2344	120.00	38.7840		-.02	-.04	-.02

## MIXTURE NO 27 (Hiza, et al. [14])

0.94067 C<sub>2</sub>H<sub>6</sub> + 0.05933 N<sub>2</sub>

3.850	21.4718	105.00	29.9481		-.02	-.01	-.03
4.630	21.2912	110.00	29.9481		.03	.02	.03
5.472	21.0845	115.00	29.9481		-.01	-.04	-.04
6.383	20.8998	120.00	29.9481		-.72	.01	.00

## MIXTURE NO 28 (Hiza, et al. [14])

0.60949 C<sub>3</sub>H<sub>8</sub> + 0.39051 nC<sub>4</sub>H<sub>10</sub>

	14.6487	115.00	49.5749		-.01	-.02	-.01
	14.5521	120.00	49.5749		.02	.00	.02

## MIXTURE NO 29 (Hiza, et al. [14])

0.60650 C<sub>3</sub>H<sub>8</sub> + 0.39350 nC<sub>4</sub>H<sub>10</sub>

	14.1343	140.00	49.6169		.00	-.03	.00
	14.0333	145.00	49.6169		.00	.00	.00
	13.9346	150.00	49.6169		.02	.05	.02

## MIXTURE NO 30 (Hiza, et al. [14])

0.58692 C<sub>3</sub>H<sub>8</sub> + 0.41308 nC<sub>4</sub>H<sub>10</sub>

	14.6839	110.00	49.8915		.01	.04	.01
	14.1748	135.00	49.8915		-.03	-.06	-.03
	14.0786	140.00	49.8915		.00	-.02	.00

## MIXTURE NO 31 (Hiza, et al., [14])

0.49030 C<sub>3</sub>H<sub>8</sub> + 0.50970 iC<sub>4</sub>H<sub>10</sub>

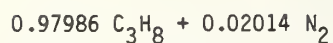
	14.3080	105.00	51.2468		-.01	-.04	-.01
	14.2136	110.00	51.2468		-.01	-.05	.00
	14.1219	115.00	51.2468		.02	-.03	.02
	14.0257	120.00	51.2468		.01	-.04	.01
	13.9300	125.00	51.2468		.00	-.04	.00
	13.8342	130.00	51.2468		-.01	-.04	-.01

## MIXTURE NO 32 (Hiza, et al. [14])



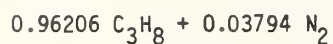
P	D	T	MW	RKM	HS	CELL	CS
	13.9718	125.00	51.0650		.01	-.03	.01
	13.8737	130.00	51.0650		-.01	-.04	-.01

## MIXTURE NO 33 (Hiza, et al. [14])



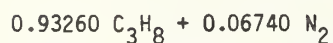
3.567	16.2131	110.00	43.7733		-.01	-.04	-.01
4.712	16.0931	115.00	43.7733		-.02	-.05	-.02

## MIXTURE NO 34 (Hiza, et al. [14])



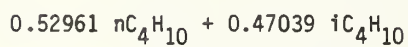
4.955	16.4638	105.00	43.4870		.02	-.03	.01
6.708	16.3410	110.00	43.4870		.00	-.04	.00

## MIXTURE NO 35 (Hiza, et al. [14])



8.795	16.7084	105.00	43.0132		.20	.11	.18
6.313	16.8055	100.00	43.0132		.04	-.07	.01

## MIXTURE NO 36 (Hiza, et al. [14])



	12.6943	125.00	58.1243		-.01	-.03	-.01
	12.6133	130.00	58.1243		.01	-.01	.01
	12.5271	135.00	58.1243		-.01	-.04	-.01
	12.4447	140.00	58.1243		.00	-.02	.00

## MIXTURE NO 37 (Hiza and Haynes [15])



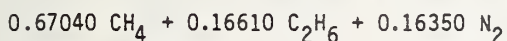
.476	24.9975	105.00	20.1852	.02	.04	.06	.02
.747	24.6696	110.00	20.1852	-.03	.00	.00	-.02
1.119	24.3515	115.00	20.1852	.01	.02	.02	.01
1.616	24.0335	120.00	20.1852	.07	.07	.07	.06

## MIXTURE NO 38 (Hiza and Haynes [15])



P	D	T	MW	RKM	HS	CELL	CS
.427	20.5342	110.00	30.0903	- .03	.02	.00	-.03
.636	20.3497	115.00	30.0903	- .01	.03	-.02	-.02
.638	20.3567	115.00	30.0903	.03	.06	.01	.01
.914	20.1786	120.00	30.0903	.12	.10	.04	.06
.914	20.1803	120.00	30.0903	.12	.11	.05	.07
1.280	19.9858	125.00	30.0903	.10	.08	.01	.04

## MIXTURE NO 39 (Hiza and Haynes [15])



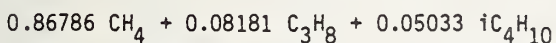
3.688	25.8587	105.00	20.3301	.57	.01	.28	.00
4.813	25.4598	110.00	20.3301	.64	- .03	.27	-.01
6.181	25.0466	115.00	20.3301	.79	.02	.25	-.05
7.731	24.6359	120.00	20.3301	.70	.42	.31	-.04

## MIXTURE NO 40 (Hiza and Haynes [15])



7.190	24.9084	105.00	24.5861	2.06	.01	.61	.07
9.494	24.5350	110.00	24.5861	2.55	- .01	.64	.04
12.372	24.1433	115.00	24.5861	3.72	.24	.65	-.06

## MIXTURE NO 41 (Miller and Hiza [25])



.466	24.9239	100.00	20.4561	- .17	.04	.11	-.03
.769	24.4200	108.00	20.4561	- .17	.01	.05	-.04
1.327	23.9676	115.00	20.4561	- .18	- .01	.02	-.05

## MIXTURE NO 42 (Hiza and Haynes [15])



2.817	25.3950	105.00	20.1181	.17	.08	.24	-.01
3.620	25.0153	110.00	20.1181	.10	.02	.23	-.05
4.549	24.6465	115.00	20.1181	.08	.08	.33	.01
5.610	24.2667	120.00	20.1181	.02	*	.44	.04

\* The hard sphere solution for the density of N<sub>2</sub> failed.

## MIXTURE NO 43 (Haynes [9])

0.89071 CH<sub>4</sub> + 0.04998 nC<sub>4</sub>H<sub>10</sub> + 0.05931 N<sub>2</sub>

P	D	T	MW	RKM	HS	CELL	CS
2.400	25.3450	110.00	18.8562	- .23	.00	.01	.03
3.145	24.9440	115.00	18.8562	- .25	- .04	-.02	.01
4.082	24.5383	120.00	18.8562	- .38	*	-.02	.00
5.196	24.1141	125.00	18.8562	- .32	*	-.04	-.04

## MIXTURE NO 44 (Miller and Hiza [25])

0.85317 CH<sub>4</sub> + 0.05077 C<sub>2</sub>H<sub>6</sub> + 0.04855 C<sub>3</sub>H<sub>8</sub> + 0.04751 nC<sub>4</sub>H<sub>10</sub>

1.038	24.6056	110.04	20.1165	.02	.15	.10	.06
1.464	24.2712	115.00	20.1165	.00	.11	.04	.02

## MIXTURE NO 45 (Haynes [9])

0.85133 CH<sub>4</sub> + 0.05759 C<sub>2</sub>H<sub>6</sub> + 0.04808 C<sub>3</sub>H<sub>8</sub> + 0.04300 nC<sub>4</sub>H<sub>10</sub>

1.180	24.3243	115.00	20.0092	- .04	.07	.00	-.01
1.700	23.9965	120.00	20.0092	.00	.10	.02	.03
2.374	23.6586	125.00	20.0092	.05	.11	.04	.05
3.232	23.3108	130.00	20.0092	.04	.11	.05	.05
4.301	22.9634	135.00	20.0092	.08	.13	.11	.09

## MIXTURE NO 46 (Haynes [9])

0.84566 CH<sub>4</sub> + 0.07924 C<sub>2</sub>H<sub>6</sub> + 0.05060 C<sub>3</sub>H<sub>8</sub> + 0.02450 nC<sub>4</sub>H<sub>10</sub>

1.167	24.5569	115.00	19.6051	.00	.04	.00	-.01
1.683	24.2126	120.00	19.6051	.02	.04	-.01	-.01
2.350	23.8698	125.00	19.6051	.08	.07	.03	.03
3.201	23.5204	130.00	19.6051	.12	.11	.09	.07

## MIXTURE NO 47 (Haynes [9])

0.86040 CH<sub>4</sub> + 0.04600 C<sub>2</sub>H<sub>6</sub> + 0.04790 C<sub>3</sub>H<sub>8</sub> + 0.04570 iC<sub>4</sub>H<sub>10</sub>

1.186	24.2654	115.00	19.9552	- .14	.01	.04	-.03
1.710	23.9371	120.00	19.9552	- .10	.04	.07	.01
2.387	23.5860	125.00	19.9552	- .10	.01	.05	-.01
3.248	23.2331	130.00	19.9552	- .13	- .01	.06	-.02
4.320	22.8637	135.00	19.9552	- .18	- .07	.05	-.07

\* The hard sphere solution for the density of N<sub>2</sub> failed.

MIXTURE NO 48 (Haynes [9])

0.85378 CH<sub>4</sub> + 0.05178 C<sub>2</sub>H<sub>6</sub> + 0.04703 C<sub>3</sub>H<sub>8</sub> + 0.04741 iC<sub>4</sub>H<sub>10</sub>

P	D	T	MW	RKM	HS	CELL	CS
1.190	24.2100	115.00	20.0838	- .14	.01	.04	-.03
1.706	23.8779	120.00	20.0838	- .14	.01	.04	-.02
2.379	23.5324	125.00	20.0838	- .13	- .02	.02	-.04
3.238	23.1834	130.00	20.0838	- .15	- .04	.03	-.05

MIXTURE NO 49 (Miller and Hiza [25])

0.85378 CH<sub>4</sub> + 0.05178 C<sub>2</sub>H<sub>6</sub> + 0.04703 C<sub>3</sub>H<sub>8</sub> + 0.04741 iC<sub>4</sub>H<sub>10</sub>

.972	24.5434	110.02	20.0838	- .14	.03	.06	-.01
1.429	24.2154	115.01	20.0838	- .12	.02	.05	-.01

MIXTURE NO 50 (Hiza and Haynes [15])

0.85260 CH<sub>4</sub> + 0.04830 C<sub>2</sub>H<sub>6</sub> + 0.05070 C<sub>3</sub>H<sub>8</sub> + 0.04840 N<sub>2</sub>

1.581	25.8910	105.00	18.7223	.01	- .04	.03	-.07
2.138	25.5081	110.00	18.7223	- .09	- .07	.03	-.07
2.827	25.1224	115.00	18.7223	- .05	- .06	.05	-.06
3.650	24.7283	120.00	18.7223	- .08	*	.08	-.06

MIXTURE NO 51 (Haynes [9])

0.85892 CH<sub>4</sub> + 0.11532 C<sub>2</sub>H<sub>6</sub> + 0.01341 C<sub>3</sub>H<sub>8</sub> + 0.00705 nC<sub>4</sub>H<sub>10</sub> + 0.00530 iC<sub>4</sub>H<sub>10</sub>

1.185	25.0957	115.00	18.5565	.05	- .02	-.01	-.03
1.706	24.7131	120.00	18.5565	.03	- .06	-.05	-.07
2.372	24.3294	125.00	18.5565	.02	- .07	-.05	-.09
3.225	23.9490	130.00	18.5565	.05	- .02	.01	-.06

MIXTURE NO 52 (Hiza and Haynes [15])

0.85442 CH<sub>4</sub> + 0.05042 C<sub>2</sub>H<sub>6</sub> + 0.04038 C<sub>3</sub>H<sub>8</sub> + 0.02901 nC<sub>4</sub>H<sub>10</sub> + 0.02577 iC<sub>4</sub>H<sub>10</sub>

.515	24.8775	105.00	20.1885	.09	.25	.25	.16
.818	24.5382	110.00	20.1885	.00	.17	.15	.09
1.190	24.2083	115.00	20.1885	.00	.15	.12	.08
1.695	23.8859	120.00	20.1885	.05	.19	.15	.13

MIXTURE NO 53 (Haynes [9])

0.84558 CH<sub>4</sub> + 0.08153 C<sub>2</sub>H<sub>6</sub> + 0.04778 C<sub>3</sub>H<sub>8</sub> + 0.01252 nC<sub>4</sub>H<sub>10</sub> + 0.01259 iC<sub>4</sub>H<sub>10</sub>

1.166	24.5586	115.00	19.5838	.01	.05	.04	.01
1.680	24.2180	120.00	19.5838	.04	.07	.05	.03
2.348	23.8688	125.00	19.5838	.08	.08	.08	.04
3.188	23.5154	130.00	19.5838	.10	.10	.12	.07

\* The hard sphere solution for the density of N<sub>2</sub> failed.

## MIXTURE NO 54 (Haynes [9])

0.81249 CH <sub>4</sub> + 0.08484 C <sub>2</sub> H <sub>6</sub> + 0.04931 C <sub>3</sub> H <sub>8</sub> + 0.02708 nC <sub>4</sub> H <sub>10</sub> + 0.02628 N <sub>2</sub>							
P	D	T	MW	RKM	HS	CELL	CS
2.214	24.4562	115.00	20.0706	.01	.01	.03	-.02
2.874	24.1119	120.00	20.0706	.00	*	.04	-.01
3.768	23.7507	125.00	20.0706	.02	*	.02	-.05
4.793	23.3954	130.00	20.0706	-.02	-3.67	.07	-.03

## MIXTURE NO 55 (Hiza and Haynes [15])

0.79090 CH <sub>4</sub> + 0.05600 C <sub>2</sub> H <sub>6</sub> + 0.05000 C <sub>3</sub> H <sub>8</sub> + 0.04770 nC <sub>4</sub> H <sub>10</sub> + 0.05540 N <sub>2</sub>							
P	D	T	MW	RKM	HS	CELL	CS
1.933	24.8080	105.00	20.9017	.04	.10	.12	.05
2.530	24.4664	110.00	20.9017	.02	.02	.03	-.02

## MIXTURE NO 56 (Miller and Hiza [25])

0.79054 CH <sub>4</sub> + 0.05597 C <sub>2</sub> H <sub>6</sub> + 0.04996 C <sub>3</sub> H <sub>8</sub> + 0.04762 nC <sub>4</sub> H <sub>10</sub> + 0.05591 N <sub>2</sub>							
P	D	T	MW	RKM	HS	CELL	CS
2.158	24.8354	105.03	20.9029	.15	.21	.23	.15

## MIXTURE NO 57 (Haynes [9])

0.80940 CH <sub>4</sub> + 0.04542 C <sub>2</sub> H <sub>6</sub> + 0.05050 C <sub>3</sub> H <sub>8</sub> + 0.04667 iC <sub>4</sub> H <sub>10</sub> + 0.04801 N <sub>2</sub>							
P	D	T	MW	RKM	HS	CELL	CS
3.005	24.1487	115.00	20.6355	.02	-.02	-.03	-.04
3.863	23.8075	120.00	20.6355	-.14	*	.00	-.03
4.874	23.4518	125.00	20.6355	-.12	*	.01	-.05
6.125	23.0893	130.00	20.6355	-.18	-5.06	.05	-.08

## MIXTURE NO 58 (Hiza and Haynes [15])

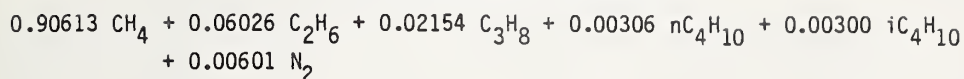
0.80600 CH <sub>4</sub> + 0.04680 C <sub>2</sub> H <sub>6</sub> + 0.04820 C <sub>3</sub> H <sub>8</sub> + 0.05000 iC <sub>4</sub> H <sub>10</sub> + 0.04900 N <sub>2</sub>							
P	D	T	MW	RKM	HS	CELL	CS
2.039	24.7803	105.00	20.7423	-.03	.08	.03	.01
2.550	24.4327	110.00	20.7423	-.09	-.02	-.06	-.06
3.135	24.1039	115.00	20.7423	.06	.00	-.02	-.02
3.790	23.7707	120.00	20.7423	-.10	*	-.01	-.02

## MIXTURE NO 59 (Miller and Hiza [25])

0.80545 CH <sub>4</sub> + 0.04671 C <sub>2</sub> H <sub>6</sub> + 0.04817 C <sub>3</sub> H <sub>8</sub> + 0.04998 iC <sub>4</sub> H <sub>10</sub> + 0.04969 N <sub>2</sub>							
P	D	T	MW	RKM	HS	CELL	CS
2.273	24.7831	105.06	20.7476	.00	.10	.05	.03

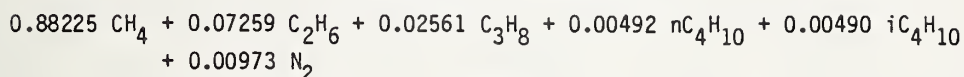
\* The hard sphere solution for the density of N<sub>2</sub> failed.

## MIXTURE NO 60 (Haynes [9])



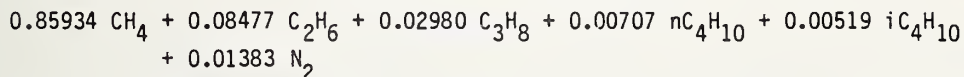
P	D	T	MW	RKM	HS	CELL	CS
1.478	25.3834	115.00	17.8195	.03	- .01	.01	-.01
2.043	24.9894	120.00	17.8195	.08	.00	.05	.02
2.785	24.5702	125.00	17.8195	.04	.00	.03	-.02
3.722	24.1578	130.00	17.8195	.06	-1.08	.11	.02

## MIXTURE NO 61 (Haynes [9])



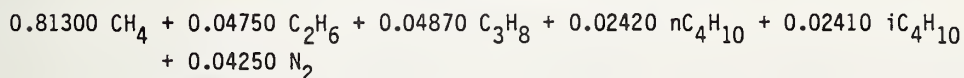
1.639	25.2023	115.00	18.3094	.09	.04	.07	.04
2.247	24.8047	120.00	18.3094	.06	.00	.04	.00
3.022	24.4022	125.00	18.3094	.04	.00	.03	-.03

## MIXTURE NO 62 (Haynes [9])



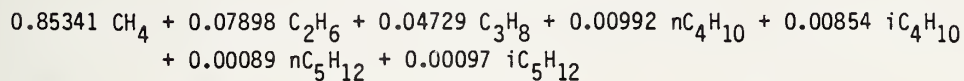
1.812	25.0384	115.00	18.7496	.12	.06	.09	.06
2.441	24.6661	120.00	18.7496	.12	*	.11	.07
3.223	24.2880	125.00	18.7496	.19	.00	.16	.09
4.222	23.8981	130.00	18.7496	.17	-2.12	.20	.10

## MIXTURE NO 63 (Hiza and Haynes [15])



1.834	24.8496	105.00	20.6168	.03	.12	.10	.05
2.807	24.5159	110.00	20.6168	.02	.08	.06	.03
3.384	24.1783	115.00	20.6168	.09	.06	.05	.03
6.039	23.8577	120.00	20.6168	.04	*	.11	.08

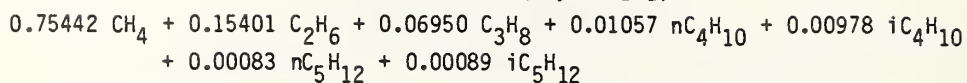
## MIXTURE NO 64 (Haynes [9])



.787	25.0063	110.00	19.3588	.01	.02	.02	-.01
1.172	24.6566	115.00	19.3588	.00	- .01	-.01	-.03
1.686	24.3079	120.00	19.3588	.02	.00	.00	-.02
2.351	23.9525	125.00	19.3588	.05	.01	.03	-.01
3.210	23.5883	130.00	19.3588	.06	.02	.06	.00

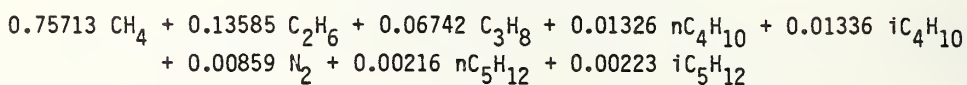
\* The hard sphere solution for the density of N<sub>2</sub> failed.

MIXTURE NO 65 (Haynes [9])



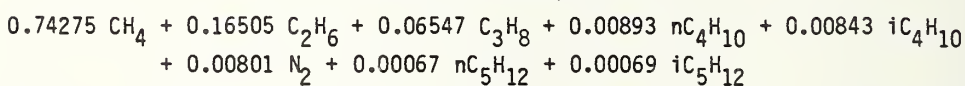
P	D	T	MW	RKM	HS	CELL	CS
.723	24.2529	110.00	21.1060	- .02	.00	-.01	-.04
1.081	23.9619	115.00	21.1060	.04	.04	.03	.01
1.549	23.6535	120.00	21.1060	.07	.04	.02	.01
2.153	23.3351	125.00	21.1060	.04	.01	.00	-.01

MIXTURE NO 66 (Haynes [9])



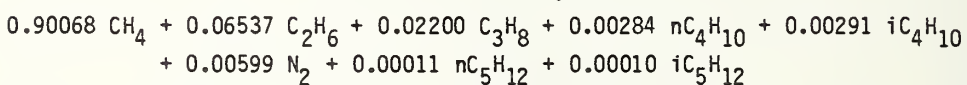
1.155	24.1809	110.00	21.3094	.09	.07	.08	.04
1.595	23.8731	115.00	21.3094	.12	.05	.05	.02
2.155	23.5709	120.00	21.3094	.12	.00	.08	.05
2.873	23.2644	125.00	21.3094	.15	.00	.12	.08
3.744	22.9514	130.00	21.3094	.22	-1.42	.16	.11

MIXTURE NO 67 (Haynes [9])



1.158	24.3141	110.00	21.0976	.02	-.02	.00	-.05
1.584	24.0160	115.00	21.0976	.09	.01	.02	-.01
2.093	23.6937	120.00	21.0976	.03	.00	-.03	-.06
2.853	23.3804	125.00	21.0976	.05	.00	-.01	-.05

MIXTURE NO 68 (Haynes [9])



1.456	25.3600	115.00	17.9026	.05	.01	.03	.01
2.024	24.9656	120.00	17.9026	.08	.00	.06	.03
2.762	24.5450	125.00	17.9026	.03	.00	.03	-.03
3.698	24.1289	130.00	17.9026	.02	-1.13	.07	-.02

Appendix B. Computer Program and Equation Parameters for the  
Extended Corresponding States Model

The program listings in Appendix F include the extended corresponding states method described in section 2. To use the program in its present form one must make one of the two possible calls to SUBROUTINE PDMIX(P,D,T,X) (lines LNG 1 through LNG 9). The two possible calls are:

CALL PDMIX(P,D,T,X)

or

CALL PMIX(P,D,T,X)

When the call to PDMIX(P,D,T,X) is made the input variables are: P (pressure in bars); T (temperature in kelvin); and X which is a matrix of the mole fraction of the components of the mixture in the following order:

- X(1) = mole fraction of methane
- X(2) = mole fraction of ethane
- X(3) = mole fraction of propane
- X(4) = mole fraction of normal butane
- X(5) = mole fraction of isobutane
- X(6) = mole fraction of nitrogen
- X(7) = mole fraction of normal pentane
- X(8) = mole fraction of isopentane

No other components are allowed and if one or more of the above components are absent, a zero should be inserted in the appropriate matrix element. The program then calculates a density and it is returned in the argument list as D (density in moles/liter).

When a call to PMIX(P,D,T,X) is made all of the above are the same except that the roles of P and D are interchanged, i.e., D is an input variable and P is calculated by the program.

The range of the program is 90 to 150 kelvin for the saturated liquid phase of any of the pure components of  $\text{CH}_4$ ,  $\text{C}_2\text{H}_6$ ,  $\text{C}_3\text{H}_8$ ,  $\text{nC}_4\text{H}_{10}$ ,  $\text{iC}_4\text{H}_{10}$ ,  $\text{N}_2$ ,  $\text{nC}_4\text{H}_{12}$  or  $\text{iC}_4\text{H}_{12}$  or any mixture of those fluids. The program will extrapolate to higher pressures (higher than saturation pressure) but the user is reminded that such a calculation is an extrapolation and should be used with caution.

Other subprograms required:

SUBROUTINE MIX DATA, line LNG 95, Appendix F

SUBROUTINE DATA CH4, line LNG 162, Appendix F

FUNCTION FINDM, line LNG 217, Appendix F

FUNCTION SATL, line LNG 236, Appendix F

SUBROUTINE PROPS, line LNG 248, Appendix F

The equation of state from which  $Z_0$  and  $G_0$  by eqs (1) and (2) may be derived is:

$$\begin{aligned}
P = & \rho RT + \rho^2(N_1 T + N_2 T^{1/2} + N_3 + N_4/T + N_5/T^2) \\
& + \rho^3(N_6 T + N_7 + N_8/T + N_9/T^2) \\
& + \rho^4(N_{10} T + N_{11} + N_{12}/T) + \rho^5(N_{13}) \\
& + \rho^6(N_{14}/T + N_{15}/T^2) + \rho^7(N_{16}/T) \\
& + \rho^8(N_{17}/T + N_{18}/T^2) + \rho^9(N_{19}/T^2) \\
& + \rho^3(N_{20}/T^2 + N_{21}/T^3) \exp(-\gamma\rho^2) \\
& + \rho^5(N_{22}/T^2 + N_{23}/T^4) \exp(-\gamma\rho^2) \\
& + \rho^7(N_{24}/T^2 + N_{25}/T^3) \exp(-\gamma\rho^2) \\
& + \rho^9(N_{26}/T^2 + N_{27}/T^4) \exp(-\gamma\rho^2) \\
& + \rho^{11}(N_{28}/T^2 + N_{29}/T^3) \exp(-\gamma\rho^2) \\
& + \rho^{13}(N_{30}/T^2 + N_{31}/T^3 + N_{32}/T^4) \exp(-\gamma\rho^2)
\end{aligned} \tag{B-1}$$

The computer subroutine PROPS(PP,DD,TT), lines "LNG 248 through LNG 371 in Appendix F" are the FORTRAN statements for eq (B-1) and the derivative  $(\partial P/\partial \rho)_T$ .

The parameters for eq (B-1) as applied to methane are given in table 2 and in the FORTRAN SUBROUTINE DATA CH4, lines LNG 162 through LNG 216, Appendix F.

The parameters for eqs (5) and (6), (9) and (10) are given in table 3 and 4 and in the FORTRAN SUBROUTINE MIX DATA (IBASE), lines LNG 95 through LNG 161, Appendix F.

Table 2. Methane Coefficients  $N_i$  for Eq B-1.

$R$	$=$	$0.08205616$	$N_{16}$	$=$	$-0.529609525984 \times 10^{-3}$
$\gamma$	$=$	$0.0096$	$N_{17}$	$=$	$0.152264286004 \times 10^{-4}$
$N_1$	$=$	$-0.187027997685 \times 10^{-1}$	$N_{18}$	$=$	$-0.109952182842 \times 10^{-1}$
$N_2$	$=$	$0.103387108009 \times 10$	$N_{19}$	$=$	$0.191395549929 \times 10^{-3}$
$N_3$	$=$	$-0.155387625619 \times 10^2$	$N_{20}$	$=$	$0.386470003746 \times 10^5$
$N_4$	$=$	$0.772311478564 \times 10^3$	$N_{21}$	$=$	$-0.157930582612 \times 10^7$
$N_5$	$=$	$-0.377103300895 \times 10^5$	$N_{22}$	$=$	$0.195270144401 \times 10^3$
$N_6$	$=$	$0.846818843475 \times 10^{-3}$	$N_{23}$	$=$	$0.165996081629 \times 10^7$
$N_7$	$=$	$-0.496415884529$	$N_{24}$	$=$	$0.603051146711$
$N_8$	$=$	$0.869909352414 \times 10^2$	$N_{25}$	$=$	$0.376485162808 \times 10^2$
$N_9$	$=$	$-0.322821592493 \times 10^5$	$N_{26}$	$=$	$0.125593680622 \times 10^{-2}$
$N_{10}$	$=$	$-0.395843026318 \times 10^{-4}$	$N_{27}$	$=$	$-0.343570032513 \times 10^2$
$N_{11}$	$=$	$0.266772318035 \times 10^{-1}$	$N_{28}$	$=$	$-0.540945094139 \times 10^{-5}$
$N_{12}$	$=$	$-0.304010057839 \times 10$	$N_{29}$	$=$	$0.185622284663 \times 10^{-2}$
$N_{13}$	$=$	$0,191584507536 \times 10^{-3}$	$N_{30}$	$=$	$0.770786979245 \times 10^{-8}$
$N_{14}$	$=$	$-0.195587933458 \times 10^{-3}$	$N_{31}$	$=$	$-0.286868318650 \times 10^{-5}$
$N_{15}$	$=$	$0.607479967879 \times 10$	$N_{32}$	$=$	$0.372376961647 \times 10^{-4}$

Table 3. Coefficients for Eqs 5 and 6.

$n_1 = -0.109495$	$n_4 = -4.14192$
$n_2 = 0.919454$	$n_5 = 0.444850$
$n_3 = -4.01525$	
$n_6 = 0.356808$	$n_8 = 0.893323$
$n_7 = 1.02619$	$n_9 = 0.761533$

	w	$P_c^*$ (bar)	$T_c$ (K)	$V_c$ ( $\text{cm}^3/\text{mol}$ )	M	Fluid No.
$\text{CH}_4$	0.0109	45.956967	190.555	98.522	16.04303	1
$\text{C}_2\text{H}_6$	0.110427	48.60314	305.5	146.2	30.07012	2
$\text{C}_3\text{H}_8$	0.154837	42.445123	370.	200.	44.09721	3
$n\text{C}_4\text{H}_{10}$	0.176372	38.295398	425.	251.62	58.1243	4
$i\text{C}_4\text{H}_{10}$	0.150115	36.88998	408.1	263.	58.1243	5
$\text{N}_2$	0.0291791	33.542557	126.2	89.827	28.0134	6
$n\text{C}_5\text{H}_{12}$	0.234320	33.812152	469.6	304.	72.15139	7
$i\text{C}_5\text{H}_{12}$	0.288886	31.988302	460.39	306.	72.15139	8

\*Note: The large number of significant figures given for critical pressure is necessary to reproduce the  $Z_c$  ( $Z_c = P_c V_c / RT_c$ ) in the least squares fit of the data.  $P_c$ 's have been converted to bar from atmospheres.

Table 4. Binary Interaction Coefficients for Eqs 9 and 10.  
Fluid numbers are given in table 3.

i	1	2	3	4	5	6	7	8
1	1	1.00514	1.01922	1.04243	1.05048	1.01009	1.06	1.06
2	1	1	1.00599	1.01616	1.02369	1.02127	1.02	1.02
3	1	1	1	1.00172	1.01140	1.04606	1.01	1.01
4	1	1	1	1	0.997114	1.20955	1.0	1.0
5	1	1	1	1	1	1.13889	1.0	1.0
6	1	1	1	1	1	1	1.0	1.0
7	1	1	1	1	1	1	1	1.0
8	1	1	1	1	1	1	1	1

i	1	2	3	4	5	6	7	8
1	1	1.01127	0.988608	0.983130	0.986978	0.953430	0.98	0.98
2	1	1	0.999961	0.972223	0.998886	0.939622	0.99	0.99
3	1	1	1	0.985547	1.03099	0.912209	0.99	0.99
4	1	1	1	1	0.976416	0.849200	0.99	0.99
5	1	1	1	1	1	0.857310	0.99	0.99
6	1	1	1	1	1	1	0.99	0.99
7	1	1	1	1	1	1	1	1.0
8	1	1	1	1	1	1	1	1

Table 5. Values for Checking Calculations Using Corresponding States Equations.\*

$$0.6975 \text{ CH}_4 + 0.156 \text{ C}_2\text{H}_6 + 0.092 \text{ C}_3\text{H}_8 + 0.029 \text{ nC}_4\text{H}_{10} + 0.014 \text{ iC}_4\text{H}_{10} + 0.0115 \text{ N}_2$$

Temperature K	Density in moles/liter	Pressure, bar
95	24.333	1
100	24.067	1.1
105	23.796	1.2

\* Included for check purposes only; these values are calculated from the corresponding states model and are not experimental data.

Appendix C. Computer Program and Equation Parameters for the  
Hard Sphere Model

The program listing that follows is for the hard sphere model described in section 3. To use the program in its present form one must make the following reference to the computer program:

$$\text{DEN} = \text{RODEN}(\text{P}, \text{T}, \text{X})$$

where DEN is density in moles/liter, P is pressure in bars, T is temperature in kelvin, and X is a matrix of the mole fractions of the components of the mixture in the following order:

- X(1) = mole fraction of methane
- X(2) = mole fraction of ethane
- X(3) = mole fraction of propane
- X(4) = mole fraction of normal butane
- X(5) = mole fraction of isobutane
- X(6) = mole fraction of nitrogen
- X(7) = mole fraction of normal pentane
- X(8) = mole fraction of isopentane

Note: the inclusion of the pentanes is due to Rodosevich and Miller [33] and no optimization of parameters has been included in this work for mixtures with pentane as a component.

The range of the program is 90 to 150 kelvin for the saturated liquid phase of mixtures of  $\text{CH}_4$ ,  $\text{C}_2\text{H}_6$ ,  $\text{C}_3\text{H}_8$ ,  $n\text{C}_4\text{H}_{10}$ ,  $i\text{C}_4\text{H}_{10}$ ,  $\text{N}_2$ ,  $n\text{C}_5\text{H}_{12}$  and  $i\text{C}_5\text{H}_{12}$ . The program will calculate densities of any of the pure components but they will be from a different model (i.e., some from an equation of state ( $\text{CH}_4$  and  $\text{N}_2$ ) and some from the equations for saturated liquid densities. Therefore in its present form, extrapolation to higher pressures is possible but the reliability of the results is questionable.

Other subprograms required:

SUBROUTINE FM, lines LNG 435 to 529, Appendix F  
SUBROUTINE ZERO, lines LNG 617 to 623, Appendix F  
FUNCTION FIND V1, lines LNG 530 to 548, Appendix F  
FUNCTION FIND G1, lines LNG 549 to 560, Appendix F  
FUNCTION EXCESS, lines LNG 561 to 616, Appendix F  
FUNCTION FIND M, lines LNG 217 to 234, Appendix F  
SUBROUTINE PROPS, lines LNG 248 to 371, Appendix F  
SUBROUTINE DATA CH4, lines LNG 162 to 216, Appendix F  
SUBROUTINE DATA N2, lines LNG 372 to 415, Appendix F

The parameters for eq (11), section 3 are given in table 6, and in lines LNG 462 through LNG 466 in Appendix F.

The binary interaction parameters  $j_{ij}$  and  $k_{ij}$  in eqs (15) and (16), section 3 are given in table 7 and in lines LNG 447 through LNG 461 in Appendix F.

Table 6. Coefficients for Eq 11.

Fluid	$a_i$	$S_i$	$c_i$	Fluid No.
CH <sub>4</sub>	$2.755 \times 10^5$	$3.676 \times 10^{-8}$	1.00	1
C <sub>2</sub> H <sub>6</sub>	$7.773 \times 10^5$	$4.158 \times 10^{-8}$	1.50	2
C <sub>3</sub> H <sub>8</sub>	$14.165 \times 10^5$	$4.644 \times 10^{-8}$	1.67	3
nC <sub>4</sub> H <sub>10</sub>	$22.733 \times 10^5$	$5.051 \times 10^{-8}$	1.83	4
iC <sub>4</sub> H <sub>10</sub>	$21.279 \times 10^5$	$5.056 \times 10^{-8}$	1.79	5
N <sub>2</sub>	$1.718 \times 10^5$	$3.546 \times 10^{-8}$	1.03	6
nC <sub>5</sub> H <sub>12</sub>	$30.550 \times 10^5$	$5.389 \times 10^{-8}$	1.91	7
iC <sub>5</sub> H <sub>12</sub>	$42.946 \times 10^5$	$5.706 \times 10^{-8}$	2.11	8

$$b_i = (2)(3.14159)(6.025 \times 10^{23})S_i^3/3$$

Table 7. Binary Interaction Parameters for Eqs 15 and 16.

		$j_{ij}$													
$i$	$j$	1	2	3	4	5	6	7	8						
1	0	-0.388616	$\times 10^{-2}$	-0.120932	$\times 10^{-1}$	-0.231577	$\times 10^{-1}$	-0.238349	$\times 10^{-1}$	-0.997547	$\times 10^{-2}$	-0.326	$\times 10^{-1}$	0.458	$\times 10^{-1}$
2	0	-0.2162	$\times 10^{-2}$	-0.400910	$\times 10^{-2}$	-0.812712	$\times 10^{-2}$	-0.143976	$\times 10^{-1}$	-0.3	$\times 10^{-2}$	-0.4	$\times 10^{-2}$	0.0	0.0
3	0	0.761571	$\times 10^{-3}$	0	0.222150	$\times 10^{-2}$	-0.383743	$\times 10^{-2}$	-0.24014	$\times 10^{-1}$	0.0	0.0	0.0	0.0	0.0
4	0	0	0	0	0	0	-0.576043	$\times 10^{-1}$	-0.576043	$\times 10^{-1}$	0.0	0.0	0.0	0.0	0.0
5	0	0	0	0	0	0	-0.576043	$\times 10^{-1}$	0	0	0	0	0	0	0
6	0	0	0	0	0	0	0	0	0	0	0	0	0	0	0
7	0	0	0	0	0	0	0	0	0	0	0	0	0	0	0
8	0	0	0	0	0	0	0	0	0	0	0	0	0	0	0

		$k_{ij}$													
$i$	$j$	1	2	3	4	5	6	7	8						
1	0	0.298830	$\times 10^{-2}$	0.597378	$\times 10^{-1}$	0.110893	0.100298	0.197290	$\times 10^{-1}$	0.14	0.1745	0.2	$\times 10^{-1}$	0.3	$\times 10^{-1}$
2	0	0.14527	$\times 10^{-1}$	0.67703	$\times 10^{-1}$	0.346632	$\times 10^{-1}$	0.529034	$\times 10^{-1}$	0.14719	0.0	0.0	0.0	0.0	0.0
3	0	0.249291	$\times 10^{-1}$	0	0.199213	$\times 10^{-1}$	-0.838212	$\times 10^{-2}$	0.154365	0.154365	0.0	0.0	0.0	0.0	0.0
4	0	0	0	0	0	0	0	0	0	0	0	0	0	0	0
5	0	0	0	0	0	0	0	0	0	0	0	0	0	0	0
6	0	0	0	0	0	0	0	0	0	0	0	0	0	0	0
7	0	0	0	0	0	0	0	0	0	0	0	0	0	0	0
8	0	0	0	0	0	0	0	0	0	0	0	0	0	0	0

Appendix D. Computer Program and Parameters for the Revised  
Klosek and McKinley Model

The program listing and tables that follow are for the Revised Klosek and McKinley model described in section 4. The method may be used in two ways.

First using the equation:

$$V_{\text{mix}} = \sum X_i V_i - [k_1 + (k_2 - k_1) X_{N_2} / 0.0425] X_{CH_4} \quad (D-1)$$

The  $V_i$ ,  $k_1$  and  $k_2$  may be obtained from tables 8, 9 and 10 and the volume of the mixture calculated. For example given the mixture of 0.8130  $CH_4$  + 0.0475  $C_2H_6$  + 0.0487  $C_3H_8$  + 0.0242  $nC_4H_{10}$  + 0.0241  $iC_4H_{10}$  + 0.0425  $N_2$  and a temperature of 105 kelvin.

The  $\sum X_i V_i$  and  $\sum X_i W_i$  are obtained from table 8.

$$\begin{aligned} \sum X_i V_i &= (.8130)(.0371113) + (.0475)(.047267) + (.0487)(.061766) \\ &+ (.0242)(.076100) + (.0241)(.077538) + (.0425)(.042565) \\ &= 0.0409453 \end{aligned}$$

$$\begin{aligned} \text{Then the } \sum X_i W_i &= (.8130)(16.04303) + (.0475)(30.07012) + (.0487)(44.09721) \\ &+ (.0242)(58.1243) + (.0241)(58.1243) + (.0425)(28.0143) \\ &= 20.6168 \text{ the molecular weight of the mixture} \end{aligned}$$

$$\text{from table 9 } k_1 = .697 \times 10^{-3}$$

$$\text{from table 10 } k_2 = .849 \times 10^{-3}$$

plugging all this into eq (D-1) gives

$$V_{\text{mix}} = .040255$$

$$1/V_{\text{mix}} = \rho_{\text{mix}} = 24.842 \text{ moles/liter}$$

This compares to the experimental value of 24.850 (Appendix A, mixture No. 63) to within 0.03%.

The same result may be obtained by using the computer program in the following way:

$$D = \text{FMKM}(T,X)$$

where T is temperature in kelvin and X is a matrix of mole fractions of the components in the following order:

- X(1) = mole fraction of methane
- X(2) = mole fraction of ethane
- X(3) = mole fraction of propane
- X(4) = mole fraction of normal butane
- X(5) = mole fraction of isobutane
- X(6) = mole fraction of nitrogen
- X(7) = mole fraction of normal pentane
- X(8) = mole fraction of isopentane

for the example: T = 105., X(1) = .8130, X(2) = .0475, X(3) = .0487, X(4) = .0242, X(5) = .0241 and X(6) = .0425.

Other subprograms required:

FUNCTION VIDEAL, lines LNG 709 through 732, Appendix F

FUNCTION SAT, lines LNG 733 through 762, Appendix F

Table 8. Volumes of Saturated Liquid of the Pure Components in Liters/mole.

T, K	CH <sub>4</sub>	C <sub>2</sub> H <sub>6</sub>	C <sub>3</sub> H <sub>8</sub>	nC <sub>4</sub> H <sub>10</sub>	iC <sub>4</sub> H <sub>10</sub>	N <sub>2</sub>	nC <sub>5</sub> H <sub>12</sub>	iC <sub>5</sub> H <sub>12</sub>
90.	.035441	.046081	.060461	.074708	.076084	.037543	.089173	.089243
92.	.035649	.046235	.060632	.074891	.076274	.038081	.089379	.089454
94.	.035861	.046390	.060804	.075075	.076466	.038650	.089586	.089666
96.	.036077	.046547	.060977	.075259	.076659	.039254	.089793	.089878
98.	.036298	.046704	.061151	.075445	.076853	.039897	.090000	.090091
100.	.036524	.046863	.061325	.075631	.077047	.040586	.090208	.090304
102.	.036755	.047023	.061501	.075818	.077243	.041327	.090416	.090518
104.	.036992	.047185	.061677	.076006	.077440	.042128	.090624	.090733
106.	.037234	.047348	.061855	.076194	.077637	.043002	.090833	.090948
108.	.037481	.047512	.062033	.076384	.077836	.043963	.091042	.091163
110.	.037735	.047678	.062212	.076574	.078035	.045031	.091252	.091379
112.	.037995	.047845	.062392	.076765	.078236	.046231	.091462	.091596
114.	.038262	.048014	.062574	.076957	.078438	.047602	.091673	.091814
116.	.038536	.048184	.062756	.077150	.078640	.049179	.091884	.092032
118.	.038817	.048356	.062939	.077344	.078844	.050885	.092095	.092251
120.	.039106	.048529	.063124	.077539	.079049	.052714	.092307	.092470
122.	.039404	.048704	.063309	.077734	.079255	.054679	.092520	.092690
124.	.039710	.048881	.063496	.077931	.079462	.056797	.092733	.092911
126.	.040025	.049059	.063684	.078128	.079671	.059085	.092947	.093133
128.	.040350	.049239	.063873	.078327	.079880	.061565	.093161	.093355
130.	.040685	.049421	.064063	.078526	.080091	.064263	.093376	.093578
molecular weight*	16.04303	30.07012	44.09721	58.1243	58.1243	28.0143	72.15139	72.15139

52

\* See section 6 for an explanation of values of molecular weight.

Table 9. Correction Factor  $k_1 \times 10^3$ .

T/W	16	17	18	19	20	21	22	23	24	25
90	-.005	.120	.220	.340	.430	.515	.595	.660	.725	.795
95	-.006	.135	.260	.380	.500	.590	.665	.740	.810	.885
100	-.007	.150	.300	.425	.575	.675	.755	.830	.910	.990
105	-.007	.165	.340	.475	.635	.735	.840	.920	1.045	1.120
110	-.008	.180	.375	.535	.725	.835	.950	1.055	1.155	1.245
115	-.009	.220	.440	.610	.810	.945	1.065	1.180	1.280	1.380
120	-.01	.250	.500	.695	.920	1.055	1.205	1.330	1.450	1.550
125	-.013	.295	.590	.795	1.035	1.210	1.385	1.525	1.640	1.750
130	-.015	.345	.700	.920	1.200	1.370	1.555	1.715	1.860	1.990
135	-.017	.400	.825	1.060	1.390	1.590	1.800	1.950	2.105	2.272

Table 10. Correction Factor  $k_2 \times 10^3$ .

T/W	16	17	18	19	20	21	22	23	24	25
90	-.004	.10	.22	.35	.50	.60	.69	.78	.86	.95
95	-.005	.12	.28	.43	.59	.71	.83	.94	1.05	1.14
100	-.007	.16	.34	.49	.64	.79	.94	1.08	1.17	1.27
105	-.01	.24	.42	.61	.75	.91	1.05	1.19	1.33	1.45
110	-.015	.32	.59	.77	.92	1.07	1.22	1.37	1.52	1.71
115	-.024	.41	.72	.95	1.15	1.22	1.3	1.45	1.65	2.00
120	-.032	.60	.91	1.23	1.43	1.63	1.85	2.08	2.30	2.45
125	-.043	.71	1.13	1.48	1.73	1.98	2.23	2.48	2.75	2.90
130	-.058	.95	1.46	1.92	2.20	2.42	2.68	3.00	3.32	3.52
135	-.075	1.30	2.00	2.40	2.60	3.00	3.40	3.77	3.99	4.23

## Appendix E. Computer Program for the Cell Model

The program listings for the cell model start at line LNG 763 and continue on to the end of Appendix F. As is mentioned in section 4, no details of the model are given here only the program listing. To use the program in its present form one must make the following reference to the computer program:

```
CALL ECKNON(P,D,T,X)
```

where P is input pressure in bars, D is the output density in moles/liter, T is the input temperature in kelvins and X is a matrix of the mole fractions of the components of the mixture in the following order:

- X(1) = mole fraction of methane
- X(2) = mole fraction of ethane
- X(3) = mole fraction of propane
- X(4) = mole fraction of normal butane
- X(5) = mole fraction of isobutane
- X(6) = mole fraction of nitrogen
- X(7) = mole fraction of normal pentane
- X(8) = mole fraction of isopentane

## Appendix F. Computer Programs

Listing of computer programs for all four models. See the sections on the individual models for a list of subprograms needed for each model.

The programs are written in FORTRAN IV and are operational on a CDC 6600 computer.

	SUBROUTINE PDMIX(P,D,T,X)	LNG	1
C	FOR A CALL TO PDMIX, P,T AND X ARE INPUT. P IS IN BAR,T IS IN	LNG	2
C	KELVIN AND D IS OUTPUT IN THE UNITS OF MOLES/LITER	LNG	3
C	FOR A CALL TO P MIX, D,T AND X ARE INPUT AND P IS OUTPUT, THE	LNG	4
C	UNITS ARE THE SAME	LNG	5
C	THE X MATRIX MUST CONTAIN THE MOL FRACTION OF THE ALLOWABLE FLUIDS	LNG	6
C	IN THE FOLLOWING ORDER,1=C1,2=C2,3=C3,4=NC4,5=IC4,6=N2,7=NC5,8=IC5	LNG	7
C	PLACE A ZERO IN THE ELEMENTS OF X WHERE THAT PARTICULAR GAS IS NOT	LNG	8
C	PRESENT	LNG	9
	DIMENSION ZATA(10,10),ATA(10,10),TC(10),VC(10),ZC(10),AC(10),W(10)	LNG	10
	1,PC(10),CF(9)	LNG	11
	DIMENSION THETA(10,10),TH(10,10),PHI(10,10),PH(10,10),F(10,10),FH	LNG	12
	1(10,10),H(10,10),HH(10,10),VR(10,10),TR(10,10),X(10)	LNG	13
	COMMON/DATA M/ZATA,ATA,TC,VC,W,TCO,VCO,ACO,ZCO,RR,R,OMEGO,AC,ZC,N	LNG	14
	1,PC,CF	LNG	15
	DATA(IE=0)	LNG	16
	D=0.0 \$ PI=P/1.01325	LNG	17
	GO TO 4	LNG	18
	ENTRY PMIX	LNG	19
	P=0.0	LNG	20
	IP=1	LNG	21
	GO TO 5	LNG	22
4	IP=0	LNG	23
5	CONTINUE	LNG	24
	IF(IE.GT.0)GO TO 6	LNG	25
	IE=1	LNG	26
	CALL DATA CH4	LNG	27
	IBASE=L=1	LNG	28
	CALL MIX DATA(IBASE)	LNG	29
6	CONTINUE	LNG	30
	DO 1 I=1,N	LNG	31
	F(I,I)=H(I,I)=1.	LNG	32
	THETA(I,I)=1.	LNG	33
1	PHI(I,I)=1.	LNG	34
	DO 30 J=1,30	LNG	35
	HX=FXHX=0.0	LNG	36
	DO 10 I=1,N	LNG	37
	FH(I,I)=F(I,I)	LNG	38
	HH(I,I)=H(I,I)	LNG	39
	IF(X(I).LT..0001)GO T O 10	LNG	40
	F(I,I)=(TC(I)/TC(L))*THETA(I,I)	LNG	41
	H(I,I)=(VC(I)/VC(L))*PHI(I,I)	LNG	42
10	CONTINUE	LNG	43
	DO 11 IA=1,N	LNG	44
	DO 11 IB=1,N	LNG	45
	IF(X(IA).LT..0001)GO TO 11	LNG	46
	IF(X(IB).LT..0001)GO TO 11	LNG	47
	FAB=ZATA(IA,IB)*(F(IA,IA)* F(IB,IB))**.5	LNG	48
	HAB=ATA(IA,IB)*(.5*H(IA,IA)**(1./3.)+.5*H(IB,IB)**(1./3.))**3	LNG	49
	HX=HX+X(IA)*X(IB)*HAB	LNG	50
	FXHX=FXHX+X(IA)*X(IB)*HAB*FAB	LNG	51
11	CONTINUE	LNG	52
	FX=FXHX/HX	LNG	53
	PRO=PI*HX/FX	LNG	54
	TRO=T/FX	LNG	55
	DEN=D*HX	LNG	56
	IF(IP.EQ.1)GO TO 8	LNG	57
	DD=SATL(TRO)*1000.+1.	LNG	58
9	DEN=FIND M(PRO,TRO,DD)	LNG	59
8	CONTINUE	LNG	60
	IF(DEN.LE.0.0) GO TO 33	LNG	61
	VRO=1000./DEN	LNG	62
	DO 12 I=1,N	LNG	63

```

IF(X(I).LT..0001)GO TO 12                                LNG 64
VR(I,I)=VRO*PHI(I,I)/VCO                                LNG 65
TR(I,I)=TRO*THETA(I,I)/TCO                              LNG 66
IF(VR(I,I).GT.2.)VR(I,I)=2.                             LNG 67
IF(VR(I,I).LT..5)VR(I,I)=.5                             LNG 68
TH(I,I)=THETA(I,I)                                       LNG 69
THETA(I,I)=1.+(AC(I)-OMEGO)*(CF(1)-CF(2)*ALOG(TR(I,I))+(CF(3)-CF(4
1)/TR(I,I))*VR(I,I)-CF(5)))                             LNG 70
PH(I,I)=PHI(I,I)                                         LNG 71
PHI(I,I)=(1.+(AC(I)-OMEGO)*(CF(6)*(VR(I,I)-CF(7))-CF(8)*(VR(I,I)
1-CF(9))*ALOG(TR(I,I))))*ZCO/ZC(I)                       LNG 72
12 CONTINUE                                              LNG 73
DO 13 I=1,N                                              LNG 74
IF(X(I).LT..0001)GO TO 13                                LNG 75
IF(ABS ((FH(I,I)-F(I,I))/F(I,I)).GT..001)GO TO 30        LNG 76
IF(ABS ((HH(I,I)-H(I,I))/H(I,I)).GT..001)GO TO 30        LNG 77
IF(ABS ((TH(I,I)-THETA(I,I))/THETA(I,I)).GT..001)GO TO 30 LNG 78
IF(ABS ((PH(I,I)-PHI(I,I))/PHI(I,I)).GT..001)GO TO 30   LNG 79
13 CONTINUE                                              LNG 80
GO TO 31                                                  LNG 81
30 CONTINUE                                              LNG 82
33 PRINT 100,P,DEN,T                                     LNG 83
100 FORMAT(* ITTERATION FAILED AT*,3F10.4)                LNG 84
STOP                                                      LNG 85
31 D=DEN/HX                                              LNG 86
THC=THETA(6,6)                                          LNG 87
IF(IP.EQ.0)GO TO 32                                     LNG 88
CALL PRESS(P,DEN,TRO)                                   LNG 89
PI=1.01325*P*FX/HX                                     LNG 90
32 RETURN                                               LNG 91
END                                                       LNG 92
SUBROUTINE MIX DATA(IBASE)                             LNG 93
DIMENSION ZATA(10,10),ATA(10,10),TC(10),VC(10),ZC(10),AC(10),W(10) LNG 94
1,PC(10),CF(9)                                          LNG 95
COMMON/DATA M/ZATA,ATA,TC,VC,W,TCO,VCO,ACO,ZCO,RR,R,OMEGO,AC,ZC,N LNG 96
1,PC,CF                                                  LNG 97
DATA(PC=45.356,47.96757,41.89008,37.79462,36.40758,33.10393) LNG 98
DATA(TC=190.555,305.5,370.,425.,408.1,126.2)           LNG 99
DATA(W=16.04303,30.07012,44.09721,58.1243,58.1243,28.0134) LNG 100
DATA(VC=98.522,146.2,200.,251.62,263.00,89.827)        LNG 101
DATA(AC=.0109,.110427,.154837,.176372,.150115,.0291791) LNG 102
DATA(R=82.05606),(RR=8.3144),(N=6)                     LNG 103
DATA(CF=-.109495,.919454,-4.01525,-4.14192,.444850,.356808,
11.02619,.893323,.761533)                               LNG 104
DATA(ATA(1,2)=1.00514),(ATA(1,3)=1.01922),(ATA(1,4)=1.04243),
1(ATA(1,5)=1.05048),(ATA(1,6)=1.01009),                 LNG 105
A(ATA(2,3)=1.00599),(ATA(2,4)=1.01616),                 LNG 106
2(ATA(2,5)=1.02369),(ATA(2,6)=1.02127),(ATA(3,4)=1.00172),
3(ATA(3,5)=1.01140),(ATA(3,6)=1.04606),(ATA(4,5)=.997114),
4(ATA(4,6)=1.20955),(ATA(5,6)=1.13889)                 LNG 107
DATA(ZATA(1,2)=1.01127),(ZATA(1,3)=.988608),(ZATA(1,4)=.983130),
1(ZATA(1,5)=.986978),(ZATA(1,6)=.953430),(ZATA(2,3)=.999961),
2(ZATA(2,4)=.972223),(ZATA(2,5)=.998886),(ZATA(2,6)=.939622),
3(ZATA(3,4)=.985547),(ZATA(3,5)=1.03099),(ZATA(3,6)=.912209),
4(ZATA(4,5)=.976416),(ZATA(4,6)=.849200),(ZATA(5,6)=.857310)
L=IBASE                                                  LNG 108
N=8                                                       LNG 109
N1=N-1                                                   LNG 110
PC(7)=33.37                                             LNG 111
PC(8)=31.57                                             LNG 112
TC(7)=469.6                                             LNG 113
TC(8)=460.39                                           LNG 114
VC(7)=304.                                             LNG 115
VC(8)=304.                                             LNG 116
VC(9)=304.                                             LNG 117
VC(10)=304.                                            LNG 118
VC(11)=304.                                            LNG 119
VC(12)=304.                                            LNG 120
VC(13)=304.                                            LNG 121
VC(14)=304.                                            LNG 122
VC(15)=304.                                            LNG 123
VC(16)=304.                                            LNG 124
VC(17)=304.                                            LNG 125
VC(18)=304.                                            LNG 126

```

VC(8)=306.	LNG 127
W(7)=72.15139	LNG 128
W(8)=72.15139	LNG 129
AC(7)=.234320	LNG 130
AC(8)=.288886	LNG 131
ATA(1,7)=ATA(1,8)=1.06	LNG 132
ATA(2,7)=ATA(2,8)=1.02	LNG 133
ATA(3,7)=ATA(3,8)=1.01	LNG 134
ATA(4,7)=ATA(4,8)=1.	LNG 135
ATA(5,7)=ATA(5,8)=1.	LNG 136
ATA(6,7)=ATA(6,8)=1.	LNG 137
ATA(7,8)=1.	LNG 138
ZATA(1,7)=ZATA(1,8)=.98	LNG 139
ZATA(2,7)=ZATA(2,8)=.99	LNG 140
ZATA(3,7)=ZATA(3,8)=.99	LNG 141
ZATA(4,7)=ZATA(4,8)=.99	LNG 142
ZATA(5,7)=ZATA(5,8)=.99	LNG 143
ZATA(6,7)=ZATA(6,8)=.99	LNG 144
ZATA(7,8)=1.	LNG 145
DO 3 J=1,N1	LNG 146
J1=J+1	LNG 147
DO 3 K=J1,N	LNG 148
ZATA(K,J)=ZATA(J,K)	LNG 149
3 ATA(K,J)=ATA(J,K)	LNG 150
DO 4 I=1,N	LNG 151
4 ATA(I,I)=ZATA(I,I)=1.	LNG 152
PCO=PC(L)	LNG 153
VCO=VC(L)	LNG 154
TCO=TC(L)	LNG 155
OMEGO=AC(L)	LNG 156
ZCO=PCO*VCO/TCO/R	LNG 157
DO 5 I=1,N	LNG 158
5 ZC(I)=PC(I)*VC(I)/TC(I)/R	LNG 159
RETURN	LNG 160
END	LNG 161
SUBROUTINE DATA CH4	LNG 162
C INITIALIZES THE EQUATION OF STATE CONSTANTS TO METHANE	LNG 163
DIMENSION G(32),VP(9),GI(11)	LNG 164
COMMON/DATA/G,R,GAMMA,VP,DTP	LNG 165
DIMENSION A(10)	LNG 166
COMMON/SATC/A	LNG 167
R=.08205616	LNG 168
GAMMA=-.0096	LNG 169
A(1)=190.555	LNG 170
A(2)=10.23	LNG 171
A(3)=18.404156472	LNG 172
A(4)=7.3498921512	LNG 173
A(5)=-1.4313160833	LNG 174
A(6)=A(7)=0.0	LNG 175
G( 1)=-.187027997685E-01	LNG 176
G( 2)=.103387108009E+01	LNG 177
G( 3)=-.155387625619E+02	LNG 178
G( 4)=.772311478564E+03	LNG 179
G( 5)=-.377103300895E+05	LNG 180
G( 6)=.846818843475E-03	LNG 181
G( 7)=-.496415884529E+00	LNG 182
G( 8)=.869909352414E+02	LNG 183
G( 9)=-.322821592493E+05	LNG 184
G(10)=-.395843026318E-04	LNG 185
G(11)=.266772318035E-01	LNG 186
G(12)=-.304010057839E+01	LNG 187
G(13)=.191584507536E-03	LNG 188
G(14)=-.195587933458E-03	LNG 189

G(15)= .607479967879E+01	LNG 190
G(16)=-.529609525984E-03	LNG 191
G(17)= .152264286004E-04	LNG 192
G(18)=-.109952182842E-01	LNG 193
G(19)= .191395549929E-03	LNG 194
G(20)= .386470003746E+05	LNG 195
G(21)=-.157930582612E+07	LNG 196
G(22)= .195270144401E+03	LNG 197
G(23)= .165996081629E+07	LNG 198
G(24)= .603051146711E+00	LNG 199
G(25)= .376485162808E+02	LNG 200
G(26)= .125593680622E-02	LNG 201
G(27)=-.343570032513E+02	LNG 202
G(28)=-.540945094139E-05	LNG 203
G(29)= .185622284663E-02	LNG 204
G(30)= .770786979245E-08	LNG 205
G(31)=-.286868318650E-05	LNG 206
G(32)= .372376961647E-04	LNG 207
VP(1)=4.77748580	LNG 208
VP(2)=1.76065363	LNG 209
VP(3)=-.56788894	LNG 210
VP(4)=1.32786231	LNG 211
VP(5)=1.5	LNG 212
VP(6)=.1159	LNG 213
VP(7)=90.68	LNG 214
VP(8)=190.555	LNG 215
END	LNG 216
FUNCTION FIND M(P,T,D)	LNG 217
C SOLVES THE EQUATION OF STATE OF METHANE FOR DENSITY GIVEN P AND T	LNG 218
DD=D	LNG 219
TT=T	LNG 220
DO 10 I=1,50	LNG 221
CALL PRESS(PP,DD,TT)	LNG 222
P2=PP	LNG 223
IF(ABS (P-P2)-1.E-7*P)20,20,1	LNG 224
1 CALL DPDD(PP,DD,TT)	LNG 225
DP=PP	LNG 226
CORR=(P2-P)/DP	LNG 227
IF(ABS (CORR)-1.E-7*DD)20,20,10	LNG 228
10 DD=DD-CORR	LNG 229
FIND M=0	LNG 230
RETURN	LNG 231
20 FIND M=DD	LNG 232
RETURN	LNG 233
END	LNG 234
FUNCTION SATL(T)	LNG 235
C CALCULATES THE SATURATED LIQUID DENSITY OF METHANE	LNG 236
DIMENSION A(10)	LNG 237
COMMON/SATC/A	LNG 238
IF(T.GT.A(1))GO TO 1	LNG 239
X=(1.-T/A(1))	LNG 240
SATL=A(2)+A(3)*X**(.35)+A(4)*X+A(5)*X**(4./3.)+A(6)*X**(5./3.	LNG 241
1)+A(7)*X**2	LNG 242
SATL=SATL/1000.	LNG 243
RETURN	LNG 244
1 SATL=1.E20	LNG 245
RETURN	LNG 246
END	LNG 247
SUBROUTINE PROPS(PP,DD,TT)	LNG 248
C EQUATION OF STATE FOR METHANE AND NITROGEN	LNG 249
DIMENSION X(33)	LNG 250
DIMENSION B(33),G(32)	LNG 251
EQUIVALENCE (B,X)	LNG 252

COMMON/DATA/G,R,GAMMA	
DATA(ID=1)	LNG 253
DATA(IZ=1)	LNG 254
1 CONTINUE	LNG 255
D=DD	LNG 256
P=PP	LNG 257
T=TT	LNG 258
GM=GAMMA	LNG 259
D2=D*D	LNG 260
D3=D2*D	LNG 261
D4=D3*D	LNG 262
D5=D4*D	LNG 263
D6=D5*D	LNG 264
D7=D6*D	LNG 265
D8=D7*D	LNG 266
D9=D8*D	LNG 267
D10=D9*D	LNG 268
D11=D10*D	LNG 269
D12=D11*D	LNG 270
D13=D12*D	LNG 271
TS=SQRT ( T)	LNG 272
T2=T*T	LNG 273
T3=T2*T	LNG 274
T4=T3*T	LNG 275
T5=T4*T	LNG 276
F=EXP (GM*D2)	LNG 277
GO TO (100,200),K	LNG 278
ENTRY PRESS	LNG 279
K=1	LNG 280
GO TO 1	LNG 281
100 CONTINUE	LNG 282
B( 1)=D2*T	LNG 283
B( 2)=D2*TS	LNG 284
B( 3)=D2	LNG 285
B( 4)=D2/T	LNG 286
B( 5)=D2/T2	LNG 287
B( 6)=D3*T	LNG 288
B( 7)=D3	LNG 289
B( 8)=D3/T	LNG 290
B( 9)=D3/T2	LNG 291
B(10)=D4*T	LNG 292
B(11)=D4	LNG 293
B(12)=D4/T	LNG 294
B(13)=D5	LNG 295
B(14)=D6/T	LNG 296
B(15)=D6/T2	LNG 297
B(16)=D7/T	LNG 298
B(17)=D8/T	LNG 299
B(18)=D8/T2	LNG 300
B(19)=D9/T2	LNG 301
B(20)=D3*F/T2	LNG 302
B(21)=D3*F/T3	LNG 303
B(22)=D5*F/T2	LNG 304
B(23)=D5*F/T4	LNG 305
B(24)=D7*F/T2	LNG 306
B(25)=D7*F/T3	LNG 307
B(26)=D9*F/T2	LNG 308
B(27)=D9*F/T4	LNG 309
B(28)=D11*F/T2	LNG 310
B(29)=D11*F/T3	LNG 311
B(30)=D13*F/T2	LNG 312
B(31)=D13*F/T3	LNG 313
B(32)=D13*F/T4	LNG 314
	LNG 315

102	P=0	LNG 316
	DO 101 I=1,32	LNG 317
101	P=P+B(I)*G(I)	LNG 318
	P=P+R*D*T	LNG 319
	PP=P	LNG 320
	RETURN	LNG 321
	ENTRY DPDD	LNG 322
	K=2	LNG 323
	GO TO 1	LNG 324
200	CONTINUE	LNG 325
	F1=2.00*F*GM*D	LNG 326
	F21=3.000*F*D2 +F1*D3	LNG 327
	F22=5.000*F*D4 +F1*D5	LNG 328
	F23=7.000*F*D6 +F1*D7	LNG 329
	F24=9.000*F*D8 +F1*D9	LNG 330
	F25=11.00*F*D10+F1*D11	LNG 331
	F26=13.00*F*D12+F1*D13	LNG 332
	B( 1)=2.00*D*T	LNG 333
	B( 2)=2.00*D*TS	LNG 334
	B( 3)=2.00*D	LNG 335
	B( 4)=2.00*D/T	LNG 336
	B( 5)=2.00*D/T2	LNG 337
	B( 6)=3.00*D2*T	LNG 338
	B( 7)=3.00*D2	LNG 339
	B( 8)=3.00*D2/T	LNG 340
	B( 9)=3.00*D2/T2	LNG 341
	B(10)=4.00*D3*T	LNG 342
	B(11)=4.00*D3	LNG 343
	B(12)=4.00*D3/T	LNG 344
	B(13)=5.00*D4	LNG 345
	B(14)=6.00*D5/T	LNG 346
	B(15)=6.00*D5/T2	LNG 347
	B(16)=7.00*D6/T	LNG 348
	B(17)=8.00*D7/T	LNG 349
	B(18)=8.00*D7/T2	LNG 350
	B(19)=9.00*D8/T2	LNG 351
	B(20)=F21/T2	LNG 352
	B(21)=F21/T3	LNG 353
	B(22)=F22/T2	LNG 354
	B(23)=F22/T4	LNG 355
	B(24)=F23/T2	LNG 356
	B(25)=F23/T3	LNG 357
	B(26)=F24/T2	LNG 358
	B(27)=F24/T4	LNG 359
	B(28)=F25/T2	LNG 360
	B(29)=F25/T3	LNG 361
	B(30)=F26/T2	LNG 362
	B(31)=F26/T3	LNG 363
	B(32)=F26/T4	LNG 364
202	P=0	LNG 365
	DO 201 I=1,32	LNG 366
201	P=P+B(I)*G(I)	LNG 367
	P=P+R*T	LNG 368
	PP=P	LNG 369
	RETURN	LNG 370
	END	LNG 371
	SUBROUTINE DATA N2	LNG 372
C	INITIALIZES THE EQUATION OF STATE CONSTANTS TO NITROGEN	LNG 373
	DIMENSION G(32),VP(9),GI(11)	LNG 374
	COMMON/DATA/G,R,GAMMA,VP,DTP	LNG 375
	R=8.20539E-2	LNG 376
	GAMMA=-.0056	LNG 377
	G( 1)= 0.136224769272827E-02	LNG 378

```

G( 2)= 0.107032469908591E 00 LNG 379
G( 3)= -0.243900721871413E 01 LNG 380
G( 4)= 0.341007449376470E 02 LNG 381
G( 5)= -0.422374309466167E 04 LNG 382
G( 6)= 0.105098600246494E-03 LNG 383
G( 7)= -0.112594826522081E-01 LNG 384
G( 8)= 0.142600789270907E-03 LNG 385
G( 9)= 0.184698501609007E 05 LNG 386
G(10)= 0.811140082588776E-07 LNG 387
G(11)= 0.233011645038006E-02 LNG 388
G(12)= -0.507752586350986E 00 LNG 389
G(13)= 0.485027881931214E-04 LNG 390
G(14)= -0.113656764115364E-02 LNG 391
G(15)= -0.707430273540575E 00 LNG 392
G(16)= 0.751706648852680E-04 LNG 393
G(17)= -0.111614119537424E-05 LNG 394
G(18)= 0.368796562233495E-03 LNG 395
G(19)= -0.201317691347729E-05 LNG 396
G(20)= -0.169717444755949E 05 LNG 397
G(21)= -0.119719240044192E 06 LNG 398
G(22)= -0.975218272038281E 02 LNG 399
G(23)= 0.554639713151823E 05 LNG 400
G(24)= -0.179920450443470E 00 LNG 401
G(25)= -0.256582926077184E 01 LNG 402
G(26)= -0.413707715090789E-03 LNG 403
G(27)= -0.256245415300293E 00 LNG 404
G(28)= -0.124222373740063E-06 LNG 405
G(29)= 0.103556535840165E-04 LNG 406
G(30)= -0.538699166558303E-09 LNG 407
G(31)= -0.757415412839596E-08 LNG 408
G(32)= 0.585367172069521E-07 LNG 409
VP(1)=5.1113192094 $ VP(2)=6.482667539E-1 LNG 410
VP(3)=-1.5108730916E-1 $ VP(4)=7.4028493342E-1 LNG 411
VP(5)=1.5 $ VP(6)=.123 $ VP(7)=63.15 $ VP(8)=126.26 LNG 412
VP(9)=0.0 LNG 413
DTP=31.0 LNG 414
RETURN $ END LNG 415
FUNCTION VPN(TT) LNG 416
C CALCULATES THE VAPOR PRESSURE OF BOTH METHANE AND NITROGEN LNG 417
DIMENSION G(32),VP(9) LNG 418
COMMON/DATA/G,R,GAMMA,VP,DTP LNG 419
T=TT LNG 420
X=(1.-VP(7)/T)/(1.-VP(7)/VP(8)) LNG 421
VPN=VP(6)*EXP(VP(1)*X+VP(2)*X*X+VP(3)*X**3+VP(9)*X**4+VP(4)*X* LNG 422
1(1.-X)**VP(5)) LNG 423
RETURN LNG 424
END LNG 425
FUNCTION RODEN(P,T,X) LNG 426
C THE HARD SPHERE MODEL,SEE SUBROUTINE FM FOR THE ARGUMENT LIST LNG 427
DIMENSION X(10) LNG 428
CALL FM(P,T,X,V,G) LNG 429
D=28. LNG 430
V=V+V IDEL(P,D,T,X) LNG 431
RODEN=1000./V LNG 432
RETURN LNG 433
END LNG 434
SUBROUTINE FM(Q,T,X,V9,G9) LNG 435
C PREDICTION OF EXCESS PROPERTIES WITH LHW POTENTIAL, COMP 1-METH LNG 436
C ANE,COMP 2-ETHANE,COMP 3-PROPANE,COMP 4 N-BUTANE,COMP 5-I-BUT LNG 437
C ANE, COMP 6-NITROGEN, COMP 7-NORMAL PENTANE,COMP 8-ISOPENTANE LNG 438
C ADV CRYO ENGR. VOL. 19 (1973)-REPROGRAMED BY R. MCCARTY,2/22/74 LNG 439
C ARGUMENTS ARE X-MOLE FRACTIONS,T-TEMPERATURE,Q-PRESSURE,V9-EXCESS LNG 440
C VOLUME,G9-EXCESS GIBBS ENERGY, FIRST THREE ARE INPUT,LAST TWO ARE LNG 441

```

```

C   OUTPUT,INPUT IS IN KELVINS AND BAR,                                LNG 442
    DIMENSION A(8),B(8) ,S(8),V(8),G(8),C(8,8),D(8,8),K(8,8),      LNG 443
    1J(8,8),E(8),Y(8),O(8),X(10)                                     LNG 444
    TYPE REAL J,K,N1                                                LNG 445
    DATA(KEY=1)                                                    LNG 446
    DATA(J(1,2)=-.00388616),(J(1,3)=-.0120932),(J(1,4)=-.0231577), LNG 447
    A(J(1,5)=-.0238349),(J(1,6)=-.00997547),(J(1,7)=-.0326),(J(1,8)= LNG 448
    B-.0458),(J(2,4)=-.00400910),(J(2,5)=-.00812712),(J(2,6)=-.0143976) LNG 449
    C,(J(2,7)=-.003),(J(2,8)=-.004),(J(3,4)=+.0007615710),(J(3,5)=-.003 LNG 450
    D83743),(J(3,6)=-.024014),(J(3,7)=0.0),(J(3,8)=0.0),(J(4,5)=.002221 LNG 451
    E50),(J(4,7)=.0),(J(4,8)=.0),(J(5,6)=-.0576043),(J(4,6)=-.0576043), LNG 452
    F(J(5,7)=.0),(J(5,8)=0.0),(J(6,7)=-.04),(J(6,8)=-.05),(J(7,8)=.0) LNG 453
    G ,(J(2,3)=-.002162)                                           LNG 454
    DATA(K(1,2)=.00298830),(K(1,3)=.0597378),(K(1,4)=.110893),( LNG 455
    AK(1,5)=.100298),(K(1,6)=.0197290),(K(1,7)=.14),(K(1,8)=.1745), LNG 456
    B(K(2,4)=.0677703),(K(2,5)=.0346632),(K(2,6)=.0529034),(K(2,7)= LNG 457
    C.02),(K(2,8)=.03),(K(3,4)=.0249291),(K(3,5)=-.00838212),(K(4,5)=.0 LNG 458
    D199213),(K(4,6)=.154365 ),(K(4,7)=.0),(K(4,8)=.0),(K(5,6)=.154365) LNG 459
    E,(K(5,7)=.0),(K(5,8)=.0),(K(6,7)=.15),(K(6,8)=.18),(K(7,8)=0.0) LNG 460
    F,(K(2,3)=.014527),(K(3,6)=.14719),(K(3,7)=0.0),(K(3,8)=0.0) LNG 461
    DATA(S=3.676E-8,4.158E-8,4.644E-8,5.051E-8,5.056E-8,3.546E-8, LNG 462
    15.389E-8,5.706E-8)                                           LNG 463
    DATA(A=2.755E+5,7.773E+5,14.165E+5,22.733E+5,21.279E+5,1.718E+5, LNG 464
    130.550E+5,42.946E+5)                                         LNG 465
    DATA(O=1.,1.5,1.67,1.83,1.79,1.03,1.91,2.11)                 LNG 466
C   THESE ARE THE ACENTRICITY FACTORS (FOR MOLECULAR SHAPES,ETC.) *** LNG 467
    DATA(Y=35.,45.,60.,75.,75.,40.,90.,105.)                     LNG 468
    DATA(P1=3.14159),(N1=6.025E+23),(R=8.3143 )                  LNG 469
    IF(KEY.EQ.0)GO TO 1                                           LNG 470
    KEY=0                                                           LNG 471
    DO 2 I=1,8                                                      LNG 472
    J(I,I)=0.0                                                       LNG 473
    K(I,I)=0.0                                                       LNG 474
    DO 2 M=I,8                                                      LNG 475
    J(M,I)=J(I,M)                                                  LNG 476
    2 K(M,I)=K(I,M)                                                LNG 477
    1 CONTINUE                                                      LNG 478
    P=Q*.1                                                           LNG 479
    IW=8                                                            LNG 480
    DO 10 I=1,IW                                                    LNG 481
    10 E(I)=O(I)                                                    LNG 482
    DO 15 I=1,IW                                                    LNG 483
    15 B(I)=(2./3.)*P1*N1*S(I)**3                                  LNG 484
    DO 20 I=1,IW                                                    LNG 485
    DO 20 M=1,IW                                                    LNG 486
    D(I,M) =(((B(I)**( 1./3. ) + B(M) ** ( 1./3.))/ 2. )*(1.-J(I,M) )) LNG 487
    1 **3                                                           LNG 488
    20 C( I , M ) = ( 1. - K( I , M ) ) * ( A(I)* A(M) ) ** ( 1. / 2. ) * LNG 489
    1( D( I , M ) **2 / ( B(I) * B(M) ) ) ** ( 1./2. )           LNG 490
    A2=0 $ B2=0                                                    LNG 491
    E2=0 $ V2=0                                                    LNG 492
    DO 25 I=1,IW                                                    LNG 493
    V2=V2+X(I)*Y(I)                                                LNG 494
    DO 25 M=1,IW                                                    LNG 495
    E2=E2+X(I)*X(M)*(E(I)+E(M))/2.                                LNG 496
    A2 = A2 + X(I) * X(M) * C( I , M )                             LNG 497
    25 B2=B2+X(I)*X(M)*D(I,M)                                       LNG 498
    V6=V2                                                           LNG 499
    DO 30 I = 1, IW                                                LNG 500
    A3 = A(I)                                                       LNG 501
    B3 = B(I)                                                       LNG 502
    E3 = E(I)                                                       LNG 503
    V2 = Y(I)                                                       LNG 504

```

```

V1 = FIND V1( A3, B3, E3, R, V2, P, T) LNG 505
G1 = FIND G1( A3, B3, E3, R, V2, P, T) LNG 506
V(I) = V1 LNG 507
30 G(I) = G1 LNG 508
A3=A2 LNG 509
B3=B2 LNG 510
E3=E2 LNG 511
V2=V6 LNG 512
V1=FIND V1(A3,B3,E3,R,V2,P,T) LNG 513
C G1=FIND G1(A3,B3,E3,R,V2,P,T) LNG 514
V7=V1 LNG 515
G7=G1 LNG 516
C EXCEAS VOLUME AND GIBS ENERGY LNG 517
V9=0 LNG 518
G9=0 LNG 519
DO 35 I=1,IW LNG 520
V9=V9-X(I)*V(I) LNG 521
35 G9=G9-X(I)*G(I) LNG 522
W9 = -V9 LNG 523
H9 = -G9 LNG 524
V9=V9+V7 LNG 525
G9=G9+G7 LNG 526
VIWW=V(IWW) LNG 527
RETURN LNG 528
END LNG 529
FUNCTION FIND V1( A3, B3, E3,R, V2, P, T ) LNG 530
C SOLVES THE HARD SPHERE EQUATION OF STATE FOR VOLUME GIVEN P AND T LNG 531
C A2 IS THE CONSTANT A, B2 IS THE CONSTANT B, E3 IS THE ACENTRICITY LNG 532
INDEX = 0 LNG 533
1 V1 = V2 LNG 534
X1 = B3 / ( 4. * V1 ) LNG 535
F2 = (( 1. + X1 + X1**2) / ( 1. - X1)**3) * E3 -A3 / ( V1 * R * T) LNG 536
1- (P * V1) / ( R*T) LNG 537
F3 = A3 / (R*T*V1**2) - P/ (R*T) LNG 538
F3 = F3 - ((( X1 + 2.* X1**2) * ( 1 - X1) + 3* ( 1. + X1 + X1**2) LNG 539
1* X1) / (( 1. - X1 )**4 * V1)) * E3 LNG 540
V2 = V1 - F2/ F3 LNG 541
IF( ABS( (V2 - V1) / V2) .LT. .00001 ) GO TO 2 LNG 542
INDEX = INDEX + 1 LNG 543
IF( INDEX .LT. 250 ) GO TO 1 LNG 544
2 V1 = V2 LNG 545
FIND V1 = V2 LNG 546
RETURN LNG 547
END LNG 548
FUNCTION FIND G1( A3, B3, E3,R, V2, P, T ) LNG 549
C CALCULATES THE GIBBS FREE ENERGY FOR THE HARD SPHERE EOS LNG 550
V1 = V2 LNG 551
X1 = B3 / ( 4. * V1 ) LNG 552
G1 =ALOG( 1. / ( 1. - X1 )) +(3. *X1) / ( 1. - X1) + ( 3. * X1**2) LNG 553
1 / ( 2. * ( 1. - X1 )**2) LNG 554
G1 = G1 - A3 / ( E3 * R * T*V1 ) + ( P * V1) / ( E3 * R * T ) -1.0 LNG 555
1 - ALOG( V1 ) LNG 556
G1 = R * T * E3 * G1 LNG 557
FIND G1 = G1 LNG 558
RETURN LNG 559
END LNG 560
FUNCTION EXCESS(P,DD,T,X) LNG 561
C CALCULATES THE EXCESS OR IDEAL VOLUM DEPENDING ON THE ENTRY LNG 562
DIMENSION X(10),F(10) LNG 563
KR=0 LNG 564
GO TO 1 LNG 565
ENTRY V IDEL LNG 566
KR=1 LNG 567

```

1	CONTINUE	LNG 568
	CALL ZERO(F)	LNG 569
	IF(X(1).LE..000001)GO TO 2	LNG 570
	CALL DATA CH4	LNG 571
	IF(T.GT.190.555)GO TO 12	LNG 572
	PM=VPN(T)+.00001	LNG 573
	DELP=P-PM	LNG 574
	D=SAT(T,1)	LNG 575
	CALL DPDD(DP,D,T)	LNG 576
	DELD=DELP/DP	LNG 577
	D=DELD+D	LNG 578
	F(1)=X(1)*1000./D	LNG 579
	GO TO 2	LNG 580
12	D=FINDD M(P,T,DD)	LNG 581
	IF(D.LE.0.0)D=1000.	LNG 582
	F(1)=X(1)*1000./D	LNG 583
2	IF(X(2).LE..000001)GO TO 3	LNG 584
	F(2)=X(2)*1000./SAT(T,2)	LNG 585
3	IF(X(3).LE..000001)GO TO 4	LNG 586
	F(3)=X(3)*1000./SAT(T,3)	LNG 587
4	IF(X(4).LE..00001)GO TO 5	LNG 588
	F(4)=X(4)*1000./SAT(T,4)	LNG 589
5	IF(X(5).LE..00001)GO TO 6	LNG 590
	F(5)=X(5)*1000./SAT(T,5)	LNG 591
6	IF(X(7).LE..00001)GO TO 61	LNG 592
	F(7)=X(7)*1000./SAT(T,7)	LNG 593
61	IF(X(8).LE..00001)GO TO 62	LNG 594
	F(8)=X(8)*1000./SAT(T,8)	LNG 595
62	IF(X(6).LE..00001)GO TO 8	LNG 596
	CALL DATA N2	LNG 597
	IF(T.GT.126.6)GO TO 7	LNG 598
	PN=VPN(T)+.000001	LNG 599
	DELP=P-PN	LNG 600
	D=SAT(T,6)	LNG 601
	CALL DPDD(DP,D,T)	LNG 602
	F(6)=X(6)*1000./(D+DELP/DP)	LNG 603
	GO TO 8	LNG 604
7	D=FINDD M(P,T,DD)	LNG 605
	IF(D.LE.0.0)D=1000.	LNG 606
	F(6)=X(6)*1000./D	LNG 607
8	V=1000./DD	LNG 608
	VS=0	LNG 609
	DO 21 I=1,8	LNG 610
21	VS=VS+F(I)	LNG 611
	EXCESS=V-VS	LNG 612
	IF(KR.GT.0)EXCESS=VS	LNG 613
	CALL DATA CH4	LNG 614
	RETURN	LNG 615
	END	LNG 616
	SUBROUTINE ZERO(X)	LNG 617
C	INITIALIZES THE COMPONENT MATRIX TO 0	LNG 618
	DIMENSION X(10)	LNG 619
	DO 1 I=1,10	LNG 620
1	X(I)=0.0	LNG 621
	RETURN	LNG 622
	END	LNG 623
	FUNCTION FMKM(T,X)	LNG 624
C	THE REVISED KLOSEK AND MCKINLEY METHOD,THE INPUT IS TEMPERATURE	LNG 625
C	AND THE COMPONENT MATRIX. TEMPERATURE IS IN KELVIN,OUTPUT IS	LNG 626
C	DENSITY IN MOLES PER LITER. THE ALLOWABLE COMPONENTS ARE C1,C2,C3	LNG 627
C	NC4,IC4,N2,NC5,IC5 IN THAT ORDER. THIS METHOD SHOULD NOT BE USED	LNG 628
C	FOR MIXTURES WITH LESS THAN 60% METHANE, OR FOR MIXTURES CONTAININ	LNG 629
C	MORE THAN 4% NITROGEN OR MORE THAN 4% EACH OF NC4 OR IC4 OR MORE	LNG 630

C	THAN 2% TOTAL OF NC5 AND IC5.	LNG 631
	DIMENSION TM(100),TN(100),X(10),Q(8)	LNG 632
	DATA(Q=16.04303,30.07012,44.09721,58.1243,58.1243,28.0134,72.1513	LNG 633
	19,72.15139)	LNG 634
	DATA((TM(I),I=1,10)=-.005,.12,.22,.34,.43,.515,.595,.66,.725,.795)	LNG 635
	DATA((TM(I),I=11,20)=-.006,.135,.26,.38,.5,.59,.665,.74,.81,.885)	LNG 636
	DATA((TM(I),I=21,30)=-.007,.15,.3,.425,.575,.675,.755,.83,.91,.99)	LNG 637
	DATA((TM(I),I=31,40)=-.007,.165,.34,.475,.635,.735,.84,.92,1.045,	LNG 638
	A1.12)	LNG 639
	DATA((TM(I),I=41,50)=-.008,.19,.375,.535,.725,.835,.95,1.055,1.155	LNG 640
	A,1.245)	LNG 641
	DATA((TM(I),I=51,60)=-.009,.22,.44,.61,.81,.945,1.065,1.18,1.28,	LNG 642
	A1.38)	LNG 643
	DATA((TM(I),I=61,70)=-.01,.25,.5,.695,.92,1.055,1.205,1.33,1.45,	LNG 644
	A1.55)	LNG 645
	DATA((TM(I),I=71,80)=-.013,.295,.59,.795,1.035,1.21,1.385,1.525,	LNG 646
	11.64,1.75)	LNG 647
	DATA((TM(I),I=81,90)=-.015,.345,.7,.92,1.2,1.37,1.555,1.715,	LNG 648
	A1.86,1.99)	LNG 649
	DATA((TM(I),I=91,100)=-.017,.4,.825,1.06,1.39,1.59,1.8,1.95,	LNG 650
	A2.105,2.272)	LNG 651
	DATA((TN(I),I=1,10)=-.004,.1,.22,.35,.5,.6,.69,.78,.86,.95)	LNG 652
	DATA((TN(I),I=11,20)=-.005,.12,.28,.43,.59,.71,.83,.94,1.05,1.14)	LNG 653
	DATA((TN(I),I=21,30)=-.007,.16,.34,.49,.64,.79,.94,1.08,1.17,1.27)	LNG 654
	DATA((TN(I),I=31,40)=-.01,.24,.42,.61,.75,.91,1.05,1.19,1.33,1.45)	LNG 655
	DATA((TN(I),I=41,50)=-.015,.32,.59,.77,.92,1.07,1.22,1.37,1.52,	LNG 656
	11.71)	LNG 657
	DATA((TN(I),I=51,60)=-.024,.41,.72,.95,1.15,1.22,1.3,1.45,1.65,2.)	LNG 658
	DATA((TN(I),I=61,70)=-.032,.6,.91,1.23,1.43,1.63,1.85,2.08,2.3,	LNG 659
	12.45)	LNG 660
	DATA((TN(I),I=71,80)=-.043,.71,1.13,1.48,1.73,1.98,2.23,2.48,2.75	LNG 661
	1,2.9)	LNG 662
	DATA((TN(I),I=81,90)=-.058,.95,1.46,1.92,2.2,2.42,2.68,3.,	LNG 663
	A3.32,3.52)	LNG 664
	DATA((TN(I),I=91,100)=-.075,1.3,2.,2.4,2.6,3.,3.4,3.77,	LNG 665
	A3.99,4.23)	LNG 666
	IF(X(1).LT..00001)GO TO 20	LNG 667
	AW=0.0	LNG 668
	DO 1 I=1,8	LNG 669
1	AW=AW+X(I)*Q(I)	LNG 670
	VI=VIDEAL(T,X)	LNG 671
	J=1	LNG 672
	IF(T.GE.95.)J=11	LNG 673
	IF(T.GE.100.)J=21	LNG 674
	IF(T.GE.105.)J=31	LNG 675
	IF(T.GE.110.)J=41	LNG 676
	IF(T.GE.115.)J=51	LNG 677
	IF(T.GE.120.)J=61	LNG 678
	IF(T.GE.125.)J=71	LNG 679
	IF(T.GE.130.)J=81	LNG 680
	JJ=J+9	LNG 681
	W=15.	LNG 682
	DO 5 I=J,JJ	LNG 683
	W=W+1.	LNG 684
	IF(AW.GT.W)GO TO 5	LNG 685
	GO TO 6	LNG 686
5	CONTINUE	LNG 687
	I=JJ	LNG 688
6	DIF1=AW-W	LNG 689
	J=I-1	LNG 690
	FK=(TM(I)-TM(J))*DIF1+TM(I)	LNG 691
	FK1=(TM(I+10)-TM(J+10))*DIF1+TM(I+10)	LNG 692
	IT=(T+.00001)/5.	LNG 693

```

DIF2=T-IT*5 LNG 694
IF(T.GE.135.)DIF2=T-130. LNG 695
IF(T.LT.90.)DIF2=T-90. LNG 696
FK=FK+(FK1-FK)*DIF2/5. LNG 697
IF(X(6).LT..0001)GO TO 17 LNG 698
FKN=(TN(I)-TN(J))*DIF1+TN(I) LNG 699
FK1=(TN(I+10)-TN(J+10))*DIF1+TN(I+10) LNG 700
FKN=FKN+(FK1-FKN)*DIF2/5. LNG 701
FK=FK+(FKN-FK)*X(6)/.0425 LNG 702
17 FK=FK/1000. LNG 703
FMKM=1./(VI-FK*X(1)) LNG 704
RETURN LNG 705
20 FMKM=0.0 LNG 706
RETURN LNG 707
END LNG 708
FUNCTION V IDEAL(T,X) LNG 709
C CALCULATES THE IDEAL VOLUME OF A MIXTURE FOR THE K AND M METHOD LNG 710
DIMENSION X(10) LNG 711
V=0 LNG 712
J=0 LNG 713
IF(X(6).GT..0001.AND.T.GT.115.)J=1 LNG 714
DO 10 I=1,8 LNG 715
IF(X(I).LE..000001)GO TO 10 LNG 716
IF(J.GT.0.AND.I.EQ.6)GO TO 10 LNG 717
V=V+X(I)/SAT(T,I) LNG 718
10 CONTINUE LNG 719
IF(J.EQ.1)V=V+X(6)/SATN2(T) LNG 720
VIDEAL=V LNG 721
RETURN LNG 722
END LNG 723
FUNCTION SATN2(T) LNG 724
C CALCULATES A PSEUDO SATURATED LIQUID DENSITY FOR N2 ABOVE 115 K LNG 725
IF(T.LT.115.)GO TO 1 LNG 726
DELT=(T-115.) LNG 727
SATN2=SAT(115.,6)+DELT*(SAT(115.05,6)-SAT(114.95,6))/1 LNG 728
RETURN LNG 729
1 SATN2=SAT(T,6) LNG 730
RETURN LNG 731
END LNG 732
FUNCTION SAT(T,I) LNG 733
C CALCUALTES THE PURE FLUID DENSITIES FOR THE K AND M METHOD LNG 734
C UNITS ARE DEG K AND MOLES/LITER LNG 735
DIMENSION A(7,8) LNG 736
DATA((A(I),I=1,7)=190.555,10.16,18.65812322,6.712030737, LNG 737
1-.9472019702,0.0,0.0) LNG 738
DATA((A(I),I=8,14)=305.33, LNG 739
1 6.86,12.55205121,13.43284373,-19.00461066,11.07715985,0.0) LNG 740
DATA((A(I),I=15,21)=369.82,5.,8.684458671,18.04085714,-29.46261356 LNG 741
1,16.43559114,0.0) LNG 742
DATA((A(I),I=22,28)=425.16,3.92, LNG 743
1 7.286062567,11.96307859,-19.87591962, LNG 744
211.60211932,0.0) LNG 745
DATA((A(I),I=29,35)=408.13,3.8, LNG 746
1 7.657535400,8.145251283,-13.10582462, LNG 747
28.145894091,0.0) LNG 748
DATA((A(I),I=36,42)=126.2,11.21,19.39216835,26.01408462,-39.497587 LNG 749
191,23.32977312,0.0) LNG 750
DATA((A(I),I=43,49)=469.6,3.285,-.0362004993,59.00202990, LNG 751
1-93.44193819,43.66780833,0.0) LNG 752
DATA((A(I),I=50,56)=460.39,3.271,2.946310456,35.50770979, LNG 753
1-57.41242993,28.15898339,0.0) LNG 754
IF(T.GT.A(1,I))GO TO 1 LNG 755
X=(1.-T/A(1,I)) LNG 756

```



	COMMON/UNITS/ITC,IPC,T,TMAX,DT,P,PMAX,DP,PS	LNG 820
	SWITCH = 0	LNG 821
1	CALL ZERO1	LNG 822
C	THE NEXT VALUES ARE SET TO PREVENT UNDER/OVER FLOWS	LNG 823
	TMAX = 100.0	LNG 824
	DT = 100.0	LNG 825
	PMAX = 100.0	LNG 826
	DP = 100.0	LNG 827
	PS = 100.0	LNG 828
	CALL INPUT(Q)	LNG 829
	CODE=0	LNG 830
	ITC=0	LNG 831
	IPC=0	LNG 832
	P=PIN/1.01325	LNG 833
	T=TIN	LNG 834
	IF(T.GT.(160.)) GO TO 19	LNG 835
8	CALL PZERO(CTMX)	LNG 836
	MWM = 0	LNG 837
	DO 9 I = 1,NC	LNG 838
	MWM = MWM + (X(I)*MW(I))	LNG 839
9	CONTINUE	LNG 840
10	DO 11 I = 1,NC	LNG 841
	TBI(I) = T / TS(I)	LNG 842
	CALL VOLUME(TBI(I),VBI(I),JPUR,NC)	LNG 843
	TBIM(I) = T / TSIM(I)	LNG 844
	CALL VOLUME(TBIM(I),VBIM(I),JMIX,NC)	LNG 845
11	CONTINUE	LNG 846
	VM = 0.0	LNG 847
	DO 12 I = 1,NC	LNG 848
	VM = VM + (X(I)*VBIM(I)*VSIM(I))	LNG 849
12	CONTINUE	LNG 850
	TMP = ( T * 1.8) - (459.67)	LNG 851
	DO 13 I = 1,NC	LNG 852
	VHOLD(I) = VBI(I)	LNG 853
	VPHOLD(I) = VBIM(I)	LNG 854
	PP = (P*TS(I))/US(I)	LNG 855
	VBIMP(I) = VBI(I)	LNG 856
	CALL PRES(PP,VBIMP(I),TBI(I),NC)	LNG 857
	VBI(I) = VBIMP(I)	LNG 858
	PP = (P * TSIM(I)) / USIM(I)	LNG 859
	VBIMP(I) = VBIM(I)	LNG 860
	CALL PRES(PP,VBIMP(I),TBIM(I),NC)	LNG 861
	VBIM(I) = VBIMP(I)	LNG 862
13	CONTINUE	LNG 863
	VMP = 0.0	LNG 864
	DO 14 I = 1,NC	LNG 865
	VMP = VMP + (X(I)*VBIMP(I)*VSIM(I))	LNG 866
	PD(I) = VBIMP(I) * VSIM(I)	LNG 867
14	CONTINUE	LNG 868
	DENS=MWM/VMP	LNG 869
	DOUT=DENS*1000./MWM	LNG 870
	RETURN	LNG 871
19	DOUT=0.0	LNG 872
	RETURN	LNG 873
	END	LNG 874
	SUBROUTINE ZERO1	LNG 875
	COMMON /RUN/A(361)	LNG 876
	COMMON /DAT/B(224)	LNG 877
	DO 1 I = 1,361	LNG 878
1	A(I) = 0.0	LNG 879
	DO 2 I = 1,224	LNG 880
2	B(I) = 0.0	LNG 881
		LNG 882

```

RETURN LNG 883
END LNG 884
SUBROUTINE INPUT(Q) LNG 885
DIMENSION NNO( 8),SIGM( 8),EPSI( 8),LAMB( 8),NAME(2, 8),SNO( 8),MO LNG 886
1L( 8),CT( 8),TCH( 8),VCH( 8),ECH( 8),AR( 8),AZ( 8),Q(8) LNG 887
TYPE INTEGER CNT1,CNT2,SWITCH LNG 888
TYPE REAL MWM,INCR,KIJ,MW,MOL,LAM,LAMB LNG 889
COMMON /RUN/ID(12),X(12),NAM(2,12),C12(12,12),R(12),Z(12),S(12),VS LNG 890
1(12),TS(12),US(12),SG(12),EP(12),LAM(12),NC,MW(12),AIJ(12,12),PST( LNG 891
212),TCT(12) LNG 892
COMMON /DAT/TBI(12),VBI(12),TBIM(12),VBIM(12),C(12),SGIM(12),SIM(1 LNG 893
12),EPIM(12),PIM(12),SIN(12),VSIM(12),USIM(12),TSIM(12),DVBIM(12),P LNG 894
2D(12),PV(12),RHO(12),VBIMP(12),TTM(12),MWM,CNT1,CNT2,TOLD(12),INCR LNG 895
3(12),SWITCH,JPC,JPCS,JMIX,DENS,VEX,HEX,GEX,TMP,VMP,TP LNG 896
COMMON/PAR/KIJ( 8, 8),AJI( 8, 8) LNG 897
DATA SIGM/ LNG 898
*0.991000,1.029000,1.155000,1.278000,1.388752,1.392995, LNG 899
*1.47162,1.47217/ LNG 900
DATA EPSI/ LNG 901
*0.640000,0.909000,1.69800,2.237000,2.705262,2.545907, LNG 902
*3.76195,3.68336/ LNG 903
DATA LAMB/ LNG 904
*1.053604,0.986325,1.227117,1.408519,1.473346,1.461676, LNG 905
*1.698790,1.695012/ LNG 906
DATA MOL/ LNG 907
*28.01600,16.04200,30.06800,44.09400,58.12000,58.12000, LNG 908
*72.146000,72.146000/ LNG 909
DATA SNO/ LNG 910
*10.00000,10.00000,10.00000,10.00000,10.00000,10.00000, LNG 911
*10.00000,10.00000/ LNG 912
DATA CT/ LNG 913
*126.0600,190.5600,305.4300,369.8200,425.1600,408.0300, LNG 914
*469.65,460.39/ LNG 915
DATA TCH/ LNG 916
*112.7699,170.9645,256.8311,294.7255,340.7867,322.6109, LNG 917
*411.0100,403.3200/ LNG 918
DATA VCH/ LNG 919
*26.01846,29.04010,40.88188,54.60301,68.72075,69.44272, LNG 920
*84.90197,84.99830/ LNG 921
DATA ECH/ LNG 922
*1393.000,1977.000,3695.000,4867.000,5886.652,5539.895, LNG 923
*8186.000,8015.000/ LNG 924
DATA AR/ LNG 925
*1.000000,1.000000,1.000000,1.000000,1.000000,1.000000, LNG 926
*1.000000,1.000000/ LNG 927
DATA AZ/ LNG 928
*10.00000,10.00000,10.00000,10.00000,10.00000,10.00000, LNG 929
*10.00000,10.00000/ LNG 930
DO 4 I=2,6 LNG 931
4 X(I)=Q(I-1) LNG 932
X(1)=Q(6) LNG 933
X(7)=Q(7) LNG 934
X(8)=Q(8) LNG 935
NC=0 LNG 936
DO 1 I=1,8 LNG 937
IF(X(I).LE.0.0)GO TO 1 LNG 938
NC=NC+1 LNG 939
X(NC)=X(I) LNG 940
ID(NC)=I LNG 941
1 CONTINUE LNG 942
DO 2 I = 1,NC LNG 943
J = ID(I) LNG 944
R(I) = AR(J) LNG. 945

```

```

Z(I) = AZ(J) LNG 946
S(I) = SNO(J) LNG 947
TS(I)= TCH(J) LNG 948
US(I)= ECH(J) LNG 949
SG(I) = SIGM(J) LNG 950
TCT(I) = CT(J) LNG 951
EP(I) = EPSI(J) LNG 952
LAM(I) = LAMB(J) LNG 953
VS(I) = VCH(J) LNG 954
MW(I) = MOL(J) LNG 955
2 CONTINUE LNG 956
DO 3 I = 1,NC LNG 957
DO 3 J = 1,NC LNG 958
M = ID(I) LNG 959
L = ID(J) LNG 960
C12(I,J) = KIJ(M,L) LNG 961
C12(J,I) = KIJ(L,M) LNG 962
AIJ(I,J) = AJI(M,L) LNG 963
AIJ(J,I) = AJI(L,M) LNG 964
3 CONTINUE LNG 965
RETURN LNG 966
END LNG 967
END LNG 968
SUBROUTINE PZERO(TRT) LNG 969
TYPE INTEGER CNT1,CNT2,SWITCH LNG 970
TYPE REAL MWM,INCR,KIJ,MW,MOL,LAM,LAMB LNG 971
COMMON /RUN/ID(12),X(12),NAM(2,12),C12(12,12),R(12),Z(12),S(12),VS LNG 972
1(12),TS(12),US(12),SG(12),EP(12),LAM(12),NC,MW(12),AIJ(12,12),PST( LNG 973
212),TCT(12) LNG 974
COMMON /DAT/TBI(12),VBI(12),TBIM(12),VBIM(12),C(12),SGIM(12),SIM(1 LNG 975
12),EPIM(12),PIM(12),SIN(12),VSIM(12),USIM(12),TSIM(12),DYBIM(12),P LNG 976
2D(12),PV(12),RHO(12),VBIMP(12),TTM(12),MWM,CNT1,CNT2,TOLD(12),INCR LNG 977
3(12),SWITCH,JPC,JPCS,JMIX,DENS,VEX,HEX,GEX,TMP,VMP,TP LNG 978
COMMON/PAR/KIJ( 8, 8),AJI( 8, 8) LNG 979
COMMON /UNITS/ITC,IPC,T,TMAX,DT,P,PMAX,DP,PS LNG 980
IF(NC.EQ.1) TRT = T/TCT(1) LNG 981
IF(NC.GT.1) CALL TCM(TRT) LNG 982
IF(NC.GT.1) TRT = T/TRT LNG 983
IF(NC.EQ.1) CALL PURE(TRT,TRT,R(1),RXX) LNG 984
DO 1 I = 1,NC LNG 985
TCXX = T/TCT(I) LNG 986
IF(NC.GT.1) CALL PURE(TCXX,TRT,R(I),RTR) LNG 987
JPC = 0 LNG 988
IF(TRT.GT.(.87)) JPC = 2 LNG 989
IF(TRT.GT.(1.0)) JPC = 1 LNG 990
IF(NC.EQ.1) RTR = RXX LNG 991
C THERE ARE SEVERAL OTHER FORMS OF THESE EQUATIONS LNG 992
C REFER TO ORIGINAL ARTICLES FOR VALUES TO USE LNG 993
S(I) = RTR * Z(I) - 2. * RTR + 2. LNG 994
SIM(I) = S(I) LNG 995
LNG 996
SG(I) = (VS(I)/RTR ) **(.1/.3.) LNG 997
EP(I) = US(I) / S(I) LNG 998
C(I) = LAM(I) * (2176./((185.6)*(1.98726))) LNG 999
TTM(I) = TS(I) LNG1000
TOLD(I) = TS(I) LNG1001
INCR(I) = (20.0) LNG1002
1 CONTINUE LNG1003
JPUR = 0 LNG1004
CNT1 = 1 LNG1005
CNT2 = 1 LNG1006
JMIX = 0 LNG1007
2 DEN = 0 LNG1008

```

DO 3 I = 1,NC	LNG1009
DEN = DEN + (X(I) * SIM(I))	LNG1010
3 CONTINUE	LNG1011
DO 4 I = 1,NC	LNG1012
PIM(I) = (X(I) * SIM(I)) / DEN	LNG1013
4 CONTINUE	LNG1014
DO 6 I = 1,NC	LNG1015
SGIM(I) = 0.0	LNG1016
DO 6 J = 1,NC	LNG1017
M = I	LNG1018
N = J	LNG1019
IF(I.GT.J) M = J	LNG1020
IF(I.GT.J) N = I	LNG1021
IF(I.EQ.J) GO TO 5	LNG1022
TRUDX = (AIJ(N,M)/(T/TTM(I)))	LNG1023
IF(TRUDX.LT.(-180.0)) GO TO 5	LNG1024
SGIM(I) = SGIM(I) + ((PIM(J) * (((SG(I)**(1./3.) + SG(J)**(1./3.))	LNG1025
1/(2.0))**3))* (AIJ(M,N) * EXP(AIJ(N,M)/(T/TTM(I))))	LNG1026
GO TO 6	LNG1027
5 SGIM(I) = SGIM(I) + (PIM(J) * (((SG(I)**(1./3.) + SG(J)**(1./3.))	LNG1028
1/(2.0))**3 )	LNG1029
6 CONTINUE	LNG1030
DEN = 0.0	LNG1031
DO 7 I = 1,NC	LNG1032
DEN = DEN + (PIM(I)* SGIM(I)* SGIM(I))	LNG1033
7 CONTINUE	LNG1034
DO 8 I = 1,NC	LNG1035
SIN(I) =(S(I) * (SGIM(I)**(2.))) / DEN	LNG1036
8 CONTINUE	LNG1037
	LNG1038
DO 9 I = 1,NC	LNG1039
TEST = (1.0) - (SIM(I) / SIN(I))	LNG1040
TEST = ABS (TEST)	LNG1041
IF(TEST.GT.(0.00001)) GO TO 10	LNG1042
9 CONTINUE	LNG1043
GO TO 12	LNG1044
10 DO 11 I = 1,NC	LNG1045
SIM(I) =(SIM(I) + SIN(I)) / (2.0)	LNG1046
11 CONTINUE	LNG1047
CNT1 = CNT1 + 1	LNG1048
IF(CNT1.GT.250) GO TO 12	LNG1049
GO TO 2	LNG1050
12 DO 14 I = 1,NC	LNG1051
SIM(I) = SIN(I)	LNG1052
EPIM(I) = 0.0	LNG1053
DO 14 J = 1,NC	LNG1054
K = I	LNG1055
L = J	LNG1056
IF(J.LT.I) K = J	LNG1057
IF(J.LT.I) L = I	LNG1058
IF(I.EQ.J) GO TO 13	LNG1059
TRUDX = C12(L,K) / (T/TTM(I))	LNG1060
IF(TRUDX.LT.(-180.0)) GO TO 13	LNG1061
EPIM(I) = EPIM(I) + ((PIM(J) * SQRT(EP(I)*EP(J)))*	LNG1062
1(C12(K,L) * EXP((C12(L,K) / (T/TTM(I))))))	LNG1063
GO TO 14	LNG1064
13 EPIM(I) = EPIM(I) + (PIM(J) * SQRT(EP(I) * EP(J)))	LNG1065
14 CONTINUE	LNG1066
C ASSUME NUMBER OF MOLS OF MIXTURE = 1.0	LNG1067
DO 15 I = 1,NC	LNG1068
VSIM(I) = R(I) * (SGIM(I)**(3.0))	LNG1069
USIM(I) = SIM(I) * EPIM(I)	LNG1070
TSIM(I) = USIM(I) / ((1.98726) * C(I))	LNG1071

15 CONTINUE	LNG1072
DO 16 I = 1,NC	LNG1073
TEST = (1.0) - (TSIM(I)/TTM(I))	LNG1074
TEST = ABS(TEST)	LNG1075
IF(TEST.GT.(0.00001)) GO TO 17	LNG1076
16 CONTINUE	LNG1077
RETURN	LNG1078
17 DO 20 I = 1,NC	LNG1079
IF(TSIM(I) - TTM(I))18,20,19	LNG1080
18 TNEW = TTM(I) - INCR(I)	LNG1081
IF(TNEW.EQ.TOLD(I)) INCR(I) = INCR(I) / (2.0)	LNG1082
IF(TNEW.EQ.TOLD(I)) GO TO 18	LNG1083
TOLD(I) = TTM(I)	LNG1084
TTM(I) = TNEW	LNG1085
GO TO 20	LNG1086
19 TNEW = TTM(I) + INCR(I)	LNG1087
IF(TNEW.EQ.TOLD(I)) INCR(I) = INCR(I) / (2.0)	LNG1088
IF(TNEW.EQ.TOLD(I)) GO TO 19	LNG1089
TOLD(I) = TTM(I)	LNG1090
TTM(I) = TNEW	LNG1091
20 CONTINUE	LNG1092
CNT2 = CNT2 + 1	LNG1093
IF(CNT2.GT.250) RETURN	LNG1094
GO TO 2	LNG1095
END	LNG1096
SUBROUTINE PURE(TZ,T,Z,R)	LNG1097
DIMENSION A(15)	LNG1098
IF(TZ.LT.(.8653525)) R = Z	LNG1099
IF(TZ.LT.(.8653525)) GO TO 2	LNG1100
IF(T.LT.(.8653525)) R = Z	LNG1101
IF(T.LT.(.8653525)) GO TO 2	LNG1102
IF(T.GT.(1.0)) TA = 1.0	LNG1103
IF(T.LE.(1.0)) TA = T	LNG1104
DATA A/.9184780,-.1530647,-.1090050,.8073883,1.441803,	LNG1105
1-10.85944,-6.041687,51.26758,.9062500,-108.9805,28.88672,	LNG1106
2106.1406,-45.78125,-38.43750,20.56250/	LNG1107
R = 0.0	LNG1108
TT = (TA - (.9267292)) / (.7267517E-01)	LNG1109
DO 1 K = 1,14	LNG1110
R = R + A(16-K)	LNG1111
R = R * TT	LNG1112
1 CONTINUE	LNG1113
R = R + A(1)	LNG1114
2 RETURN	LNG1115
END	LNG1116
SUBROUTINE VOLUME(T,V,J,NC)	LNG1117
TR = T	LNG1118
IF(TR.GT.(1.00)) GO TO 4	LNG1119
V = 0.5	LNG1120
1 VT = (1.0) + (0.1*TR*V**(4.0))	LNG1121
ERR = (1.0) - (V/VT)	LNG1122
TEST = ABS(ERR)	LNG1123
IF(TEST.LE.(0.00001)) GO TO 2	LNG1124
V = VT	LNG1125
GO TO 1	LNG1126
2 V = V**(3.0)	LNG1127
3 RETURN	LNG1128
4 V = ((((((10.06600 *TR)-24.79837)*TR)+23.260722)*TR)-6.686880)	LNG1129
GO TO 3	LNG1130
END	LNG1131
SUBROUTINE BETA(P,DV,T,V,KK)	LNG1132
	LNG1133
	LNG1134

TYPE REAL AF,BF,CF,DF,EF,AG,BG,CG,DG,P,DV,T,V,F,F1,G,G1,DEN,EG	LNG1135
TYPE REAL C,B1,B2,B3	LNG1136
DIMENSION C(11)	LNG1137
DATA AF/O.11566564E+02/,BF/-0.53510144E+01/,CF/-0.74598207E-01/,	LNG1138
1DF/O.67068653E+00/,EF/-0.11939887E+00/,AG/O.62721813E+01/,	LNG1139
2BG/O.47698365E+00/,CG/-0.16023080E+01/,DG/O.49837746E+00/,	LNG1140
3EG/-0.42639183E-01/	LNG1141
F = AF +(BF*V)+(CF*V*V)+ (DF*V*V*V)+(EF*V*V*V*V)	LNG1142
IF(F.LT.(0.0)) GO TO 1	LNG1143
F1 = (BF+(CF*V*2.E+00)+(DF*V*V*3.E+00)+(EF*V*V*V*4.E+00))*	LNG1144
1T * EXP(F)	LNG1145
G = AG+(BG*V)+(CG*V*V)+(DG*V*V*V)+(EG*V*V*V*V)	LNG1146
IF(G.LT.(0.00)) GO TO 1	LNG1147
G1 = (BG+(CG*V*2.E+00)+(DG*V*V*3.E+00+(EG*V*V*V*4.E+00))) * EXP(G	LNG1148
1)	LNG1149
G1 = -G1	LNG1150
DEN = F1 + G1	LNG1151
DV = (1.E+00) / DEN	LNG1152
IF(DV.GT.(0.0).OR.DV.LT.(-1.0E+00)) GO TO 1	LNG1153
GO TO 2	LNG1154
DATA C/- .118659822E+02, -.5509099E+00, .4172102E+01, -.8996686E+00,	LNG1155
1-.1500376E+01, -.1958324E+00, -.2788988E+01, .5195283E+00,	LNG1156
2.3734878E+01, .1361904E+00, .4671948E-01/	LNG1157
1 B1 = C(1) + C(2)*T + C(3)*V	LNG1158
B2 = C(4)*((V+C(5))**(2 ))*EXP((C(6))*((T+C(7))**(2 )))	LNG1159
B3 = C(11) * (V+C(8))**(C(9))/(T**(C(10)))	LNG1160
DV = B1 + B2 + B3	LNG1161
DV = EXP(DV)	LNG1162
DV = - DV	LNG1163
2 RETURN	LNG1164
END	LNG1165
SUBROUTINE PRES(A,B,C,NC)	LNG1166
TYPE REAL H,P,V,T,K1,K2,K3,K4,VT,PT	LNG1167
P = A	LNG1168
V = B	LNG1169
T = C	LNG1170
H = 1.E-02	LNG1171
IF(H.GT.P) H = P	LNG1172
ASSIGN 3 TO KK	LNG1173
1 CALL BETA(P,K1,T,V,NC)	LNG1174
K1 = H * K1	LNG1175
VT = V + ((0.5E+00) *K1)	LNG1176
PT = P + ((0.5E+00)*H)	LNG1177
CALL BETA(PT,K2,T,VT,NC)	LNG1178
K2 = K2 * H	LNG1179
VT = V + ((0.5E+00) *K2)	LNG1180
CALL BETA(PT,K3,T,VT,NC)	LNG1181
K3 = K3 * H	LNG1182
PT = P + H	LNG1183
VT = V + ( K3)	LNG1184
CALL BETA(PT,K4,T,VT,NC)	LNG1185
K4 = K4 * H	LNG1186
V = V + (((K1 + (2.E+00*K2) + (2.E+00*K3) + K4) / (6.E+00)) )	LNG1187
P = P - H	LNG1188
IF(P.EQ.(0.0)) GO TO 4	LNG1189
IF(P.LT.(0.0)) GO TO 2	LNG1190
GO TO 1	LNG1191
2 GO TO KK , (3,4)	LNG1192
3 P = P + H	LNG1193
H = P	LNG1194
ASSIGN 4 TO KK	LNG1195
GO TO 1	LNG1196
4 A = P	LNG1197

B = V	LNG1198
C = T	LNG1199
RETURN	LNG1200
END	LNG1201
SUBROUTINE TCM(TMC)	LNG1202
TYPE REAL NUM	LNG1203
TYPE INTEGER CNT1,CNT2,SWITCH	LNG1204
TYPE REAL MWM,INCR,KIJ,MW,MOL,LAM,LAMB	LNG1205
DIMENSION VCI(6),TH(12)	LNG1206
COMMON /RUN/ID(12),X(12),NAM(2,12),C12(12,12),R(12),Z(12),S(12),VS	LNG1207
1(12),TS(12),US(12),SG(12),EP(12),LAM(12),NC,MW(12),AIJ(12,12),PST(	LNG1208
212),TCT(12)	LNG1209
COMMON /DAT/TBI(12),VBI(12),TBIM(12),VBIM(12),C(12),SGIM(12),SIM(1	LNG1210
12),EPIM(12),PIM(12),SIN(12),VSIM(12),USIM(12),TSIM(12),DVBIM(12),P	LNG1211
2D(12),PV(12),RHO(12),VBIMP(12),TTM(12),MWM,CNT1,CNT2,TOLD(12),INCR	LNG1212
3(12),SWITCH,JPC,JPCS,JMIX,DENS,VEX,HEX,GEX,TMP,VMP,TP	LNG1213
COMMON/PAR/KIJ( 8, 8),AJI( 8, 8)	LNG1214
COMMON/UNITS/ITC,IPC,T,TMAX,DT,P,PMAX,DP,PS	LNG1215
DATA VCI/ 1.44,1.59,2.27,3.18,4.03,4.21/	LNG1216
DO 1 I = 1,NC	LNG1217
J = ID(I)	LNG1218
V = VCI(J)**(2./3.)	LNG1219
TH(I) = X(I) * V	LNG1220
1 CONTINUE	LNG1221
TTZ = 0.0	LNG1222
DO 2 I = 1,NC	LNG1223
TTZ = TTZ + TH(I)	LNG1224
2 CONTINUE	LNG1225
DO 3 I = 1,NC	LNG1226
TH(I) = TH(I) / TTZ	LNG1227
3 CONTINUE	LNG1228
SUM1 = 0.0	LNG1229
SUM2 = 0.0	LNG1230
K = NC - 1	LNG1231
DO 5 I = 1,K	LNG1232
L = I + 1	LNG1233
DO 4 J = L,NC	LNG1234
TTZ = (TCT(I)-TCT(J))/(TCT(I)+TCT(J))	LNG1235
TTZ= ABS(TTZ)	LNG1236
T12 = ((((((TTZ*(-3.038))+(5.443))*TTZ)+(-1.343))*TTZ)	LNG1237
1 + (0.287))*TTZ) - (.0076)	LNG1238
T12 = T12*(TCT(I) + TCT(J)) * (0.9)	LNG1239
SUM2 = SUM2 + ((2.)*TH(I)*TH(J)*T12)	LNG1240
4 CONTINUE	LNG1241
SUM1 = SUM1 + (TH(I)*TCT(I))*(1.8)	LNG1242
5 CONTINUE	LNG1243
TMC = SUM1 + SUM2 + (TH(NC)*TCT(NC))*(1.8)	LNG1244
V = 0.0	LNG1245
DO 6 I = 1,NC	LNG1246
	LNG1247
J = ID(I)	LNG1248
TH(I) = X(I) * VCI(J)	LNG1249
V = V + TH(I)	LNG1250
6 CONTINUE	LNG1251
DO 7 I = 1,NC	LNG1252
TH(I) = TH(I) / V	LNG1253
7 CONTINUE	LNG1254
TMM = 0.0	LNG1255
DO 9 I = 1,NC	LNG1256
DO 8 J = 1,NC	LNG1257
M = ID(I)	LNG1258
N = ID(J)	LNG1259
NUM = (VCI(M)**(1./3.)) * (VCI(N)**(1./3.))	LNG1260

```

NUM = SQRT(NUM)
DEN = (0.5)*((VCI(M)**(1./3.))+(VCI(N)**(1./3.)))
NUM = NUM / DEN
NUM = NUM**(3.)
AKIJ = (1.0) - NUM
TCIJ = (1.0 - AKIJ) * SQRT(TCT(I)*TCT(J)*1.8*1.8)
TMM = TMM + TH(I)*TH(J)*TCIJ
8 CONTINUE
9 CONTINUE
TCMP = TMM + (10.0)
ICT = 0
TPO = TMM + (10.0)
10 TR = (T*1.8)/TCMP
NUM = (2901.01) -((5738.92)*TR) +((2849.85)*TR*TR)
1 + ((1.74127)/ (1.01 - TR))
NUM = NUM * (TR - (1.0))
IF(NUM.LT.(-180.)) DD = 0
IF(NUM.LT.(-180.)) GO TO 11
DD = EXP(NUM)
C THE STATEMENT ABOVE MAY RESULT IN AN UNDERFLOW SENSE LIGHT
C ON SOME OPERATING SYSTEMS WHEN THE NUMBER NUM IS A LARGE
C NEGATIVE NUMBER. THE LARGE NEGATIVE VALUE IS PROPER AND
C THE CORRECT ANSWER FOR DD IS ZERO.
11 TCMP = TMM + ((TMC-TMM)*DD)
TEST = (1.0) - (TCMP/TPO)
TEST = ABS(TEST)
IF(TEST.LT.(.0001)) GO TO 12
ICT = ICT + 1

IF(ICT.GT.250) GO TO 12
TPO = TCMP
GO TO 10
12 TMC = TCMP/(1.8)
RETURN
END
SUBROUTINE BLOCK
TYPE REAL KIJ,AJI
DIMENSION KIJ(8,8),AJI(8,8)
COMMON /PAR/ KIJ,AJI
DATA KIJ/
*0.000000,.293E-07,.911E-06,.0030498,0.001000,0.001000,0.001000,
*0.001000,1.088608,0.000000,.188E-10,.463E-06,.462E-08,.120E-03,
*0.001000,0.001000,1.098880,1.078910,0.000000,.517E-06,.535E-06,
*.188E-10,0.001000,0.001000,.8578232,1.146026,1.009559,0.000000,
*.546E-06,.136E-05,0.001000,0.001000,0.995000,1.287762,.9868486,
*.9690485,0.000000,.541E-06,0.001000,0.001000,1.178993,1.266327,
*1.016231,.9976706,.9435714,0.000000,0.001000,0.001000,0.950000,
*1.000000,1.000000,1.000000,1.000000,1.000000,0.000000,0.001000,
*0.995000,1.000000,1.000000,1.000000,1.000000,1.000000,1.000000,
*0.000000/
DATA AJI/
*0.000000,.161E-04,.257E-06,.0003462,0.001000,0.001000,0.001000,
*0.001000,1.014967,0.000000,.188E-10,.197E-06,.184E-05,.335E-06,
*0.001000,0.001000,1.008061,1.004105,0.000000,.142E-06,.103E-04,
*.188E-10,0.001000,0.001000,.9863463,1.011399,1.001862,0.000000,
*.105E-04,.119E-05,0.001000,0.001000,0.995000,1.024894,1.003289,
*.9987221,0.000000,.119E-05,0.001000,0.001000,.9566020,1.025269,
*1.005949,1.001225,.9968984,0.000000,0.001000,0.001000,0.995000,
*1.000000,1.000000,1.000000,1.000000,1.000000,0.000000,0.001000,
*0.995000,1.000000,1.000000,1.000000,1.000000,1.000000,1.000000,
*0.000000/
END

```

LNG1261  
LNG1262  
LNG1263  
LNG1264  
LNG1265  
LNG1266  
LNG1267  
LNG1268  
LNG1269  
LNG1270  
LNG1271  
LNG1272  
LNG1273  
LNG1274  
LNG1275  
LNG1276  
LNG1277  
LNG1278  
LNG1279  
LNG1280  
LNG1281  
LNG1282  
LNG1283  
LNG1284  
LNG1285  
LNG1286  
LNG1287  
LNG1288  
LNG1289  
LNG1290  
LNG1291  
LNG1292  
LNG1293  
LNG1294  
LNG1295  
LNG1296  
LNG1297  
LNG1298  
LNG1299  
LNG1300  
LNG1301  
LNG1302  
LNG1303  
LNG1304  
LNG1305  
LNG1306  
LNG1307  
LNG1308  
LNG1309  
LNG1310  
LNG1311  
LNG1312  
LNG1313  
LNG1314  
LNG1315  
LNG1316  
LNG1317  
LNG1318  
LNG1319  
LNG1320  
LNG1321  
LNG1322

A-246

*J. Chem. Thermodynamics* 1982, 14, 837-854

## Mathematical models for the prediction of liquefied-natural-gas densities<sup>a</sup>

R. D. McCARTY

*Thermophysical Properties Division, National Engineering Laboratory,  
National Bureau of Standards, Boulder, Colorado 80303, U.S.A.**(Received 27 October 1980; in revised form 25 January 1982)*

Three mathematical models of the equation of state for liquid mixtures simulating liquefied natural gas (LNG) are discussed and compared. The adjustable parameters for each model have been optimized using the same set of experimental data, consisting of over 280 new ( $p, V, T, x$ ) points taken at the National Bureau of Standards in Boulder, Colorado. It is estimated that each of the models will predict LNG densities over its range of validity to within 0.1 per cent of the true values, given the pressure, temperature, and composition of the mixture. Deviation plots and a detailed performance evaluation are given for each model. The range of validity varies slightly among the models but in general the range of the study included the saturated liquid from 90 to 135 K.

### 1. Introduction

A project was begun at the National Bureau of Standards in Boulder, Colorado in the summer of 1972, with an ultimate goal of obtaining one or more models of the equation of state of liquefied-natural-gas-like (LNG-like) mixtures which could be used to predict the density of any LNG mixture with a total uncertainty of less than 0.1 per cent given the pressure, temperature, and composition of the liquid. LNG-like mixtures for the purposes of this paper are defined as mixtures of  $N_2$ ,  $CH_4$ ,  $C_2H_6$ ,  $C_3H_8$ ,  $n-C_4H_{10}$ , and  $i-C_4H_{10}$  with mole fractions of  $N_2$ ,  $n-C_4H_{10}$ , and  $i-C_4H_{10}$  restricted to 0.05 or less. The project was sponsored by a consortium of 18 international energy companies through a grant administered by the American Gas Association, with the hope of providing a means to an equitable custody transfer of large quantities of LNG. A series of papers reporting the results of experimental measurements performed during this project have been previously published in this Journal and the present paper is a part of that series.<sup>(1-5)</sup> The purpose of this paper is to report an analysis of three models which are believed to have achieved the 0.1 per cent total-uncertainty goal.

No equation of state can be more accurate than experimental data. Therefore, experimental ( $p, V, T, x$ ) values of comparable or greater accuracy and of adequate scope were a necessary condition to the success of the project. At the time when this

<sup>a</sup> This work is a contribution of the National Bureau of Standards, not subject to copyright.

project was initiated a survey of the existing values revealed that such a set did not exist, and a major experimental program was initiated. Over the next six years comprehensive ( $p, V, T, x$ ) results for the saturated liquid state of the major components ( $N_2, CH_4, C_2H_6, C_3H_8, i-C_4H_{10}, n-C_4H_{10}$ ) of LNG as well as their binary and multicomponent mixtures were obtained. These results are reported elsewhere.<sup>(1-7)</sup> and will not be repeated here. However, a synopsis of the experimental values is given in a later section.

## 2. Selection of models

A preliminary investigation of the existing equations of state of a mixture, revealed a multitude of possibilities from which to choose. Rather than relying on a single model it was decided to select several which would represent the various categories of models found in the literature, thus enhancing the possibility of achieving the 0.1 per cent accuracy goal of the project.

The choices were made on the basis of past performance for other fluids, and likelihood of success. An effort was also made to choose one model which would be representative of a general category of approaches which could be identified as being basically different from each other. On these bases three models were selected: the extended corresponding-states model<sup>(8)</sup> which, while it is complex, allows a great deal of flexibility; a hard-sphere model<sup>(9)</sup> which has demonstrated capabilities; and the Klosek and McKinley<sup>(10)</sup> model which is very simple in principle and totally empirical. From time to time as the project continued other methods and models were suggested by co-workers and the sponsoring companies but only two of these were investigated in any detail: (a) Watson's<sup>(11)</sup> method, investigated to the point where it became obvious that it was unsuitable without some major modifications; (b) Hiza's<sup>(12)</sup> new empirical method, found to work well for restricted ranges of composition and temperature.

## 3. Data used

The experimental densities for saturated liquid of the pure components of LNG given in references 1 and 7 have been used here both as data for optimization procedures and as pure-fluid data for calculating the molar volumes  $V_i$  of the components (see equations 19 and 21). Table 1 presents these data in the form of coefficients to an equation for the saturated liquid density and table 2 summarizes the data used from references 1, 2, 3, and 7.

References 5 and 6 contain 110 ( $p, V, T, x$ ) points for a total of 27 different multicomponent mixtures which, with one exception, were used for comparison purposes only. The data for the ternary system:  $(0.05931N_2 + 0.89071CH_4 + 0.04998n-C_4H_{10})$  from reference 6 were used to obtain the  $N_2-n-C_4H_{10}$  binary interaction parameters, which are also used for the  $N_2-i-C_4H_{10}$  binary interaction parameters given in sections 4 and 5. No other ( $p, V, T, x$ ) values have been used in the development of the mathematical models in the following sections.

The use of values from a single source was the intent from the beginning of the

TABLE 1. Saturated-liquid densities of the pure fluids

$$(\rho - \rho_c)/(\text{mol} \cdot \text{dm}^{-3}) = a(1 - T/T_c)^{0.35} + \sum_{i=1}^3 b_i(1 - T/T_c)^{1+(i-1)3}$$

 where  $T_c$  and  $\rho_c$  are the critical temperature and amount-of-substance density

	CH <sub>4</sub>	C <sub>2</sub> H <sub>6</sub>	C <sub>3</sub> H <sub>8</sub>	<i>i</i> -C <sub>4</sub> H <sub>10</sub>
<i>a</i>	18.65812	12.55205	8.684459	7.657535
<i>b</i> <sub>1</sub>	6.712030	13.43284	18.04086	8.145251
<i>b</i> <sub>2</sub>	-0.9472020	-19.00461	-29.46261	-13.10582
<i>b</i> <sub>3</sub>	0	11.07716	16.43559	8.145894
<i>T</i> <sub>c</sub> /K	190.555	305.33	369.82	408.13
$\rho_c/(\text{mol} \cdot \text{dm}^{-3})$	10.16	6.86	5.00	3.80
<i>M</i> /(g · mol <sup>-1</sup> ) <sup>a</sup>	16.04303	30.07012	44.09721	58.1243
	<i>n</i> -C <sub>4</sub> H <sub>10</sub>	N <sub>2</sub>	<i>i</i> -C <sub>5</sub> H <sub>12</sub> <sup>b</sup>	<i>n</i> -C <sub>5</sub> H <sub>12</sub> <sup>b</sup>
<i>a</i>	7.286063	19.39217	2.946310456	-0.0362004993
<i>b</i> <sub>1</sub>	11.96308	26.01408	35.50770979	59.0020299
<i>b</i> <sub>2</sub>	-19.87592	-39.49759	-57.41242943	-93.44193819
<i>b</i> <sub>3</sub>	11.60211	23.32977	28.15898339	43.66780833
<i>T</i> <sub>c</sub> /K	425.16	126.20	460.39	469.6
$\rho_c/(\text{mol} \cdot \text{dm}^{-3})$	3.92	11.21	3.271	3.285
<i>M</i> /(g · mol <sup>-1</sup> ) <sup>a</sup>	58.1243	28.0134	72.15139	72.15139

<sup>a</sup> The project under which the work reported here was done started in 1972. The molar masses *M* were calculated using the values for C, H, and N accepted at that time. The values for H and C were changed slightly by the 1976 Commission on Atomic Weights. For the sake of consistency we have continued to use the previous values. The maximum error in density of any of the fluids resulting from using the newer values is 0.003 per cent.

<sup>b</sup> Towards the end of the project, *i*-pentane and *n*-pentane were added to the list of possible components in the LNG-like mixtures. No experimental (*p*, *V*, *T*) values for these two pure fluids were taken as part of this project; the constants in table 1 for the saturated amount-of-substance densities of these fluids were derived from the results of McClune.<sup>(28)</sup>

project, the purpose being to eliminate systematic differences which almost always occur when values from more than one source are used. The development of the mathematical models was done simultaneously with the acquisition of the experimental values; this procedure allowed almost immediate consistency checks between the experimental results for various different compositions of a binary mixture as well as for comparisons with data from other sources.<sup>(10, 11, 13-16)</sup> These comparisons verified, in many cases, the anticipated systematic differences in multisource data.

#### 4. Extended corresponding states

A theoretical development of the thermodynamic equations for the extended corresponding states method may be found in a paper by Rowlinson and Watson<sup>(17)</sup> and only those equations necessary for this particular application will be given here. Other important work on this method has been done by Leach<sup>(8)</sup> in developing models for the shape factors and by Mollerup<sup>(18)</sup> and Mollerup and Rowlinson<sup>(19)</sup>

TABLE 2. Experimental measurements used, their temperature ranges  $T_1$  to  $T_2$ , and the ranges of the mole fraction  $x$  of the most volatile component in binary mixtures

Fluid or binary mixture	Reference	$T_1$ /K	$T_2$ /K	$x$	No. of points
$N_2$	7	95	120	pure fluid	19
$CH_4$	1	105	160	pure fluid	11
$C_2H_6$	1	100	270	pure fluid	22
$C_3H_8$	1	100	288	pure fluid	16
$n-C_4H_{10}$	2	135	300	pure fluid	12
$i-C_4H_{10}$	2	115	300	pure fluid	12
$n-C_5H_{12}$	28	148	249	pure fluid	21
$i-C_5H_{12}$	28	125	254	pure fluid	20
$xN_2 + (1-x)CH_4$	2	105	140	0.05 to 0.5	21
$xN_2 + (1-x)C_2H_6$	2	105	120	0.06	4
$xN_2 + (1-x)C_3H_8$	2	105	115	0.02 to 0.07	6
$xCH_4 + (1-x)C_2H_6$	2	105	140	0.35 to 0.68	20
$xCH_4 + (1-x)C_3H_8$	2	105	130	0.3 to 0.85	20
$xCH_4 + (1-x)i-C_4H_{10}$	2, 3	110	140	0.48 to 0.92	17
$xCH_4 + (1-x)n-C_4H_{10}$	2, 3 <sup>a</sup>	115	140	0.58 to 0.93	23
$xC_2H_6 + (1-x)C_3H_8$	2	105	140	0.50 to 0.67	10
$xC_2H_6 + (1-x)i-C_4H_{10}$	2	105	130	0.69 to 0.72	6
$xC_2H_6 + (1-x)n-C_4H_{10}$	2	110	140	0.65 to 0.67	8
$xC_3H_8 + (1-x)i-C_4H_{10}$	2	105	130	0.49 to 0.50	8
$xC_3H_8 + (1-x)n-C_4H_{10}$	2	110	150	0.58 to 0.61	8
$xi-C_4H_{10} + (1-x)n-C_4H_{10}$	2	125	140	0.47	4

<sup>a</sup> The results for  $(0.91674CH_4 + 0.08326n-C_4H_{10})$  from reference 3 were not used because they appear to be inconsistent with later results<sup>(4)</sup> for nearly the same composition.

who combined the work of Leach<sup>(8)</sup> with an equation of state for methane by Goodwin<sup>(20)</sup> to produce a model for LNG-like mixtures. The same general approach as used by Mollerup<sup>(18)</sup> is used here except that the shape-factor functions of Leach<sup>(8)</sup> have been refitted to the pure fluid values experimentally obtained at this laboratory on this project<sup>(1,7)</sup> and an equation of state by McCarty<sup>(21)</sup> has been used for methane. Interim results of this study can be found in references 21 and 22. The differences between the interim results mentioned above and the final results, given here, are minor and the previously published equations may be used. More details on the performance of the extended-corresponding-states method are given later in this section.

The extended-corresponding-states method is defined by the equations:

$$Z_i(p, T) = Z_0(ph_{ii,0}/f_{ii,0}, T/f_{ii,0}), \quad (1)$$

$$G_i(p, T) = f_{ii,0}G_0(ph_{ii,0}/f_{ii,0}, T/f_{ii,0}) - RT \ln(h_{ii,0}), \quad (2)$$

where  $Z$  is the compression factor,  $G$  is the Gibbs free energy,  $p$  is pressure, and  $T$  is thermodynamic temperature. The subscript  $_0$  denotes a reference fluid (in this case methane) and the subscript  $_i$  denotes the fluid for which properties are to be obtained via the equation of state for the reference fluid and the transformation variables  $f_{ii,0}$  and  $h_{ii,0}$ . The double subscript  $_{ii}$  is introduced now to facilitate the extension later to mixtures. Two equations, (1) and (2), are necessary to define uniquely the

transformation variables  $f_{ii,0}$  and  $h_{ii,0}$ . The equation of state for methane by McCarty<sup>(21)</sup> was constructed using a hypothetical saturation line for both liquid and vapor down to 43 K. This construction is necessary to represent realistically the very low reduced temperatures of the heavier hydrocarbons and was accomplished without changing the performance of the equation of state above the triple-point temperature of methane. The equation of state for the reference fluid is

$$\begin{aligned}
 p = \rho RT + \rho^2(N_1 T + N_2 T^{1/2} + N_3 + N_4/T + N_5/T^2) + \rho^3(N_6 T + N_7 + N_8/T + N_9/T^2) \\
 + \rho^4(N_{10} T + N_{11} + N_{12}/T) + \rho^5(N_{13}) + \rho^6(N_{14}/T + N_{15}/T^2) + \rho^7(N_{16}/T) \\
 + \rho^8(N_{17}/T + N_{18}/T^2) + \rho^9(N_{19}/T^2) + \rho^3(N_{20}/T^2 + N_{21}/T^3) \exp(-\gamma\rho^2) \\
 + \rho^5(N_{22}/T^2 + N_{23}/T^4) \exp(-\gamma\rho^2) + \rho^7(N_{24}/T^2 + N_{25}/T^3) \exp(-\gamma\rho^2) \\
 + \rho^9(N_{26}/T^2 + N_{27}/T^4) \exp(-\gamma\rho^2) + \rho^{11}(N_{28}/T^2 + N_{29}/T^3) \exp(-\gamma\rho^2) \\
 + \rho^{13}(N_{30}/T^2 + N_{31}/T^3 + N_{32}/T^4) \exp(-\gamma\rho^2), \quad (3)
 \end{aligned}$$

where  $p$  is pressure,  $T$  is thermodynamic temperature, and  $\rho$  is amount-of-substance density. The coefficients  $N_i$  are given in table 3.

TABLE 3. Coefficients  $N_i$  of equation (4) for  $\text{CH}_4$ <sup>a</sup>

$R = 0.831434 \times 10^{-2} \text{ MPa} \cdot \text{dm}^3 \cdot \text{mol}^{-1} \cdot \text{K}^{-1}$ ,	$\gamma = 0.0096 \text{ dm}^6 \cdot \text{mol}^{-2}$ ,
$N_1 = -0.189506118654 \times 10^{-1} \text{ dm}^6 \cdot \text{mol}^{-2} \cdot \text{K}^{-1}$ ,	$N_2 = 0.104756987190 \times 10 \text{ dm}^6 \cdot \text{mol}^{-2} \cdot \text{K}^{-1/2}$ ,
$N_3 = -0.157446511658 \times 10^1 \text{ dm}^6 \cdot \text{mol}^{-2}$ ,	$N_4 = 0.782544605655 \times 10^2 \text{ dm}^6 \cdot \text{mol}^{-2} \cdot \text{K}$ ,
$N_5 = -0.382099919632 \times 10^4 \text{ dm}^6 \cdot \text{mol}^{-2} \cdot \text{K}^2$ ,	$N_6 = 0.858039193151 \times 10^{-4} \text{ dm}^9 \cdot \text{mol}^{-3} \cdot \text{K}^{-1}$ ,
$N_7 = -0.502993394999 \times 10^{-1} \text{ dm}^9 \cdot \text{mol}^{-3}$ ,	$N_8 = 0.881435651333 \times 10^1 \text{ dm}^9 \cdot \text{mol}^{-3} \cdot \text{K}$ ,
$N_9 = -0.327098978594 \times 10^4 \text{ dm}^9 \cdot \text{mol}^{-3} \cdot \text{K}^2$ ,	$N_{10} = -0.401087946417 \times 10^{-5} \text{ dm}^{12} \cdot \text{mol}^{-4} \cdot \text{K}^{-1}$ ,
$N_{11} = 0.270307051249 \times 10^{-2} \text{ dm}^{12} \cdot \text{mol}^{-4}$ ,	$N_{12} = -0.308038191105 \times 10 \text{ dm}^{12} \cdot \text{mol}^{-4} \cdot \text{K}$ ,
$N_{13} = 0.194123002261 \times 10^{-4} \text{ dm}^{15} \cdot \text{mol}^{-5}$ ,	$N_{14} = -0.198179473576 \times 10^{-4} \text{ dm}^{18} \cdot \text{mol}^{-6} \cdot \text{K}$ ,
$N_{15} = 0.615529077453 \times 10 \text{ dm}^{18} \cdot \text{mol}^{-6} \cdot \text{K}^2$ ,	$N_{16} = -0.536626852203 \times 10^{-4} \text{ dm}^{21} \cdot \text{mol}^{-7} \cdot \text{K}$ ,
$N_{17} = 0.154281787794 \times 10^{-5} \text{ dm}^{24} \cdot \text{mol}^{-8} \cdot \text{K}$ ,	$N_{18} = -0.111409049265 \times 10^{-2} \text{ dm}^{24} \cdot \text{mol}^{-8} \cdot \text{K}^2$ ,
$N_{19} = 0.193931540966 \times 10^{-4} \text{ dm}^{27} \cdot \text{mol}^{-9} \cdot \text{K}^2$ ,	$N_{20} = 0.391590731296 \times 10^4 \text{ dm}^9 \cdot \text{mol}^{-3} \cdot \text{K}^2$ ,
$N_{21} = -0.160023162832 \times 10^6 \text{ dm}^9 \cdot \text{mol}^{-3} \cdot \text{K}^3$ ,	$N_{22} = 0.197857473814 \times 10^2 \text{ dm}^{15} \cdot \text{mol}^{-5} \cdot \text{K}^2$ ,
$N_{23} = 0.168195529711 \times 10^6 \text{ dm}^{15} \cdot \text{mol}^{-5} \cdot \text{K}^4$ ,	$N_{24} = 0.611041574405 \times 10^{-1} \text{ dm}^{21} \cdot \text{mol}^{-7} \cdot \text{K}^2$ ,
$N_{25} = 0.381473591215 \times 10^1 \text{ dm}^{21} \cdot \text{mol}^{-7} \cdot \text{K}^3$ ,	$N_{26} = 0.127257796890 \times 10^{-3} \text{ dm}^{27} \cdot \text{mol}^{-9} \cdot \text{K}^2$ ,
$N_{27} = -0.348122335444 \times 10^1 \text{ dm}^{27} \cdot \text{mol}^{-9} \cdot \text{K}^4$ ,	$N_{28} = -0.548112616636 \times 10^{-6} \text{ dm}^{33} \cdot \text{mol}^{-11} \cdot \text{K}^2$ ,
$N_{29} = 0.188081779935 \times 10^{-3} \text{ dm}^{33} \cdot \text{mol}^{-11} \cdot \text{K}^3$ ,	$N_{30} = 0.780999906720 \times 10^{-9} \text{ dm}^{34} \cdot \text{mol}^{-13} \cdot \text{K}^2$ ,
$N_{31} = -0.290669323872 \times 10^{-6} \text{ dm}^{39} \cdot \text{mol}^{-13} \cdot \text{K}^3$ ,	$N_{32} = 0.377310956389 \times 10^{-5} \text{ dm}^{39} \cdot \text{mol}^{-13} \cdot \text{K}^4$ .

<sup>a</sup> An existing wide-range equation of state for  $\text{CH}_4$  was used for the base fluid to facilitate the extension of this work to a wider range of pressures and temperatures in the future. The large number of digits in the coefficients given here is necessary to insure the validity of the calculated pressure in some areas of the ( $p$ ,  $T$ ) surface.

The  $f_{ii,0}$  and  $h_{ii,0}$  are then defined as

$$f_{ii,0} = (T_{ii}^c/T_0^c)\theta_{ii}(T_i^r, V_i^r), \quad (4)$$

$$h_{ii,0} = (V_{ii,0}^c/V_0^c)\phi_{ii,0}(T_i^r, V_i^r), \quad (5)$$

where the superscript <sup>c</sup> denotes the critical property and  $T_i^r = T/T_{ii}^c$  and  $V_i^r = V/V_{ii}^c$ . The  $\theta_{ii}(T_i^r, V_i^r)$  and  $\phi_{ii,0}(T_i^r, V_i^r)$  are called shape factors, where

$$\theta_{ii,0} = 1 + (w_i - w_0)\{a_1 - a_2 \ln T_i^r + (a_3 - a_4/T_i^r)(V_i^r - a_5)\}, \quad (6)$$

and

$$\phi_{ii,0} = (Z_0^c/Z_i^c)[1 + (w_i - w_0)\{b_1(V_i^r - b_2) - b_3(V_i^r - b_4)\ln T_i^r\}], \quad (7)$$

where the  $T_i^r$  and  $V_i^r$  are as before and  $w_i$  is a fluid-dependent parameter.

The  $a_j$ 's and  $b_j$ 's are fluid-independent parameters and  $Z_0^c/Z_i^c$  is the ratio of the compression factors at the critical point. The  $a_j$ 's,  $b_j$ 's, and  $w_i$ 's were estimated by least squares using the experimental data from (1) and (2) and simultaneous fitting techniques. The parameters  $a_j$ ,  $b_j$ ,  $w_i$ , and the critical properties are given in table 4.

TABLE 4. Coefficients for corresponding-states equations (6) and (7)

$$a_1 = -0.109495, \quad a_2 = 0.919454, \quad a_3 = -4.01525, \quad a_4 = -4.14192, \quad a_5 = 0.444850$$

$$b_1 = 0.356808, \quad b_2 = 1.02619, \quad b_3 = 0.893323, \quad b_4 = 0.761533$$

	$w$	$p_c^a$ MPa	$T_c$ K	$V_c$ $\text{cm}^3 \cdot \text{mol}^{-1}$	$M$ $\text{g} \cdot \text{mol}^{-1}$	Fluid no.
$\text{N}_2$	0.029179	3.3542557	126.2	89.827	28.0134	6
$\text{CH}_4$	0.0109	4.59570	190.555	98.522	16.04303	1
$\text{C}_2\text{H}_6$	0.110427	4.860314	305.5	146.2	30.07012	2
$\text{C}_3\text{H}_8$	0.154837	4.2445123	370	200	44.09721	3
$n\text{-C}_4\text{H}_{10}$	0.176372	3.8295398	425	251.62	58.1243	4
$i\text{-C}_4\text{H}_{10}$	0.150115	3.688998	408.1	263	58.1243	5
$n\text{-C}_5\text{H}_{12}$	0.234320	3.3812152	469.6	304	72.15139	7
$i\text{-C}_5\text{H}_{12}$	0.288886	3.1988302	460.39	306	72.15139	8

<sup>a</sup> The large number of significant figures given for critical pressure is necessary to reproduce the  $Z_c$  ( $Z_c = p_c V_c / RT_c$ ) in the least-squares fit.

Equations (6) and (7) were originally proposed by Leach<sup>(19)</sup> with  $w_i$  as the acentric factor, which allows the extension of the equations to any fluid with a minimum of information about that fluid. Here,  $w_i$  was treated as an adjustable parameter to provide for the greatest possible accuracy in the limited range of pressure and temperature of interest.

The extension of the above to mixtures is accomplished through the equations:

$$f_{ij,0} = \varepsilon_{ij}(f_{ii,0}f_{jj,0})^{1/2}, \quad (8)$$

$$h_{ij,0} = \eta_{ij}(\frac{1}{2}h_{ii,0}^{1/3} + \frac{1}{2}h_{jj,0}^{1/3})^3, \quad (9)$$

$$h_{x,0} = \sum_i \sum_j x_i x_j h_{ij,0}, \quad (10)$$

$$f_{x,0} h_{x,0} = \sum_i \sum_j x_i x_j f_{ij,0} h_{ij,0}, \quad (11)$$

where  $x_i$  and  $x_j$  are the mole fractions of the pure components.

The  $\varepsilon_{ij}$  and the  $\eta_{ij}$  are binary interaction parameters determined by least squares from ( $p$ ,  $V$ ,  $T$ ,  $x$ ) values for binary mixtures as outlined in section 3. The  $f_{x,0}$  and  $h_{x,0}$  are now the transformation variables to transform the equation of state of the reference fluid to an equation of state for the mixture specified by  $p$ ,  $T$ , and  $x$ . The  $\eta_{ij}$ 's and  $\varepsilon_{ij}$ 's for the corresponding-states method are given in table 5.

Of the three models presented here, the extended-corresponding-states model is superior to the other two in most respects. It covers the widest range of composition,

TABLE 5. Binary interaction coefficients for corresponding states equations (8) and (9). Fluid numbers  $i$  are given in table 4

$i, j$	1	2	3	4	5	6	7	8
	$\eta_{ij}$							
1	1	1.00514	1.01922	1.04243	1.05048	1.01009	1.06	1.06
2		1	1.00599	1.01616	1.02369	1.02127	1.02	1.02
3			1	1.00172	1.01140	1.04606	1.01	1.01
4				1	0.997114	1.20955	1.0	1.0
5					1	1.13889	1.0	1.0
6						1	1.0	1.0
7							1	1.0
8								1
	$\epsilon_{ij}$							
$i, j$	1	2	3	4	5	6	7	8
1	1	1.01127	0.988608	0.983130	0.986978	0.953430	0.98	0.98
2		1	0.999961	0.972223	0.998886	0.939622	0.99	0.99
3			1	0.985547	1.03099	0.912209	0.99	0.99
4				1	0.976416	0.849200	0.99	0.99
5					1	0.857310	0.99	0.99
6						1	0.99	0.99
7							1	0.99
8								1

the widest range of pressure and temperature, and is probably the most accurate, although the last is hard to substantiate. Of the approximately 285 experimental ( $p, V, T, x$ ) points reported in references 2 to 6, only 14 differ by more than 0.1 per cent in density from the value predicted by this extended-corresponding-states model. Of these 14 points 11 (see below) are judged to have an experimental uncertainty greater than the 0.1 per cent. Figure 1 presents the deviations between calculated and experimental densities for these 14 points. Deviations between predicted and experimental densities of the other 271 ( $p, V, T, x$ ) points are published in reference 23. No restrictions as to pressure, temperature, or composition (within the data from references 2 to 6) need be placed on the model. The other two models have pressure-, temperature-, and composition-range restrictions. In preliminary accounts (references 21 and 22), some reservations were expressed about the accuracy of the calculation methods because of the disagreement between experimental and calculated densities for a few binary and multicomponent system which contained methane and butanes as components. This disagreement has since been resolved by more experimental measurements which have been made<sup>(4,6)</sup> on mixtures of similar composition and in some cases the same composition (more measurements on the same sample). As a result of the additional measurements<sup>(4,6)</sup> some of the unpublished multicomponent mixture results for systems containing methane and butanes were discarded,<sup>(6)</sup> and some of the already published binary systems containing (methane +  $n$ -butane) were judged to be uncertain by more than 0.1 per cent in density. The published results<sup>(2,4)</sup> which are believed to be uncertain by more than 0.1 per cent are detailed in table 2. As a result of the additional values

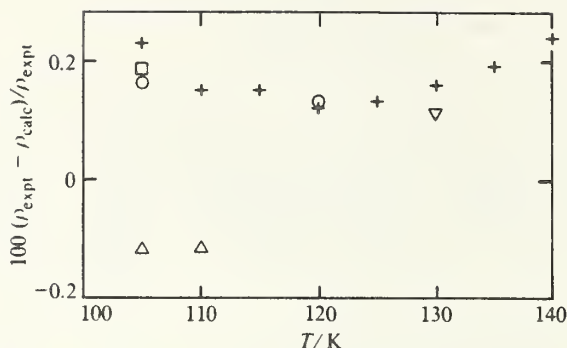


FIGURE 1. Relative deviations exceeding 0.1 per cent between densities calculated by the extended-corresponding-states method and *all* of the  $(p, V, T, x)$  mixture values taken in this project.<sup>(2-6)</sup> +, 0.91674CH<sub>4</sub> + 0.8326*n*-C<sub>4</sub>H<sub>10</sub>; □, 0.06740N<sub>2</sub> + 0.93260C<sub>3</sub>H<sub>8</sub>; △, 0.00859N<sub>2</sub> + 0.75713CH<sub>4</sub> + 0.13585C<sub>2</sub>H<sub>6</sub> + 0.06742C<sub>3</sub>H<sub>8</sub> + 0.01326*n*-C<sub>4</sub>H<sub>10</sub> + 0.01336*i*-C<sub>4</sub>H<sub>10</sub> + 0.00216*n*-C<sub>5</sub>H<sub>12</sub> + 0.00223*i*-C<sub>5</sub>H<sub>12</sub>; ○, 0.85442CH<sub>4</sub> + 0.05042C<sub>2</sub>H<sub>6</sub> + 0.04038C<sub>3</sub>H<sub>8</sub> + 0.02901*n*-C<sub>4</sub>H<sub>10</sub> + 0.02577*i*-C<sub>4</sub>H<sub>10</sub>; ∇, 0.74920CH<sub>4</sub> + 0.25080C<sub>3</sub>H<sub>8</sub>.

obtained in the experimental program, subsequent to the models published in references 21 and 22, very slight changes were made in the binary interaction parameters: CH<sub>4</sub>-*i*-C<sub>4</sub>H<sub>10</sub>, CH<sub>4</sub>-*n*-C<sub>4</sub>H<sub>10</sub>, N<sub>2</sub>-*i*-C<sub>4</sub>H<sub>10</sub>, and N<sub>2</sub>-*n*-C<sub>4</sub>H<sub>10</sub>. These changes have a negligible effect on density calculations for LNG-like mixtures, *i.e.* where the mole fractions of N<sub>2</sub>, *i*-C<sub>4</sub>H<sub>10</sub>, and *n*-C<sub>4</sub>H<sub>10</sub> are individually less than 0.05. Therefore, either the models presented here or those in references 21 and 22 may be used to predict the density of an LNG mixture to within 0.1 per cent of its true value.

The accuracy claim of 0.1 per cent in density must be qualified by specifying ranges of pressure and temperature as well as components. For each of the three models the qualifications will be different; in the case of the extended-corresponding-states model the temperature range is 95 to 135 K for saturated liquid pressures. The component restrictions are minimal, *i.e.* any combination of mole fractions of N<sub>2</sub>, CH<sub>4</sub>, C<sub>2</sub>H<sub>6</sub>, C<sub>3</sub>H<sub>8</sub>, *n*-C<sub>4</sub>H<sub>10</sub>, and *i*-C<sub>4</sub>H<sub>10</sub>, as long as liquid-liquid phase separation does not occur. The total mole fraction of *n*-C<sub>5</sub>H<sub>12</sub> and *i*-C<sub>5</sub>H<sub>12</sub> must not be more than 0.02. The above restrictions are based on the performance of the model when compared to the set of results from this laboratory.<sup>(1-7)</sup> Comparisons with other sources have been made.<sup>(9, 24, 25, 26)</sup> With a few exceptions the comparisons have revealed our values to be internally consistent to better than the 0.1 per cent accuracy claim given here. Rodosevich's values<sup>(16)</sup> are in agreement with ours to within 0.1 per cent in density but do not extend the range of pressure and temperature upon which the extended-corresponding-states model is based. A comparison of calculated and experimental densities from Rodosevich<sup>(16)</sup> and Rodosevich and Miller<sup>(9)</sup> is given in figure 2. Orrit and Laupretre<sup>(24)</sup> have published  $(p, V, T, x)$  values for LNG-like mixtures which agree reasonably well with this model as shown in figure 3, but again contain no points which would expand the scope of the set used here.

Nunes *et al.*<sup>(25)</sup> have measured  $(p, V, T, x)$  for (methane + nitrogen) at low temperatures in the compressed liquid to several tens of megapascals. These results

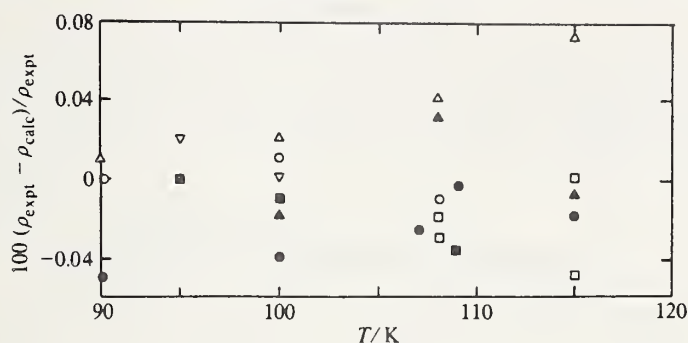


FIGURE 2. Typical relative deviations between densities calculated by the extended-corresponding-states method and experimental densities from Rodosevich<sup>(16)</sup> and Rodosevich and Miller.<sup>(9)</sup> ○, 0.9206CH<sub>4</sub> + 0.0794*n*-C<sub>4</sub>H<sub>10</sub>; △, 0.9262CH<sub>4</sub> + 0.0738C<sub>3</sub>H<sub>8</sub>; □, 0.9737CH<sub>4</sub> + 0.0263C<sub>3</sub>H<sub>8</sub>; ▽, 0.9206CH<sub>4</sub> + 0.0794*n*-C<sub>4</sub>H<sub>10</sub>; ■, 0.9462CH<sub>4</sub> + 0.0538*i*-C<sub>4</sub>H<sub>10</sub>; ●, 0.8409CH<sub>4</sub> + 0.1086C<sub>2</sub>H<sub>6</sub> + 0.0505N<sub>2</sub>; ▲, 0.8303CH<sub>4</sub> + 0.1001C<sub>2</sub>H<sub>6</sub> + 0.0493C<sub>3</sub>H<sub>8</sub> + 0.0203*n*-C<sub>4</sub>H<sub>10</sub>.

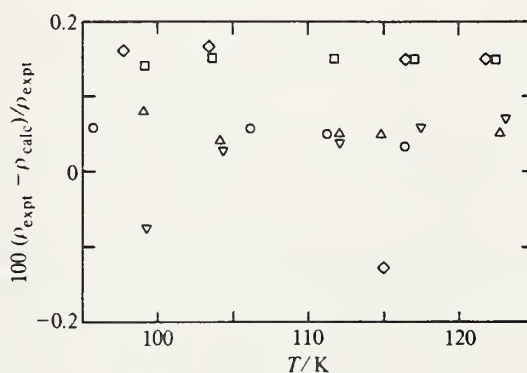


FIGURE 3. Typical relative deviations between densities calculated by the extended-corresponding-states method and experimental densities from Orrit and Laupretre.<sup>(24)</sup> ▽, 0.009N<sub>2</sub> + 0.95CH<sub>4</sub> + 0.026C<sub>2</sub>H<sub>6</sub> + 0.015C<sub>3</sub>H<sub>8</sub>; □, 0.009N<sub>2</sub> + 0.90CH<sub>4</sub> + 0.053C<sub>2</sub>H<sub>6</sub> + 0.028C<sub>3</sub>H<sub>8</sub> + 0.012*n*-C<sub>4</sub>H<sub>10</sub>; △, 0.009N<sub>2</sub> + 0.93CH<sub>4</sub> + 0.026C<sub>2</sub>H<sub>6</sub> + 0.015C<sub>3</sub>H<sub>8</sub> + 0.012*n*-C<sub>4</sub>H<sub>10</sub> + 0.008*i*-C<sub>4</sub>H<sub>10</sub>; ◇, 0.006N<sub>2</sub> + 0.89CH<sub>4</sub> + 0.056C<sub>2</sub>H<sub>6</sub> + 0.024C<sub>3</sub>H<sub>8</sub> + 0.012*n*-C<sub>4</sub>H<sub>10</sub> + 0.012*i*-C<sub>4</sub>H<sub>10</sub> + 0.005*i*-C<sub>5</sub>H<sub>12</sub>; ○, 0.01N<sub>2</sub> + 0.70CH<sub>4</sub> + 0.16C<sub>2</sub>H<sub>6</sub> + 0.09C<sub>3</sub>H<sub>8</sub> + 0.029*n*-C<sub>4</sub>H<sub>10</sub> + 0.014*i*-C<sub>4</sub>H<sub>10</sub> + 0.0005*n*-C<sub>5</sub>H<sub>12</sub> + 0.0011*i*-C<sub>5</sub>H<sub>12</sub>.

agree very well with the extended-corresponding-states model with the exception of one isotherm (see figure 4) which again suggests some internal systematic differences.

Finally Straty and Diller<sup>(27)</sup> have measured several hundred ( $p, V, T, x$ ) points for (methane + nitrogen) over a wide range of  $p, V$ , and  $T$  including compressed liquid and gas. Figure 5 is a summary of the agreement of the corresponding-states model discussed here with these results. Figure 5 demonstrates that the model is well behaved and reasonable when extrapolated beyond the range of the present data set, but that the extrapolation is limited by the range of  $p$  and  $T$  of the equation of state

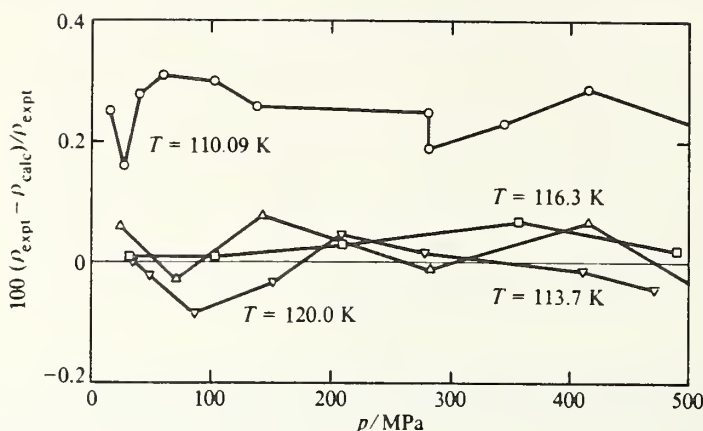


FIGURE 4. Typical relative deviations between densities calculated by the extended-corresponding-states method and experimental densities from Nunes *et al.*<sup>(25)</sup> for (0.497CH<sub>4</sub> + 0.503N<sub>2</sub>).

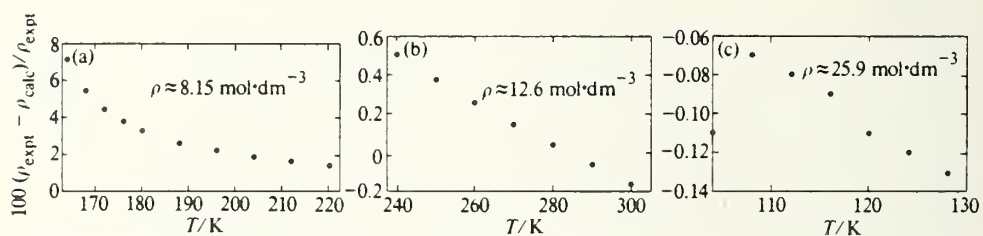
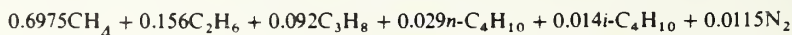


FIGURE 5. Typical relative deviations between densities calculated by the extended-corresponding-states method and experimental densities from Straty and Diller<sup>(27)</sup> for (0.50115N<sub>2</sub> + 0.49884CH<sub>4</sub>).

for the base fluid, *i.e.* 90 to 350 K with pressures to 35 MPa. No comparisons with or calculations of the thermodynamic properties of mixtures have been made with any of the models presented here and calculations of this sort are not recommended because of the extreme emphasis placed on  $(p, V, T, x)$  and the complete absence of consideration of other thermodynamic properties during the development of the models. Table 6 contains amount-of-substance densities for purposes of checking the method.

TABLE 6. Values for checking calculations using corresponding-states equations. These are included for check purposes only; they are calculated from the corresponding-states model and are not experimental values



$T/\text{K}$	$\rho/(\text{mol}\cdot\text{dm}^{-3})$	$p/\text{MPa}$
95	24.333	0.1013250
100	24.067	0.1114575
105	23.796	0.1215900

### 5. Hard-sphere model

The hard-sphere model presented here is a refit of the model proposed by Rodosevich and Miller<sup>(9)</sup> which is one of many modifications of the Longuet-Higgins and Widom model,<sup>(26)</sup> and was chosen to be included in this study as a representative example of the application of the hard-sphere equation-of-state concept to the correlation of ( $p, V, T, x$ ) data.

The equation of state from reference 9 is

$$pV/RT = c(1 + y + y^2)/(1 - y)^3 - a/RTV, \quad (12)$$

where  $a$ ,  $b$ , and  $c$  are adjustable parameters and  $y = b/4V$ . The equation is applied to mixtures by assuming the one-fluid theory and applying the mixing rules:

$$a_m = \sum_i \sum_j a_{ij} x_i x_j, \quad (13)$$

$$b_m = \sum_i \sum_j b_{ij} x_i x_j, \quad (14)$$

$$c_m = \sum_i \sum_j c_{ij} x_i x_j. \quad (15)$$

The combining rules are:

$$b_{ij} = \left\{ \frac{1}{2}(b_{ii}^{1/3} + b_{jj}^{1/3})(1 - j_{ij}) \right\}^3, \quad (16)$$

$$a_{ij} = (a_{ii} a_{jj})^{1/2} (b_{ij}^2 / b_{ii} b_{jj})^{1/2} (1 - k_{ij}), \quad (17)$$

$$c_{ij} = (c_{ii} + c_{jj})/2. \quad (18)$$

The parameters  $j_{ij}$  and  $k_{ij}$  are now the binary interaction parameters. The  $a$ 's,  $b$ 's,  $c$ 's,  $j_{ij}$ 's, and  $k_{ij}$ 's are given in tables 7 and 8. The excess volume is calculated using the equation of state and

$$V^E = \tilde{V}_m - \sum_i \tilde{V}_i x_i \quad (19)$$

where  $\tilde{V}_m$  and the  $\tilde{V}_i$  are calculated *via* the equations (12) through (18) and then

$$V_m = \sum_i V_i x_i + V^E \quad (20)$$

where the  $V^E$  is from equation (19) and the  $V_i$  are experimental. The  $V_i$  in this case were calculated from the equations for the liquid density of the pure fluids given in table 1.

The above equations are the same as they originally appeared in Rodosevich and Miller<sup>(9)</sup> and only the  $j_{ij}$ 's and  $k_{ij}$ 's have been revised on the basis of the ( $p, V, T, x$ )

TABLE 7. Coefficients for the hard-sphere model of equation (12):  $b = 2\pi L S_i^3/3$  where  $L$  denotes Avogadro's constant and the  $S_i$ 's are the pure-fluid coordination numbers

Fluid	$a_i/(\text{dm}^6 \cdot \text{mol}^{-2} \cdot \text{MPa})$	$S_i/(\text{dm} \cdot \text{mol}^{-1/3})$	$c_i$	Fluid no. $i$
N <sub>2</sub>	$1.718 \times 10^5$	$3.546 \times 10^{-8}$	1.03	6
CH <sub>4</sub>	$2.755 \times 10^5$	$3.676 \times 10^{-8}$	1	1
C <sub>2</sub> H <sub>6</sub>	$7.773 \times 10^5$	$4.158 \times 10^{-8}$	1.5	2
C <sub>3</sub> H <sub>8</sub>	$14.165 \times 10^5$	$4.644 \times 10^{-8}$	1.67	3
<i>n</i> -C <sub>4</sub> H <sub>10</sub>	$22.733 \times 10^5$	$5.051 \times 10^{-8}$	1.83	4
<i>i</i> -C <sub>4</sub> H <sub>10</sub>	$21.279 \times 10^5$	$5.056 \times 10^{-8}$	1.79	5

TABLE 8. Binary interaction parameters for the hard-sphere model of equations (16) and (17). See table 4 for identification of  $i$  and  $j$ 

$i, j$	1	2	3	4	5	6	7	8	
				$j_{ij}$					
1	0	-0.00388616	-0.0120932	-0.0231577	-0.0238349	-0.00997547	-0.0326	0.0458	
2		0	-0.002162	-0.00400910	-0.00812712	-0.0143976	-0.003	-0.004	
3			0	0.000761571	-0.00383743	-0.024014	0	0	
4				0	0.00222150	-0.0576043	0	0	
5					0	-0.0576043	0	0	
6						0	-0.04	-0.05	
7							0	0	
8								0	
				$k_{ij}$					
$i, j$	1	2	3	4	5	6	7	8	
1	0	0.00298830	0.0597378	0.110893	0.100298	0.0197290	0.14	0.1745	
2		0	0.014527	0.067703	0.0346632	0.0529034	0.02	0.03	
3			0	0.024291	-0.00838212	0.14719	0	0	
4				0	0.0199213	0.154365	0	0	
5					0	0.154365	0	0	
6						0	0.15	0.18	
7								0	
8									

binary-mixture set as outlined in section 3. An attempt was made to optimize the  $a$ ,  $b$ , and  $c$  parameters for each pure fluid on the basis of the new pure-fluid values; however, the results were disappointing, and no perceptible improvement in the prediction of mixture properties was achieved. The results did suggest, however, that the introduction of a temperature dependence to the  $a$ ,  $b$ , and  $c$  parameters would improve the performance of the equation of state for pure fluids.

This method has one disadvantage not present in the extended-corresponding-states method which causes the method to be restricted to temperatures below 120 K for mixtures which contain  $N_2$ . As the method is applied here, it is an excess-volume method, and therefore when the temperature of the mixture approaches the critical temperature of one of the component fluids the method fails. Since the critical temperature of  $N_2$  is about 126 K, calculations for mixtures containing  $N_2$  should not be made with this method for temperatures above 120 K. This added restriction on the method reduces the original set of 285 experimental ( $p, V, T, x$ ) points<sup>(2-6)</sup> to 251. Figure 6 shows all of the points within the new set of 251 for which calculated and experimental densities differ by more than 0.1 per cent. Conclusions may be drawn from the deviations shown in figure 6. First, even with a reduced total number of points for comparison, the total number of deviations between calculated and experimental densities for the hard-sphere model which exceed the 0.1 per cent criterion, is far more than for the extended-corresponding-states model. Second, the method degrades for all mixtures regardless of components as the temperature becomes greater than 115 K.

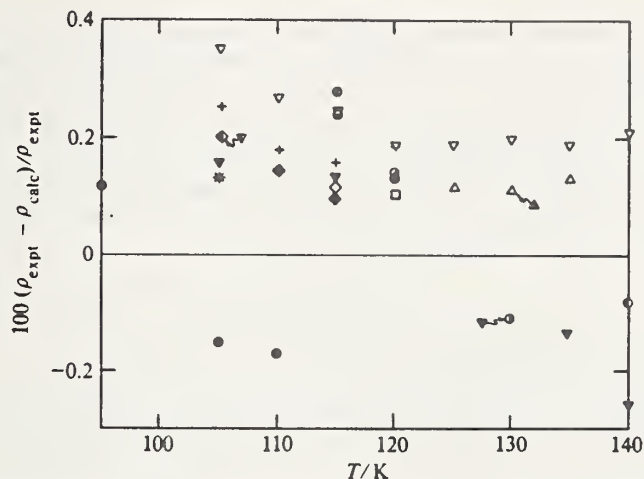


FIGURE 6. Relative deviations exceeding 0.1 per cent between experimental densities and densities calculated by the hard-sphere method. The comparison set is about 250 ( $p, V, T, x$ ) points from references 2 to 6.  $\bullet$ ,  $0.92780\text{CH}_4 + 0.07220n\text{-C}_4\text{H}_{10}$ ;  $\nabla$ ,  $0.91674\text{CH}_4 + 0.08326n\text{-C}_4\text{H}_{10}$ ;  $\circ$ ,  $0.77982\text{CH}_4 + 0.22018n\text{-C}_4\text{H}_{10}$ ;  $\blacktriangledown$ ,  $0.77762\text{CH}_4 + 0.22238n\text{-C}_4\text{H}_{10}$ ;  $\nabla$ ,  $0.58828\text{CH}_4 + 0.41172n\text{-C}_4\text{H}_{10}$ ;  $\diamond$ ,  $0.30349\text{N}_2 + 0.69651\text{CH}_4$ ;  $\bullet$ ,  $0.49242\text{N}_2 + 0.50758\text{CH}_4$ ;  $\blacktriangledown$ ,  $0.06740\text{N}_2 + 0.93260\text{C}_3\text{H}_8$ ;  $\square$ ,  $0.34242\text{CH}_4 + 0.31372\text{C}_2\text{H}_6 + 0.34386\text{C}_3\text{H}_8$ ;  $\ominus$ ,  $0.33800\text{N}_2 + 0.34140\text{CH}_4 + 0.32060\text{C}_2\text{H}_6$ ;  $\blacklozenge$ ,  $0.85317\text{CH}_4 + 0.05077\text{C}_2\text{H}_6 + 0.04855\text{C}_3\text{H}_8 + 0.04751n\text{-C}_4\text{H}_{10}$ ;  $\blacktriangle$ ,  $0.84566\text{CH}_4 + 0.07924\text{C}_2\text{H}_6 + 0.05060\text{C}_3\text{H}_8 + 0.02450n\text{-C}_4\text{H}_{10}$ ;  $\triangle$ ,  $0.85133\text{CH}_4 + 0.05759\text{C}_2\text{H}_6 + 0.04808\text{C}_3\text{H}_8 + 0.04300n\text{-C}_4\text{H}_{10}$ ;  $+$ ,  $0.85442\text{CH}_4 + 0.05042\text{C}_2\text{H}_6 + 0.04038\text{C}_3\text{H}_8 + 0.02901n\text{-C}_4\text{H}_{10} + 0.02577i\text{-C}_4\text{H}_{10}$ ;  $\blacklozenge$ ,  $0.05540\text{N}_2 + 0.79090\text{CH}_4 + 0.05600\text{C}_2\text{H}_6 + 0.05000\text{C}_3\text{H}_8 + 0.04770n\text{-C}_4\text{H}_{10}$ ;  $*$ ,  $0.04250\text{N}_2 + 0.81300\text{CH}_4 + 0.04750\text{C}_2\text{H}_6 + 0.04870\text{C}_3\text{H}_8 + 0.02420n\text{-C}_4\text{H}_{10} + 0.02410i\text{-C}_4\text{H}_{10}$ .

Figure 7 shows deviations greater than 0.1 per cent between experimental densities and those calculated by the hard-sphere method for all mixtures in the 251-point comparison set which are LNG-like, *i.e.* all multicomponent mixtures with 60 moles per cent or more of  $\text{CH}_4$  but with 5 moles per cent or less of each of  $\text{N}_2$ ,  $i\text{-C}_4\text{H}_{10}$ , and  $n\text{-C}_4\text{H}_{10}$ . The points above 120 K for those mixtures containing  $\text{N}_2$  have been

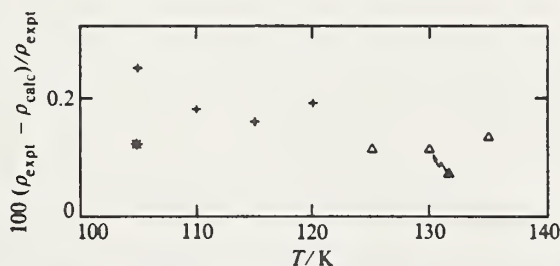


FIGURE 7. Relative deviations exceeding 0.1 per cent between experimental densities and densities calculated by the hard-sphere method. The comparison set is about 60 ( $p, V, T, x$ ) points for LNG-like mixtures from references 4, 5, and 7.  $\blacktriangle$ ,  $0.84566\text{CH}_4 + 0.07924\text{C}_2\text{H}_6 + 0.05060\text{C}_3\text{H}_8 + 0.02450n\text{-C}_4\text{H}_{10}$ ;  $\triangle$ ,  $0.85133\text{CH}_4 + 0.05759\text{C}_2\text{H}_6 + 0.04808\text{C}_3\text{H}_8 + 0.04300n\text{-C}_4\text{H}_{10}$ ;  $+$ ,  $0.85442\text{CH}_4 + 0.05042\text{C}_2\text{H}_6 + 0.04038\text{C}_3\text{H}_8 + 0.02901n\text{-C}_4\text{H}_{10} + 0.02577i\text{-C}_4\text{H}_{10}$ ;  $*$ ,  $0.04250\text{N}_2 + 0.81300\text{CH}_4 + 0.04750\text{C}_2\text{H}_6 + 0.04870\text{C}_3\text{H}_8 + 0.02420n\text{-C}_4\text{H}_{10} + 0.02410i\text{-C}_4\text{H}_{10}$ .

excluded. This newly-defined comparison set now contains 60 ( $p, V, T, x$ ) points. Excluding the 5 points (see above) which have been judged to be experimentally uncertain by more than the 0.1 per cent criterion as explained in the section on the extended-corresponding-states model, we are still left with 4 points outside the 0.1 per cent tolerance which did not appear on the extended-corresponding-states deviation plot. All of these four deviations occur at temperatures greater than 120 K. Therefore the restriction of 120 K as an upper limit in temperature must be placed on the method regardless of the composition.

### 6. A revised Klosek and McKinley method

The Klosek and McKinley method<sup>(10)</sup> is a totally empirical method and was included in this study because of its simplicity and its widespread use in the LNG industry. Very early in the study it became apparent that the original form of the method would not work for mixtures in which  $N_2$  was present, even at mole fractions of 0.04 or less. The original method was proposed as

$$V_{\text{mix}} = \sum_i x_i V_i - kx(\text{CH}_4) \quad (21)$$

where  $V_{\text{mix}}$  is the volume of the mixture,  $x_i$  and  $V_i$  are the mole fraction and molar volume of component  $i$  and the summation is taken over all components including  $\text{CH}_4$ ,  $x(\text{CH}_4)$  is the mole fraction of  $\text{CH}_4$ , and  $k$  is a correction factor obtained from a

TABLE 9. Molar volumes  $V_i$  of saturated liquid of the pure components at temperatures  $T$  at intervals close enough to allow linear interpolation

$T/K$	$\text{CH}_4$	$\text{C}_2\text{H}_6$	$\text{C}_3\text{H}_8$	$n\text{-C}_4\text{H}_{10}$	$i\text{-C}_4\text{H}_{10}$	$\text{N}_2$	$n\text{-C}_5\text{H}_{12}$	$i\text{-C}_5\text{H}_{12}$
	$V_i/(\text{dm}^3 \cdot \text{mol}^{-1})$							
90	0.035441	0.046081	0.060461	0.074708	0.076084	0.037543	0.089173	0.089243
92	0.035649	0.046235	0.060632	0.074891	0.076274	0.038081	0.089379	0.089454
94	0.035861	0.046390	0.060804	0.075075	0.076466	0.038650	0.089586	0.089666
96	0.036077	0.046547	0.060977	0.075259	0.076659	0.039254	0.089793	0.089878
98	0.036298	0.046704	0.061151	0.075445	0.076853	0.039897	0.090000	0.090091
100	0.036524	0.046863	0.061325	0.075631	0.077047	0.040586	0.090208	0.090304
102	0.036755	0.047023	0.061501	0.075818	0.077243	0.041327	0.090416	0.090518
104	0.036992	0.047185	0.061677	0.076006	0.077440	0.042128	0.090624	0.090733
106	0.037234	0.047348	0.061855	0.076194	0.077637	0.043002	0.090833	0.090948
108	0.037481	0.047512	0.062033	0.076384	0.077836	0.043963	0.091042	0.091163
110	0.037735	0.047678	0.062212	0.076574	0.078035	0.045031	0.091252	0.091379
112	0.037995	0.047845	0.062392	0.076765	0.078236	0.046231	0.091462	0.091596
114	0.038262	0.048014	0.062574	0.076957	0.078438	0.047602	0.091673	0.091814
116	0.038536	0.048184	0.062756	0.077150	0.078640	0.049179	0.091884	0.092032
118	0.038817	0.048356	0.062939	0.077344	0.078844	0.050885	0.092095	0.092251
120	0.039106	0.048529	0.063124	0.077539	0.079049	0.052714	0.092307	0.092470
122	0.039404	0.048704	0.063309	0.077734	0.079255	0.054679	0.092520	0.092690
124	0.039710	0.048881	0.063496	0.077931	0.079462	0.056797	0.092733	0.092911
126	0.040025	0.049059	0.063684	0.078128	0.079671	0.059085	0.092947	0.093133
128	0.040350	0.049239	0.063873	0.078327	0.079880	0.061565	0.093161	0.093355
130	0.040685	0.049421	0.064063	0.078526	0.080091	0.064263	0.093376	0.093578

table or graph. The  $V_i$  and  $k$  are temperature dependent and in addition  $k$  is dependent upon the mean molar mass of the mixture.

The revised equation is

$$V_{\text{mix}} = \sum_i x_i V_i - \{k_1 + (k_2 - k_1)x(\text{N}_2)/0.0425\}x(\text{CH}_4), \quad (22)$$

where quantities are the same as in equation (21) except that a second correction factor has been added and  $x(\text{N}_2)$  is the mole fraction of  $\text{N}_2$ . Tables 9, 10, and 11 give values for the  $V_i$ ,  $k_1$ , and  $k_2$ , which are spaced so that linear interpolation is adequate in both variables (*i.e.* temperature and molar mass).

The pure-fluid volumes in table 9 are taken from the equations in section 3 with the exception of that of  $\text{N}_2$  above 115 K which is a linear extrapolation of the 115 K point using the slope of the curve at that point. The  $k$  factors in tables 10 and 11 have been obtained graphically from the multicomponent ( $p, V, T, x$ ) data of references 4 and 6 and from multicomponent densities calculated using the extended-corresponding-states method.

TABLE 10. Correction factor  $k_1$  for the Klosek and McKinley method as a function of temperature  $T$  and molar mass  $M$

$M/(\text{g} \cdot \text{mol}^{-1})$	16	17	18	19	20	21	22	23	24	25
$T/\text{K}$	$10^3 k_1 / (\text{cm}^3 \cdot \text{mol}^{-1})$									
90	-0.005	0.120	0.220	0.340	0.430	0.515	0.595	0.660	0.725	0.795
95	-0.006	0.135	0.260	0.380	0.500	0.590	0.665	0.740	0.810	0.885
100	-0.007	0.150	0.300	0.425	0.575	0.675	0.755	0.830	0.910	0.990
105	-0.007	0.165	0.340	0.475	0.635	0.735	0.840	0.920	1.045	1.120
110	-0.008	0.190	0.375	0.535	0.725	0.835	0.950	1.055	1.155	1.245
115	-0.009	0.220	0.440	0.610	0.810	0.945	1.065	1.180	1.280	1.380
120	-0.010	0.250	0.500	0.695	0.920	1.055	1.205	1.330	1.450	1.550
125	-0.013	0.295	0.590	0.795	1.035	1.210	1.385	1.525	1.640	1.750
130	-0.015	0.345	0.700	0.920	1.200	1.370	1.555	1.715	1.860	1.990
135	-0.017	0.400	0.825	1.060	1.390	1.590	1.800	1.950	2.105	2.272

TABLE 11. Correction factor  $k_2$  for the Klosek and McKinley method as a function of temperature  $T$  and molar mass  $M$

$M/(\text{g} \cdot \text{mol}^{-1})$	16	17	18	19	20	21	22	23	24	25
$T/\text{K}$	$10^3 k_2 / (\text{cm}^3 \cdot \text{mol}^{-1})$									
90	-0.004	0.10	0.22	0.35	0.50	0.60	0.69	0.78	0.86	0.95
95	-0.005	0.12	0.28	0.43	0.59	0.71	0.83	0.94	1.05	1.14
100	-0.007	0.16	0.34	0.49	0.64	0.79	0.94	1.08	1.17	1.27
105	-0.01	0.24	0.42	0.61	0.75	0.91	1.05	1.19	1.33	1.45
110	-0.015	0.32	0.59	0.77	0.92	1.07	1.22	1.37	1.52	1.71
115	-0.024	0.41	0.72	0.95	1.15	1.22	1.30	1.45	1.65	2.00
120	-0.032	0.60	0.91	1.23	1.43	1.63	1.85	2.08	2.30	2.45
125	-0.043	0.71	1.13	1.48	1.73	1.98	2.23	2.48	2.75	2.90
130	-0.058	0.95	1.46	1.92	2.20	2.42	2.68	3.00	3.32	3.52
135	-0.075	1.30	2.00	2.40	2.60	3.00	3.40	3.77	3.99	4.23

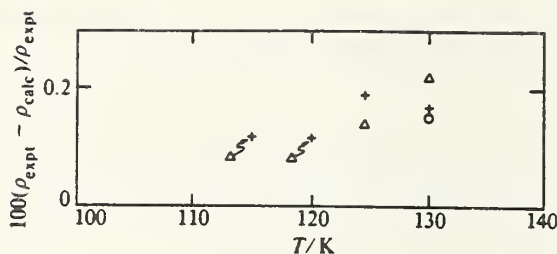


FIGURE 8. Relative deviations exceeding 0.1 per cent between experimental densities and densities calculated by the revised Klosek and McKinley method. The comparison set is about 60 ( $p, V, T, x$ ) points for LNG-like mixtures from references 4, 5, and 7.  $\circ$ ,  $0.84566\text{CH}_4 + 0.07924\text{C}_2\text{H}_6 + 0.05060\text{C}_3\text{H}_8 + 0.02450n\text{-C}_4\text{H}_{10}$ ;  $+$ ,  $0.85934\text{CH}_4 + 0.08477\text{C}_2\text{H}_6 + 0.02980\text{C}_3\text{H}_8 + 0.00707n\text{-C}_4\text{H}_{10} + 0.00519i\text{-C}_4\text{H}_{10}$ ;  $\triangle$ ,  $0.00859\text{N}_2 + 0.75713\text{CH}_4 + 0.13585\text{C}_2\text{H}_6 + 0.06742\text{C}_3\text{H}_8 + 0.01326n\text{-C}_4\text{H}_{10} + 0.01336i\text{-C}_4\text{H}_{10} + 0.00216n\text{-C}_5\text{H}_{12} + 0.00223i\text{-C}_5\text{H}_{12}$ .

The composition limits of the revised Klosek and McKinley method are the most severe of any of the three methods given here. This method should not be used for LNG-like mixtures, unless they contain at least 60 moles per cent of  $\text{CH}_4$ , less than 4 moles per cent of  $\text{N}_2$ , less than 4 moles per cent of each of  $i\text{-C}_4\text{H}_{10}$  and  $n\text{-C}_4\text{H}_{10}$ , and less than 2 moles per cent in all of  $i\text{-C}_5\text{H}_{12}$  and  $n\text{-C}_5\text{H}_{12}$ .

There are 61 experimental ( $p, V, T, x$ ) points from references 4 and 6 which fall within the composition limits outlined above. Figure 8 shows all of the deviations between calculated and experimental densities in this 61-point comparison set which exceed the 0.1 per cent criterion. Figure 8 exhibits the same sort of deviation trend as is found in figure 7. In figure 8 all of the deviations are at 115 K and above; therefore, the claim of 0.1 per cent accuracy with this method must be restricted to temperatures below 115 K.

## 7. Conclusions

On the basis of the performance of the three models and subject to composition and temperature range restrictions as outlined earlier in this paper; it is estimated that, given the pressure, temperature, and composition of LNG, any one of the three models presented here may be used to predict the density to within 0.1 per cent of the true value. As was mentioned before, no model or method can be any better than the experimental values used to develop it; therefore the above accuracy claim depends strongly on the accuracy of the experimental values. The estimated uncertainty of the experimental values<sup>(1-7)</sup> used here is 0.1 per cent or less, with a precision of a few hundredths of a per cent. With the exceptions already detailed in sections 3 and 4, the correlations presented here provide no basis for questioning the claims of the experimenters.

This entire study including the experimental work has provided valuable experience in the problem of mathematically modelling the equation of state of a mixture, and the lessons learned therefrom are worth passing along to future workers in the field. Having accurate and internally consistent experimental results has always

been an important factor in equation-of-state development for pure substances but in the case of the equation of state of mixtures it is absolutely essential. Without internally consistent results the job is hopeless, especially if the accuracy of the equation of state is important.

The value of conducting the experimental and modelling program simultaneously has also been clearly demonstrated, for without the parallel efforts in this project the experimental problems with some of the mixtures containing butane would never have been detected.

Of the three methods presented here, the extended-corresponding-states model has proved to be more accurate and more versatile than either of the other two. However, over the very restricted range of composition and temperature of liquefied natural gas, no one method seems to be more accurate than the other.

Interim results of this study were reported by Haynes *et al.*<sup>(22)</sup> and McCarty<sup>(21)</sup> both of which contain earlier versions of the mathematical models presented here. The earlier versions in references 21 and 22 are only slightly different from the present ones, the main difference being in the  $\text{CH}_4\text{-C}_4\text{H}_{10}$  binary interaction parameters for the extended-corresponding-states method and the hard-sphere method; however, for calculations of the density of LNG, the difference is inconsequential. The user of any of these models is cautioned to read carefully the limitations associated with each model given in the relevant individual section.

Computer programs for the three models presented here are available from the Thermophysical Properties Division of the National Bureau of Standards in Boulder, Colorado. A complete listing of these programs and more detailed instructions on how to use them is published elsewhere.<sup>(23)</sup>

## REFERENCES

1. Haynes, W. M.; Hiza, M. J. *J. Chem. Thermodynamics* **1977**, *9*, 179.
2. Hiza, M. J.; Haynes, W. M.; Parrish, W. R. *J. Chem. Thermodynamics* **1977**, *9*, 873.
3. Haynes, W. M. Orthobaric liquid densities of methane + isobutane and methane + normal butane mixtures at low temperatures (to be published).
4. Hiza, M. J.; Haynes, W. M. *J. Chem. Thermodynamics* **1980**, *12*, 1.
5. Haynes, W. M. *J. Chem. Thermodynamics* **1982**, *14*, 603.
6. Miller, R. C.; Hiza, M. J. *Fluid Phase Equilibria* **1978**, *2*, 49.
7. Haynes, W. M.; Hiza, M. J.; Frederick, N. V. *Rev. Sci. Instrum.* **1976**, *47*, 1237.
8. Leach, J. W. Molecular structure correction for applying the theory of corresponding states to non-spherical pure fluids and mixtures. Ph.D. Thesis. Rice University. **1967**.
9. Rodosevich, J. B.; Miller, R. C. *Adv. Cryog. Eng.* **1974**, *19*, 339.
10. Klosek, J.; McKinley, C. *Proc. First Int. Conf. on LNG, Chicago*. **1968**, paper 22.
11. Watson, K. M. *Ind. Eng. Chem.* **1943**, *35*, 4, 399.
12. Hiza, M. J. *Fluid Phase Equilibria* **1978**, *2*, 27.
13. Shana'a, M. Y.; Canfield, F. B. *Trans. Faraday Soc.* **1968**, *64*, 2281.
14. Bloomer, O. T.; Parent, J. D. *Chem. Eng. Prog. Symp. Ser.* **1952**, *49*, 11.
15. Orrit, J.; Olives, J. F. Distributed at 4th International Conference on Liquefied Natural Gas. Algeria. **1974**.
16. Rodosevich, J. B. Measurements and prediction of liquefied natural gas densities. M.Sc. Thesis. University of Wyoming. **1973**.
17. Rowlinson, J. S.; Watson, I. D. *Chem. Eng. Sci.* **1969**, *24*, 1565.
18. Mollerup, J. *Adv. Cryog. Eng.* **1975**, *20*, 172.
19. Mollerup, J.; Rowlinson, J. S. *Chem. Eng. Sci.* **1974**, *29*, 1373.
20. Goodwin, R. D.; Prydz, R. *J. Res. Natl Bur. Stand. (U.S.) Sect. A* **1972**, *76*, 1-81.

21. McCarty, R. D. *Natl Bur. Stand. (U.S.), Interagency Report NBSIR 77-867*. 1977.
22. Haynes, W. M.; Hiza, M. J.; McCarty, R. D. Proc. Fifth International Conference on LNG, Düsseldorf Vol. 2. Institute of Gas Technology, Chicago, Ill. 1977, Section III. Paper 11.
23. McCarty, R. D. *Natl Bur. Stand. (U.S.), Tech. Note 1030*. 1980.
24. Orrit, J. E.; Laupretre, J. M. *Adv. Cryog. Eng.* 1978, 23, 573.
25. Nunes da Ponte, M.; Streett, W. B.; Staveley, L. A. K. *J. Chem. Thermodynamics* 1978, 10, 151.
26. Longuet-Higgins, H. C.; Widom, B. *Mol. Phys.* 1964, 8, 549.
27. Straty, G. C.; Diller, D. E. *J. Chem. Thermodynamics* 1980, 12, 937.
28. McClune, C. R. *Cryogenics* 1976, 16, 289.

## AN EMPIRICAL EXCESS VOLUME MODEL FOR ESTIMATING LIQUEFIED NATURAL GAS DENSITIES

M.J. HIZA

*Cryogenics Division, Institute for Basic Standards, National Bureau of Standards, Boulder, Colorado 80302 (U.S.A.)*

(Received August 22nd, 1977)

### ABSTRACT

Hiza, M.J., 1978. An empirical excess volume model for estimating liquefied natural gas densities. *Fluid Phase Equilibria*, 2: 27–38.

The mathematical model presented herein was developed to represent excess volumes at saturation for multicomponent liquid mixtures of nitrogen and the low molecular weight alkanes between 105 and 120 K. Parameters of the model were determined from experimental excess volumes for binary liquid mixtures of nitrogen, methane, ethane, propane, isobutane, and normal butane. Comparisons made with selected experimental excess volumes reported in the literature for multicomponent liquid mixtures of the above components demonstrate the predictive capability of the model in two simple forms. An extension of the model to include mixtures containing isopentane and normal pentane is also proposed. Pure component molar volumes are given at 0.5 K intervals from 105 to 116 K to facilitate the use of the present model in estimating liquefied natural gas (LNG) densities.

### BACKGROUND

Analysis of consistency and the prediction of orthobaric (saturated) liquid molar volumes of multicomponent mixtures requires a reliable mechanism to account for the effect of each component as a function of composition and temperature. Of specific interest here are multicomponent liquid mixtures of natural gas components; viz. nitrogen, methane, ethane, propane, isobutane, and normal butane. A simple and reliable empirical model in this specific area is most attractive because it offers an alternative to the more complex theoretical models for predicting orthobaric LNG (Liquefied Natural Gas) densities for custody transfer.

At temperatures where all components present in the liquid mixture are subcritical, the logical subject of an empirical model is the liquid mixture excess volume. The development of such a model into a useable (predictive) form requires a consistent set of density data for the pure components and for the

possible binary systems, each at several compositions, in the temperature range of interest.

The empirical models of Klosek and McKinley (1968) and of Miller (1974) are of this type. The first, using mixture molecular weight as the correlating parameter, does not properly account for the presence of nitrogen in the mixture nor does it include adequate information on the temperature dependence of excess volume. The second, basically a more sound approach, treats the presence of nitrogen separately, uses an effective ethane mole fraction as the correlating parameter for the hydrocarbon contribution, and includes significantly more information on temperature dependence, as well as pressure effects. However, both models were based on relatively incomplete data sets and some of the features of each were, of necessity, based on educated guesses. For example, accurate orthobaric liquid density data for nitrogen + ethane, nitrogen + propane, and binary mixtures of ethane, propane, isobutane, and normal butane were not available at the time these earlier models were developed. In addition, both models were intended only for use with methane-rich mixtures. Neither will correctly predict the excess volume at saturation of a simple equimolar liquid mixture of methane, ethane, and propane.

The empirical excess volume model proposed here was developed with due consideration of the deficiencies in the models of Klosek and McKinley (1968) and of Miller (1974). It is based on the self-consistent orthobaric liquid densities for the pure components (Haynes et al., 1976; Haynes and Hiza, 1977) and for the binary mixtures (Hiza et al., 1977) obtained in the NBS LNG density project. The excess volumes for the methane + butanes and nitrogen + methane reported by Miller (1974) and Rodosevich and Miller (1973) were also used. The excess volumes reported by Miller (1974) and Rodosevich and Miller (1973) are generally consistent with those from the NBS data within an imprecision equivalent to about 0.1 percent in the mixture molar volumes (Hiza et al., 1977). All excess volumes reported in these references were calculated from:

$$V^E = V_m - \sum_i x_i [V_i + \beta_i V_i (P_i - P_m)] \quad (1)$$

where  $V$  is the molar volume,  $P$  is the saturation pressure,  $x$  is the mole fraction, and  $\beta$  is the isothermal compressibility. Subscripts  $m$  and  $i$  refer to the mixture and to the pure components, respectively. In all cases the isothermal compressibilities were taken from Rowlinson (1969) for nitrogen and methane, and from Miller (1974) for ethane. Isothermal compressibility adjustments to the molar volumes of propane, isobutane, and normal butane were not made in deriving excess volumes from the NBS data. Neglecting isothermal compressibility adjustments to the molar volumes of propane and the high-molecular weight alkanes has no significant effect on the results.

#### FORMULATION OF THE EXCESS VOLUME MODEL

The present model is based on excess volume ratios relative to the well-defined methane + ethane and nitrogen + methane binary systems, treating

the hydrocarbon + hydrocarbon and nitrogen + hydrocarbon contributions separately. Eqns. 2, 3 and 4 describe this model in general terms.

$$V_t^E = V_{CC}^E + V_{NC}^E \quad (2)$$

where

$$V_{CC}^E(@x_1^*) = V_{12}^E \left[ 1 + \left( \frac{V_{13}^E}{V_{12}^E} - 1 \right) \frac{x_3}{(1-x_1^*)} + \left( \frac{V_{14}^E}{V_{12}^E} - 1 \right) \frac{x_4}{(1-x_1^*)} + \left( \frac{V_{15}^E}{V_{12}^E} - 1 \right) \frac{x_5}{(1-x_1^*)} + \dots \right] \quad (3)$$

and

$$V_{NC}^E(@x_N) = V_{N1}^E \left[ 1 + \left( \frac{V_{N2}^E}{V_{N1}^E} - 1 \right) \frac{x_2}{(1-x_N)} + \left( \frac{V_{N3}^E}{V_{N1}^E} - 1 \right) \frac{x_3}{(1-x_N)} + \dots \right] \quad (4)$$

In these equations  $V^E$  is excess molar volume and  $x$  is the component mole fraction. The subscripts t, CC, and NC refer to total, hydrocarbon + hydrocarbon, and nitrogen + hydrocarbon, respectively. The subscript N refers to nitrogen and 1, 2, 3, 4, and 5 refer to methane, ethane, propane, isobutane and normal butane, respectively. In eqn. (3), the excess volumes for methane + ethane ( $V_{12}^E$ ), etc. are taken at a pseudo mole fraction of methane,  $x_1^*$ , equal to the sum of the actual methane and nitrogen mole fractions,  $x_1 + x_N$ . In eqn. (4), the excess volumes for nitrogen + methane ( $V_{N1}^E$ ), etc. are taken at the actual nitrogen mole fraction in the mixture,  $x_N$ . Obviously, if no nitrogen is present in the mixture  $V_t^E = V_{CC}^E$  and eqn. (4) is not needed.

In this approach, it is assumed that contributions from heavy hydrocarbon + heavy hydrocarbon interactions are negligible. In the temperature range of interest, this assumption is valid since experimental excess volumes for binary mixtures of ethane, propane, isobutane, and normal butane are nearly zero (Hiza et al., 1977).

The values of  $V_{12}^E$  and  $V_{13}^E$  in  $\text{cm}^3/\text{mol}$  in eqn. (3) are evaluated from a temperature dependent Redlich-Kister expansion of the following form:

$$V_{ij}^E = x_i x_j [(a_0 + a_1 T + a_2 T^2) + (b_0 + b_1 T + b_2 T^2)(2x_i - 1) + (c_0 + c_1 T + c_2 T^2)(2x_i - 1)^2] \quad (5)$$

at  $x_i = x_1^* = x_1 + x_N$  and  $x_j = 1 - x_1^*$ .  $T$  is the temperature in Kelvin. The coefficients of eqn. (5) obtained from the NBS data for the methane + ethane and methane + propane systems are given in Table 1. The coefficients for the methane + propane system are the same as those presented earlier (Hiza et al., 1977); those for the methane + ethane system are slightly different from the earlier values (Hiza et al., 1977) since a few points, obtained by vapor recircu-

TABLE 1

Coefficients of Eq. (5) for the methane + ethane and methane + propane systems

	methane + ethane	methane + propane
$a_0$	-14.89469	-11.96725
$a_1$	0.2770596	0.236748
$a_2$	-0.001473116	-0.001429237
$b_0$	-37.98245	16.59465
$b_1$	0.6427122	-0.3212125
$b_2$	-0.002783724	0.001398221
$c_0$	0	-52.93613
$c_1$	0	0.9887147
$c_2$	0	-0.004667488

lation and composition analyses of liquid samples (Hiza and Haynes, 1978), were added to determine the coefficients given here. The applicable temperature ranges for these coefficients are 105 to 135 K for methane + ethane and 105 to 130 K for methane + propane. For convenience values of  $A = a_0 + a_1T + a_2T^2$ ,  $B = b_0 + b_1T + b_2T^2$ , and  $C = c_0 + c_1T + c_2T^2$  are given at a few specific temperatures in Tables 2 and 3 for methane + ethane and methane + propane, respectively.

There are few data points available for the methane + isobutane and methane + normal butane systems. Thus, it is not possible to represent the excess volumes for these systems analytically. The ratios of excess volumes for the methane + butane systems to the excess volume for the methane + ethane system were determined at several compositions in the methane rich region at approximately 108 K. For purposes of this correlation these ratios have been assumed to be constant. These are

$$V_{14}^E/V_{12}^E = 2.0 \quad (6)$$

and

$$V_{15}^E/V_{12}^E = 2.5 \quad (7)$$

where subscripts 4 and 5 refer to isobutane and normal butane, respectively.

Thus eqn. (3) reduces to

$$V_{CC}^E(@x_1^*) = V_{12}^E \left[ 1 + \left( \frac{V_{13}^E}{V_{12}^E} - 1 \right) \frac{x_3}{(1-x_1^*)} + \frac{x_4}{(1-x_1^*)} + \frac{1.5x_5}{(1-x_1^*)} \right] \quad (8)$$

With some loss in precision, the ratios of the excess volumes for the methane + propane system to the methane + ethane system above 30 mole percent methane can be represented as a function of  $x_1^*$  only. With this modification,

TABLE 2

Redlich—Kister coefficients at specific temperatures for the methane + ethane system

$T$ (K)	$A$ ( $a_0 + a_1T + a_2T^2$ )	$B$ ( $b_0 + b_1T + b_2T^2$ )
105	-2.044536	-1.188226
108	-2.154678	-1.038889
108.15	-2.160881	-1.032738
110	-2.242838	-0.967168
115	-2.514795	-0.885297
120	-2.860408	-0.942612

TABLE 3

Redlich—Kister coefficients at specific temperatures for the methane + propane system

$T$ (K)	$A$ ( $a_0 + a_1T + a_2T^2$ )	$B$ ( $b_0 + b_1T + b_2T^2$ )	$C$ ( $c_0 + c_1T + c_2T^2$ )
105	-2.866048	-1.717276	-0.580142
108	-3.069086	-1.787450	-0.596522
108.15	-3.079914	-1.790298	-0.599547
110	-3.218738	-1.820251	-0.654118
115	-3.642889	-1.853315	-0.961468
120	-4.138503	-1.816468	-1.502193

eqn. (8) becomes

$$V_{CC}^E(@x_1^*) = V_{12}^E \left[ 1 + (0.6075x_1^* + 0.1664) \frac{x_3}{(1-x_1^*)} + \frac{x_4}{(1-x_1^*)} + \frac{1.5x_5}{(1-x_1^*)} \right] \quad (9)$$

In examining the nitrogen + hydrocarbon data, it was noted that the excess volumes for the nitrogen + ethane and nitrogen + propane systems are essentially the same; and, at low nitrogen content, these and the excess volumes for nitrogen + methane are almost linear functions of the nitrogen mole fraction (up to about 10 mole percent for nitrogen in methane). Without the benefit of experimental data, it was assumed that excess volumes for the nitrogen + butane systems are approximately the same as those for the nitrogen + propane system. Therefore, eqn. (4) was reduced to

$$V_{NC}^E(@x_N) = V_{N1}^E \left[ 1 + \frac{0.87(1-x_1^*)}{(1-x_N)} \right] \quad (10)$$

where

$$V_{N1}^E = x_N \left[ 2.8842 - \frac{134.196}{126.2 - T} \right] \quad (11)$$

The applicable temperature range of eqn. (11) is 91 to 120 K. For temperatures above 115 K, this equation should not be used for nitrogen concentrations in excess of 5 mole percent.

#### MODEL LIMITATIONS

In the applicable temperature range, i.e. 105 to 120 K, limitations of the present empirical model are due primarily to insufficient or lack of data for certain binary systems. The available data are inadequate to describe the temperature and composition dependence of excess volumes for either of the methane + butane systems. Above 115 K, more data are needed for the nitrogen + methane system to adequately describe the composition dependence of excess volumes for mixtures containing more than 5 mole percent nitrogen. And finally there is a lack of any experimental information on properties of the nitrogen + butane systems.

Therefore, between 105 and 115 K, this model should not be used for multicomponent LNG mixtures containing more than 10 mole percent of nitrogen, isobutane, or normal butane. Between 115 and 120 K, the uncertainties of predicted excess volumes are expected to become unacceptably large ( $>0.15\%$  of the mixture molar volume) for multicomponent LNG mixtures containing more than 5 mole percent nitrogen. For mixtures containing only methane, ethane, and propane, the model should be applicable from 30 to 100 mole percent of methane from 105 to 120 K, and probably to somewhat higher temperatures. It is believed that, within these limits of composition and temperature, the uncertainty in predicted excess volumes for multicomponent LNG mixtures is equivalent to about  $\pm 0.15\%$  of the mixture molar volume. Best results are expected in the middle of the applicable temperature range, i.e., 110–115 K, particularly if eqn. (9) is used instead of eqn. (8).

Some comparisons between experimental excess volumes for selected multicomponent mixtures of LNG components from the literature and predicted results using both eqns. (8) and (9) are given in Table 4. In almost all cases, the predicted excess volumes are less than the experimental values, and only for the mixture containing 72 mole percent of methane with ethane and propane (Shana'a and Canfield, 1968) does the difference exceed 0.15% of the mixture molar volume. The average difference between predicted and experimental excess volumes is about  $-0.09\%$  of the mixture molar volume. Comparisons are also being made with excess volumes from experimental multicomponent mixture measurements in the NBS LNG density project, and these will be published with the data in the near future.

#### ESTIMATING DENSITIES OF LNG, INCLUDING PENTANES

Use of the present model for estimating the orthobaric molar volume, and thus the density, of a liquefied natural gas mixture at a desired temperature and saturation pressure follows directly from eqn. (1). A consistent set of pure

TABLE 4

Comparisons of predicted and experimental excess volumes ( $\text{cm}^3/\text{mol}$ ) for multicomponent liquid mixtures of LNG components reported in the literature

Data source	Mixture composition	T (K)	$V_m$	$V_{\text{exp}}^E$	$V_{\text{calc.}}^E$ eqn. (8), (10)	$\frac{100 \Delta V^E}{V_m}$ (exp. - calc.) (%)	$V_{\text{calc.}}^E$ eqn. (9), (10)	$\frac{100 \Delta V^E}{V_m}$ (exp. - calc.) (%)
Rodosevich and Miller, 1973	0.8466 CH <sub>4</sub>	108	39.322	-0.46	-0.448	-0.03	-0.457	-0.01
	0.1025 C <sub>2</sub> H <sub>6</sub>	115	40.096	-0.55	-0.504	-0.12	-0.498	-0.13
	0.0509 C <sub>3</sub> H <sub>8</sub>							
Shana'a and Canfield, 1968	0.3884 CH <sub>4</sub>	108.15	47.288	-0.598	-0.546	-0.11	-0.547	-0.11
	0.3216 C <sub>2</sub> H <sub>6</sub>							
	0.2900 C <sub>3</sub> H <sub>8</sub>							
Shana'a and Canfield, 1968	0.7238 CH <sub>4</sub>	108.15	41.160	-0.730	-0.634	-0.23	-0.650	-0.19
	0.1668 C <sub>2</sub> H <sub>6</sub>							
	0.1094 C <sub>3</sub> H <sub>8</sub>							
Rodosevich, 1973	0.8679 CH <sub>4</sub>	108	40.951	-0.59	-0.589	-0.00	-0.606	+0.04
	0.0818 C <sub>3</sub> H <sub>8</sub>	115	41.724	-0.69	-0.669	-0.05	-0.657	-0.08
	0.0503 iC <sub>4</sub> H <sub>10</sub>							
Miller, 1974	0.8303 CH <sub>4</sub>	108	39.95	-0.56	-0.540	-0.05	-0.550	-0.03
	0.1001 C <sub>2</sub> H <sub>6</sub>	115	40.73	-0.64	-0.605	-0.09	-0.600	-0.10
	0.0493 C <sub>3</sub> H <sub>8</sub>							
	0.0203 nC <sub>4</sub> H <sub>10</sub>							
Rodosevich and Miller, 1973	0.0505 N <sub>2</sub>	108	38.400	-0.56	-0.536	-0.06	-0.536	-0.06
	0.8409 CH <sub>4</sub>	115	39.261	-0.85	-0.816	-0.09	-0.816	-0.09
	0.1086 C <sub>2</sub> H <sub>6</sub>							
Rodosevich and Miller, 1973	0.0447 N <sub>2</sub>	108	38.549	-0.50	-0.454	-0.12	-0.465	-0.09
	0.9055 CH <sub>4</sub>							
	0.0497 C <sub>3</sub> H <sub>8</sub>							

component molar volumes adjusted to the mixture vapor pressure at the same temperature are needed to make this calculation.

The saturated liquid molar volumes of nitrogen and the alkanes through the butanes are readily obtained from the expression

$$\rho - \rho_c = a \left(1 - \frac{T}{T_c}\right)^{0.35} + \sum_{i=1}^3 b_i \left(1 - \frac{T}{T_c}\right)^{(i+2)/3} \quad (12)$$

with the parameters given by Haynes et al. (1976) and Haynes and Hiza (1977). In this expression  $\rho$  is the density in mol/l,  $T$  is the temperature in Kelvin, and the subscript c denotes the critical point. For isopentane and normal pentane, saturated liquid molar volumes between 105 and 120 K can be obtained by extrapolation of the data of Orrit and Laupretre (1978) or of McClune (1976). Densities from these investigators are generally within 0.1% of the NBS values for the lower molecular weight alkanes. In his paper, McClune gives the constants for a quadratic expression in temperature which he used to extrapolate the densities for isopentane and normal pentane down to 93 K. In the present paper, the densities given by Orrit and Laupretre for isopentane (from 124.925 to 253.794 K) and for normal pentane (from 148.879 to 249.011 K) were fitted to eqn. (12) with values of  $\rho_c$  and  $T_c$  taken from Kudchadker et al. (1968). These parameters of eqn. (12) are given in Table 5. Compared with molar volumes between 120 and 105 K from McClune's extrapolation, molar volumes obtained from the fit of the data of Orrit and Laupretre are larger for isopentane by 0.14–0.15% and smaller for normal pentane by 0.09–0.29%. With the small concentrations of pentanes normally encountered in LNG mixtures, these differences are not significant.

Of common interest is the molar volume or density at a temperature where the total vapor pressure of the liquid mixture is about atmospheric pressure. For mixtures containing mole fractions of 0.85–0.97 methane, 0.03–0.09 ethane, and up to 0.016 nitrogen, 0.03 propane, 0.01 butanes, and 0.0023 pentanes, Giarratano and Collier (1977) report a calculated boiling point temperature range from about 106.5 K with a nitrogen mole fraction of 0.016 to about 113.2 K with no nitrogen. The pure component molar volumes given in Table 6 at 0.5 K increments from 105 to 116 K and at 120 K can be used

TABLE 5  
Parameters of eqn. (12) for isopentane and normal pentane

	isopentane	normal pentane
$a$	2.946310	-0.03620055
$b_1$	35.50771	59.00203
$b_2$	-57.41243	-93.44194
$b_3$	28.15898	43.66781
$T_c$ (K)	460.39	469.60
$\rho_c$ (mol/l)	3.271	3.285

TABLE 6  
Liquid molar volumes ( $\text{cm}^3/\text{mol}$ ) for the pure components of LNG

$T$ (K)	$V_{\text{N}_2}$	$V_{\text{CH}_4}$	$V_{\text{C}_2\text{H}_6}$	$V_{\text{C}_3\text{H}_8}$	$V_{\text{C}_4\text{H}_{10}}$	$V_{\text{C}_4\text{H}_{10}}$	$V_{\text{C}_4\text{H}_{10}}$	$V_{\text{C}_5\text{H}_{12}}$	$V_{\text{C}_5\text{H}_{12}}$
105.0	43.138	37.112	47.266	61.766	77.538	76.100	90.840	90.728	
105.5	43.408	37.173	47.307	61.810	77.588	76.147	90.894	90.781	
106.0	43.687	37.234	47.348	61.855	77.637	76.194	90.948	90.833	
106.5	43.977	37.295	47.389	61.899	77.687	76.242	91.001	90.885	
107.0	44.276	37.357	47.430	61.944	77.736	76.289	91.055	90.938	
107.5	44.588	37.419	47.471	61.988	77.786	76.336	91.109	90.990	
108.0	44.911	37.481	47.512	62.033	77.836	76.384	91.163	91.042	
108.5	45.247	37.544	47.553	62.078	77.886	76.431	91.217	91.095	
109.0	45.598	37.607	47.595	62.122	77.935	76.479	91.271	91.147	
109.5	45.964	37.671	47.636	62.167	77.985	76.526	91.325	91.199	
110.0	46.348	37.735	47.678	62.212	78.035	76.574	91.379	91.252	
110.5	46.748	37.800	47.719	62.257	78.085	76.622	91.434	91.304	
111.0	47.169	37.864	47.761	62.302	78.136	76.670	91.488	91.357	
111.5	47.610	37.930	47.803	62.347	78.186	76.717	91.542	91.410	
112.0	48.077	37.995	47.845	62.392	78.236	76.765	91.596	91.462	
112.5	48.569	38.061	47.887	62.438	78.286	76.813	91.651	91.515	
113.0	49.089	38.128	47.929	62.483	78.337	76.861	91.705	91.567	
113.5	49.641	38.195	47.971	62.528	78.387	76.909	91.759	91.620	
114.0	50.230	38.262	48.014	62.574	78.438	76.957	91.814	91.673	
114.5	50.857	38.330	48.056	62.619	78.488	77.005	91.868	91.725	
115.0	51.529	38.398	48.099	62.665	78.539	77.054	91.923	91.778	
115.5	52.252	38.467	48.141	62.710	78.590	77.102	91.977	91.831	
116.0	53.033	38.536	48.184	62.756	78.640	77.150	92.032	91.884	
120.0	62.884	39.106	48.529	63.124	79.049	77.539	92.470	92.307	

\* Molar volumes of nitrogen adjusted to 1 bar.

directly to calculate the ideal contribution to the mixture molar volume when the mixture vapor pressure is about *one bar*. The molar volumes given in Table 5 for nitrogen were adjusted to one bar using isothermal compressibilities given by the following expression

$$\beta_{N_2}(\text{bar}^{-1}) = -0.001032 + 0.051368/(126.2 - T). \quad (13)$$

The molar volumes given for all of the other fluids are the orthobaric (saturation) values. Values for isopentane and normal pentane were calculated from eqn. (12) and the parameters given in Table 5. Though the isothermal compressibility correction has little effect on the methane molar volume at the conditions considered here, one can determine the magnitude of the pressure effect using the following expression to obtain the isothermal compressibility for methane:

$$\beta_{CH_4}(\text{bar}^{-1}) = -0.0001595 + 0.029488/(190.555 - T) \quad (14)$$

Between 105 and 120 K, eqns. (13) and (14) represent isothermal compressibilities listed by Rowlinson (1969) within 4% for nitrogen and within 2% for methane. At the same temperatures eqn. (14) gives isothermal compressibilities for methane that are smaller but within 3% of those taken from the more recent data of Goodwin (1974).

There are no experimental data in the literature from which excess volume ratios of methane + pentanes to methane + ethane can be derived. However, for the present purpose estimates of these ratios were made by inspection of the excess volume ratios of methane + propane, methane + isobutane, and methane + normal butane to methane + ethane. Based on these estimates, eqn. (9) can be rewritten to include the pentanes as follows:

$$V_{CC}^E(@x_1^*) = V_{12}^E \left[ 1 + (0.6075x_1^* + 0.1664) \frac{x_3}{(1-x_1^*)} + \frac{x_4}{(1-x_1^*)} + \frac{1.5x_5}{(1-x_1^*)} + \frac{2.2x_6}{(1-x_1^*)} + \frac{3.1x_7}{(1-x_1^*)} \right] \quad (15)$$

In eqn. (15), subscripts 6 and 7 refer to isopentane and normal pentane, respectively. For the nitrogen + hydrocarbon contribution,  $V_{NC}^E$ , to the total excess volume,  $V_t^E$ , of mixtures containing small amounts of pentanes, eqns. (10) and (11) should be used without modification.

## CONCLUSION

For liquid mixtures containing nitrogen and the low molecular weight alkanes all at subcritical temperatures, the mathematical excess volume model proposed here combined with the consistent set of experimental pure component densities now available, allow reasonable estimates of the orthobaric liquid densities of mixtures containing these components within defined composition limits. For the special case involving some typical LNG compositions

over a limited temperature range (105 to 115 K), liquid mixture densities can be predicted with the present method with an inaccuracy of  $\pm 0.15\%$  or less. Additional LNG type mixtures data, consistent with the pure component and binary mixtures data used here, would more clearly identify the composition and uncertainty limits of the present model.

#### ACKNOWLEDGMENTS

The contribution of M.J. Brown to the reduction of the data is gratefully acknowledged. Partial support of this work was provided by British Gas Corp., Chicago Bridge and Iron Co., Columbia Gas Service Corp., Distrigas Corp., Easco Gas LNG, Inc., El Paso Natural Gas, Gaz de France, Marathon Oil Co., Mobil Oil Corp., Natural Gas Pipeline Co., Phillips Petroleum Co., Shell International Gas, Ltd., Sonatrach, Southern California Gas Co., Tennessee Gas Pipeline Co., Texas Eastern Transmission Co., Tokyo Gas Co., Ltd., and Transcontinental Gas Pipe Line Corp., through a grant administered by the American Gas Association, Inc.

#### REFERENCES

- Giarratano, P.J. and Collier, R.S., 1977. Evaluation of capacitance densitometry for LNG mixtures with low nitrogen composition. *Ind. Eng. Chem., Proc. Design and Development*, 16: 330-336.
- Goodwin, R.D., 1974. The thermophysical properties of methane, from 90 to 500 K at pressures to 700 bar. *Nat. Bur. Stand. (U.S.), Tech. Note 653*, 274 pp.
- Haynes, W.M. and Hiza, M.J., 1977. Measurements of the orthobaric liquid densities of methane, ethane, propane, isobutane, and normal butane. *J. Chem. Thermodynam.*, 9: 179-187.
- Haynes, W.M., Hiza, M.J. and Frederick, N.V., 1976. Magnetic suspension densimeter for measurements on fluids of cryogenic interest. *Rev. Sci. Instrum.*, 47: 1237-1250.
- Hiza, M.J. and Haynes, W.M., 1978. Liquid mixture excess volumes and total vapor pressures using a magnetic suspension densimeter with compositions determined by chromatographic analysis: methane + ethane. In: K.D. Timmerhaus (Ed.), *Advances in Cryogenic Engineering*, Vol. 23, Plenum, New York, paper M-6 (in press).
- Hiza, M.J., Haynes, W.M. and Parrish, W.R., 1977. Orthobaric liquid densities and excess volumes for binary mixtures of low molar-mass alkanes and nitrogen between 105 and 140 K. *J. Chem. Thermodynam.*, 9: 873-896.
- Klosek, J. and McKinley, C., 1968. Densities of liquefied natural gas and low molecular weight hydrocarbons. In: J.W. White and A.E.S. Neumann (Editors), *Proceedings of First International Conference on LNG*, Institute of Gas Technology, Chicago, Ill., Paper 22, Session 5.
- Kudchadker, A.P., Alani, G.H. and Zwolinski, B.J., 1968. The critical constants of organic substances. *Chem. Rev.*, 68: 659-735.
- McClune, C.R., 1976. Measurement of the densities of liquefied hydrocarbons from  $-100$  to  $-180^{\circ}\text{C}$  (173 to 93 K). *Cryogenics*, 16: 289-295.
- Miller, R.C., 1974. Estimating the densities of natural gas mixtures. *Chem. Eng.*, 81 (No. 23): 134-135.
- Orrit, J. and Laupretre, J.M. 1978. Density of liquefied natural gas constituents. In: K.D. Timmerhaus (Ed.), *Advances in Cryogenic Engineering*, Vol. 23, Plenum, New York, paper M-4 (in press). (see also: Orrit, J. and Olives, J.F., 1974. Density of liquefied

- natural gas and its components. Unpublished report distributed at 4th International Conference on Liquefied Natural Gas, Algeria, 16 pp).
- Rodosevich, J.B., 1973. Measurement and prediction of liquefied natural gas densities. M.S. Thesis, Univ. of Wyoming, Laramie, 83 pp.
- Rodosevich, J.B. and Miller, R.C., 1973. Experimental liquid mixture densities for testing and improving correlations for liquefied natural gas. *A.I.Ch.E.J.*, 19: 729—735.
- Rowlinson, J.S., 1969. *Liquids and liquid mixtures*. 2nd edn., Butterworths, London, 371 pp.
- Shana'a, M.Y. and Canfield, F.B., 1968. Liquid density and excess volume of light hydrocarbon mixtures at  $-165^{\circ}\text{C}$ . *Trans. Faraday Soc.*, 64 (No. 549, Part 9): 2281—2286.

*A concentric cylinder capacitor has been used to measure the orthobaric liquid dielectric constants of multicomponent mixtures of the major components of liquefied natural gas (LNG) to an accuracy of approximately  $\pm 0.05\%$  at temperatures from 110 to 130 K. These mixtures ranged from a ternary mixture containing nitrogen, methane, and normal butane to four to eight component methane rich (74 to 90 mol %) mixtures containing up to 5 mol % of nitrogen, 16 mol % of ethane, 7 mol % of propane, 5 mol % of the butanes, and 0.44 mol % of the pentanes. Some of these mixtures were prepared to simulate commercial LNG compositions. Experimental densities previously reported for these mixtures have been combined with the mixture dielectric constant data to calculate values of the Clausius-Mossotti (CM) function and the excess CM function. Pure component experimental CM functions for LNG components except for propane and isobutane have been combined with the mixture data in the development of a simple calculational technique for the prediction of LNG densities to an uncertainty of approximately  $\pm 0.15\%$  based on a knowledge of the composition and dielectric constant of the liquid mixtures. In fitting the data, pseudo values of the CM function are derived for the slightly polar components, propane and isobutane, while constraining the mixture excess CM function to be zero.*

## Prediction of liquefied natural gas (LNG) densities from new experimental dielectric constant data

W.M. Haynes and R.D. McCarty

**Key words:** liquefied natural gas, density, dielectric constant

A large-scale project has been carried out at this laboratory to provide one or more mathematical models to predict the density of a liquefied natural gas (LNG) mixture to within an uncertainty of 0.1%, given the temperature, composition and pressure of the liquid mixture. Such models will serve as a basis for custody transfer. The mathematical models developed for this purpose have ranged from simple empirical models<sup>1-4</sup> to those that are theoretically based<sup>2-4</sup> and, consequently, much more complex.

In order to develop and test such models, a comprehensive, accurate and consistent set of density data has been obtained for the major components<sup>5,6</sup> of LNG and for mixtures<sup>7-10</sup> of these components. Most of these data were obtained with a magnetic suspension densimeter.<sup>5,7,11</sup> Prior to the completion of the LNG density project, the apparatus was completely rebuilt because of the need to extend the pressure capability of the apparatus.<sup>12</sup> During the reconstruction of the apparatus, it was decided to include a capacitor inside the sample space so that simultaneous measurements of dielectric constant and density could be performed on the same fluid samples. The new apparatus was subsequently used to complete the measurements for the LNG density project. The measurements with the new apparatus included density and dielectric constant data for binary mixtures of methane with either isobutane or normal butane<sup>10</sup> and for multicomponent mixtures<sup>9</sup> with up to eight components, some simulating commercial LNG compositions. The experimental densities for the multicomponent mixtures were reported as a function of temperature and pressure in an earlier paper.<sup>9</sup> The dielectric constant measurements that were performed at the same time were not published along with the density data since, at the time of the measurements and analysis of the density data, there were insufficient pure fluid dielectric constant data

for LNG components at low temperatures to analyse properly the dielectric constant results. Thus, one of the major purposes of this paper is to present the dielectric constant data for multicomponent mixtures of LNG components, for which the pressure density temperature properties have been reported previously.

The dielectric constant of a fluid is closely related to its density through the Clausius-Mossotti (CM) function. In fact, dielectric constant measurements can serve as a simple and reliable substitute for density measurements. In the custody transfer of LNG, densities are usually determined either by direct density measurements with a commercially available instrument or indirectly using a calculation based on measurements of composition and temperature. One technique employed in commercial densimeters is based on a density determination through the application of capacitance (or dielectric constant) measurements.

The dielectric constant data for multicomponent mixtures of LNG components have been combined with the previously reported density data to develop a simple calculational scheme for the prediction of LNG densities based on measurements of the dielectric constant and composition of the liquid mixture. This procedure provides an alternative approach to the complex models<sup>2-4</sup> that have been previously used for prediction of LNG densities. Additionally, the procedure presented here can be used as a relatively simple check against any of the other LNG density determination methods, whether by direct or indirect means. It should be emphasized that, in most cases, it is much easier to perform accurate and precise measurements of dielectric constant than of density.

The prediction of LNG and LPG (liquefied petroleum gas) densities and heating values from dielectric constant

0011-2275/83/080421-06 \$03.00 © 1983 Butterworth & Co (Publishers) Ltd.

measurements has been investigated by Miller and colleagues.<sup>13-15</sup> However, their work for LNG<sup>13</sup> was based primarily on binary mixture data, along with two ternary mixtures, and did not include pentanes. The present study probably includes the only experimental dielectric constant data that have been obtained for multicomponent mixtures simulating commercial LNG compositions.

## Experimental

The experimental apparatus, procedures, and uncertainties have been described in detail elsewhere.<sup>9,10,12</sup> The dielectric constant measurements were performed using a concentric cylinder capacitor with a vacuum capacitance of approximately 20 pF. The dielectric constant was obtained from measurements of the ratio of the capacitance with liquid between the electrodes to the vacuum capacitance. Capacitances were measured to a resolution of  $10^{-6}$  pF, which is equivalent to the stability of the vacuum capacitance. Based on reproducibility of binary mixture dielectric constant measurements<sup>10</sup> with the same capacitor, the uncertainty in the dielectric constant data for the multicomponent mixtures investigated in the present work should be no larger than 0.05%.

Density data<sup>9</sup> were obtained simultaneously with the dielectric constant results for the mixtures investigated here. The devices for measuring density and dielectric constant were contained in a single sample cell; therefore, measurements of these properties were made on the same liquid samples. During the course of the mixture measurements, data were obtained for liquid methane, prior to filling the cell with each new mixture sample, as a control on the measurement process for determining density. The dielectric constant data for liquid methane (usually at 120 K), obtained along with the density data, agreed to better than 0.02% with the results of Straty and Goodwin.<sup>16</sup> Vacuum capacitances were measured for each new filling of the cell.

From an analysis of the density measurement technique, it has been shown that the total systematic error in the density determination is approximately 0.05%.<sup>5</sup> Combined with the 0.05% uncertainty in the dielectric constant, it is estimated that the maximum uncertainty in the derived values of the Clausius-Mossotti function is 0.15%.

## Results

The experimental orthobaric liquid dielectric constants of mixtures of LNG components are presented in Table 1 as a function of temperature (IPTS-68), pressure, and density. As noted in a preceding section, the vapour pressure and density data that were obtained simultaneously with the dielectric constant results have been discussed in detail.<sup>9</sup> The compositions of the mixtures were determined gravimetrically except those for mixtures m, n, and p. For these mixtures the compositions were determined by analyses of the prepared mixtures using a gas chromatograph with a thermal conductivity detector.

Small adjustments were made to the observed dielectric constants to account for differences in compositions between the prepared gas mixtures and the liquid mixtures condensed into the equilibrium cell, which resulted from vapour occupying a small part of the sample space. The maximum correction was less than 0.03%, which was for mixture a at 125 K. All other corrections were of the order of 0.01% or less. For mixtures containing only hydrocar-

bons, the vapour composition was assumed to be pure methane. For mixtures with nitrogen as a constituent, the vapour composition was estimated from partial-pressure calculations using available phase-equilibrium data for nitrogen-methane mixtures.<sup>17,18</sup>

The experimental dielectric constants,  $\epsilon$ , have been combined with the experimental densities,  $\rho$ , to calculate values for the Clausius-Mossotti function  $CM$ , from the relation,

$$CM = \left( \frac{\epsilon - 1}{\epsilon + 2} \right) \frac{1}{\rho} \quad (1)$$

The excess Clausius-Mossotti function ( $CM^E$ ), analogous to the definition of the excess volume of a liquid mixture, is given by the expression,

$$CM^E = CM - \sum_i x_i CM_i \quad (2)$$

where  $CM$ , as defined above, refers to the Clausius-Mossotti function of the liquid mixture at a given temperature at saturation pressure,  $x_i$  is the mole fraction of component  $i$ , and  $CM_i$  is the Clausius-Mossotti function of component  $i$  at the same temperature and pressure as the mixture. Along an isotherm, the  $CM$  function is a very slowly varying function; therefore, adjustments of the pure component  $CM_i$ 's to the saturation pressure of the mixture are sufficiently small to neglect.

In the calculation of  $CM_i$ 's, the pure fluid orthobaric liquid densities were obtained from expressions given in references 1, 5, and 6. The dielectric constants for nitrogen were taken from Ely and Straty<sup>19</sup>; for methane from Straty and Goodwin<sup>16</sup>; for ethane from Weber<sup>20</sup>; and for propane, isobutane, and normal butane from Haynes and Younglove.<sup>21</sup> For the pentanes, no dielectric constant data could be found in the literature for temperatures less than 223 K. Therefore, dielectric constant values for the pentanes at temperatures between 110 and 130 K have been estimated by a linear extrapolation of higher temperature results.<sup>15,22-26</sup> The values used for saturated liquid isopentane ranged from 2.138 at 110 K to 2.105 at 130 K, while for normal pentane the values varied from 2.123 at 110 K to 2.092 at 130 K. These extrapolated values are estimated to be accurate to better than  $\pm 1\%$ . An uncertainty of 1% in the dielectric constant for either of the pentanes corresponds to a change of less than  $0.0008 \text{ cm}^3 \text{ mol}^{-1}$  in the mole fraction average of the  $CM_i$ 's ( $\sum_i x_i CM_i$ ) for mixture o, which contains the largest amount of the pentanes (approximately 0.2 mol% for each pentane) of the mixtures investigated here. A change of  $8 \times 10^{-4} \text{ cm}^3 \text{ mol}^{-1}$  represents less than 0.01% of the mixture  $CM$  function.

From the results presented in Table 1, several observations concerning trends in the behaviour of the excess  $CM$  function can be noted. For the measurements of the present study, the  $CM^E$ 's are generally small and positive and decrease with increasing temperature. (For the same mixtures, the excess volumes were negative, increasing in magnitude (more negative) with increasing temperature.<sup>9</sup>) The maximum observed excess  $CM$  function for the mixtures of this study was approximately 0.25% of the mixture  $CM$  function. Those mixtures that contain the largest fractions of the polar components, propane and isobutane, are characterized by the largest excess  $CM$  functions. This behaviour was expected based on dielectric constant and density

**Table 1.** Orthobaric liquid dielectric constants  $\epsilon$  and Clausius-Mossotti functions  $CM$  of multicomponent mixture of LNG components

$T, K$	$P, MPa$	$\rho_{\text{expt}}, \text{mol dm}^{-3}$	$\epsilon$	$CM, \text{cm}^3 \text{mol}^{-1}$	$CM^E, \text{cm}^3 \text{mol}^{-1}$	$\frac{10^2(\rho_{\text{expt}} - \rho_{\text{calc}})}{\rho_{\text{expt}}}$	$\frac{10^2(\rho_{\text{expt}} - \rho_{\text{FIT}})}{\rho_{\text{expt}}}$
a - 0.05931 N <sub>2</sub> + 0.89071 CH <sub>4</sub> + 0.04998 nC <sub>4</sub> H <sub>10</sub> (MW = 18.8562)							
110.00	0.2400	25.3450	1.65978	7.1130	0.0068	-0.095	-0.058
115.00	0.3145	24.9440	1.64742	7.1160	0.0069	-0.097	-0.100
120.00	0.4082	24.5383	1.63497	7.1188	0.0071	-0.100	-0.140
125.00	0.5196	24.1141	1.62203	7.1218	0.0069	-0.097	-0.181 <sup>†</sup>
b - 0.86040 CH <sub>4</sub> + 0.04600 C <sub>2</sub> H <sub>6</sub> + 0.04790 C <sub>3</sub> H <sub>8</sub> + 0.04570 iC <sub>4</sub> H <sub>10</sub> (MW = 19.9552)							
115.00	0.1186	24.2654	1.70983	7.8852	0.0092	-0.117	0.036
120.00	0.1710	23.9371	1.69759	7.8815	0.0043	-0.055	0.082
125.00	0.2387	23.5868	1.68523	7.8832	0.0042	-0.053	0.061 <sup>†</sup>
130.00	0.3248	23.2331	1.67269	7.8836	0.0026	-0.033	0.056 <sup>†</sup>
135.00	0.4320	22.8637	1.65999	7.8870	0.0041	-0.052	0.013 <sup>†</sup>
c - 0.85378 CH <sub>4</sub> + 0.05178 C <sub>2</sub> H <sub>6</sub> + 0.04703 C <sub>3</sub> H <sub>8</sub> + 0.04741 iC <sub>4</sub> H <sub>10</sub> (MW = 20.0838)							
115.00	0.1191	24.2100	1.71285	7.9304	0.0115	-0.145	0.005
120.00	0.1706	23.8779	1.70061	7.9288	0.0088	-0.111	0.026
125.00	0.2379	23.5324	1.68823	7.9296	0.0078	-0.098	0.071 <sup>†</sup>
130.00	0.3238	23.1834	1.67570	7.9293	0.0055	-0.069	0.019 <sup>†</sup>
d - 0.85133 CH <sub>4</sub> + 0.05759 C <sub>2</sub> H <sub>6</sub> + 0.04808 C <sub>3</sub> H <sub>8</sub> + 0.04300 nC <sub>4</sub> H <sub>10</sub> (MW = 20.0092)							
115.00	0.1180	24.3243	1.70951	7.8632	0.0090	-0.114	-0.009
120.00	0.1700	23.9965	1.69758	7.8619	0.0052	-0.066	0.008
125.00	0.2374	23.6586	1.68553	7.8621	0.0024	-0.031	0.006 <sup>†</sup>
130.00	0.3232	23.3108	1.67330	7.8631	0.0003	-0.004	-0.007 <sup>†</sup>
135.00	0.4301	22.9634	1.66120	7.8645	-0.0012	0.015	-0.025 <sup>†</sup>
e - 0.84566 CH <sub>4</sub> + 0.07924 C <sub>2</sub> H <sub>6</sub> + 0.05060 C <sub>3</sub> H <sub>8</sub> + 0.02450 nC <sub>4</sub> H <sub>10</sub> (MW = 19.6051)							
115.00	0.1167	24.5569	1.70224	7.7241	0.0028	-0.036	0.077
120.00	0.1683	24.2126	1.69016	7.7244	0.0008	-0.010	0.073
125.00	0.2350	23.8698	1.67791	7.7219	-0.0024	0.031	0.106 <sup>†</sup>
130.00	0.3201	23.5204	1.66557	7.7198	-0.0098	0.127	0.132 <sup>†</sup>
f - 0.04801 N <sub>2</sub> + 0.80940 CH <sub>4</sub> + 0.04542 C <sub>2</sub> H <sub>6</sub> + 0.05050 C <sub>3</sub> H <sub>8</sub> + 0.04667 iC <sub>4</sub> H <sub>10</sub> (MW = 20.6355)							
115.00	0.3005	24.1487	1.69935	7.8284	0.0195	-0.249	-0.090
120.00	0.3863	23.8075	1.68708	7.8273	0.0172	-0.220	-0.075
125.00	0.4874	23.4518	1.67464	7.8285	0.0165	-0.211	-0.092 <sup>†</sup>
130.00	0.6125	23.0893	1.66152	7.8248			-0.043 <sup>†</sup>
g - 0.02628 N <sub>2</sub> + 0.81249 CH <sub>4</sub> + 0.08484 C <sub>2</sub> H <sub>6</sub> + 0.04931 C <sub>3</sub> H <sub>8</sub> + 0.02708 nC <sub>4</sub> H <sub>10</sub> (MW = 20.0706)							
115.00	0.2214	24.4562	1.69916	7.7283	0.0150	-0.194	-0.083
120.00	0.2874	24.1119	1.68701	7.7278	0.0120	-0.155	-0.077
125.00	0.3768	23.7507	1.67487	7.7322	0.0134	-0.173	-0.133 <sup>†</sup>
130.00	0.4793	23.3954	1.66264	7.7331			-0.145 <sup>†</sup>
h - 0.85892 CH <sub>4</sub> + 0.11532 C <sub>2</sub> H <sub>6</sub> + 0.01341 C <sub>3</sub> H <sub>8</sub> + 0.00530 iC <sub>4</sub> H <sub>10</sub> + 0.00705 nC <sub>4</sub> H <sub>10</sub> (MW = 18.5565)							
115.00	0.1185	25.0957	1.68091	7.3711	0.0006	-0.008	0.028
120.00	0.1706	24.7131	1.66863	7.3749	0.0021	-0.028	-0.022
125.00	0.2372	24.3294	1.65622	7.3771	0.0012	-0.016	-0.052 <sup>†</sup>
130.00	0.3225	23.9490	1.64364	7.3760	-0.0030	0.041	-0.037 <sup>†</sup>

Table 1. continued

$T, K$	$P, MPa$	$\rho_{\text{expt}}, \text{mol dm}^{-3}$	$\epsilon$	$CM, \text{cm}^3 \text{mol}^{-1}$	$CM^E, \text{cm}^3 \text{mol}^{-1}$	$\frac{10^2(\rho_{\text{expt}} - \rho_{\text{calc}})}{\rho_{\text{expt}}}$	$\frac{10^2(\rho_{\text{expt}} - \rho_{\text{FIT}})}{\rho_{\text{expt}}}$
i - 0.84558 CH <sub>4</sub> + 0.08153 C <sub>2</sub> H <sub>6</sub> + 0.04778 C <sub>3</sub> H <sub>8</sub> + 0.01259 iC <sub>4</sub> H <sub>10</sub> + 0.01252 nC <sub>4</sub> H <sub>10</sub> (MW = 19.5838)							
115.00	0.1166	24.5586	1.70334	7.7334	0.0094	-0.122	-0.000
120.00	0.1680	24.2180	1.69122	7.7323	0.0062	-0.080	0.014
125.00	0.2348	23.8688	1.67899	7.7322	0.0035	-0.045	0.014 <sup>†</sup>
130.00	0.3188	23.5154	1.66656	7.7309	-0.0006	0.008	0.032 <sup>†</sup>
j - 0.00601 N <sub>2</sub> + 0.90613 CH <sub>4</sub> + 0.06026 C <sub>2</sub> H <sub>6</sub> + 0.02154 C <sub>3</sub> H <sub>8</sub> + 0.00300 iC <sub>4</sub> H <sub>10</sub> + 0.00306 nC <sub>4</sub> H <sub>10</sub> (MW = 17.8195)							
115.00	0.1478	25.3834	1.65987	7.1030	0.0057	-0.080	-0.025
120.00	0.2043	24.9894	1.64698	7.0991	-0.0005	0.007	0.031
125.00	0.2785	24.5702	1.63408	7.1013	-0.0011	0.016	-0.001 <sup>†</sup>
130.00	0.3722	24.1578	1.62098	7.0989			0.033 <sup>†</sup>
k - 0.00973 N <sub>2</sub> + 0.88225 CH <sub>4</sub> + 0.07259 C <sub>2</sub> H <sub>6</sub> + 0.02561 C <sub>3</sub> H <sub>8</sub> + 0.00490 iC <sub>4</sub> H <sub>10</sub> + 0.00492 nC <sub>4</sub> H <sub>10</sub> (MW = 18.3094)							
115.00	0.1639	25.2023	1.67011	7.2448	0.0081	-0.112	0.155
120.00	0.2247	24.8047	1.65731	7.2456	0.0067	-0.093	0.144
125.00	0.3022	24.4022	1.64434	7.2455	0.0037	-0.051	-0.055 <sup>†</sup>
l - 0.01383 N <sub>2</sub> + 0.85934 CH <sub>4</sub> + 0.08477 C <sub>2</sub> H <sub>6</sub> + 0.02980 C <sub>3</sub> H <sub>8</sub> + 0.00519 iC <sub>4</sub> H <sub>10</sub> + 0.00707 nC <sub>4</sub> H <sub>10</sub> (MW = 18.7496)							
115.00	0.1812	25.0384	1.67817	7.3638	0.0076	-0.103	-0.027
120.00	0.2441	24.6661	1.66553	7.3609	0.0024	-0.033	0.012
125.00	0.3223	24.2880	1.65268	7.3569	-0.0045	0.061	0.066 <sup>†</sup>
130.00	0.4222	23.8981	1.63968	7.3542			0.103 <sup>†</sup>
m - 0.85341 CH <sub>4</sub> + 0.07898 C <sub>2</sub> H <sub>6</sub> + 0.04729 C <sub>3</sub> H <sub>8</sub> + 0.00854 iC <sub>4</sub> H <sub>10</sub> + 0.00992 nC <sub>4</sub> H <sub>10</sub> + 0.00097 iC <sub>5</sub> H <sub>12</sub> + 0.00089 nC <sub>5</sub> H <sub>12</sub> (MW = 19.3587)							
110.00	0.0787	25.0063	1.71025	7.6552	0.0100	-0.131	0.013
115.00	0.1172	24.6566	1.69823	7.6572	0.0098	-0.128	-0.013
120.00	0.1686	24.3079	1.68611	7.6573	0.0078	-0.102	-0.014
125.00	0.2351	23.9525	1.67385	7.6576	0.0054	-0.071	-0.017 <sup>†</sup>
130.00	0.3210	23.5883	1.66137	7.6578	0.0028	-0.037	-0.020 <sup>†</sup>
n - 0.75442 CH <sub>4</sub> + 0.15401 C <sub>2</sub> H <sub>6</sub> + 0.06950 C <sub>3</sub> H <sub>8</sub> + 0.00978 iC <sub>4</sub> H <sub>10</sub> + 0.01057 nC <sub>4</sub> H <sub>10</sub> + 0.00089 iC <sub>5</sub> H <sub>12</sub> + 0.00083 nC <sub>5</sub> H <sub>12</sub> (MW = 21.1060)							
110.00	0.0723	24.2529	1.74897	8.2374	0.0193	-0.234	-0.053
115.00	0.1081	23.9619	1.73738	8.2338	0.0137	-0.166	-0.011
120.00	0.1549	23.6535	1.72575	8.2353	0.0131	-0.159	-0.028
125.00	0.2153	23.3351	1.71406	8.2390	0.0139	-0.169	-0.074 <sup>†</sup>
o - 0.00859 N <sub>2</sub> + 0.75713 CH <sub>4</sub> + 0.13585 C <sub>2</sub> H <sub>6</sub> + 0.06742 C <sub>3</sub> H <sub>8</sub> + 0.01336 iC <sub>4</sub> H <sub>10</sub> + 0.01326 nC <sub>4</sub> H <sub>10</sub> + 0.00223 iC <sub>5</sub> H <sub>12</sub> + 0.00216 nC <sub>5</sub> H <sub>12</sub> (MW = 21.3094)							
110.00	0.1155	24.1809	1.74764	8.2502	0.0136	-0.165	0.015
115.00	0.1595	23.8731	1.73600	8.2521	0.0135	-0.164	-0.008
120.00	0.2155	23.5709	1.72406	8.2486	0.0080	-0.097	0.033
125.00	0.2873	23.2644	1.71227	8.2473	0.0038	-0.046	0.049 <sup>†</sup>
130.00	0.3744	22.9514	1.70017	8.2447			0.082 <sup>†</sup>
p - 0.00801 N <sub>2</sub> + 0.74275 CH <sub>4</sub> + 0.16505 C <sub>2</sub> H <sub>6</sub> + 0.06547 C <sub>3</sub> H <sub>8</sub> + 0.00843 iC <sub>4</sub> H <sub>10</sub> + 0.00893 nC <sub>4</sub> H <sub>10</sub> + 0.00069 iC <sub>5</sub> H <sub>12</sub> + 0.00067 nC <sub>5</sub> H <sub>12</sub> (MW = 21.0976)							
110.00	0.1158	24.3141	1.74469	8.1790	0.0154	-0.188	-0.015
115.00	0.1584	24.0160	1.73307	8.1767	0.0109	-0.133	0.014
120.00	0.2093	23.6937	1.72140	8.1816	0.0137	-0.167	-0.046
125.00	0.2853	23.3804	1.70971	8.1826	0.0117	-0.143	-0.058 <sup>†</sup>

Table 1. continued

<i>T</i> , K	<i>P</i> , MPa	$\rho_{\text{expt}}$ , mol dm <sup>-3</sup>	$\epsilon$	<i>CM</i> , cm <sup>3</sup> mol <sup>-1</sup>	<i>CM</i> <sup>E</sup> , cm <sup>3</sup> mol <sup>-1</sup>	$\frac{10^2(\rho_{\text{expt}} - \rho_{\text{calc}})}{\rho_{\text{expt}}}$	$\frac{10^2(\rho_{\text{expt}} - \rho_{\text{FIT}})}{\rho_{\text{expt}}}$
$q - 0.00599 \text{ N}_2 + 0.90068 \text{ CH}_4 + 0.06537 \text{ C}_2\text{H}_6 + 0.02200 \text{ C}_3\text{H}_8 + 0.00291 \text{ iC}_4\text{H}_{10}$ $+ 0.00284 \text{ nC}_4\text{H}_{10} + 0.00010 \text{ iC}_5\text{H}_{12} + 0.00011 \text{ nC}_5\text{H}_{12}$ (MW = 17.9026)							
115.00	0.1456	25.3600	1.66189	7.1274	0.0031	-0.043	0.013
120.00	0.2024	24.9656	1.64901	7.1242	-0.0024	0.034	0.058
125.00	0.2762	24.5450	1.63624	7.1286	-0.0008	0.012	-0.004 <sup>†</sup>
130.00	0.3698	24.1289	1.62319	7.1284			-0.001 <sup>†</sup>

*MW*, molecular weight; *T*, temperature (IPTS-68); *P*, pressure;  $\rho_{\text{expt}}$ , experimental density; *CM*<sup>E</sup>, excess Clausius-Mossotti function calculated from equation 2;  $\rho_{\text{calc}}$ , density calculated from equation 3 using experimental *CM*<sub>*i*</sub>'s from literature;  $\rho_{\text{FIT}}$ , density calculated from equation 3 using *CM*<sub>*i*</sub> values for propane and isobutane determined from least squares by fitting multicomponent mixture data.

<sup>†</sup>Data not used in fit to equation 3

measurements of binary mixtures of LNG components containing either propane or isobutane.<sup>10,13</sup> For those mixtures containing nitrogen, excess *CM* functions are not given for temperatures above 125 K since the critical temperature of nitrogen is approximately 126.2 K.

Combining (1) and (2) and assuming that the *CM* function of the mixture is a mole fraction average of the pure component *CM*<sub>*i*</sub>'s, ie, *CM*<sup>E</sup> = 0, then a density ( $\rho_{\text{calc}}$ ) of the mixture can be calculated from the relation,

$$\rho_{\text{calc}} = \left( \frac{\epsilon - 1}{\epsilon + 2} \right) \cdot \left( \sum_i x_i CM_i \right)^{-1} \quad (3)$$

Differences between experimental and calculated densities from (3) are presented in the next to last column of Table 1. These differences are equivalent to the ratios of the excess *CM* functions to the mixture *CM* functions (*CM*<sup>E</sup>/*CM*). In other words, assuming *CM*<sup>E</sup> = 0, it is possible to predict the densities of the LNG-like mixtures investigated here within 0.25% from measurements of the dielectric constant, composition, and temperature of the liquid mixture. This would not meet the 0.1% uncertainty level desired in LNG custody transfer applications. However, by making minor modifications to the *CM*<sub>*i*</sub>'s in (3), it is possible to reduce the density uncertainty to near the desired 0.1% goal, as discussed in the next section.

### Calculational technique

In the preceding section, it has been observed that the densities calculated from (3), using available experimental *CM* data for the pure components, can differ by as much as 0.25% from the experimental densities for the LNG-like mixtures investigated here. In general, those mixtures that exhibit the largest differences contain significant amounts of the slightly polar components, propane and isobutane. Subsequently, an effort was initiated to develop a simple mathematical procedure that could be used to predict LNG densities to within an uncertainty of approximately 0.1% from an input of dielectric constant and composition. This calculational technique would incorporate new pseudo values of the *CM* functions of propane and isobutane to account for the relatively large *CM*<sup>E</sup> values observed for mixtures containing these constituents.

The ranges of temperature and composition over which the calculational technique would be applicable

should be defined. The normal boiling point of LNG mixtures is approximately the same as that of pure methane (112 K); thus, the temperature range for the calculational scheme was selected to be 110 to 120 K. The compositions of the mixtures from the present study cover ranges that encompass almost any that might be encountered in LNG custody transfer applications. The extent to which the calculational procedure can be used for compositions outside the range of the present data is not known.

Since the *CM* function varies slowly as a function of temperature (or density) for a liquid along the saturation curve, the *CM* value for each of the pure components of LNG is assumed to be constant from 110 to 120 K. The *CM* values for the saturated liquid at 115 K are used for each of the nonpolar components. Then, new pseudo values of the *CM* function are determined for propane and isobutane (given in Table 2 along with the *CM*<sub>*i*</sub>'s for the nonpolar components) by a least squares fit of (3) using the mixture data in Table 1 for temperatures between 110 and 120 K. These pseudo values for the *CM* function for propane and isobutane are determined by constraining the *CM* function for LNG mixtures to be equal to the mole fraction average of the pure component *CM* values, ie, for *CM*<sup>E</sup> = 0. The new pseudo values for the *CM* function determined from fitting the data are approximately 1.1 and 0.4% larger than experimental *CM* values<sup>21</sup> for propane and isobutane, respectively. The pseudo values are substantially smaller (1.5 to 2.0%) than the infinite dilution values deduced by Pan et al.<sup>13</sup> from binary mixture data for methane with either propane or isobutane.

In the last column of Table 1, comparisons between experimental densities ( $\rho_{\text{expt}}$ ) and values ( $\rho_{\text{FIT}}$ ) calculated from (3) with *CM*<sub>*i*</sub>'s from Table 2 are presented. At temperatures from 110 to 120 K for the mixtures studied here, all deviations between the experimental and calculated densities, using the pseudo values for the *CM* function for propane and isobutane, are less than 0.1% except for mixture a at 120 K (0.14%) and mixture k at 115 K (0.15%) and at 120 K (0.14%). The deviation of greater than 0.1% for mixture a is likely the result of using a constant *CM* value for nitrogen over a 10 K range for a mixture that contains a relatively significant amount (6%) of nitrogen. For temperatures between 110 and 120 K, the average deviation or bias between experimental and calculated densities is -0.001%, while the average absolute deviation is 0.044%. Above 120 K, at temperatures for which the data were not used in the fit, the average absolute deviation was 0.058%. Maximum

**Table 2. Values of the Clausius-Mossotti function for LNG components to be used in (3) to calculate LNG densities**

Component	$CM_i, \text{cm}^3 \text{mol}^{-1}$
Nitrogen	4.3984
Methane	6.5490
Ethane	11.063
Propane	(16.1612)
Isobutane	(21.2305)
Normal butane	20.303
Isopentane	25.151
Normal pentane	24.868

Pseudo values for propane and isobutane (in parentheses) were determined from least squares analysis by fitting the multicomponent mixture data of present study. The  $CM$  functions for the other components are experimental saturated liquid values at 115 K

deviation (0.18%) was for mixture a at 125 K; this mixture contains a relatively large amount of nitrogen, which has a critical temperature of approximately 126.2 K.

### Conclusion

Dielectric constant data are reported for multicomponent mixtures of LNG components at temperatures from 110 to 130 K. Density results obtained simultaneously with the dielectric constant data for these mixtures had been published previously. These density and dielectric constant data have been used to develop a simple, alternative approach for determining densities of LNG mixtures to within an uncertainty of less than 0.15% based on measurements of the dielectric constant and composition of the liquid mixture. Composition measurements are required in determining LNG densities with any correlation or prediction method. It is a relatively simple and straightforward task to perform accurate and precise dielectric constant measurements compared to direct density measurements. The extent to which the calculation can be extrapolated beyond the composition ranges of the mixtures investigated here is unknown. However, the compositions of the present study were selected to cover the ranges that would be encountered in most LNG custody transfer applications.

### Authors

The authors are at the Chemical Engineering Science Division, National Engineering Laboratory, National Bureau of Standards, Boulder, Colorado 80303. Paper received 2 March 1983. The contributions of M.J. Hiza in the prepara-

tion of the mixtures is gratefully acknowledged. This work was carried out at the National Bureau of Standards under the sponsorship of British Gas Corp., Chicago Bridge and Iron Co., Columbia Gas Service Corp., Distrigas Corp., Easco Gas LNG, Inc., El Paso Natural Gas, Gaz de France, Marathon Oil Co., Mobil Oil Corp., Natural Gas Pipeline Co., Phillips Petroleum Co., Shell International Gas Ltd., Sonatrach, Southern California Gas Co., Tennessee Gas Pipeline Co., Texan Eastern Transmission Co., Tokyo Gas Co., Ltd., and Transcontinental Gas Pipe Line Corp., through a grand administered by the American Gas Association, Inc.

### References

- 1 Hiza, M.J. *Fluid Phase Equilibria* 2 (1978) 27
- 2 McCarty, R.D. Nat Bur Stand (US), Interagency Report NBSIR 77-867 (1977)
- 3 McCarty, R.D. Nat Bur Stand (US), Technical Note 1030 (1980)
- 4 McCarty, R.D. *J Chem Thermodynamics* 14 (1982) 837
- 5 Haynes, W.M., Hiza, M.J., Frederick, N.V. *Rev Sci Instrum* 47 (1976) 1237
- 6 Haynes, W.M., Hiza, M.J. *J Chem Thermodynamics* 9 (1977) 179
- 7 Hiza, M.J., Haynes, W.M., Parrish, W.R. *J Chem Thermodynamics* 9 (1977) 873
- 8 Hiza, M.J., Haynes, W.M. *J Chem Thermodynamics* 12 (1980) 1
- 9 Haynes, W.M. *J Chem Thermodynamics* 14 (1982) 603
- 10 Haynes, W.M. Orthobaric liquid densities and dielectric constants of (methane + isobutane) and (methane + normal butane) at low temperatures, submitted to *J Chem Thermodynamics*
- 11 Haynes, W.M. *Rev Sci Instrum* 48 (1977) 39
- 12 Haynes, W.M. Apparatus for density and dielectric measurements to 35 MPa on fluids of cryogenic interest, submitted to *J Res Nat Bur Stand (US)*
- 13 Pan, W.P., Mady, M.H., Miller, R.C. *AIChE J* 21 (1975) 283
- 14 Thompson, Jr., R.T., Miller, R.C. *Advances in Cryogenic Engineering* 25 (1980) 698
- 15 Luo, C.C., Miller, R.C. *Oryogenics* 21 (1981) 85
- 16 Straty, G.C., Goodwin, R.D. *Oryogenics* 13 (1973) 712
- 17 Parrish, W.R., Hiza, M.J. *Advances in Cryogenic Engineering* 19 (1974) 300
- 18 Kidnay, A.J., Miller, R.C., Parrish, W.R., Hiza, M.J. *Cryogenics* 15 (1975) 531
- 19 Ely, J.F., Straty, G.C. *J Chem Phys* 61 (1973) 712
- 20 Weber, L.A. *J Chem Phys* 65 (1976) 446
- 21 Haynes, W.M., Younglove, B.A. *Advances in Cryogenic Engineering* 27 (1982) 883
- 22 Brazier, D.W., Freeman, G.R. *Can J Chem* 47 (1969) 893
- 23 Mopsik, F.J. *J Chem Phys* 50 (1969) 2559
- 24 Moliton, A., Gerbier, J. *Revue de Physique Appliquee* 6 (1971) 273
- 25 Belinskii, B.A., Ikramov, Sh. Kh. *Soviet Physics-Acoustics* 18 (1973) 300
- 26 Dagg, I.R., Reesor, G.E. *Can J Phys* 52 (1974) 29

U.S. DEPT. OF COMM. <b>BIBLIOGRAPHIC DATA SHEET</b> <i>(See instructions)</i>	1. PUBLICATION OR REPORT NO. NBS Monogr. 172	2. Performing Organ. Report No.	3. Publication Date October 1983
4. TITLE AND SUBTITLE LIQUEFIED NATURAL GAS DENSITIES: SUMMARY OF RESEARCH PROGRAM AT THE NATIONAL BUREAU OF STANDARDS			
5. AUTHOR(S) W. M. Haynes, R. D. McCarty and M. J. Hiza			
6. PERFORMING ORGANIZATION <i>(If joint or other than NBS, see instructions)</i> NATIONAL BUREAU OF STANDARDS DEPARTMENT OF COMMERCE WASHINGTON, D.C. 20234		7. Contract/Grant No.	8. Type of Report & Period Covered Final
9. SPONSORING ORGANIZATION NAME AND COMPLETE ADDRESS <i>(Street, City, State, ZIP)</i> British Gas Corp.; Chicago Bridge and Iron Co.; Columbia Gas Service Corp.; Distrigas Corp.; Easco Gas LNG, Inc.; El Paso Natural Gas; Gaz de France; Marathon Oil Co.; Mobil Oil Corp.; Natural Gas Pipeline Co.; Phillips Petroleum Co.; Shell International Gas, Ltd.; Sonatrach; Southern California Gas Co.; Tennessee Gas Pipeline Co.; Texas Eastern Transmission Co.; Tokyo Gas Co., Ltd.; Transcontinental Gas Pipe Line Corp.			
10. SUPPLEMENTARY NOTES <p style="text-align: center;">Library of Congress Catalog Card Number: 83-600608</p> <input type="checkbox"/> Document describes a computer program; SF-185, FIPS Software Summary, is attached.			
11. ABSTRACT <i>(A 200-word or less factual summary of most significant information. If document includes a significant abstract, this section should be omitted.)</i> This report summarizes the results of a project concerning the densities of liquefied natural gas (LNG) and its components. This project, initiated in the Properties of Fluids Section of the Cryogenics Division of the National Bureau of Standards in July 1972, was carried out under the sponsorship of a consortium of eighteen energy companies. The experimental part of this project has included the following accomplishments: (a) development of a magnetic suspension densimeter for absolute density measurements on liquids, including liquid mixtures in equilibrium with their vapor, at temperatures from 90 to 300 K; (b) orthobaric liquid density measurements on the major components of LNG, which include nitrogen (95-120 K), methane (105-160 K), ethane (100-270 K), propane (100-288.7 K), isobutane (115-300 K), and normal butane (135-300 K); (c) orthobaric liquid density measurements on approximately thirty-five binary mixtures of the above components for all combinations except nitrogen + butane systems, primarily in the temperature range of 105 to 130 K; and (d) orthobaric liquid density measurements on twenty-seven multicomponent mixtures (105-120 K), including several LNG-like mixtures with up to eight components. The total uncertainty of a single density measurement is approximately 0.1 percent at low temperatures and decreases to approximately 0.06 percent at room temperature. The estimated standard deviation of a single density measurement is less than 0.02 percent. The density data have been used to optimize, test, and compare several mathematical models as to their suitability for the calculation of LNG densities for custody transfer. Models selected for optimization and testing included an extended corresponding states method, a hard sphere model, a cell model, and an empirical model due to Klosek and McKinley. The ultimate goal of this project was to produce one or more mathematical models that could be used to predict the density of any LNG mixture to within an uncertainty of 0.1 percent from an input of pressure, temperature, and composition. After revisions based on the new experimental data from this project, each of the models investigated here satisfy this goal for typical LNG compositions. The limitations and ranges of validity of the various models are discussed. Also presented are techniques for predicting LNG densities from dielectric constant measurements and from excess volume calculations. The last section of this report consists of publications that provide a complete and detailed account of the results of this project.			
12. KEY WORDS <i>(Six to twelve entries; alphabetical order; capitalize only proper names; and separate key words by semicolons)</i> Binary mixtures; density; experimental data; liquefied natural gas; magnetic suspension densimeter; multicomponent mixtures; prediction methods; pure fluids.			
13. AVAILABILITY <input checked="" type="checkbox"/> Unlimited <input type="checkbox"/> For Official Distribution. Do Not Release to NTIS <input checked="" type="checkbox"/> Order From Superintendent of Documents, U.S. Government Printing Office, Washington, D.C. 20402. <input type="checkbox"/> Order From National Technical Information Service (NTIS), Springfield, VA. 22161		14. NO. OF PRINTED PAGES 241	15. Price







# NBS TECHNICAL PUBLICATIONS

## PERIODICALS

**JOURNAL OF RESEARCH**—The Journal of Research of the National Bureau of Standards reports NBS research and development in those disciplines of the physical and engineering sciences in which the Bureau is active. These include physics, chemistry, engineering, mathematics, and computer sciences. Papers cover a broad range of subjects, with major emphasis on measurement methodology and the basic technology underlying standardization. Also included from time to time are survey articles on topics closely related to the Bureau's technical and scientific programs. As a special service to subscribers each issue contains complete citations to all recent Bureau publications in both NBS and non-NBS media. Issued six times a year. Annual subscription: domestic \$18; foreign \$22.50. Single copy, \$4.25 domestic; \$5.35 foreign.

## NONPERIODICALS

**Monographs**—Major contributions to the technical literature on various subjects related to the Bureau's scientific and technical activities.

**Handbooks**—Recommended codes of engineering and industrial practice (including safety codes) developed in cooperation with interested industries, professional organizations, and regulatory bodies.

**Special Publications**—Include proceedings of conferences sponsored by NBS, NBS annual reports, and other special publications appropriate to this grouping such as wall charts, pocket cards, and bibliographies.

**Applied Mathematics Series**—Mathematical tables, manuals, and studies of special interest to physicists, engineers, chemists, biologists, mathematicians, computer programmers, and others engaged in scientific and technical work.

**National Standard Reference Data Series**—Provides quantitative data on the physical and chemical properties of materials, compiled from the world's literature and critically evaluated. Developed under a worldwide program coordinated by NBS under the authority of the National Standard Data Act (Public Law 90-396).

**NOTE:** The principal publication outlet for the foregoing data is the Journal of Physical and Chemical Reference Data (JPCRD) published quarterly for NBS by the American Chemical Society (ACS) and the American Institute of Physics (AIP). Subscriptions, reprints, and supplements available from ACS, 1155 Sixteenth St., NW, Washington, DC 20056.

**Building Science Series**—Disseminates technical information developed at the Bureau on building materials, components, systems, and whole structures. The series presents research results, test methods, and performance criteria related to the structural and environmental functions and the durability and safety characteristics of building elements and systems.

**Technical Notes**—Studies or reports which are complete in themselves but restrictive in their treatment of a subject. Analogous to monographs but not so comprehensive in scope or definitive in treatment of the subject area. Often serve as a vehicle for final reports of work performed at NBS under the sponsorship of other government agencies.

**Voluntary Product Standards**—Developed under procedures published by the Department of Commerce in Part 10, Title 15, of the Code of Federal Regulations. The standards establish nationally recognized requirements for products, and provide all concerned interests with a basis for common understanding of the characteristics of the products. NBS administers this program as a supplement to the activities of the private sector standardizing organizations.

**Consumer Information Series**—Practical information, based on NBS research and experience, covering areas of interest to the consumer. Easily understandable language and illustrations provide useful background knowledge for shopping in today's technological marketplace.

*Order the above NBS publications from: Superintendent of Documents, Government Printing Office, Washington, DC 20402.*

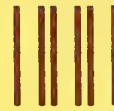
*Order the following NBS publications—FIPS and NBSIR's—from the National Technical Information Services, Springfield, VA 22161.*

**Federal Information Processing Standards Publications (FIPS PUB)**—Publications in this series collectively constitute the Federal Information Processing Standards Register. The Register serves as the official source of information in the Federal Government regarding standards issued by NBS pursuant to the Federal Property and Administrative Services Act of 1949 as amended, Public Law 89-306 (79 Stat. 1127), and as implemented by Executive Order 11717 (38 FR 12315, dated May 11, 1973) and Part 6 of Title 15 CFR (Code of Federal Regulations).

**NBS Interagency Reports (NBSIR)**—A special series of interim or final reports on work performed by NBS for outside sponsors (both government and non-government). In general, initial distribution is handled by the sponsor; public distribution is by the National Technical Information Services, Springfield, VA 22161, in paper copy or microfiche form.

**U.S. Department of Commerce**  
National Bureau of Standards

Washington, D.C. 20234  
Official Business  
Penalty for Private Use \$300



POSTAGE AND FEES PAID  
U.S. DEPARTMENT OF COMMERCE  
COM-215

SPECIAL FOURTH-CLASS RATE  
BOOK